Universität Hamburg
DER FORSCHUNG | DER LEHRE | DER BILDUNG

Molecular mechanisms of hypoxia tolerance in the phocid seal brain

---

Cumulative dissertation

with the aim of achieving a

doctoral degree (Dr. rer. nat.)

at the

Faculty of Mathematics,

Informatics and Natural Sciences,

Department of Biology

of the University of Hamburg

submitted by

Gerrit A. Martens from Hannover

- Hamburg, 2023 –

“The time has come," the Walrus said, "to talk of many things: Of shoes - and ships - and sealing wax - of cabbages - and kings - And why the sea is boiling hot - And whether pigs have wings.” - The Walrus and the Carpenter, Through the Looking-Glass, Lewis Carroll

1st Evaluator: Prof. Dr. Susanne Dobler

2nd Evaluator: Dr. Andrej Fabrizius

Examination Board: Dr. Cornelia Geßner, Prof. Dr. Markus Fischer, Prof. Dr. Baris Tursun (chair)

Oral defense: 12 June 2023

1 Contents

Included publications

Martens, Gerrit A.; Geßner, Cornelia; Folkow, Lars P.; Creydt, Marina; Fischer, Markus; Burmester, Thorsten (2023): The roles of brain lipids and polar metabolites in the hypoxia tolerance of deep-diving pinnipeds. In *Journal of Experimental Biology*, Article jeb.245355. DOI: 10.1242/jeb.245355.

Martens, Gerrit A.; Geßner, Cornelia; Osterhof, Carina; Hankeln, Thomas; Burmester, Thorsten (2022): Transcriptomes of Clusterin- and S100B-transfected neuronal cells elucidate protective mechanisms against hypoxia and oxidative stress in the hooded seal (*Cystophora cristata*) brain. In *BMC Neuroscience* 23 (1), p. 59. DOI: 10.1186/s12868-022-00744-6.

Martens, Gerrit A.; Folkow, Lars P.; Burmester, Thorsten; Geßner, Cornelia (2022): Elevated antioxidant defence in the brain of deep-diving pinnipeds. In *Frontiers in Physiology*. 13, Article 1064476. DOI: 10.3389/fphys.2022.1064476.

2 Summary

Marine mammals have undergone a fascinating transition from a life on land, back to an aquatic environment. Various physiological adaptations have evolved to facilitate their diving lifestyle such as enhanced oxygen stores and a profound diving response, including a reduced heart beat (bradycardia) and restriction of blood flow to vital organs (peripheral vasoconstriction), i.e., the brain and heart. Nevertheless, central oxygen stores may be depleted during extensive diving bouts, resulting in low tissue oxygen levels (hypoxia). Remarkably, isolated brain slices of the hooded seal (*Cystophora cristata*) survive extended periods of severe hypoxia in comparison to other mammals. However, this intrinsic hypoxia tolerance of the hooded seal brain is not well understood. In this study, different molecular targets and pathways were therefore analyzed, i.e., brain lipids and polar metabolites (Chapter I), the neuroprotective genes Clusterin (CLU) and S100B (Chapter II) and antioxidant expression and activity (Chapter III) that may contribute to the intrinsic hypoxia tolerance of the hooded seal brain.

In an untargeted lipidomics approach the lipid composition of deep-diving pinnipeds, the hooded seal and the harp seal (*Pagophilus groenlandicus*), was compared to terrestrial relatives, the ferret (*Mustela putorius furo*) and the mouse (*Mus musculus*) (Chapter I). A general increase of sphingomyelin species was observed in adult, but not juvenile, pinnipeds. Maintenance of the axon enwrapping myelin sheath may be necessary for efficient signal transduction in the pinniped brain, but may develop with diving ability. However, when analyzing the lipidome of hooded seal brain samples, incubated at hypoxia and oxidative stress *in vitro*, no changes in lipid content could be determined. Increased sphingomyelin levels may therefore reflect a constitutive adaptation to recurrent hypoxic conditions. In substrate assays, low levels of the neurotransmitter glutamate were determined, which may decrease even further during hypoxia. A reduced capacity for glutamatergic neurotransmission coincides with previous studies and may reduce the energy expenditure and oxygen consumption, when oxygen supply becomes scarce. Elevated levels of glucose and lactate may indicate an enhanced glycolytic capacity and may support reduced oxidative metabolism in the hooded seal brain.

Previous transcriptomics studies determined opposing trends regarding aerobic capacity in the hooded seal brain, but observed high expression of the genes CLU and S100B. Both are associated with various neurodegenerative diseases, but their functions and molecular mechanisms remain ambiguous. Thus, the transcriptomes of neuronal cells were analyzed, which were separately transfected with two isoforms of CLU (nCLU, sCLU) and S100B and exposed to different oxygen regimes (Chapter II). Interestingly, overexpression of sCLU and S100B already influenced gene expression of the neuronal cells at normoxic conditions. Both genes may confer increased glycolytic metabolism and reduced mitochondrial aerobic respiration. Furthermore, S100B may reduce neurotransmission through the

opioid signaling pathway, while sCLU may promote protein homeostasis (proteostasis) and mitochondrial autophagy (mitophagy). These processes were enhanced at normoxic conditions, but gene expression was not markedly different when neuronal cells were exposed to oxidative stress. However, the cells demonstrated elevated viability at this condition. Thus, the observed changes in gene expression may prepare the hooded seal brain for upcoming stress conditions.

A known adaptation of marine mammals are their constitutively elevated levels of antioxidants to detoxify reactive oxygen species (ROS), which is especially relevant when surfacing after extensive diving bouts. However, the antioxidant defence in the brain of diving mammals has not been the focus of studies so far. Therefore, the expression and activity of selected antioxidants in different brain regions were determined, i.e., the visual cortex, cerebellum and hippocampus, of the hooded seal and harp seal compared to mice (Chapter III). Especially antioxidants involved in the glutathione system were highly expressed and active in the pinniped brain. In constrast to glutathione, the thioredoxin and glutaredoxin system were not similarly upregulated and may thus not be as important in the antioxidant defence of the pinniped brain or only react once facing acute stress situations.

The present work describes molecular alterations in the pinniped brain and provides the basis for additional studies on the hypoxia tolerance of the hooded seal brain. Understanding the adaptation of marine mammals to their aquatic environment may aid in conservation projects as well as provide insights for human medicine.

3 Zusammenfassung

Meeressäuger haben einen faszinierenden Übergang vom Land zurück in eine aquatische Umgebung durchlaufen. Verschiedene physiologische Anpassungen haben sich entwickelt, um ein Leben in der Tiefe zu ermöglichen, wie z. B. erhöhte Sauerstoffspeicher und eine tiefgreifende Tauchreaktion mit reduziertem Herzschlag (Bradykardie) und einer Einschränkung des Blutflusses zu lebenswichtigen Organen (periphere Vasokonstriktion) wie Gehirn und Herz. Dennoch werden ihre zentralen Sauerstoffvorräte bei ausgedehnten Tauchgängen erschöpft, was zu einem niedrigen Sauerstoffgehalt im Gewebe (Hypoxie) führen kann. Bemerkenswerterweise überstehen isolierte Hirnschnitte der Klappmützenrobbe (*Cystophora cristata*) im Vergleich zu anderen Säugetieren längere Perioden starker Hypoxie. Diese intrinsische Hypoxietoleranz des Gehirns der Klappmützenrobbe ist jedoch nicht gut untersucht. In dieser Studie wurden daher verschiedene molekulare Ziele und Signalwege analysiert wie Gehirnlipide und polare Metabolite (Kapitel I), die neuroprotektiven Gene Clusterin (CLU) und S100B (Kapitel II) sowie die Expression und Aktivität von Antioxidantien (Kapitel III), welche möglicherweise an der intrinsischen Hypoxietoleranz des Klappmützengehirns mitwirken.

In einem ungezielten Lipidomik-Ansatz wurde die Lipidzusammensetzung von tieftauchenden Flossenfüßern, der Klappmützenrobbe und der Sattelrobbe (*Pagophilus groenlandicus*) mit terrestrischen Verwandten verglichen, dem Frettchen (*Mustela putorius furo*) und der Maus (*Mus musculus*) (Kapitel I). Eine allgemeine Zunahme von Sphingomyelin-Spezies bei adulten, jedoch nicht bei juvenilen Flossenfüßern wurde beobachtet. Die Aufrechterhaltung der axonumhüllenden Myelinscheide könnte für eine effiziente Signalübertragung im Flossenfüßergehirn erforderlich sein, entwickelt sich möglicherweise jedoch erst mit der Tauchfähigkeit. Bei der Analyse des Lipidoms von Gehirnproben der Klappmützenrobbe, die bei Hypoxie und oxidativem Stress *in vitro* inkubiert wurden, konnten jedoch keine Veränderungen des Lipidgehalts festgestellt werden. Erhöhte Sphingomyelinspiegel könnten daher eine konstitutive Anpassung an wiederkehrende hypoxische Zustände widerspiegeln. In Substratassays wurden geringe Konzentrationen des Neurotransmitters Glutamat festgestellt, welche bei Hypoxie sogar noch weiter abnehmen könnten. Eine reduzierte Fähigkeit zur glutamatergen Neurotransmission deckt sich mit früheren Studien und kann den Energieverbrauch und den Sauerstoffverbrauch reduzieren, wenn die Sauerstoffversorgung knapp wird. Erhöhte Glukose- und Laktatspiegel könnten auf eine erhöhte glykolytische Kapazität hinweisen und einen reduzierten oxidativen Stoffwechsel im Gehirn der Klappmützenrobbe unterstützen.

Frühere Transkriptomik-Studien ergaben gegenläufige Tendenzen bezüglich der aeroben Kapazität, zeigten jedoch eine hohe Expression der Gene CLU und S100B im Gehirn der Klappmützenrobbe auf. Beide sind mit verschiedenen neurodegenerativen Erkrankungen assoziiert, ihre Funktionen und molekularen Mechanismen bleiben jedoch weitgehend unklar. Daher wruden die Transkriptome von

Nervenzellen analysiert, die separat mit zwei Isoformen von CLU (nCLU, sCLU) und S100B transfiziert wurden und unterschiedlichen Sauerstoffregimen ausgesetzt wurden (Kapitel II). Interessanterweise beeinflusste die Überexpression von sCLU und S100B bereits die Genexpression der neuronalen Zellen unter normoxischen Bedingungen. Beide Gene könnten einen erhöhten glykolytischen Metabolismus und eine verringerte mitochondriale aerobe Atmung bewirken. Darüber hinaus könnte S100B die Neurotransmission durch den Opioid-Signalweg reduzieren, während sCLU die Proteinhomöostase (Proteostase) und die mitochondriale Autophagie (Mitophagie) fördern könnte. Während diese Prozesse unter normoxischen Bedingungen verstärkt wurden, war die Genexpression nicht merklich anders, wenn neuronale Zellen oxidativem Stress ausgesetzt waren. Die Zellen zeigten jedoch eine erhöhte Lebensfähigkeit unter dieser Bedingung. Somit könnten die beobachteten Veränderungen in der Genexpression das Gehirn der Klappmützenrobbe auf bevorstehende Stressbedingungen vorbereiten.

Eine bekannte Anpassung von Meeressäugern sind ihre konstitutiv erhöhten Gehalte an Antioxidantien zur Entgiftung reaktiver Sauerstoffspezies (ROS), was insbesondere beim Auftauchen nach ausgedehnten Tauchgängen eine wichtige Rolle spielt. Die antioxidative Abwehr im Gehirn tauchender Säugetiere stand bisher jedoch nicht im Fokus von Studien. Daher wurde die Expression und Aktivität ausgewählter Antioxidantien in verschiedenen Hirnregionen, d. h. dem visuellen Kortex, Kleinhirn und Hippocampus, von Klappmützenrobbe und Sattelrobbe im Vergleich zu Mäusen bestimmt (Kapitel III). Besonders Antioxidantien, die am Glutathionsystem beteiligt sind, zeigten eine erhöhte Expression und Aktivität im Gehirn der Flossenfüßer. Im Gegensatz zu Glutathion, zeigte das Thioredoxin- und Glutaredoxinsystem keine vergleichbare Hochregulierung und ist daher möglicherweise nicht so wichtig für die antioxidative Abwehr im Flossenfüßergehirn oder reagiert erst in akuten Stresssituationen.

Die vorliegende Arbeit beschreibt molekulare Signalwege, die im Gehirn von Flossenfüßern verändert sein könnten und liefert die Grundlage für weitere Studien zur Hypoxietoleranz im Gehirn von Klappmützenrobben. Das Verständnis der Anpassung von Meeressäugern an ihre aquatische Umgebung kann bei Naturschutzprojekten hilfreich sein und Erkenntnisse für die Humanmedizin liefern.

4 List of abbreviations

ASM	acid sphingomyelinase
ATP	adenosine triphosphate
BDNF	brain-derived neurotrophic factor
BNIP3	BCL2 (B-cell lymphoma 2) interacting protein 3
Cer	ceramide
CLU	clusterin
CV	cross validation
DEG	differentially expressed gene
ER	endoplasmic reticulum
ETC	electron transport chain
FA	fatty acid
FC	fold change
FDR	false discovery rate
FE	fold enrichment
GAP43	growth-associated protein 43
GLRX2	glutaredoxin 2
GO	gene ontology
GPX	glutathione peroxidase
GSH	glutathione
GSR	glutathione reductase
GSSG	glutathione disulfide
GST	glutathione-S-transferase
HDL	high density lipoprotein
HexCer	cerebroside
HIF	hypoxia inducible factor
IPA	ingenuity pathway analysis
LC	liquid chromatography
LDH	lactate dehydrogenase
MCT4 (SLC16A3)	monocarboxylate transporter 4 (solute carrier family 16 member 3)
MS	mass spectrometry
MUFA	monounsaturated fatty acid
nCLU	nuclear clusterin
NFE2L2 (NRF2)	nuclear factor, erythroid 2-like 2 (NF-E2-related factor 2)
NGF	nerve growth factor
OPRD1	opioid receptor delta 1
PC	phosphatidylcholine
PCA	principal component analysis
PCP4	purkinje cell protein 4
PDK1	pyruvate dehydrogenase kinase 1
PE	phosphatidylethanolamine
PI	phosphatidylinositol
PLS-DA	partial least squares-discriminant analysis
PS	phosphatidylserine
PUFA	polyunsaturated fatty acid
QC	quality control sample
qRT-PCR	quantitative real-time PCR
ROS	reactive oxygen species
sCLU	soluble clusterin
SM	sphingomyelin
SOD	superoxide dismutase
TCA	tricarboxylic acid
TPM	transcripts per million
TXNRD3	thioredoxin reductase 3
VIP	variable importance plot

5 Introduction

5.1 Return to the sea – Evolution of marine mammals

Marine mammals have undergone a fascinating transition from a life on land, conquered by Sarcopterygian fishes around 400 million years ago, back to an aquatic environment (Meyer et al. 2021; Berta et al. 2015). The return to the marine domain occurred in separate evolutionary events. While cetaceans (whales, dolphins, porpoises) and sirenians (sea-cows) emerged about 50 million years ago, pinnipeds (seals, walrus) and among them phocid seals (true seals) evolved 30–24 million years ago (Berta et al. 2022; Berta et al. 2015; Uhen 2007). Adaptation to this cold environment led to the convergent evolution of remarkable features of marine mammals such as a thick blubber insulation and a countercurrent heat exchange system (Berta et al. 2015). In addition to low temperatures, marine mammals are further challenged by high pressures and, in particular, low oxygen conditions during diving (e.g., Ponganis 2011). To facilitate this extreme lifestyle, not only anatomical adaptations, but also changes on the physiological, molecular and genetic level occurred, which will be discussed in the following sections (e.g., Davis 2014; Hindle 2020).

Tolerance to low tissue oxygen concentrations (hypoxia) also evolved in other mammals. Hibernating mammals experience recurrent hypoxia during periodic torpor and arousal bouts (Drew et al. 2001; Zhou et al. 2001; Bouma et al. 2010; Gonzalez-Riano et al. 2019), while mammals inhabiting underground burrows or high altitudes are chronically exposed to hypoxic conditions (Pamenter 2022; Ramirez et al. 2007). Studying the adaptations of hypoxia-tolerant species to their low oxygen environments is a challenging task. However, elucidating the mechanisms contributing to their hypoxia tolerance, especially on the molecular level, may not only provide insights into their fascinating physiology but may also benefit human medicine. Treatment of diseases characterized by reduced oxygen supply such as cardiac arrest or stroke may benefit from knowledge of how hypoxia-tolerant species prevent tissue damage during and after low oxygen conditions.

5.2 Physiological adaptations to an aquatic environment

Spending most of their time at sea, marine mammals developed remarkable adaptations to a diving lifestyle. In proportion to their body size, phocid seals such as the hooded seal (*Cystophora cristata*, Fig. 1) demonstrate the most exceptional breath-hold capabilities among marine mammals, which may only be exceeded by the sperm whale (*Physeter macrocephalus*) and some beaked whales (family Ziphiidae) (Fig. 2, Mirceta et al. 2013). Maximum dive depths of over 1 km and dive durations of more than 52 min have been observed for the hooded seal (Folkow and Blix 1999). In order to be able to perform such an extraordinary diving behavior, various physiological adaptations have evolved in pinnipeds (for reviews see: Ponganis 2011; Davis 2014, 2019; Blix 2018; Allen and Vázquez-Medina 2019).

Fig. 1: *Adult male hooded seal (Cystophora cristata) with inflated 'hood' © Jenny E. Ross, lifeonthinice.org*

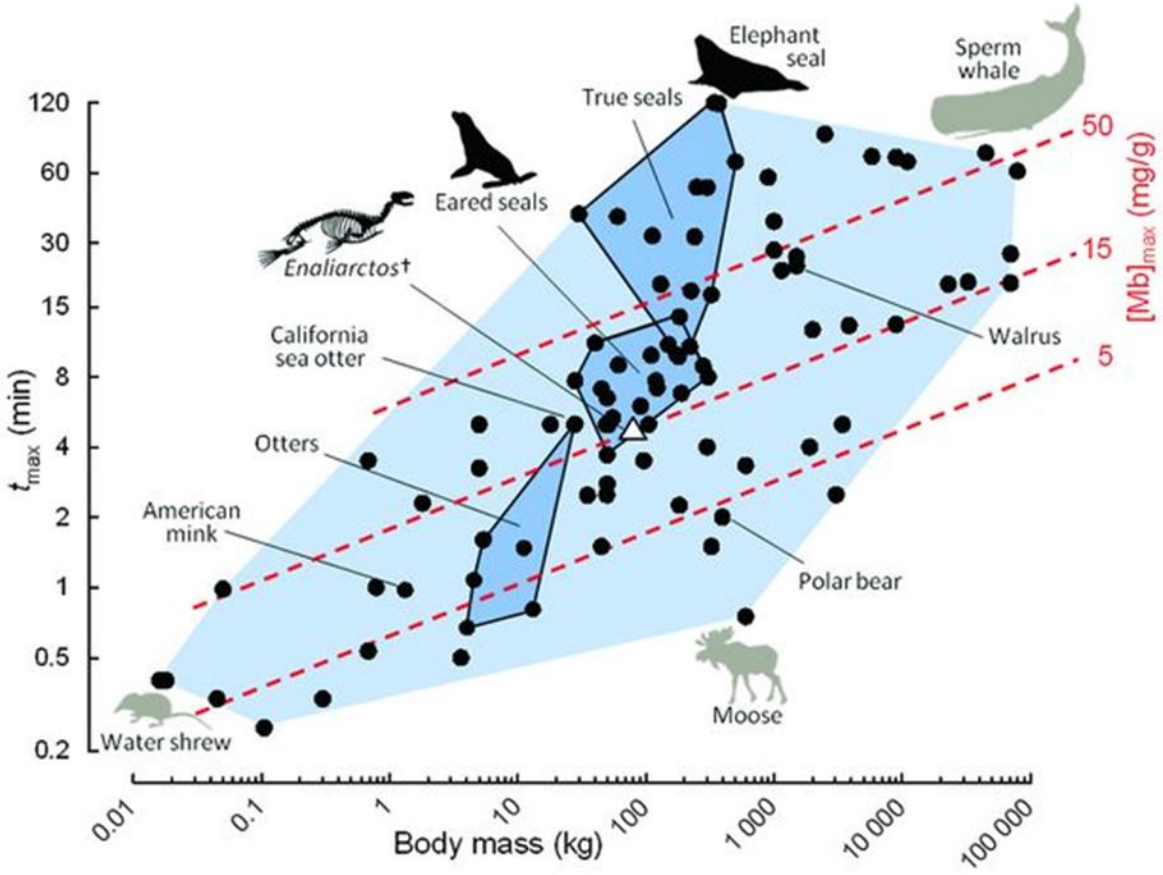

Fig. 2: *Modeling diving capacity in marine mammals. Maximal active dive time (t_{max}) and body mass in extant mammals (circles) and fossil representatives of their land-to-water transitions (triangles). Convex polygons for all mammals (light shading) and selected groups (heavy shading) are indicated. $[Mb]_{max}$: maximal skeletal muscle concentration of myoglobin, ZMb: Mb net surface charge. From Mirceta et al. (2013). Reprinted with permission from AAAS.*

Pinnipeds do not rely on lung capacity to provide oxygen during dives as the lung collapses to avoid decompression sickness-related tissue damage as shown in the diving Weddell seal (*Leptonychotes weddellii*) at depths of 25–50 m (Falke et al. 1985; Garcia Párraga et al. 2018). Thus, the lung oxygen capacity of phocid seals such as the hooded seal is somewhat smaller than in other mammals (6 ml O_2 kg^{-1} vs. 9 ml O_2 kg^{-1} in humans), whereas total oxygen stores are considerably higher (90 ml O_2 kg^{-1} vs. 25 ml O_2 kg^{-1} in humans) (Burns et al. 2007; Blix 2018). Increased blood volume of marine mammals has been an early observation (Hunter 1787), while larger hematocrit (Lenfant et al. 1969; Lenfant et al. 1970), blood hemoglobin content (Lenfant et al. 1969; Lenfant et al. 1970), muscle myoglobin content (Guyton et al. 1995; Noren and Williams 2000; Kanatous and Mammen 2010) and an enlarged spleen (Cabanac et al. 1997), contributing to overall increased oxygen storage, were discovered more recently. Interestingly, most of the oxygen stores such as myoglobin concentration are subject to postnatal development along with diving ability (Noren 2020), while hemoglobin stores are fully developed at birth as shown in the hooded seal (Geiseler et al. 2013). This suggests that the buildup of the prolonged diving capacity of marine mammals requires external stimuli and swimming activity (Geiseler et al. 2013; Noren 2020).

With cessation of breathing (apnea) pinnipeds initiate a dive response to limit energy expenditure during conditions of limited oxygen availability (Kaczmarek et al. 2018). For this purpose, the heart rate in phocid seals may be slowed (bradycardia) down to 4 beats per minute as seen in free-ranging grey seals (*Halichoerus grypus*) (Thompson and Fedak 1993; Hill et al. 1987), while blood flow is restricted to vital organs such as the heart and brain (selective peripheral vasoconstriction) as shown in Weddell seals (Zapol et al. 1979). Additionally, body core temperature may drop by 2°C (Hill et al. 1987) and brain temperature may be downregulated by as much as 2.5°C (Odden et al. 1999; Blix et al. 2010), which may result in overall decreased cerebral oxygen requirements directly observed during voluntary diving in captive grey seals (Sparling and Fedak 2004). Other marine mammals such as cetaceans exhibit a similar dive response including lung collapse, bradycardia and peripheral vasoconstriction (Ponganis 2011). However, body and brain temperature of diving whales has not been extensively studied (Ponganis 2015).

Most adult mammals, including humans, respond to low oxygen conditions by a physiological reflex, termed ‘hypoxic ventilatory response’, in order to enhance ventilation and oxygen delivery (Teppema and Dahan 2010). However, this strategy is energy-intensive and may only represent a short-term solution (Pamenter 2022). Instead, hypoxia-tolerant species such as hibernating mammals (e.g., Syrian hamster (*Mesocricetus auratus*), Arctic ground squirrel (*Urocitellus parryii*)) lower their energy expenditure by decreasing body and brain temperature and reducing blood flow and metabolism during hibernation (Drew et al. 2001; Zhou et al. 2001; Bouma et al. 2010; Gonzalez-Riano et al. 2019). Burrowing mammals (e.g., naked mole-rat (*Heterecephalus glaber*), Middle East blind mole-rat (*Spalax*

ehrenbergi)) appear to tackle chronic hypoxia by decreasing metabolic demand, while blunting the hypoxic ventilatory response (Pamenter 2022). And high altitude species (e.g., deer mouse (*Peromyscus maniculatus*), plateau zokor (*Eospalax fontanierii baileyi*)) seem to support aerobic metabolism by an enhanced blood O_2 transport capacity (McClelland and Scott 2019; Storz and Cheviron 2021; Storz 2021).

While both, pinnipeds and other hypoxia-tolerant species, demonstrate extensive efforts to cope with low oxygen supply, the former still routinely deplete their oxygen stores during repetitive diving bouts (Meir et al. 2009; Meir et al. 2013; McDonald and Ponganis 2013). Consequently, arterial oxygen partial pressure may drop to values as low as 12–23 mmHg in northern elephant seals (*Mirounga angustirostris*) (Meir et al. 2009) or 25-35 mmHg in Weddell seals (Qvist et al. 1986). The brain is among the most hypoxia-sensitive organs (Richmond 1997). Neuronal damage in the brain of terrestrial mammals already occurs at arterial oxygen tensions of 25-40 mmHg (Erecińska and Silver 2001; Lutz 2002), while in pinnipeds detrimental effects only occur when arterial oxygen partial pressure decreases to 10 mmHg (Elsner et al. 1970; Kerem and Elsner 1973). In humans, alveolar oxygen tensions of about 20 mmHg already coincided with loss of motor control (Lindholm and Lundgren 2006; Patrician et al. 2021).

Remarkably, the hooded seal brain demonstrates a profound tolerance to low oxygen conditions that cannot be explained by physiological adaptations. During and after severe hypoxia, isolated hooded seal brain slices maintained membrane potential, while neurons of non-diving species depolarized and lost their functional integrity (Fig. 3, Folkow et al. 2008; Ramirez et al. 2011; Geiseler et al. 2016). However, the molecular basis of this intrinsic hypoxia tolerance of the hooded seal brain is not well understood.

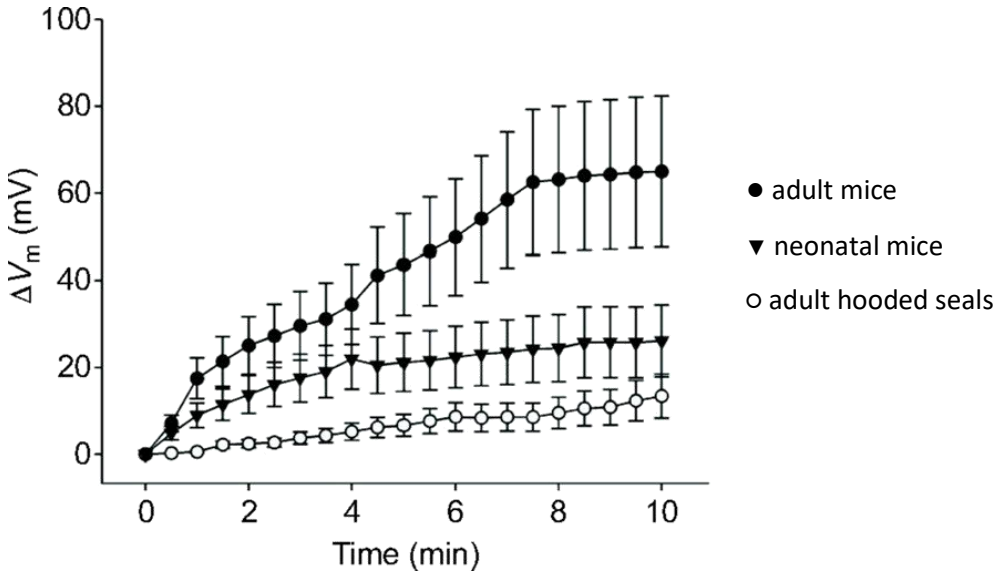

Fig. 3: *Average membrane potential changes (ΔVm) during severe hypoxia. Reprinted from Folkow et al. (2008), with permission from Elsevier.*

5.3 Energy metabolism in the mammalian brain

The mammalian brain is a highly organized structure, in which distinct tasks are performed in specialized regions. For instance, visual perception takes place in the visual cortex (Grill-Spector and Weiner 2014), control of motion (and cognition) in the cerebellum (Schmahmann et al. 2019) and navigation in (cognitive) space in the hippocampus (Bellmund et al. 2018). To perform these complex tasks the brain relies on constant supply of energy (Bélanger et al. 2011). Although it only represents 2% of the total body mass, it accounts for about 20% of the body's energy consumption (Magistretti and Allaman 2015). Most of the energy is being used for the maintenance of ion gradients, membrane potentials and neurotransmitter levels (Attwell and Laughlin 2001; Alle et al. 2009). Glutamatergic synaptic activity alone accounts for about 80% of total cortical oxidation of glucose (Sibson et al. 1998). The supply of energy substrates such as glucose is mainly facilitated by astrocytes (Chuquet et al. 2010), whose endfeet are ideally positioned to sense neuronal activity at synapses (Genoud et al. 2006) and take up glucose from intracerebral blood vessels (Kacem et al. 1998). Consequently, astrocytes primarily perform glycolysis and excrete the metabolic end product lactate into the extracellular space (Bittner et al. 2010). They additionally exhibit high concentrations of glycogen as energy stores, which can be also metabolized and secreted as lactate, when glucose becomes scarce (Brown and Ransom 2007). Neurons are subsequently able to take up released lactate, which they preferentially use for oxidative energy metabolism (Bouzier-Sore et al. 2006). Observations of this tight linkage between complementary neuronal and astrocytic metabolism led to the 'astrocyte-neuron lactate shuttle' hypothesis (Fig. 4, Pellerin and Magistretti 1994). On a side note, the brain may also utilize blood-derived ketone bodies and lactate during development, starvation (Nehlig 2004) or intense physical activity (van Hall et al. 2009), as well as oxidize various other intermediates from glucose catabolism (e.g., pyruvate, glutamate or acetate) (Zielke et al. 2009).

Interestingly, the energy metabolism in the hooded seal brain may differ from this concept. Cytochrome c, neuroglobin and lactate dehydrogenase b were primarily detected in astrocytes rather than in neurons, which suggests distinct glycolytic activity of astrocytes (Mitz et al. 2009; Hoff et al. 2016). Lactate excreted in this process may be subsequently taken up and oxidized by neurons, which has been outlined as the 'reverse lactate shuttle' hypothesis by Mitz et al. (2009). Furthermore, transcriptome studies determined genes differentially expressed in the hooded seal brain in comparison to terrestrial mammals (Fabrizius et al. 2016; Hoff et al. 2017; Geßner et al. 2022). However, genes associated with glycolytic metabolism were not particularly altered and oxidative metabolism was either found to be decreased in comparison to ferrets (*Mustela putorius furo*) or increased in comparison to mice (*Mus musculus*) (Fabrizius et al. 2016; Hoff et al. 2017; Geßner et al. 2022). The exact modification of energy metabolism in the hooded seal brain therefore remains ambiguous.

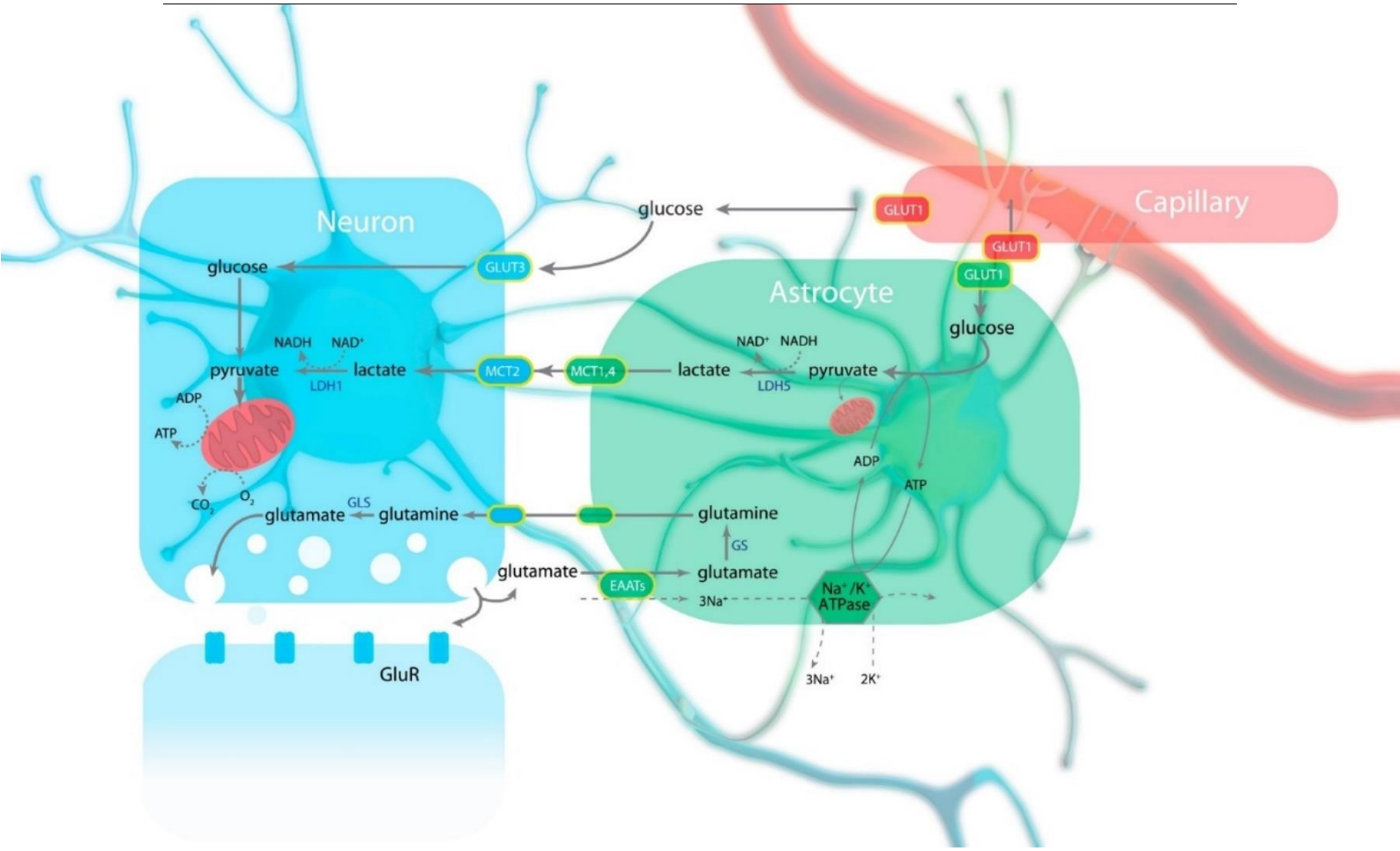

Fig. 4: *Schematic representation of the astrocyte-neuron lactate shuttle. EAAT: excitatory amino acid transporter; GluR: glutamatergic receptor; GLUT: glucose transporter; GLS: glutaminase; GS: glutamine synthetase; LDH: lactate dehydrogenase; MCT: monocarboxylate transporter. Reprinted from Magistretti and Allaman (2015), with permission from Elsevier.*

5.4 Synaptic signaling in the mammalian brain

During neuronal activity and associated glutamatergic synapse signaling, glutamate, the primary excitatory neurotransmitter in the vertebrate brain, is released into the synaptic cleft (Oltedal et al. 2008; Meldrum 2000). To terminate its action, extracellular glutamate is taken up by astrocytes through glutamate transporters (Mahmoud et al. 2019), where it is converted to glutamine by the astrocyte-specific glutamine synthetase (Martinez-Hernandez et al. 1977). Subsequently, glutamine is transported to neurons and converted back to glutamate by glutaminase to replenish the glutamate pool (Chaudhry et al. 2002; Laake et al. 1995). Glutamate can also be utilized as energy substrate in the TCA cycle and thus glutamate has to be synthesized *de novo* to compensate for its degradation (Sonnewald 2014). Replenishment of glutamate occurs in astrocytes, as the anaplerotic enzyme pyruvate carboxylase is exclusive to this neural cell type (Yu et al. 1983; Schousboe et al. 2019).

Because of this tightly regulated metabolism and dependence on oxidative energy production, the brain is especially vulnerable to pathological conditions such as disrupted blood supply (ischeamia) (Cobley et al. 2018). Ischaemia leads to low tissue oxygen levels (hypoxia), which may cause brain dysfunction in most mammals (Erecińska and Silver 2001; Lutz 2002; Lutz and Nilsson 2004). The main

reason is a decreasing level of ATP, which results in impaired uptake of glutamate and thus accumulation in the synaptic cleft, ultimately ending in overstimulation of glutamate receptors, excessive influx of calcium and depolarization of neuronal membranes (Andersen et al. 2021). These excitotoxic events are the major cause of cell death at hypoxic conditions (Choi and Rothman 1990; Belov Kirdajova et al. 2020).

Interestingly, neurons excised from the visual cortex of hooded seals at resting conditions demonstrate a decreased expression of genes involved in glutamatergic synapse signaling in comparison to mice (Geßner et al. 2022). Additionally, Hoff et al. (2017) observed a downregulation of genes associated with ion transport in brain slices exposed to hypoxia *in vitro*. Decreased neurotransmission would ultimately result in a reduction of energy expenditure and may protect against hypoxia-induced glutamate excitotoxicity in the hooded seal brain (Ramirez et al. 2007). Additionally, transcriptome studies observed high expression of the neuroprotective genes clusterin (CLU) and S100B, which may contribute to the hypoxia tolerance of the hooded seal brain (Fabrizius et al. 2016; Geßner et al. 2020; Geßner et al. 2022).

5.5 Oxidative stress in the mammalian brain

The abrupt reperfusion of tissue with oxygen after an ischemic insult can lead to the buildup of reactive oxygen species (ROS) and related tissue damage, known as ischaemia-reperfusion injury (Sun et al. 2018). ROS are a byproduct of normal cell metabolism and usually exhibit signaling functions at physiological concentrations (Dröge 2002). ROS production mainly occurs at mitochondria, which perform oxidative phosphorylation to yield energy in the form of ATP. The mitochondrial electron transport chain (ETC) terminates with the reduction of oxygen to water. However, a small portion of electrons leak from the ETC to oxygen and form superoxide radicals (Valko et al. 2007). ROS may also be generated at the endoplasmic reticulum, peroxisome and lysosomes (Milkovic et al. 2019). While physiological concentrations of ROS are beneficial for cell metabolism, excessive amounts of ROS are deleterious (Valko et al. 2007). The brain is especially susceptible to oxidative damage due to its high oxygen demand (Zielke et al. 2009; Bouzier-Sore et al. 2006) and its relatively low intrinsic antioxidant capacity (Dringen 2000). However, the two main cell types in the brain, neurons and glial cells, exhibit varying degrees of susceptibility to hypoxia and oxidative stress due to their distinct metabolic characteristics. While neurons rely on oxygen for oxidative metabolism and are likely unable to shift to anaerobic glycolysis (Herrero-Mendez et al. 2009), astrocytes (a type of glial cell) may increase glycolytic pathways, when mitochondrial respiration is inhibited (Almeida et al. 2001; Almeida et al. 2004). Additionally, astrocytes contain higher levels of antioxidants, which makes them more resistant to insults by ROS (Bélanger and Magistretti 2009). In co-culture, astrocytes may also protect neighboring neurons from oxidative stress (Bélanger and Magistretti 2009). Several neuropathological

diseases such as traumatic brain injury, stroke (causing ischaemia/reperfusion) and neurodegenerative diseases (including Alzheimer's disease, Parkinson's disease, Huntington's disease and amyotrophic lateral sclerosis) are characterized by oxidative stress (Ng and Lee 2019; Sun et al. 2018; Singh et al. 2019).

Dealing with noxious ROS generation, when surfacing after extensive diving bouts is a major challenge for pinnipeds (Zenteno-Savín et al. 2002). Rather than preventing oxidant production, seals possess a high capacity for oxidant detoxification, apparent in high concentrations and activities of enzymatic and non-enzymatic antioxidants (Vázquez-Medina et al. 2012). Especially antioxidative molecules involved in the glutathione system are elevated in plasma and various tissues of marine mammals compared to terrestrial mammals (Wilhelm Filho et al. 2002; Vázquez-Medina et al. 2006, 2007). However, the antioxidant capacity of the brains of marine mammals remains understudied. To the best of our knowledge only one study compared the antioxidative capacity of the brain of the deep-diving dwarf sperm whale (*Kogia sima*) and pygmy sperm whale (*Kogia breviceps*) to the shallow-diving bottlenose dolphin (*Tursiops truncatus*) (Cantú-Medellín et al. 2011).

5.6 Lipids in the mammalian brain

Another factor making the mammalian brain susceptible to oxidative stress is its high content of polyunsaturated fatty acids (PUFAs), which are prone to lipid peroxidation (Bazinet and Layé 2014). Glycerophospholipids, sphingolipids, and sterol lipids are the most abundant lipid species in the human brain (O'Brien and Sampson 1965). Their role has recently been found to be more than solely structural membrane elements and energy stores, but additionally appear to function as signaling molecules in various biological processes such as neurotransmission and regulation of growth (Piomelli et al. 2007). Dysregulation of lipid homeostasis has been implicated in various neurodegenerative disorders, which makes them a suitable biomarker for disease state as well as targets for brain research (Buccellato et al. 2021; Castellanos et al. 2021; Shamim et al. 2018). Additionally, lipids and especially PUFAs are a source for precursors such as omega-6 arachidonic acid (AA) and omega-3 docosahexanoic acid (DHA). The former may be converted to eicosanoids and leukotrienes which promote inflammation and vascular permeability (Mills et al. 2011; Ojo et al. 2019). The latter may form neuroprotective metabolites such as neuroprotectin D1 and other resolvins and protectins, which exhibit potent anti-inflammatory, anti-oxidant, anti-apoptotic and neurotrophic functions (Bazan 2005; Zhao et al. 2011; Mills et al. 2011; Ojo et al. 2019).

Despite being routinely exposed to ischaemia/reperfusion, marine mammals do not accumulate excessive amounts of oxidized lipids in their plasma (Wilhelm Filho et al. 2002). Lipids, especially sphingomyelins, ensheath axons to facilitate rapid conduction of action potentials and are thereby directly involved in signal transduction in the brain (Hartline 2008; Schneider et al. 2019). While the

lipid profile (lipidome) of various tissues of marine mammals has been comprehensively studied (Dannenberger et al. 2020; Simond et al. 2020; Simond et al. 2022; Tang et al. 2018; Monteiro et al. 2021a; Monteiro et al. 2021b; Bories et al. 2021; Bernier-Graveline et al. 2021; Ruiz-Hernández et al. 2022; Watson et al. 2021), to the best our knowledge only one study has looked at the brain lipidome of marine mammals (Glandon et al. 2021). Glandon et al. (2021) compared the lipid signature of neural tissue (brain, spinal cord, and spinal nerves) of stranded cetaceans to non-diving mammals (pigs, sheep). While general content and composition of lipids were similar across species, concentrations of specific lipids were not analyzed (Glandon et al. 2021).

The study of organisms adapted to extreme environments may provide valuable insights into neuroprotective mechanisms, which may help to tackle neuropathological conditions associated with hypoxia and oxidative stress. Marine mammals exhibit enormous breath-hold capacities and are routinely exposed to low oxygen conditions during diving. Thus, they represent highly suitable study animals to elucidate protective mechanisms towards conditions of hypoxia and oxidative stress.

5.7 Study animals

5.7.1 Phocid seals

In this study, members of the phocid seals, the hooded seal (*Cystophora cristata*) and the harp seal (*Pagophilus groenlandicus*) were examined, which can mostly be found in the Arctic Ocean and in the North Atlantic (Folkow et al. 1996; Folkow et al. 2004). They breed on drifting pack ice, but spend most of their time at sea, where they exploit underwater food resources in shallow to deep waters. The hooded seal routinely dives to relatively deep waters ranging from 100 to 600 m for a duration of 5 to 15 min (Folkow and Blix 1999; Andersen et al. 2013; Vacquie-Garcia et al. 2017), while the harp seal usually dives to shallow depths of less than 50 m, lasting 5 to 15 min (Folkow et al. 2004). However, maximum dive depths of over 1 km and dive durations of more than 52 min have been observed for the hooded seal (Folkow and Blix 1999), while maximum dive depths over 500 m have been recorded for harp seals (Lydersen and Kovacs 1993; Folkow et al. 2004).

Hooded seals are large, sexually dimorphic phocids (Fig. 5A). Adults are silvery-white with numerous blotches, while the head, jaws and the tops of the flippers are blackish. Pups are called ‘blue-backs’ because of their dorsal blue-gray coat (Jefferson et al. 2015). Adult males exhibit a characteristic inflatable nasal cavity in the form of a black bladder and an elastic nasal septum that can be extruded and inflated like a bright red balloon, which is mainly used for communication (Frouin-Mouy and Hammill 2021; Ballard and Kovacs 1995). Adult males reach lengths of 2.6 m and weights of 192-352 kg, while the female is slightly smaller with a length of about 2 m and weight of 145-300 kg (Jefferson et al. 2015). Sexual maturity is reached at the age of 4-6 years and 3-5 years for males and females, respectively (Miller et al. 1999; Jefferson et al. 2015). However, males are usually not able to breed

until they are larger and able to compete effectively with other males (Jefferson et al. 2015). The breeding season usually only lasts 2.5 weeks in March and early April (Jefferson et al. 2015). Pups are only weaned for an average of 4 days, the shortest period for any mammal (Stenson and Perry 1992; Bowen et al. 1985). Hooded seals typically fast during breeding and molting (Champagne et al. 2012; Thordarson et al. 2007). Their diet consists primarily of fish, but also includes crustaceans and squids. While diet composition coincides well with diving behavior, it is also subject to spatio-temporal changes in prey availibility (Haug et al. 2007; Enoksen et al. 2017). Hooded seals can live to an age of 25 to 30 years (Jefferson et al. 2015).

Harp seals exhibit the most complicated pelage pattern change of any pinniped over its lifespan (Fig. 5B). Newborns demonstrate a pure white coat for about 12 days ('whitecoats'), as they begin to molt their lanugo ('greycoat' and 'ragged jacket') and show the underlying juvenile spotted pelage ('beaters'). Juveniles ('bedlamers') start to form a 'harp' pattern on the back and sides ('spotted harp'), until the spots have completely disappeared ('old harp'). Then, the adult's base color is silvery-white to light gray, while the face, chin, upper neck and top of the head are black (Jefferson et al. 2015). Harp seals exhibit little sexual dimorphism and are on average 1.7 m long and weigh 130 kg, with females being marginally smaller than males (Perrin et al. 2009; Lavigne 2008). Males are sexually mature at 4-9 years and females at 4-7 years (Kjellqwist 1995; Sergeant 1966). Pups are born from late February to mid-March and are nursed for 12-13 days (Jefferson et al. 2015; Oftedal et al. 1989). Promiscuous mating occurs in the water and on the ice from mid- to late March (Jefferson et al. 2015). The diet of harp seals differs significantly from hooded seals as it mainly consists of crustaceans, but also includes squids and fish. Similar to hooded seals, the diet composition reflects recorded dive depths and is substantially influenced by variations in prey abundance (Lindstrøm et al. 2013; Enoksen et al. 2017). The maximum life span of a harp seal is approximately 30 years (Jefferson et al. 2015).

Pinnipeds are known for their large brains (Bininda-Emonds 2000; Herberstein et al. 2022; Eisert et al. 2014). However, their brain size is as expected for their body mass (Manger et al. 2013). Fundamental aspects of central nervous system organization are similar to other mammals (Turner et al. 2017; Sawyer et al. 2016; Hoeksema et al. 2021; Cook and Berns 2022). Hooded seals and harp seals share physiological traits of their nervous system like axon numbers within the optic nerve, which may reflect adaptation to the same aquatic environment (Mass and Supin 2003; Wohlert et al. 2016). Because of this adaptation, hooded and harp seals represent highly suitable study animals to elucidate mechanisms for dealing with low oxygen conditions.

(A)

(B)

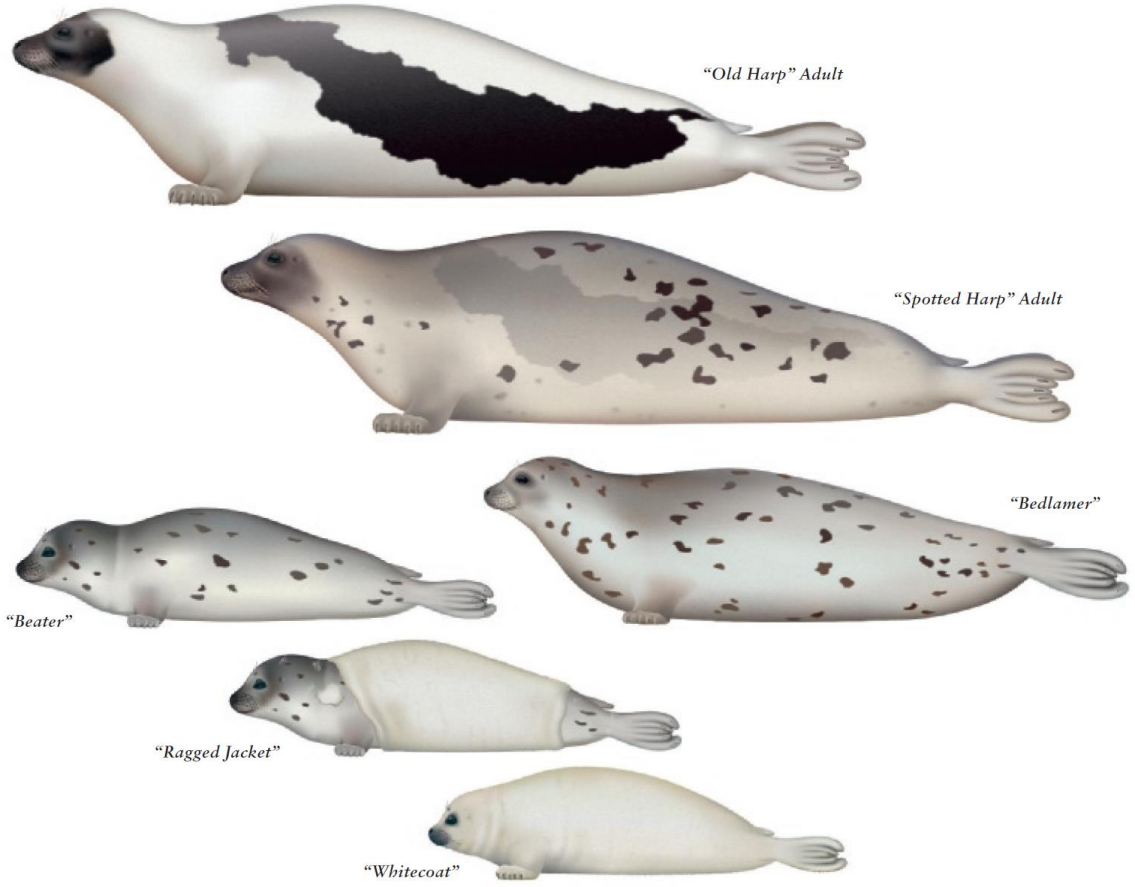

Fig. 5: *Illustrations of (A) a hooded Seal (Cystophora cristata) adult female, male and pup and (B) a harp seal (Pagophilus groenlandicus) adult, juvenile and pup at different life stages. Reprinted from Jefferson et al. (2015), with permission from Elsevier.*

5.7.2 Terrestrial mammals

In this thesis, ferrets (*Mustela putorius furo*) and house mice (*Mus musculus*) were used to compare the hooded seal and harp seal to terrestrial mammals. The closest relatives of pinnipeds are arctoid carnivores, which include procyonids (raccoons and relatives), mustelids (weasels and relatives), and ursids (bears), but which group has the closest affiliation to pinnipeds is still disputed (Fig. 6, Berta et al. 2015). Therefore, a mustelid like the ferret is an appropriate choice as terrestrial relative, while the mouse is more distantly related to pinnipeds.

The ferret is most likely domesticated from the wild European polecat (*Mustela putorius*) for hunting purposes (Davison et al. 1999). Their pelage may display the typical dark masked sable coloration of their wild polecat ancestors (Fig. 7A, Davison et al. 1999). Ferrets are on average 45 cm long with a typical slender mustelid body shape (Mitchell and Tully 2006; Wolf 2006). Ferrets exhibit sexual dimorphism with males (1.4-1.5 kg) weighing considerably more than females (0.8-0.9 kg) (Shump and Shump 1978). Sexual maturity is reached at approximately 8 to 12 months of age (Lindeberg 2008). After a mean gestation period of 41 days, females give birth to eight kits on average (Lindeberg 2008). The kits are weaned after six to eight weeks and become independent at ten weeks (Fisher 2006). As obligate carnivores, their wild ancestors naturally feed on whole small prey such as lagomorphs, rodents, amphibians and birds (Sainsbury et al. 2020). Activity may be synchronized to prey species, but is mostly nocturnal in the polecat and crepuscular in the ferret (Lode 1995; Fisher 2006). Mustelids may possess considerably high basal metabolic rates compared to other mammals of similar size (Casey and Casey 1979; Worthen and Kilgore 1981; Korhonen et al. 1983). However, contradictory results have been obtained as well (Brown and Lasiewski 1972; Harrington et al. 2003). The average life span of a ferret is 5 to 8 years (Mitchell and Tully 2006; Wolf 2006).

Ferrets have a relatively large brain compared to rodents (Herberstein et al. 2022). Cerebral structure and development such as white to gray matter ratio (Barnette et al. 2009), hippocampal location (Schwerin et al. 2017) and cortical folds (gyri) (Gilardi and Kalebic 2021) are similar to the human brain. However, cortical folding (gyrification) occurs postnatally, allowing for observations of neurodevelopment (Sawada and Watanabe 2012; Shinmyo et al. 2022; Barnette et al. 2009). Morphology and gene expression of ferret neurons and astrocytes also more closely resemble human features than do those of rodents (Long et al. 2020; Ellis et al. 2019; Roboon et al. 2022). Because of these characteristics the ferret is frequently used to study neuropathologies such as hypoxic-ischaemic brain injury (Empie et al. 2015; Schwerin et al. 2017; Wood et al. 2018; Wood et al. 2019; Wood et al. 2022; Corry et al. 2021).

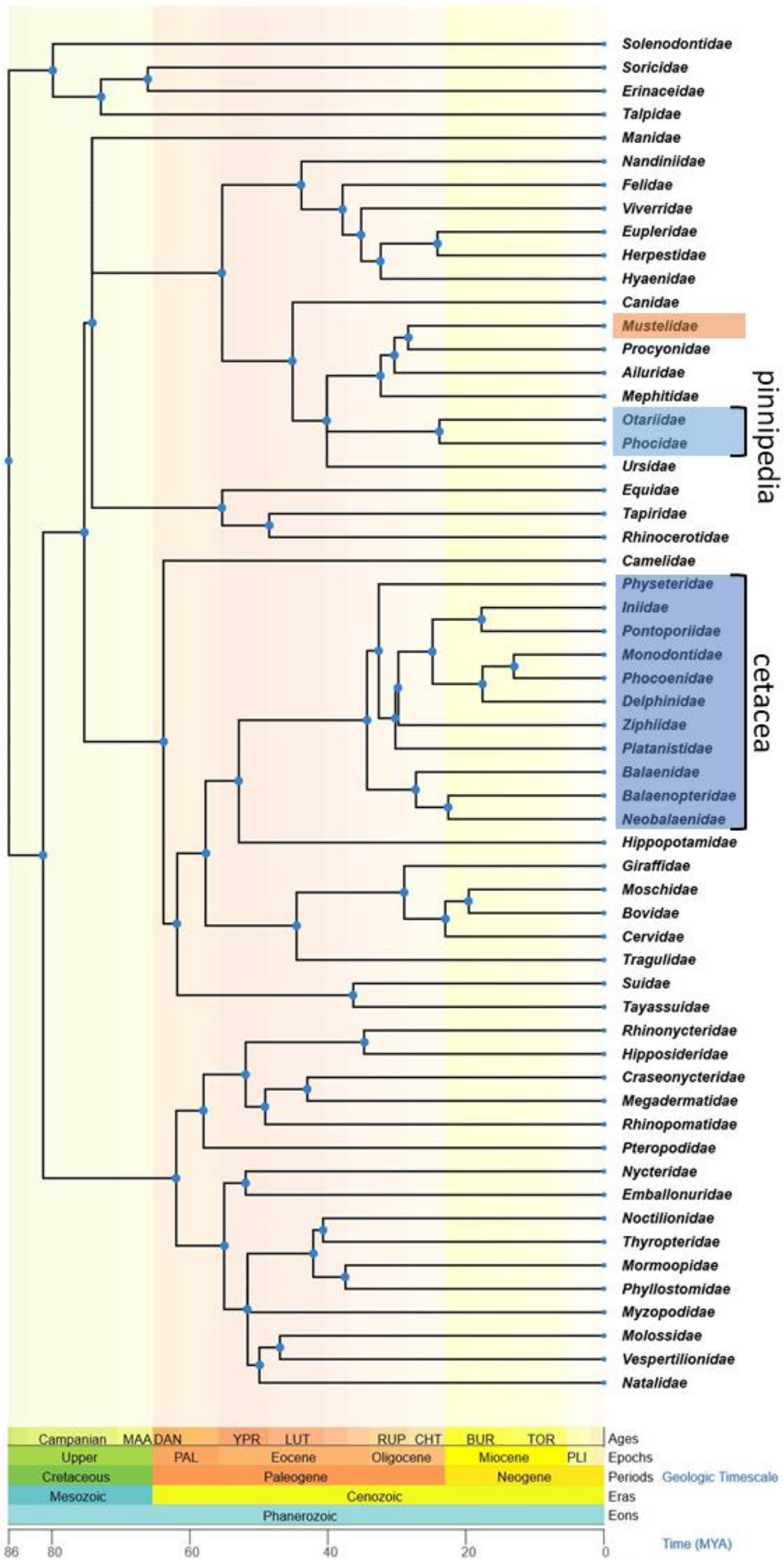

Fig. 6: *Phylogenetic tree of the Laurasiatheria superorder down to the family level with geologic timescale in millions of years (MYA). Marine mammals of the pinniped (seals, walrus) and cetacean (whales) species, as well as the terrestrial mustelid (weasels and relatives) relatives are shaded. Generated on www.timetree.org (Kumar et al. 2017)*

The house mouse is a wild rodent, originating from agricultural areas, but today largely associates with human habitation (Brown 1953). They vary in color from light brown (Fig. 7B) to black such as the laboratory mouse C57BL/6 ('black 6') strain, examined in this project (Mitchell and Tully 2006; Tully 2006; Zurita et al. 2011; Song and Hwang 2017). House mice are 8-10 cm long with a similarly long almost hairless tail and weigh 20-35 g as adults (King 1982; Eisen and Legates 1966; Berry and Jakobson 1975). House mice are omnivores and opportunistically feed on a wide variety of resources (Badan 1986; Le Roux et al. 2002). The gestation period is about 19 days long with litter sizes of about 6 to 8 young (Brown 1953; King 1982). The pups are weaned after approximately 20 days (Brown 1953). Sexual maturity is reached at about six weeks in males and at about eight weeks in age in females (Carlitz et al. 2019). House mice can usually live up to two to three years, but lifespan may be increased in genetically modified animals (Ladiges et al. 2009; Briga and Verhulst 2015).

The rodent brain exhibits some structural and functional differences to the human brain. For instance, it is lissencephalic with a low volume of white matter (Schwerin et al. 2017). The hippocampus is located, in contrast to the human brain, in a superior position making it more susceptible to brain injury (Schwerin et al. 2017). Cellular responses of neurons and astrocytes may also differ from that of humans (Zhang et al. 2016; Raju et al. 2018), but overall gene expression and synaptic connectivity appears to be similar in the human and mouse brain (Strand et al. 2007; Loomba et al. 2022; Sjöstedt et al. 2020). In spite of these differences, the mouse brain exhibits substantial homology to the human brain and is therefore commonly used to study neuropathological diseases (Johnson et al. 2015; Lodygensky et al. 2008; Loomba et al. 2022).

(A) **(B)**

Fig. 7: *Illustrations of (A) a ferret (Mustela putorius furo) and (B) a house mouse (Mus musculus). © Marcos Oliveira, natdrawings.blogspot.com*

5.8 Aims of this study

Because of their fascinating adaptation to an extreme environment, marine mammals are interesting study animals, which may provide valuable insights into mechanisms on how to prevent hypoxia and oxidative stress-induced tissue damage. Especially, the hooded seal brain demonstrates a profound tolerance to low oxygen conditions (Folkow et al. 2008; Ramirez et al. 2011; Geiseler et al. 2016). However, the molecular mechanisms involved in its intrinsic hypoxia tolerance remain elusive. Therefore, different molecular pathways were investigated in this thesis, describing how lipids and polar metabolites (Chapter I), the neuroprotective genes Clusterin (CLU) and S100B (Chapter II), and antioxidant gene expression and activity (Chapter III) are involved in the remarkable hypoxia tolerance of the hooded seal brain.

Lipids are essential building blocks of cellular membranes and exhibit diverse signaling functions (Piomelli et al. 2007). As components of the axon surrounding myelin sheath they are directly involved in efficient signal transduction (Hartline 2008). While the lipid content of various tissues of marine mammals has been extensively studied, the brain lipidome and its contribution to their hypoxia tolerance has not been the focus of studies so far. Therefore, an untargeted lipidomics analysis was performed and assays were conducted for specific polar metabolites of pinniped brain tissues in comparison to terrestrial relatives. Furthermore, lipids and polar metabolites of *in vitro* hypoxia- and oxidative stress-exposed brain tissues of hooded seals were analyzed (Chapter I).

Transcriptomics studies revealed genes differentially expressed in the hooded seal brain compared to ferrets (Fabrizius et al. 2016) and mice (Geßner et al. 2022). Particularly, the high expression of CLU and S100B is striking (Fabrizius et al. 2016; Geßner et al. 2022). Both have been associated with various neurodegenerative diseases such as Alzheimer's and Parkinson's disease in humans (Foster et al. 2019; Michetti et al. 2019). While it is being discussed if they have beneficial or deleterious functions in these diseases, their neuroprotective effects have been recently demonstrated in cell culture experiments (Geßner et al. 2020). Still, their exact molecular mechanisms remain controversial and ambiguous (Foster et al. 2019; Satapathy and Wilson 2021; Michetti et al. 2021). Here, the transcriptomes of S100B- and CLU-transfected neuronal cell lines were studied to elucidate their molecular mechanisms and targets, when exposed to different oxygen regimes (Chapter II).

An increased level of antioxidants appears to be a general feature of various tissues of marine mammals (Vázquez-Medina et al. 2012). However, the antioxidative capacity of the brain of marine mammals is underappreciated. A recent transcriptomics analysis in our lab found elevated levels of specific antioxidative genes in neurons of the hooded seal visual cortex compared to mice (Geßner et al. 2022). In this study, these findings were assessed and explored whether this characteristic feature is also true for other pinniped species and brain regions (Chapter III).

Statement of contributions

Chapter I

Martens, Gerrit A.; Geßner, Cornelia; Folkow, Lars P.; Creydt, Marina; Fischer, Markus; Burmester, Thorsten: The roles of brain lipids and polar metabolites in the hypoxia tolerance of deep-diving pinnipeds (In review at Journal of Experimental Biology)

- Contribution to study design, especially to the analysis pipeline
- Experiments: Extraction for mass spectrometry, substrate assays
- Statistical analysis: choice of suitable and informative analysis software to create an analysis pipeline, performance of all data analysis
- Interpretation of data
- Draft of the manuscript

Chapter II

Martens, Gerrit A.; Geßner, Cornelia; Osterhof, Carina; Hankeln, Thomas; Burmester, Thorsten (2022): Transcriptomes of Clusterin- and S100B-transfected neuronal cells elucidate protective mechanisms against hypoxia and oxidative stress in the hooded seal (*Cystophora cristata*) brain. In BMC Neurosci 23 (1), p. 59. DOI: 10.1186/s12868-022-00744-6.

- Organization and performance of experiments: cell culture experiments, cell viability assays, RNA preparation for sequencing, qPCR analyses
- Statistical analysis of all data (transcriptomic data, qPCR data and viability assays) and interpretation of data
- collaboration with the group of Prof. Thomas Hankeln (Johannes Gutenberg Universität, Mainz) to implement the IPA analyses
- Draft of the manuscript

Chapter III

Martens, Gerrit A.; Folkow, Lars P.; Burmester, Thorsten; Geßner, Cornelia (2022): Elevated antioxidant defence in the brain of deep-diving pinnipeds. In Front. Physiol. 13, Article 1064476. DOI: 10.3389/fphys.2022.1064476.

- Organization and performance of experiments: RNA extraction, cDNA synthesis, quantitative real time reverse transcription polymerase chain reaction (qPCR)
- Analysis of qPCR data
- Contribution to the manuscript; especially with respect to qPCR analyses and general contribution

Hamburg, 21.02.2023 — A. Fabrizius

Place, date — Andrej Fabrizius

6 Chapter I

The roles of brain lipids and polar metabolites in the hypoxia tolerance of deep-diving pinnipeds

Gerrit A. Martens[1]*, Cornelia Geßner[1], Lars P. Folkow[2], Marina Creydt[3], Markus Fischer[3], Thorsten Burmester[1]

[1] Institute of Animal Cell and Systems Biology, Biocenter Grindel, University of Hamburg, 20146 Hamburg, Germany

[2] Department of Arctic and Marine Biology, University of Tromsø – The Arctic University of Norway, Breivika, NO 9037 Tromsø, Norway

[3] Hamburg School of Food Science, Institute of Food Chemistry, University of Hamburg, 20146 Hamburg, Germany

*Corresponding author: Gerrit A. Martens

Email: gerrit.a.martens@gmail.com

Keywords: lipidome, hypoxia, oxidative stress, marine mammals, pinniped, brain

Summary statement

Efficient neurotransmission supported by increased sphingomyelin and reduced glutamate levels, as well as increased glycolytic capacity, may contribute to the hypoxia tolerance of the pinniped brain.

Published: 14 April 2023 in *Journal of Experimental Biology*

Martens, Gerrit A.; Geßner, Cornelia; Folkow, Lars P.; Creydt, Marina; Fischer, Markus; Burmester, Thorsten (2023): The roles of brain lipids and polar metabolites in the hypoxia tolerance of deep-diving pinnipeds. In *Journal of Experimental Biology*, Article jeb.245355. DOI: 10.1242/jeb.245355.

Abstract

Lipids make up more than half of the human brain's dry weight, yet the composition and function of the brain lipidome is not well characterized. Lipids not only provide the structural basis of cell membranes, but also take part in a wide variety of biochemical processes. In neurodegenerative diseases, lipids can facilitate neuroprotection and serve as diagnostic biomarkers. The study of organisms adapted to extreme environments may prove particularly valuable in understanding mechanisms that protect against stressful conditions and prevent neurodegeneration. The brain of the hooded seal (*Cystophora cristata*) exhibits a remarkable tolerance to low tissue oxygen levels (hypoxia). While neurons of most terrestrial mammals suffer irreversible damage after only short periods of hypoxia, *in vitro* experiments show that neurons of the hooded seal display prolonged functional integrity even in severe hypoxia. How the brain lipidome may contribute to the hypoxia tolerance of marine mammals has been poorly studied. We performed an untargeted lipidomics analysis, which revealed that lipid species are significantly modulated in marine mammals compared with non-diving mammals. Increased levels of sphingomyelin species may have important implications for efficient signal transduction in the seal brain. Substrate assays also revealed elevated normoxic tissue levels of glucose and lactate, which suggests an enhanced glycolytic capacity. Additionally, concentrations of the neurotransmitters glutamate and glutamine were decreased, which may indicate reduced excitatory synaptic signaling in marine mammals. Analysis of hypoxia-exposed brain tissue suggests that these represent constitutive mechanisms rather than an induced response towards hypoxic conditions.

Introduction

Lipids account for more than half of the dry weight of the human brain. However, their significance in cell metabolism has been underestimated in the past, as they have been dismissed as fixed building blocks of cell membranes and energy reserves (Lehninger 1981; Fitzner et al. 2020). Recently, more and more studies show that lipids function as signaling molecules in the human brain, as neurotransmitters and growth factors (Piomelli et al. 2007). Lipidomics studies aim to describe the complete lipid profile (lipidome) in a cell, tissue or even whole organism. Advances in experimental techniques, such as mass spectrometry, allow the comprehensive analysis of lipid species. Nevertheless, the composition and function of the brain lipidome is not well characterized in any species (Fitzner et al. 2020). The main lipids detected in the human brain include glycerophospholipids, sphingolipids and cholesterol (O'Brien and Sampson 1965). Reduced brain lipid content has been found in neurodegenerative diseases such as Alzheimer's disease, and lipids are therefore increasingly used as diagnostic biomarkers and drug targets (Buccellato et al. 2021; Castellanos et al. 2021). Lipidomics has further been suggested as a tool to study the evolution of marine mammals as well as to monitor

their health status (Rey et al. 2022). For this purpose, two independent studies have linked the blubber and plasma lipid profiles of beluga whales (*Delphinapterus leucas*) with their physiology and health state, such as inflammatory processes (Bernier-Graveline et al. 2021; Tang et al. 2018). Furthermore, lipids such as neuroprotectin D1 have been shown to reduce inflammation and apoptosis in human neuronal glial cells (Zhao et al. 2011). Studying organisms adapted to extreme environments may shed light on mechanisms that protect them from specific stress conditions that might otherwise cause neurodegeneration, and which could be of relevance in a broader context. Hooded seals (*Cystophora cristata*) and harp seals (*Pagophilus groenlandicus*) spend most of their time at sea, where they perform occasional long dives to exploit underwater food resources in shallow to deep waters. The hooded seal routinely dives to relatively deep waters ranging from 100 to 600 m for a duration of 5 to 15 min, but may dive deeper than 1 km and for durations over 1 h (Folkow and Blix 1999; Andersen et al. 2013; Vacquie-Garcia et al. 2017). The harp seal usually dives to shallower depths of 50-100 m, lasting 5 to 15 min, but dives beyond 500 m depth have also been recorded (Folkow et al. 2004). Physiological adaptations, such as elevated oxygen stores (hemoglobin, myoglobin) and a dramatic re-distribution of the blood supply involving profound peripheral vasoconstriction and bradycardia, have evolved to enable this diving lifestyle (Scholander 1940; Ponganis 2011; Blix 2018; Ramirez et al. 2007). However, during repetitive diving bouts arterial oxygen partial pressure may drop dramatically to levels that could cause neuronal damages in humans (Lutz 2002), as has been demonstrated in some other seal species (Meir et al. 2009; Qvist et al. 1986). Neurons from the hooded seal have been shown to display intrinsic tolerance properties to low oxygen conditions (hypoxia) that cannot be explained by the global physiological adaptations mentioned above. Thus, isolated hooded seal brain slices maintained both membrane potential and functional integrity (synaptic transmission) during and after exposure to severe hypoxia that resulted in loss of functional integrity in non-diving species (Folkow et al. 2008; Ramirez et al. 2011; Geiseler et al. 2016). As major components of membranes, specific neuronal lipids of diving mammals could contribute to the observed high hypoxia tolerance.

Changes in lipid structure, composition and abundance have contributed to the adaptation of marine mammals to an aquatic environment (see e.g., Strandberg et al. 2008; Liwanag et al. 2012). Divergent evolution of lipid metabolism in cetacean species is evident in positive selection, lineage-specific patterns of amino acid substitutions and functional domains in genes associated with lipid digestion, lipid storage and energy-producing pathways (Endo et al. 2018). In the visual cortex of hooded seals, two genes involved in lipid metabolism (*gdpd2*, *psap*) were among the most highly expressed genes when compared with the expression profile of a carnivoran relative, the ferret (Fabrizius et al. 2016). A genome analysis of the Weddell seal (*Leptonychotes weddellii*) and the walrus (*Odobenus rosmarus*), revealed that genes related to lipid metabolism are enriched in regions of accelerated divergence in both these pinnipeds compared to 57 other placental mammals, which strongly suggests an important

role of certain lipids in their adaptation to life in the marine environment (Noh et al. 2022). Remarkable lipid transport capabilities have been determined in the serum of the Weddell seal as evidenced by high levels of circulating cholesterol in a high-density lipoprotein (HDL)-like particle (Noh et al. 2022). Kasamatsu et al. (2009) demonstrated that serum cholesterol levels were elevated in bottlenose dolphins (*Tursiops truncatus*) and spotted seals (*Phoca largha*) compared to aquatic (West Indian manatees (*Trichechus manatus*)) and terrestrial relatives (cows and dogs). Total cholesterol for marine mammals may be as high as 393 mg/dl in adult male northern elephant seals (*Mirounga angustirostris*), but decreases to 266 mg/dl after a 3-month fasting period during the breeding season (Tift et al. 2011), while normal total cholesterol level in man (*Homo sapiens*) is 200 mg/dl (Goodman 1988). Interestingly, levels of antioxidative HDL were maintained during the breeding fast, which may prevent oxidative stress associated damage (Tift et al. 2011). Similar serum cholesterol values have been reported for other cetacean (Venn-Watson et al. 2008; Nabi et al. 2019; Kasamatsu et al. 2012; Lauderdale et al. 2021; Mello et al. 2021) and pinniped species (Kohyama and Inoshima 2017; Mazzaro et al. 2003). However, cholesterol levels vary according to season and age in cetacean species (Norman et al. 2013; Nollens et al. 2019; Nollens et al. 2020; Tsai et al. 2016) and increase in response to physical stress, as shown in killer whales (*Orcinus orca*) (Steinman et al. 2020). Hence, tightly regulated lipid mobilization may be necessary for pinniped lifestyle, e.g., during extended fasting periods during development, molting, breeding and lactation (Nordøy et al. 1993; Fowler et al. 2018).

In pinniped species, the fatty acid composition of plasma, milk, blubber, liver and muscle has been studied (Dannenberger et al. 2020; Simond et al. 2022; Watson et al. 2021), but data on the lipid composition of the pinniped brain and its potential involvement in hypoxia tolerance is not available. Data for cetacean species is more extensive, in which the lipidomes of plasma (Tang et al. 2018; Monteiro et al. 2021b), heart (Monteiro et al. 2021a), liver (Simond et al. 2022) and blubber (Bories et al. 2021; Bernier-Graveline et al. 2021; Ruiz-Hernández et al. 2022; Simond et al. 2020) have already been analyzed. Furthermore, Glandon et al. (2021) studied the lipid profile of neural tissue (brain, spinal cord, and spinal nerves) of stranded cetaceans in comparison to non-diving species (pigs, sheep). Lipid content, lipid class composition, and fatty acid signature were found to be similar across species, which may reflect a consistent functional role of lipids in the neural tissues of mammals (Glandon et al. 2021). However, specific fatty acids were not comprehensively analyzed because of sample size constraints and limited availability of tissue.

Recently, the lipid composition of membranes has been suggested to facilitate metabolic suppression in hypoxia-tolerant species by regulating activity of proteins important for ion flux (Farhat and Weber 2021). A reduction of energy expenditure will have obvious beneficial consequences on conditions of low oxygen and energy supply, and is a well-known strategy to which several specialized species resort. For instance, activity of the plasma-membrane-localized sodium-potassium ATPase (Na^+/K^+-ATPase),

an ATP-dependent ion pump, can account for 20-70 % of the oxygen expenditure of mammalian cells (Lee et al. 2020). Consequently, it has been demonstrated that hypoxia-tolerant species such as crucian carp (*Carassius carassius*) and its close relative, the goldfish (*Carassius auratus*), the naked mole rat (*Heterocephalus glaber*) and the pond slider turtle (*Trachemys scripta*) downregulate brain Na^+/K^+-ATPase in response to hypoxic conditions (Hylland et al. 1997; Farhat et al. 2021b; Farhat et al. 2021a), possibly by altering the abundance of specific fatty acids and cholesterol (Farhat et al. 2019; Farhat et al. 2020; Farhat and Weber 2021). Interestingly, genes involved in ion transport were found to be downregulated in fresh visual cortex slices of the hooded seal that had been exposed to hypoxia and reoxygenation *in vitro* (Hoff et al. 2017). Thus, in response to these stress conditions the hooded seal brain may also decrease neuronal processes to reduce energy expenditure (see e.g., Ramirez et al. 2007). Additionally, membrane lipid composition may influence glycolytic activity and mitochondrial function, but the underlying mechanisms are not well understood (Farhat and Weber 2021).

To improve our understanding of potential lipid-linked adaptations of hypoxia-tolerant species, we performed an untargeted lipidomics study comparing the brain lipidome of two marine mammals, the hooded seal and the harp seal, to those of two non-diving species, the ferret (*Mustela putorius furo*) and the house mouse (*Mus musculus*). Furthermore, we compared the lipidome of hooded seal brain tissue that had been incubated under artificial normoxic and hypoxic conditions as well as being reoxygenated after a hypoxic period, which provokes oxidative stress. Additionally, we determined substrate levels for energy metabolism and neurotransmission in brain tissue samples.

Materials and methods

Animals and Sampling

Hooded seals (*Cystophora cristata*) and harp seals (*Pagophilus groenlandicus*) were captured for other scientific purposes in March 2017 (n=3 hooded seal juveniles of both sexes), 2018 (n=1 weaned hooded seal pup, n=2 adult hooded seal females, n=3 adult harp seal females), 2019 (n=4 adult hooded seal females, n=3 adult harp seal females, n=6 hooded seal juveniles of both sexes) and 2021 (n=4 adult hooded seal females) in the pack ice of the Greenland Sea under permits from relevant Norwegian and Greenland authorities. The hooded seal pups caught in 2017 and 2019 were brought to UiT – The Arctic University of Norway, where they were maintained in a certified research animal facility in connection with other studies. At the termination of those experiments, the seals were euthanized (in 2019 and 2020, as juveniles, at age ~2 and ~1 year, respectively) according to the following protocol: the seals were sedated by intramuscular injection of zolazepam/tiletamine (Zoletil Forte Vet., Virbac S.A., France; 1.5–2.0 mg per kg of body mass), then anaesthetized using an endotracheal tube to ventilate lungs with 2–3% isoflurane (Forene, Abbott, Germany) in air and, when fully anaesthetized, they were euthanized by exsanguination via the carotid arteries. The adult hooded and harp seals were euthanized immediately following capture with a hoop net, by sedation with intramuscular injection of zolazepam/tiletamine (1.5–2.0 mg per kg of body mass), followed by catheterization of the extradural intravertebral vein and i.v. injection of an overdose of pentobarbital (Euthasol vet., Le Vet B.V., Netherlands; 30 mg per kg of body mass). The animal study was reviewed and approved by the Norwegian Animal Welfare Act and with permits from the National Animal Research Authority of Norway and Norwegian Food Safety Authority (permits no. 7247, 19305 and 22751). Samples of adult female ferrets (n=4) were received from the animal facilities of the University Medical Center Hamburg-Eppendorf (UKE) Germany. The ferrets were killed at the UKE in deep anesthesia (Ketamin/Domitor) with an overdose of pentobarbital and brain tissues were sampled by the facility's veterinarians. Adult female mice (C57BL/6, n=9) were a gift by Prof. Dr. Christian Lohr (University of Hamburg, Hamburg, Germany) and were anaesthetized with 1 ml isoflurane (Forene, Abbott, Germany) in a chamber and decapitated. All animals were handled according to the EU Directive 63 (Directive 2010/63/EU). For lipidomics of tissue exposed to hypoxia and reoxygenation, fresh visual cortex and hippocampus samples from hooded seal pups caught in 2019, as well as fresh visual cortex samples from hooded seal adults caught in 2021, were minced and placed in cooled (4 °C) artificial cerebrospinal fluid (aCSF; 128 mM NaCl, 3 mM KCl, 1.5 mM $CaCl_2$, 1 mM $MgCl_2$, 24 mM $NaHCO_3$, 0.5 mM NaH_2PO_4, 20 mM sucrose, 10 mM D-glucose) saturated with 95% O_2−5% CO_2 (normoxia) and further processed *in vitro*, as described below. For lipidomics and metabolite assays of normoxic tissue, fresh tissue of the visual cortex of all animals was frozen in liquid nitrogen and transferred to -80 °C to be stored for subsequent analysis. An overview of samples used in each study is provided in Table 1.1.

Table 1.1: Sample overview for each study. *Included animals and amount of samples (#) for each study are provided.*

Study	Animals	#
LC-MS lipidomics comparison of marine vs. terrestrial mammals	Harp seal adults	6
	Hooded seal juveniles	4
	Hooded seal adults	6
	Mouse adults	9
	Ferret adults	4
LC-MS lipidomics comparison of hypoxia-treated hooded seal brain samples	a. Hooded seal juveniles	6
	b. Hooded seal adults	4
Substrate comparison of marine vs. terrestrial mammals	Harp seal adults	3
	Hooded seal adults	4
	Mouse adults	4
Substrate comparison of hypoxia-treated hooded seal brain samples	Hooded seal juveniles	5
	Hooded seal adults	4

Hypoxia and reoxygenation treatment of brain samples

Samples in oxygenated (95% O_2–5% CO_2) aCSF were adjusted to 34 ± 0.5°C for at least 20 min. Hypoxia was introduced and maintained for 60 min after switching the gas supply to 95% N_2 and 5% CO_2, to mimic the conditions in the brain during a dive. To simulate conditions when the seal surfaces after a dive, samples were exposed to hypoxia followed by return to normoxia (95% O_2–5% CO_2) for 20 min. After treatment, hypoxia and reoxygenation samples were immediately frozen in liquid nitrogen. Samples that were kept under normoxia in aCSF for 80 min were used as controls. All samples were transferred to and stored at -80°C until later use.

Chemicals for mass spectrometry

Acetonitrile, isopropanol, methanol (all LC–MS grade), and chloroform (HPLC-grade, ammonium formate (≥95% puriss) as well as sodium hydroxide (≥99%) were purchased from Carl Roth GmbH (Karlsruhe, Germany). Formic acid (99% p.a.) and acetic acid (99% p.a.) were provided by Acros Organics (Geel, Belgium). Hexakis(1H,1H,2H-perfluoroethoxy)phosphazene was supplied by Santa Cruz Biotechnology (Dallas, TX, U.S.). Water was obtained by a Merck Millipore water purification system with a resistance of 18 MΩ (Darmstadt, Germany).

Extraction procedure for mass spectrometry

Extraction of metabolites and further analysis was performed at Hamburg School of Food Science, University of Hamburg. The extraction protocol was performed slightly modified according to the method of Bligh and Dyer (Bligh and Dyer 1959; Creydt et al. 2018). Approximately 20 mg sample was weighed into a 2.0 ml reaction tube (Eppendorf, Hamburg, Germany). Two steel balls (3.6 mm), 100 µl chloroform and 200 µl methanol were added to the sample. The mixture was homogenized in a ball

mill (1 min, 3.1 m/s Bead Ruptor 24, Omni International IM, GA, USA)). Next, 200 µl water and 100 µl chloroform were added and again processed in the ball mill (1 min, 3.1 m/s). The homogenized sample was then centrifuged (20 min, 16.000xg, 5 °C, Sigma 3-16PK, Sigma, Osterode, Germany). A quality control sample (QC) was prepared by transferring 30 µl of each sample into a new vial. The organic chloroform phase was directly used for measurement.

Mass spectrometric data acquisition

High-performance liquid chromatography coupled with electrospray ionization-quadrupole-time of flight-mass spectrometry (LC-ESI-qTOF-MS/MS) was used for metabolite identification as described previously (LC–ESI–qTOF–MS/(MS)) (Creydt et al. 2018). In brief, the LC experiments were carried out using a RP C-18 column (150 × 2.1 mm, 1.7 µm, Phenomenex, Aschaffenburg, Germany) together with a Dionex Ultimate 3000 UPLC system (Dionex, Idstein, Germany). The mobile phase consisted of water (solvent A) and mixture of acetonitrile and isopropanol (1:3, v/v) (solvent B). Both eluents contained 10 mMol/L ammonium formate for measurements in positive ionization mode and 0.02% acetic acid for measurements in negative ionization mode. The column oven was set at 50°C and the flow rate was 300 µL/min. The gradient elution was as follows: 55% B (0-2 minutes); 55% to 75% B (2-4 minutes); 75% to 100% B (4-18 minutes); 100% B (18-23 minutes), 55% B (23-24 minutes); 55% B (24-27 minutes). For measurements in positive ionization mode, 2 µL of the sample extracts were injected, whereas for analyses in negative ionization mode 8 µL were used. The samples were analyzed in randomized order, with one blank sample and one QC sample being measured after each of the five animal samples. The autosampler in which the samples were stored during the measurement was set to 4° C.

The LC system was connected to an ESI–qTOF–MS (maXis 3G, Bruker Daltonics, Bremen, Germany). The data were recorded at 1 Hz over a mass range of *m/z* 80-1100. Further parameters were: end plate offset -500 V, capillary -4500 V (positive mode) / +4500 V (negative mode), nebulizer pressure 4.0 bar, dry gas 9.0 L/min at 200 °C dry temperature. At the beginning of the measurements, the mass spectrometer was calibrated either using sodium formate clusters or sodium acetate clusters, depending on which additive was used in the solvent. At the end of each sample run, a further calibration was carried out using the cluster solutions. In the MS/MS measurements for the identification of the substances, hexakis(1H,1H,2H-perfluoroethoxy)phosphazene was used as lock mass during the entire measurement period. The recording of MS/MS spectra was carried out at 20, 40 and 60 eV.

Metabolomics Data Analysis

Acquired experimental mass spectra were recalibrated with Bruker Data Analysis Software 4.2 (Bruker Daltonics, Bremen, Germany) using the mentioned sodium formate clusters for *m/z* ratios acquired in

positive ionization mode and the sodium acetate clusters for *m/z* ratios acquired in negative ionization mode. Then, data were exported to netCDF file format. Data preprocessing was performed with R package xcms 3.6.2 (xcmsonline.scripps.edu) (Smith et al. 2006) in R version 3.6.3 (www.r-project.org) (R Core Team 2021). Parameters for processing were optimized based on existing tools and scripts (Libiseller et al. 2015; Manier et al. 2019). After reading in recalibrated netCDF files, features were detected with findChromPeaks function and CentWaveParam (peakwidth = c(10, 40), ppm = 20, snthresh = 10, mzdiff = 0.015, prefilter = c(0, 0), noise = 0)). Retention time was corrected with adjustRtime function and ObiwarpParam (binSize = 1.0). Feature correspondence was achieved with groupChromPeaks function and PeakDensityParam (sampleGroups = xdata$sample_group, bw = 1) as well as missing value imputation with fillChromPeaks function with FillChromPeaksParam (fixedRt = ChromPeakwidth/2)). ChromPeakwidth was calculated as average peak width of detected chromatographic peaks. Adducts and isotopes of features were annotated using R package CAMERA 1.40.0 (Kuhl et al. 2012). Features in the QC samples with a relative standard deviation over 30%, blank intensity contribution over 10% and QC sample count below 60% were removed before further statistical analysis.

Statistical analysis

Peak intensity tables with two sample groups (marine/terrestrial) were uploaded to MetaboAnalyst 4.0 software (www.metaboanalyst.ca) (Xia et al. 2009; Chong et al. 2019) and intensities were subjected to sum normalization and log-transformation. For univariate analysis of features, fold change calculation and t-test were performed. Features were considered significant with a false discovery rate (FDR) below $p = 0.05$. Furthermore, unsupervised multivariate analysis (PCA) and supervised multivariate analysis (PLS-DA) were calculated. Cross validation (CV) was executed with the 10-fold CV method to confirm PLS-DA models. Variable importance plot (VIP) scores of features in PLS-DA over 1 were used to further assess significant features.

Compound annotation

Significant features were annotated with MS/MS spectra using the *in silico* fragmentation tool metfRag 2.4.2 (msbi.ipb-halle.de/MetFrag). Chromatographic peaks were identified with the R package xcms 3.6.2 (Smith et al. 2006) as described above and isotopes and adducts of chromatographic peaks annotated with CAMERA 1.40.0 (Kuhl et al. 2012). If multiple MS/MS spectra per chromatographic peak were available, consensus spectra of MS/MS spectra were built with combineSpectra function (method = consensusSpectrum, mzd = 0.001, minProp = 0.8, intensityFun = median, mzFun = median). Consensus spectra and exact mass from CAMERA annotation were searched with R package metfRag 2.4.2 against LipidMaps database (Wolf et al. 2010). Search settings were: DatabaseSearchRelativeMassDeviation: 10.0, FragmentPeakMatchAbsoluteMassDeviation: 0.005,

FragmentPeakMatchRelativeMassDeviation: 10.0. Annotation reliability of non-polar candidate substances was additionally improved with LipidFrag software (Witting et al. 2017). A MetFrag as well as LipidFrag score of 1.0 represents a likely lipid identification. Example spectra of identified lipids are provided in the supplementary material (Fig. S1.1-3.6). After identification, lipid set enrichment analysis regarding lipid class, chain length and unsaturation was performed with lipidr package (Mohamed and Molendijk 2022). Briefly, samples were subjected to sum normalization and log-transformation in MetaboAnalyst 4.0 software (www.metaboanalyst.ca) as described previously. Differential analysis was then conducted with de_analysis function and enrichment determined with lsea function. A heatmap was generated with MetaboAnalyst 5.0 software (Pang et al. 2021) using the normalized data and feature autoscaling. Euclidean distance measure and Ward clustering method were used for hierarchical clustering of samples.

Substrate Assays

About 20 mg of frozen brain sample was rinsed with phosphate buffered saline, transferred into a cryo vial with 1.4 mm ceramic beads and homogenized in 50 mM tris(hydroxymethyl)aminomethane with 0.6 N HCl at an 8:1 ratio using a Fisherbrand™ Bead Mill 4 Homogenizer for 20 s at maximum speed (Thermo Fisher Scientific, Waltham, Massachusetts, U.S.). Samples were mixed with one eighth volume of 1M Tris-HCl, centrifuged (1500*g, 5 min) and supernatant used in Glucose-Glo™, Lactate-Glo™ and Glutamine/Glutamate-Glo™ Assays after manufacturer's instructions (Promega, Mannheim, Germany). Protein concentration of samples was determined by Bradford Assay using Roti®Quant solution (Carl Roth GmbH & Co. KG, Karlsruhe, Germany) and a bovine serum albumin standard curve (Carl Roth GmbH & Co. KG, Karlsruhe, Germany). Luminescence of substrate assays and absorption of Bradford Assay were measured with a DTX 880 Multimode Detector (Beckmann Coulter, Krefeld, Germany). Substrate concentration was normalized to total protein concentration and statistically analyzed with the compare_means function of the ggpubr package (Kassambara 2020) in R version 4.1.2 (www.r-project.org) (R Core Team 2021). Briefly, two sample t-tests were performed on the normally distributed data using one reference group (mouse or normoxia samples, respectively) and additionally adjusting p-values with the Benjamini-Hochberg method (FDR).

Results

Lipidomics of marine and terrestrial brain samples

Mass spectrometry data of hooded seals (*Cystophora cristata*), harp seals (*Pagophilus groenlandicus*), ferrets (*Mustela putorius furo*) and mice (*Mus musculus*) tissues from the visual cortex were collected. After splitting into marine and terrestrial mammals, PLS-DA demonstrated distinct lipidomic patterns for these groups (Fig. 1.1). The Q^2 value of the cross-validation of the measurements in the positive mode and in the negative mode were 0.98 and 0.97, respectively. Both values accordingly indicate large differences in the samples.

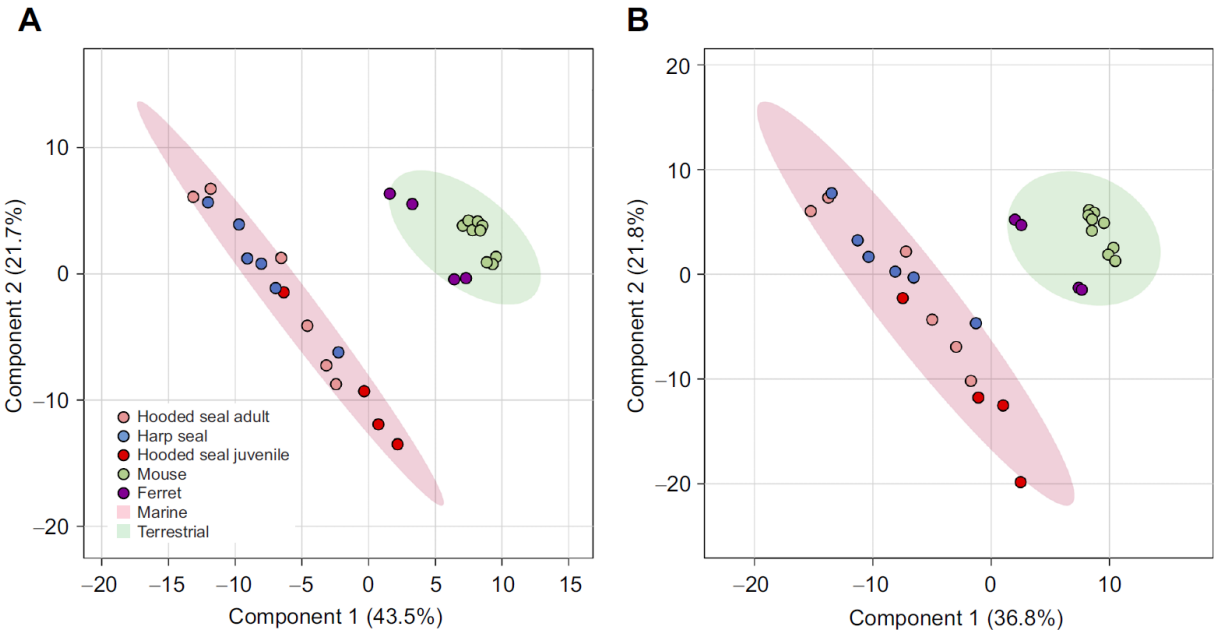

Fig. 1.1: Supervised multivariate analysis of the mass spectrometry analyses of marine mammals compared to terrestrial mammals. *Supervised multivariate analysis (PLS-DA) of high-performance liquid chromatography coupled with electrospray ionization-quadrupole-time of flight-mass spectrometry (LC-ESI-qTOF-MS/MS) performed in (A) positive ionization and (B) negative ionization mode. Marine mammals included hooded seal adults (n = 6), hooded seal juveniles (n = 4) and harp seals (n = 6) and terrestrial mammals included ferrets (n = 4) and mice (n = 9).*

Of 4072 features detected in positive ionization mode and 5720 features detected in negative ionization mode, 201 and 313 features were significantly different between marine and terrestrial mammals, respectively. After removal of low quality and isotope features, a total of 230 features (pos: 85; neg: 145) were selected for annotation by MS/MS spectra. Of 44 (pos: 29; neg: 15) annotated features (Table S1), 3 were duplicate annotations of separate features, resulting in 41 unique annotated metabolites.

The majority of annotated metabolites represented lipid classes from major components of biological membranes, such as phosphatidylcholines (PCs) with 23 features, phosphatidylethanolamines (PE) with 8 lipids and phosphatidylserines (PSs) with 3 features and phosphatidylinositols (PIs) with 2

annotated features (Table 1.2). Other classes included lipids involved in myelin sheath formation, such as sphingomyelin (SM) with 7 features and one signal probably representing a cerebroside (HexCer). While these single lipids demonstrated significant differences between marine and terrestrial mammals, fold change of whole lipid classes was not significant between groups (Fig. S1.7). Nevertheless, detected lipid classes appeared to be generally increased in the marine mammals (Fig. 1.2). SMs for example were on average 6 times higher (binary logarithm of fold change (log2FC) = 2.6) and the two PIs demonstrated an average 8-fold increase (log2FC = 3.0). The only detected HexCer was 9-fold (log2FC = 3.2) elevated, whereas the other lipid classes did not show a comparable increase (PC: log2FC = 2.0; PE: log2FC = 1.7; PS: log2FC = 1.0). Notably, 19 out of 23 PC species were significantly increased in marine mammals. Additionally, we detected a substantial amount of phospholipid plasmalogen species (PC-O and PE-O), in which fatty acids are linked to the phospholipid backbone by an alkyl or alkenyl ether instead of an ester bond. Of the 14 identified plasmalogen lipids, 12 demonstrated higher concentrations in marine mammals and an average 5-fold increase (log2FC = 2.4). However, in enrichment analyses with only the subset of plasmalogen species, no significant accumulation in the marine mammals could be determined (Fig. S1.8).

Both lipid unsaturation and chain length both influence membrane fluidity and rigidity. Adaptation of marine mammals to cold environments may have selected for lipids of shorter chain length and a higher amount of double bonds to maintain membrane fluidity. However, unsaturation of lipids (Fig. S1.9) and lipid chain length (Fig. S1.10) were not significantly different between marine and terrestrial mammals. We noted that a total chain unsaturation of 4 double bonds and a total chain length of 38 carbon atoms appeared to be decreased in seals compared with ferret and mice, whereas other unsaturation indices and chain lengths tended to be increased.

Table 1.2: Overview of annotated lipid classes. *Amount of identified significant detections (#) and functional descriptions are provided for each lipid class.*

	Lipid class	#	Function
Glycerophospholipids	Phosphatidylcholine (PC)	23	Major component of biological membranes, creating a planar lipid bilayer (van Meer et al. 2008)
	Phosphatidylethanolamine (PE)	8	Major component of biological membranes, mainly found in the inner (cytoplasmic) leaflet of the lipid bilayer; regulation of membrane curvature and thereby role in membrane budding, fission and fusion (van Meer et al. 2008)
	Phosphatidylinositol (PI)	2	Minor component on the cytosolic side of eukaryotic cell membranes, important roles in lipid signaling, cell signaling and membrane trafficking (Di Paolo and Camilli 2006)
	Phosphatidylserine (PS)	3	Localized exclusively in the cytoplasmic leaflet of biological membranes. Its exposure on the outer surface of a membrane acts as a signal for phagocytosis and consequently apoptosis (Schlegel and Williamson 2001)
Sphingolipids	Sphingomyelin (SM)	7	Part of animal cell membranes, especially in the insulating membranous myelin sheath that surrounds some nerve cell axons; involved in signal transduction (Schneider et al. 2019); hydrolyzes into ceramide (Kolesnick 1994)
	Neutral glycosphingolipids / cerebrosides (HexCer)	1	Important component of animal nerve cell membranes, regulating nerve myelin sheath formation or remyelination (Jurevics et al. 2001)

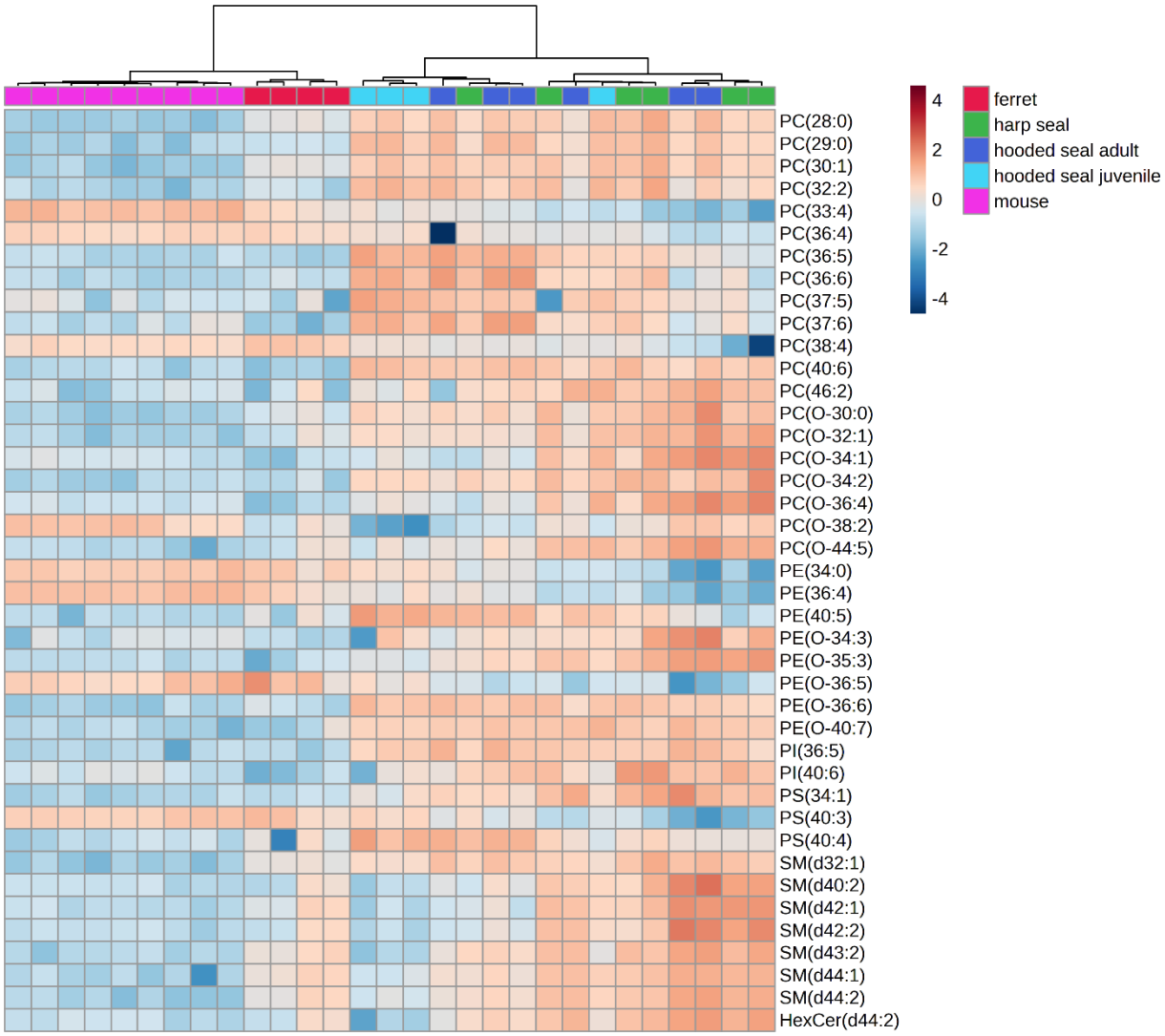

Fig. 1.2: Heatmap of identified significant lipid species with hierarchical clustering of samples. *Samples are categorized by species and age class. Lipid classes include PC: phosphatidylcholine; PE: phosphatidylethanolamine; PI: phospatidylinositol; PS: phosphatidylserine; SM: sphingomyelin; HexCer: cerebroside.*

Metabolite assays of marine and terrestrial mammals

Analysis of molecules from energy metabolism (glucose and lactate) and synaptic transmission (glutamate and glutamine) revealed substantial differences between hooded and harp seals on the one hand, and mice on the other hand (Fig. 1.3). Normalized glucose levels were significantly higher in the hooded seal cerebellum (FDR, $p < 0.01$) and visual cortex (FDR, $p < 0.05$), whereas they were only marginally higher in the harp seal cerebellum and visual cortex and hooded seal hippocampus, when compared with mice. Furthermore, concentration of lactate was significantly higher in the hooded seal (FDR, $p < 0.0001$) and harp seal hippocampus (FDR, $p < 0.05$), as well as in the hooded seal visual cortex (FDR, $p < 0.01$), as compared to mice. On the other hand, the levels of the neurotransmitters glutamine and glutamate were generally lower in seals compared to mice. Glutamate levels were significantly lower in the hooded seal cortex (FDR, $p < 0.001$) and glutamine levels were significantly lower in the

hooded seal cerebellum (FDR, $p < 0.001$), harp seal hippocampus (FDR, $p < 0.05$) and hooded seal visual cortex (FDR, $p < 0.001$). In this regard, it is important to remember that the metabolic/oxygenation state of the sampled animals and tissues sampled was not fully known, although the effects of handling the animals and samples can be predicted to some degree, as discussed in more detail in the Discussion section.

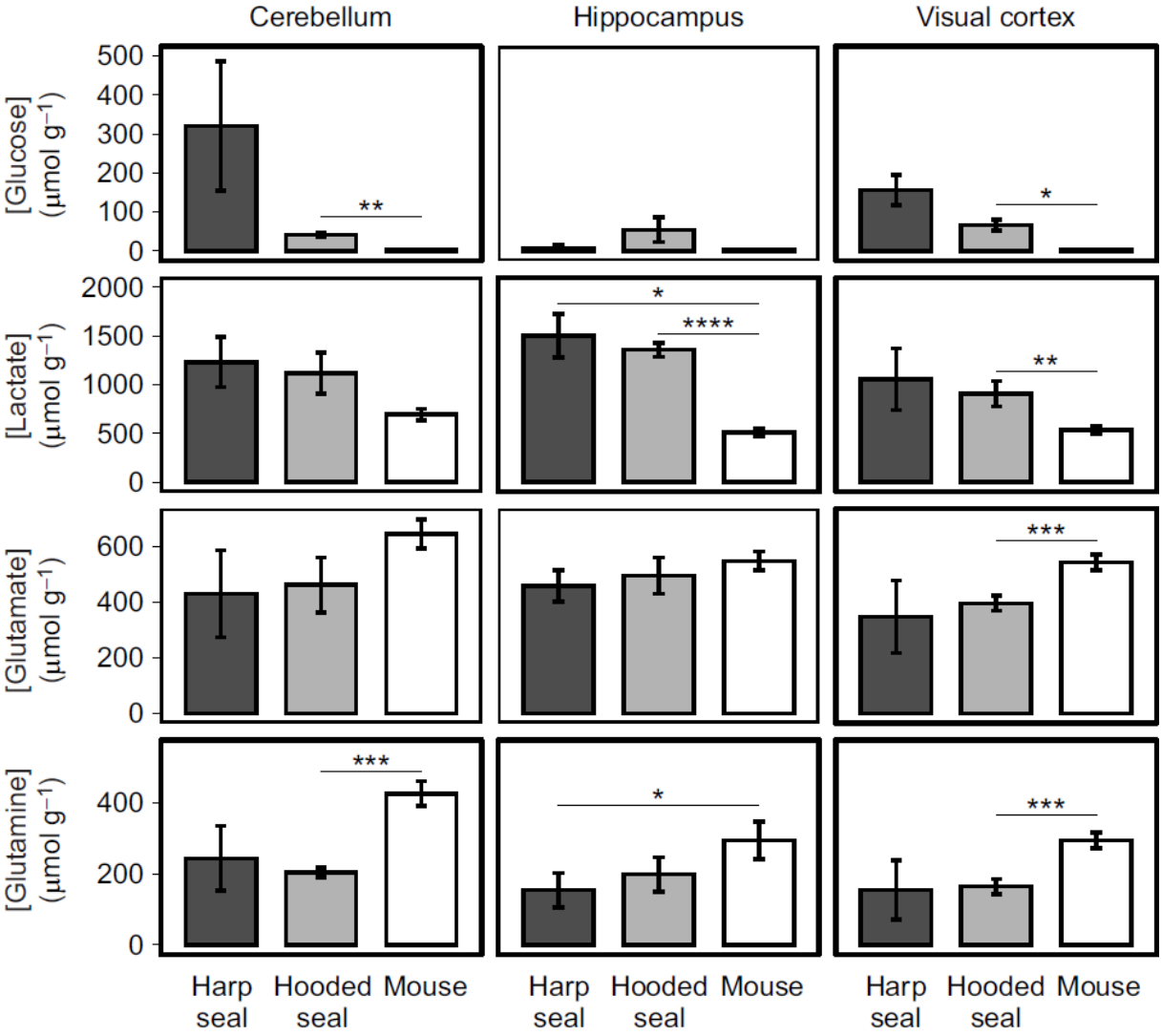

Fig. 1.3: Substrate assays of marine mammals compared to terrestrial mammals. *Substrate concentrations (mean ± s.d.) of glucose, lactate, glutamate and glutamine were normalized to total protein concentration in the harp seal (n = 3), hooded seal (n = 4) and mouse (n = 4) visual cortex, hippocampus and cerebellum, respectively. Statistical analysis was performed with two sample t-tests including Benjamini-Hochberg correction (FDR). *p < 0.05, **p < 0.01, ***p < 0.001, ****p < 0.0001.*

Lipidomics and metabolite assays of hypoxia- and reoxygenation-treated hooded seal brain samples

Fresh juvenile hooded seal visual cortices and hippocampi and adult hooded seal visual cortices were maintained *in vitro* at different oxygen regimes to emulate conditions of hypoxia and reoxygenation that hooded seals are frequently exposed to. Untargeted lipidomics analysis did not reveal significantly changed lipid levels for the different treatments. Cross validation of the PLS-DA analyses demonstrated poor predictive Q^2 values of -0.68 and 0.46, in the positive and negative mode, respectively, for the treated juvenile hooded seal brain tissue (Fig. 1.4A,B) and -0.04 and 0.12, in the positive and negative mode, respectively, for the treated adult hooded seal brain tissue (Fig. 1.4C,D). Group separation by lipid concentration therefore is inconclusive. Nevertheless, some significant differences in lactate, glutamate and glutamine concentrations were determined with substrate assays, while glucose levels were maintained across conditions and did not show significant differences between treatments (Fig. 1.5). Lactate levels were significantly lower in the visual cortex of juvenile hooded seals after reoxygenation compared with levels in normoxia (FDR, $p < 0.01$), while they were insignificantly lower after hypoxic treatment only. The same trend was found in the visual cortex of adult hooded seals, but differences were not significant. Concentration of glutamate was significantly lower in the hippocampus of juvenile hooded seals after reoxygenation (FDR, $p < 0.01$), but not after hypoxia compared to normoxia. Similarly, glutamate appears to be insignificantly lower in the visual cortex of juvenile and adult hooded seals after reoxygenation and to a lesser extent after hypoxia compared to normoxia. Glutamine levels decreased after hypoxia, but almost recovered to normoxic levels after reoxygenation. Significant differences compared to normoxia were therefore only found after hypoxic treatment of the visual cortex of juvenile (FDR, $p < 0.01$) and adult hooded seals (FDR, $p < 0.01$).

Samples that were subjected to *in vitro* incubation in aCSF under known oxygenation conditions, had a known metabolic history that is defined by the oxygenation conditions to which they were experimentally subjected (normoxia, hypoxia or hypoxia followed by reoxygenation). We here must assume that the 20 min pre-incubation of tissue in fully oxygenated aCSF was sufficient to 'reset' cells to a normoxic metabolic state, should their metabolic/oxygenation state have been disturbed because of the prior handling (animal capture procedure & metabolic effects of drugs).

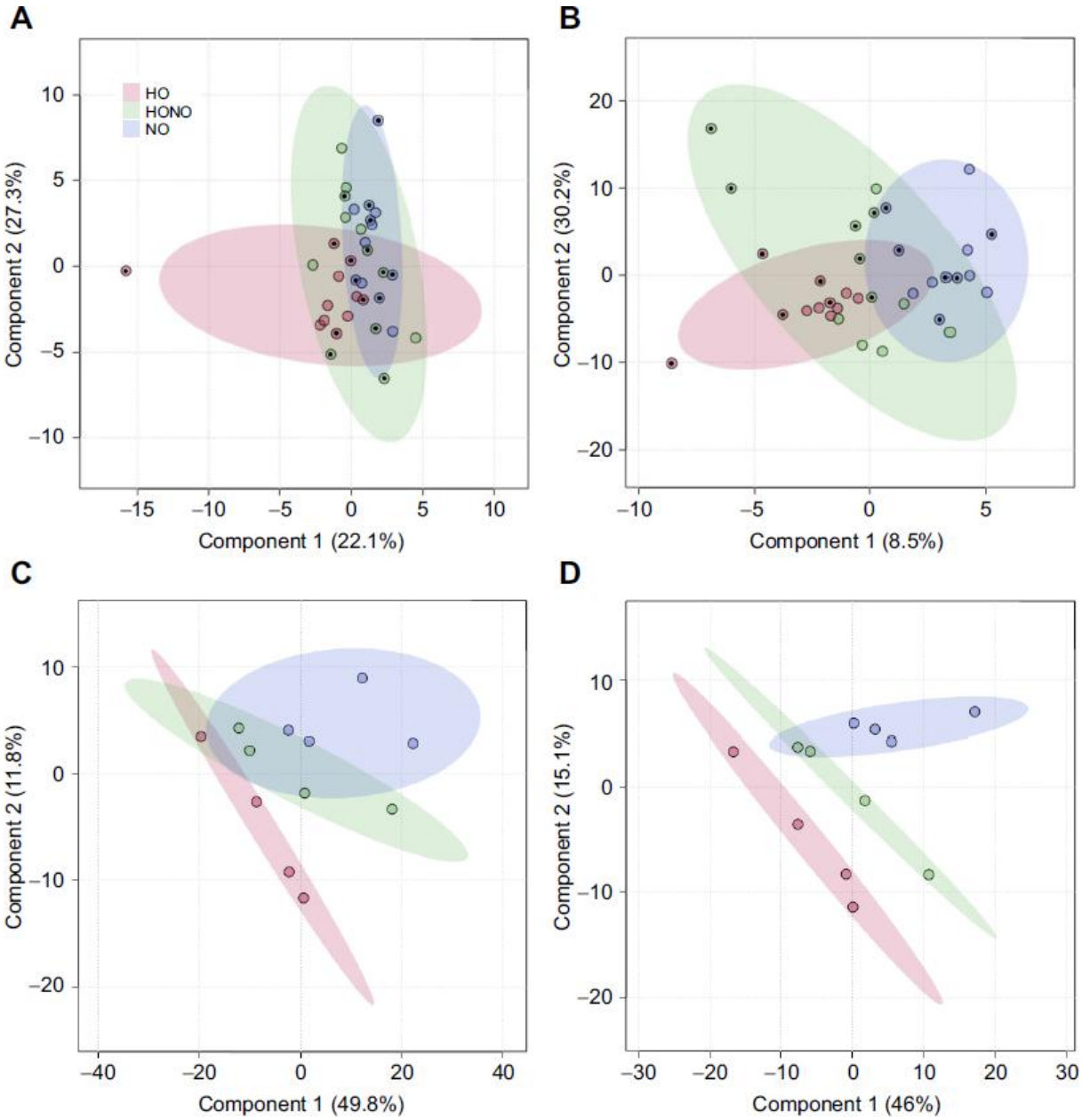

Fig. 1.4: Supervised multivariate analysis (PLS-DA) of the mass spectrometry (LC-ESI-qTOF-MS/(MS)) analyses of the hooded seal brain exposed to different oxygen regimes. *Juvenile hooded seal (n = 6) hippocampi and visual cortices (visual cortex samples marked with black dots) were exposed to normoxia (NO), hypoxia (HO) and reoxygenation (HONO) and analysed in (A) positive ionization and (B) negative ionization mode. Similarly, adult hooded seal (n = 4) visual cortices were exposed to normoxia (NO), hypoxia (HO) and reoxygenation (HONO) and analysed in (C) positive ionization and (D) negative ionization mode.*

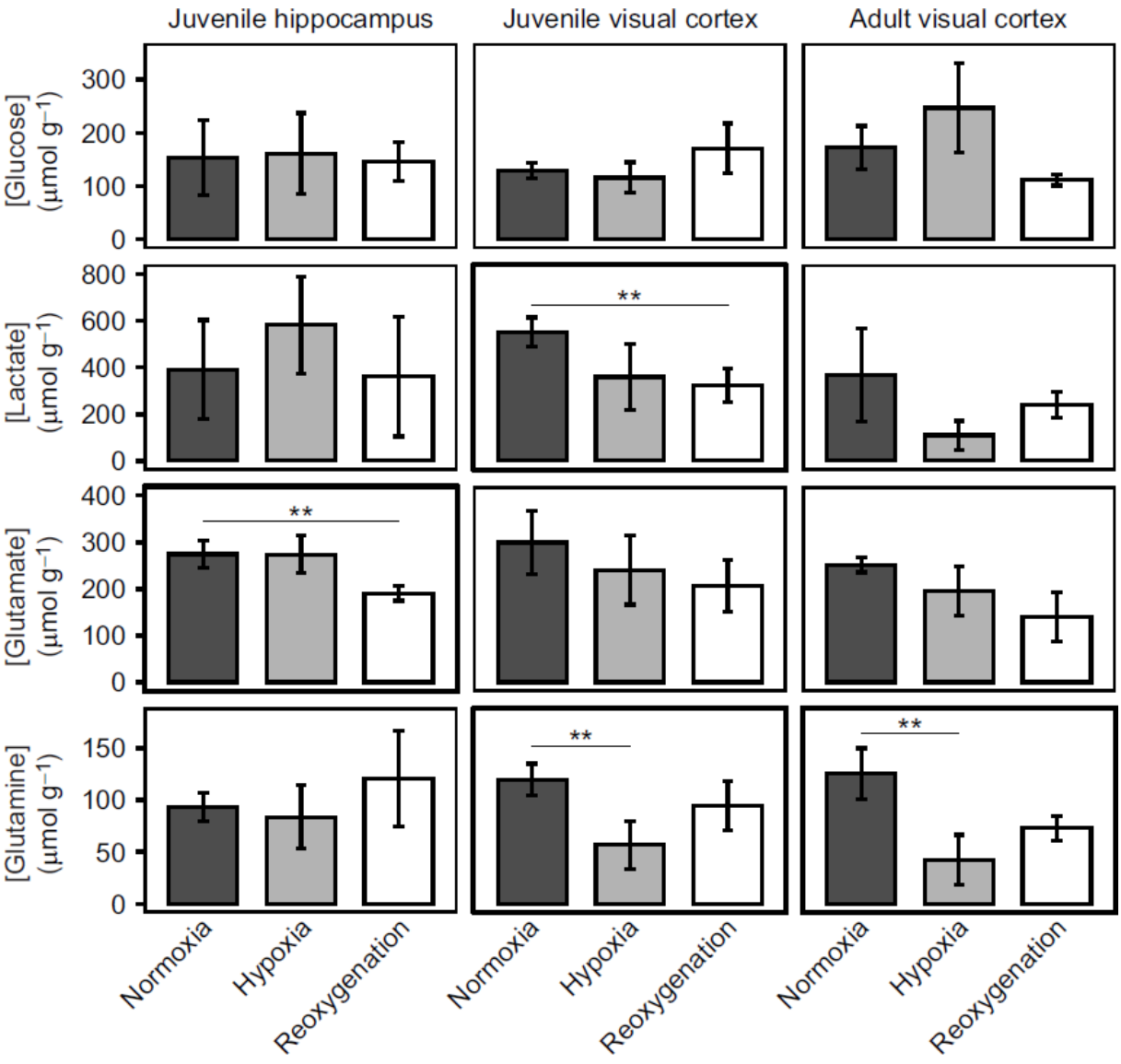

Fig. 1.5: Substrate assays of the hooded seal brain exposed to different oxygen regimes. *Substrate concentrations (mean ± s.d.) of glucose, lactate, glutamate and glutamine were normalized to total protein concentration in visual cortex and hippocampus of juvenile hooded seals (n = 5) and visual cortex of adult hooded seals (n = 4) exposed to normoxia, hypoxia and reoxygenation, respectively. Statistical analysis was performed with two sample t-tests including Benjamini-Hochberg correction (FDR). *p < 0.05, **p < 0.01, ***p < 0.001, ****p < 0.0001.*

Discussion

Lipids are ubiquitous in the brain, yet the composition and function of the brain lipidome is not well characterized (Fitzner et al. 2020). They not only provide the structural basis of cell membranes, but also take part in a wide variety of vital tasks in the brain including signal transduction (Piomelli et al. 2007). In neurodegenerative diseases, lipids may facilitate neuroprotection and serve as diagnostic biomarkers (Zhao et al. 2011; Castellanos et al. 2021). While neurons of most terrestrial (non-diving) mammals suffer irreversible damage after only short periods of low tissue oxygen levels (hypoxia), *in vitro* experiments revealed that neurons of the hooded seal show prolonged functional integrity during hypoxic conditions (Folkow et al. 2008; Geiseler et al. 2016). How the brain lipidome may contribute to the hypoxia tolerance of diving mammals has not been comprehensively studied. In this study, we performed an untargeted lipidomics analysis, which revealed that some lipid species are significantly modulated in marine mammals in comparison to terrestrial mammals. Furthermore, some metabolites involved in energy metabolism and neurotransmission appear to be regulated differently in marine than in terrestrial mammals.

The metabolic/oxygenation state of the sampled tissues

The conditions to which the animals were exposed prior to sampling affect the metabolic/oxygenation state of the sampled tissues, and this must be taken into account when interpreting data. This presumably concerns tissue metabolite and neurotransmitter levels, in particular. Unfortunately, we were unable to determine tissue oxygenation levels, but have made the following theoretical analysis of the possible effects of the various treatments:

All animals were captured and restrained before sedation, anesthesia, and euthanasia. Capture and restraint involves a certain amount of physical effort and thus represents a stressful situation for the animals, which could affect the metabolic state of the sampled brain tissue. However, even in the case of live-capture of adult seals, the capture procedure only involved moderate temporal and intense exertion for the animal, as animals typically resigned shortly (1-2 min) after being entrapped and were then immediately sedated with drugs having induction times of <1 min (Wheatley et al. 2006). During the ~10 minute interval until sedated animals were catheterized and euthanized, or intubated and manually ventilated (as was the case for some of the seals), spontaneous ventilation was somewhat depressed, presumably causing very moderate hypoxia (particularly from a seal perspective). However, manual ventilation (isoflurane in air) of those seals concerned rapidly restored normal oxygenation levels (>95% O_2 saturation), as confirmed with a pulse-oximeter with sensor attached to tongue. In other species (rat (*Rattus norwegicus*), man (*Homo sapiens*)), isoflurane, pentobarbital, ketamine (a close relative to tiletamine, which we used) and diazepam (a close relative to zolazepam, which we used) are known to all reduce brain glucose uptake (Prando et al. 2019; Kelly et al. 1986), and to

depress cerebral brain metabolic rate as a whole (de Wit et al. 1991). Since all brain tissues that were collected immediately after euthanasia were under the influence of one or more of the drugs mentioned above, we may assume that their metabolic/oxygenation state was comparable.

In contrast, those samples that were subjected to *in vitro* incubation in aCSF under known oxygenation conditions, had a known metabolic history that is defined by the oxygenation conditions to which they were experimentally subjected (normoxia, hypoxia or hypoxia followed by re-oxygenation). Here, we assume that the 20 min pre-incubation of tissue in fully oxygenated aCSF was sufficient to 'reset' cells to a normoxic metabolic state, should their metabolic/oxygenation state have been disturbed by the prior handling (animal capture procedure & metabolic effects of drugs).

Lipids and neurotransmission

Sphingolipids, especially sphingomyelin, form the myelin sheath surrounding axons and are thereby directly involved in signal transduction in the brain (Schneider et al. 2019). Myelin insulates nerve fibers, decreasing the capacitance and increasing the electrical resistance across the axonal membrane, thereby enabling rapid saltatory conduction of action potentials (Hartline 2008). We observed that sphingolipids such as cerebroside and sphingomyelin are mainly elevated in the seal brain compared to mice and ferrets, but a general significant increase of one lipid class could not be determined. A stronger sheathing of the axon would further reduce the capacitance of the axonal membrane and produce a faster conduction speed, as well as allowing a smaller number of ions to enter the fibre, thereby reducing the metabolic cost of pumping ions across the membrane (Hartline 2008). Reducing energy consumption and thereby oxygen demand may be beneficial under low oxygen conditions, as routinely experienced during diving of seals. Apart from myelin formation and signal transduction, sphingolipids can modulate various biological processes such as growth, cell migration, adhesion, apoptosis, senescence, and inflammation (Hannun and Obeid 2018). Additionally, sphingolipids can be transformed into each other. For instance, sphingomyelin can be hydrolyzed to form ceramide, which has apoptotic functions as described below (Kolesnick 1994). Ceramides may also induce negative membrane curvature, which might promote budding and vesiculation, thereby contributing to synaptic signaling (van Blitterswijk et al. 2003). Because of the variety of functions and dynamic character of sphingolipids, a general role in the hooded seal brain is not easily ascribed. However, elevated levels of sphingolipids may contribute to efficient signal transduction and reduction of energy consumption.

Glutamate is the most abundant excitatory neurotransmitter in the vertebrate nervous system (Meldrum 2000). Synaptically released glutamate is usually rapidly taken up from the extracellular space, to terminate its action (Schousboe 1981). However, energy deficiency during hypoxia leads to glutamate accumulation in the synaptic cleft, which is a major contributor to excitotoxic cell death due

to excessive calcium influx and neuronal depolarization (Belov Kirdajova et al. 2020; Choi and Rothman 1990). Blocking of glutamate receptors resulted in a delayed depolarization of neurons in hippocampal slices of mice during anoxic challenge, preventing the initiation of cell death cascades (Heit et al. 2021). In this study, we found that the neurotransmitters glutamate and its predecessor glutamine were generally decreased in the seal brain compared to the mouse brain. Furthermore, we observed that glutamine, and to a lesser extent glutamate levels decreased in response to hypoxia in the hooded seal visual cortex. Since glutamatergic signaling and the recycling of the neurotransmitters are highly energy-intensive processes (Attwell and Laughlin 2001), a reduction in glutamatergic signaling may be beneficial to i) reduce energy expenditure that is limited during hypoxia and ii) prevent neurotoxic events caused by failed glutamate reuptake from the synaptic cleft when ATP is limited under hypoxic conditions. Accordingly, a comparative transcriptomics analysis revealed that genes involved in glutamatergic transmission, e.g., glutamate receptors, were expressed at significantly lower levels, whereas genes involved in glutamate reuptake were more highly expressed in hooded seal neurons than in neurons of mice (Geßner et al. 2022). Ramirez et al. (2007) suggested that the brain of diving mammals may survive hypoxic events through depression (partial 'shut-down') of neuronal activity during diving. Later, Buck and Pamenter (2018) proposed the 'synaptic arrest' hypothesis, stating that hypoxia-tolerant species have a lower basal expression of synaptic proteins and are able to decrease their function during periods of hypoxia. Regardless of mechanism, this would lead to decreased energy expenditure during low oxygen conditions. In accordance, a reduction in glutamate and glutamine has been observed in the hypoxia-tolerant naked mole rat (*Heterocephalus glaber*) brain in response to hypoxia but only glutamine decreases in the hypoxic mouse brain (Cheng et al. 2022). Interestingly, hypoxia-preconditioning of mice also led to a decrease in glutamate, whereas inhibitory neurotransmitters, including γ-aminobutyric acid (GABA), dopamine, adenosine, and taurine were increased in the hippocampus (Liao et al. 2018). In conclusion, reduced glutamatergic signaling in the seal brain may facilitate neuronal survival during hypoxic conditions by reducing energy expenditure and neurotoxic effects.

Ceramides and mitochondrial membrane function

Ceramides are waxy lipid molecules that are composed of sphingosine and a fatty acid and they accumulate as a result of different stressors. For instance, ischemia increases ceramide levels in mouse brain tissue (Yu et al. 2000) and hypoxia induces ceramide synthesis in neuronal precursor cells (Jin et al. 2008) and neuroblastoma cells (Kang et al. 2010). Furthermore, altered ceramide metabolism is associated with various neurodegenerative diseases such as Alzheimer's disease, Parkinson's disease and Huntington's disease (Czubowicz et al. 2019). Ceramides are especially involved in modulating membrane processes and function in mitochondria (van Blitterswijk et al. 2003). They can influence the permeability of mitochondrial membranes (Siskind et al. 2002; Dadsena et al. 2019), leading to the

release of aqueous contents of mitochondria such as cytochrome c, which in turn may induce apoptosis (Ghafourifar et al. 1999; Di Paola et al. 2000; Tsujimoto and Shimizu 2000; Shimizu et al. 1999). However, the subcellular localization as well as chain length essentially influence the biological effect of ceramide species (Fugio et al. 2020). Short chain C2-ceramide (Parra et al. 2008) as well as long-chain C18-ceramide (Sentelle et al. 2012) may induce apoptosis, whereas CerS2-derived very-long-chain C20-24-ceramides may lead to protective mitophagy (Law et al. 2018). Mitophagy is the selective autophagy of dysfunctional mitochondria to reduce cellular stress (Pickles et al. 2018). Consequently, ceramides reduce mitochondrial respiratory chain processes (Di Paola et al. 2000; Gudz et al. 1997).

Here, we found that sphingomyelins, which may be transformed into ceramides by acid sphingomyelinase (ASM), are increased in harp and hooded seals. Inhibition of ASM during glutamate-induced excitotoxicity in oligodendrocytes reduced ceramide levels and enhanced cell survival (Novgorodov et al. 2018). Additionally, knockout of ASM reduced mitochondrial defects, augmented the autophagic flux and improved the brain-function recovery after traumatic brain injury (Novgorodov et al. 2019). Whether ASM is particularly active in marine mammals, thereby creating increased ceramide concentration from high levels of sphingomyelin is unknown. Nevertheless, in this study, the detected sphingomyelins had an average fatty acid chain length of 20-21 carbon atoms. Hydrolysation would therefore result in very-long-chain ceramides that could lead to mitophagy and thus reduced mitochondrial aerobic respiration (Kolesnick 1994; Law et al. 2018). Depending on the reference organism and the depth of analyses, the capacity for aerobic respiration in the hooded seal visual cortex has been shown to be decreased or increased compared with terrestrial mammals (Fabrizius et al. 2016; Geßner et al. 2022). Thus, while the transcriptome of the visual cortex (whole tissue) indicated a reduced capacity for aerobic metabolism compared to ferrets (*Mustela putorius furo*) (Fabrizius et al. 2016), a more detailed neuron-specific analysis (of excised cortical neurons) demonstrated an elevated capacity in hooded seal neurons when compared to those of mice (Geßner et al. 2022). Similarly, an increased aerobic capacity was found in the cetacean brain when compared with cattle (*Bos taurus*) brains (Krüger et al. 2020). A metabolic analysis of the hibernating Syrian hamster (*Mesocricetus auratus*) brain revealed a reversible increase of ceramides in torpor animals, which might reflect increased mitophagy during hibernation and thus processes to prevent oxidative damage (Gonzalez-Riano et al. 2019). In contrast, we could not determine a lipidomic stress response by hypoxia treatment of seal brain tissue, which might point to a constitutive rather than an induced adaptation.

Energy metabolism of glucose and lactate

At normoxic conditions, glycolytic processes might be enhanced in the seal brain, as reflected by high glucose as well as lactate levels compared with levels in the mouse brain, at least as measured in our

metabolite assays. Since these values are likely to reflect near-resting metabolite levels, and since the possible drug effects on tissue metabolic state presumably were comparable between species (see text under heading “The metabolic/oxygenation state of the sampled tissues”, above), the noted species difference may reflect a pre-adaptation of the seal brain to upcoming stress conditions, not least since elevated brain glucose levels are considered to be neuroprotective (Swanson and Choi 1993; Choi and Gruetter 2003). Recently, it has been shown that the brain not only relies on glucose as the sole energy source, but can also efficiently metabolize other substrates such as lactate (Bélanger et al. 2011). Typically, lactate is formed by glycolysis in astrocytes and subsequently transported into neurons, which convert lactate into pyruvate and utilize it in aerobic respiration to meet their high energy demands, as proposed by the ‘astrocyte-neuron lactate shuttle’ hypothesis (Pellerin and Magistretti 1994). Interestingly, the hooded seal brain exhibits an unusual distribution of cytochrome c, neuroglobin and lactate dehydrogenase b in astrocytes rather than in neurons (Mitz et al. 2009; Hoff et al. 2016). Mitz et al. (2009) therefore proposed the ‘reverse lactate shuttle’ hypothesis, in which, at normoxic conditions, lactate is shuttled to astrocytes from basically anaerobic neurons, to be converted into pyruvate and subsequently used for aerobic respiration. This would protect oxidative stress-susceptible neurons by shifting oxidative metabolism to astrocytes.

During hypoxic conditions, lactate may be transported out of the brain to limit its (glial) oxidative metabolism and its detrimental effects. An increase of the lactate level in the cerebral venous effluent has already been observed at the end of long dives of harbor seals (*Phoca vitulina*) (Kerem and Elsner 1973). In agreement, lactate concentration may have dropped in the adult and juvenile visual cortex, whereas glucose levels stayed approximately the same in our hypoxia- and reoxygenation-treated samples, possibly aided by the elevated brain glycogen stores of hooded seals (Czech-Damal et al. 2014). Czech-Damal et al. (2014) observed extended spontaneous neuronal activity in brain slices of hooded seals compared with mice, when exposed to hypoxia and ischemia, as well as in the presence of lactate. Interestingly, the monocarboxylate transporter *mct4* has been shown to be upregulated in response to hypoxia and reoxygenation in the hooded seal brain and may perform lactate efflux (Hoff et al. 2017). Generally high levels of *mct4* have been also found in hooded seal neurons in comparison to mouse neurons (Geßner et al. 2022). However, neither of these transcriptomics studies (Hoff et al. 2017; Geßner et al. 2022) suggested any distinct regulation in cerebral glucose metabolism. Nevertheless, removal of lactate may be beneficial during low oxygen conditions and may contribute to the hypoxia tolerance of the hooded seal brain. Subsequently, tissues not as sensitive to pH changes and high buffering capacities may be able to deal with high lactate concentrations (Boutilier et al. 1993; Castellini and Somero 1981).

Lipid saturation and membrane fluidity

Alterations in membrane lipid composition might be attributed to maintenance of adequate membrane fluidity (homeoviscous adaptations, see e.g., Hazel 1990). To maintain membrane fluidity in cold environments, cell membranes of marine mammals, which display substantial peripheral heterothermia (e.g., Irving and Hart 1957), might contain lipids of shorter chain lengths and with more double bonds. Williams et al. (2001) compared the erythrocyte membrane lipid composition from two deep-diving phocid seals (*Mirounga angustirostris*, *Phoca vitulina*), with that of a relatively shallow-diving otariid seal (*Callorhinus ursinus*) and with non-diving mammals (*Canis familiaris*, *Equus caballus*, *Bos taurus*). Lipid unsaturation indices and proportions of long-chain polyunsaturated fatty acids (PUFAs) were substantially higher in the phocid seals, presumably linked to the necessity to maintain a fluid membrane in cold environments (Williams et al. 2001).

We observed no significant differences in cerebral lipid saturation (Fig. S1.9) or chain length (Fig. S1.10) between seals and non-diving mammals, but noted that phospholipids with a total chain length of 38 carbon atoms tended to be decreased in marine mammals compared to terrestrial mammals. Since phospholipids contain two fatty acid chains, the average fatty acid chain length translates to 19 carbon atoms. The majority of fatty acids detected in the blubber (Wheatley et al. 2008) and muscle of Weddell seals were of similar chain length of 18 carbon atoms (Trumble et al. 2010), but in those studies no comparison to terrestrial mammals was drawn. We also noted a non-significant decrease in moderately unsaturated lipids with four double bonds in marine mammals. For comparison, more than half of the detected fatty acids in skeletal muscle tissue of Weddell seals were monounsaturated fatty acids (MUFAs), which might be important for preventing ROS damage (Trumble et al. 2010). A comprehensive analysis of phospholipids in various rat organs suggests that brain phospholipids are least enriched with PUFAs compared to the heart, kidney, and liver (Choi et al. 2018). Choi et al. (2018) argued that a decrease in membrane PUFAs might be a mechanism to protect from ischemic brain damage because of lower susceptibility to lipid peroxidation. Nevertheless, PUFAs are essential fatty acids, required for structural growth and brain development (Innis 2005). Brain phospholipids are selectively enriched in specific PUFAs, especially arachidonic acid and docosahexaenoic acid (Bazinet and Layé 2014), but their concentration may change with dietary intake (Chen et al. 2020a) – a likely scenario for marine mammals with their lipid-rich diets. Consequently, Monteiro et al. (2021a) reported higher n-3 and lower n-6 fatty acid contents of small cetaceans [common dolphin (*Delphinus delphis*), harbour porpoise (*Phocoena phocoena*), and striped dolphin (*Stenella coeruleoalba*)] hearts compared with levels in hearts of their terrestrial relatives, reflecting high availability of n-3 fatty acids in marine food chains.

Additionally, we detected a substantial amount of phospholipid plasmalogen species. The exact function of plasmalogen species remains obscure, but they are thought to act as antioxidants and facilitate membrane fusion (Dean and Lodhi 2018). Furthermore, they reduce fluidity and improve rigidity of cell membranes by favoring close alignment of lipids (Dean and Lodhi 2018; Braverman and Moser 2012). In neurons of the human brain, phosphatidylethanolamine (PE) plasmalogen species constitute over 50% of total PEs (Han et al. 2001). Here, over 60% of detected PEs represented plasmalogen species. The antioxidative functions of plasmalogens might be beneficial and although they were at mostly increased concentration in marine mammals, we could not determine a general accumulation of this lipid class.

Conclusions

Lipids are involved in a wide variety of biochemical pathways. In this study, we found that the brain lipidomes of diving mammals, the hooded seal and harp seal, differ from two terrestrial (non-diving) relatives, the mouse and ferret. While single lipids are significantly regulated, whole lipid classes did not show a significant regulation. However, sphingomyelin species were generally increased in the seals compared to the terrestrial mammals, which may be important for efficient neuronal signal transduction. Excitatory synaptic signaling may be reduced in the seal brain, as illustrated by reduced levels of glutamate and glutamine. This could represent an adaptation to prevent neurotoxic events during hypoxia. Additionally, increased neural glucose and lactate levels may be suggestive of an elevated glycolytic capacity of the seal brain. Membrane fluidity and integrity are likely to play a substantial role in the adaptation of seals to the aquatic environment. However, we found no direct evidence of altered membrane lipid chain length or unsaturation between seals and terrestrial mammals. Hypoxia and reoxygenation treatment did not induce significant changes in the brain lipidome of hooded seals, but some metabolites (e.g., glutamine) were reduced in response to hypoxia. Therefore, not only a constitutive reduction in neurotransmitter levels and synaptic signaling, but also a further decrease in response to hypoxic conditions may contribute to the hypoxia tolerance of the hooded seal brain. The present study is the first to investigate brain lipidomics in specialist diving species and provides valuable insights into the hypoxia adaptations of the pinniped brain. Future studies may further explore how hypoxia and reoxygenation influences the brain lipidome as well as polar substrates of diving compared with non-diving mammals.

Competing interests

No competing interests declared.

Authors' contributions

TB conceived the research idea and received the funding. CG and GAM developed the experimental design. MC acquired mass spectrometry data. GAM carried out the lipidome analysis with the assistance of MC and MF. GAM conducted the substrate assays and analyzed the data. LPF sampled the hooded seal and harp seal tissues and performed hypoxia and reoxygenation treatment of samples. GAM wrote the manuscript with input from all authors. All authors have read and approved the final manuscript.

Funding

This work was supported by the Deutsche Forschungsgemeinschaft (Bu956/22).

Acknowledgements

Thanks are due to the crew of R/V “Helmer Hanssen” for their support in collecting hooded and harp seal samples.

Data availability

Mass spectrometry data is available at the NIH Common Fund's National Metabolomics Data Repository (NMDR) website, the Metabolomics Workbench (Sud et al. 2016), https://www.metabolomicsworkbench.org where it has been assigned Project ID PR001514. The data can be accessed directly via it's Project DOI: http://dx.doi.org/10.21228/M80H6B. This work is supported by NIH grant U2C-DK119886.

7 Chapter II

Transcriptomes of Clusterin- and S100B-transfected neuronal cells elucidate protective mechanisms against hypoxia and oxidative stress in the hooded seal (*Cystophora cristata*) brain

Gerrit A. Martens[1]*, Cornelia Geßner[1], Carina Osterhof[2], Thomas Hankeln[2], Thorsten Burmester[1]

[1] Institute of Animal Cell and Systems Biology, Biocenter Grindel, University of Hamburg, 20146 Hamburg, Germany

[2] Institute of Organismic and Molecular Evolution, Molecular Genetics & Genome Analysis, Johannes Gutenberg University Mainz, 55128 Mainz, Germany

*Corresponding author: Gerrit A. Martens

Email: gerrit.a.martens@gmail.com

Keywords: Clusterin, S100B, hypoxia, oxidative stress, transcriptome, neurons, brain, hooded seal, marine mammals

Published: 15 October 2022 in *BMC Neuroscience*

Martens, Gerrit A.; Geßner, Cornelia; Osterhof, Carina; Hankeln, Thomas; Burmester, Thorsten (2022): Transcriptomes of Clusterin- and S100B-transfected neuronal cells elucidate protective mechanisms against hypoxia and oxidative stress in the hooded seal (*Cystophora cristata*) brain. In *BMC Neuroscience* 23 (1), p. 59. DOI: 10.1186/s12868-022-00744-6.

Abstract

Background: The hooded seal (Cystophora cristata) exhibits impressive diving skills and can tolerate extended durations of asphyxia, hypoxia and oxidative stress, without suffering from irreversible neuronal damage. Thus, when exposed to hypoxia *in vitro*, neurons of fresh cortical and hippocampal tissue from hooded seals maintained their membrane potential 4 – 5 times longer than neurons of mice. We aimed to identify the molecular mechanisms underlying the intrinsic neuronal hypoxia tolerance. Previous comparative transcriptomics of the visual cortex have revealed that S100B and clusterin (apolipoprotein J), two stress proteins that are involved in neurological disorders characterized by hypoxic conditions, have a remarkably high expression in hooded seals compared to ferrets. When overexpressed in murine neuronal cells (HN33), S100B and clusterin had neuroprotective effects when cells were exposed to hypoxia. However, their specific roles in hypoxia have remained largely unknown.

Methods: In order to shed light on potential molecular pathways or interaction partners, we exposed HN33 cells transfected with either S100B, soluble clusterin (sCLU) or nuclear clusterin (nCLU) to normoxia, hypoxia and oxidative stress for 24h. We then determined cell viability and compared the transcriptomes of transfected cells to control cells. Potential pathways and upstream regulators were identified via Gene Ontology (GO) and Ingenuity Pathway Analysis (IPA).

Results: HN33 cells transfected with sCLU and S100B demonstrated improved glycolytic capacity and reduced aerobic respiration at normoxic conditions. Additionally, sCLU appeared to enhance pathways for cellular homeostasis to counteract stress-induced aggregation of proteins. S100B-transfected cells sustained lowered energy-intensive synaptic signaling. In response to hypoxia, hypoxia-inducible factor (HIF) pathways were considerably elevated in nCLU- and sCLU-transfected cells. In a previous study, S100B and sCLU decreased the amount of reactive oxygen species and lipid peroxidation in HN33 cells in response to oxidative stress, but in the present study, these functional effects were not mirrored in gene expression changes.

Conclusions: sCLU and S100B overexpression increased neuronal survival by decreasing aerobic metabolism and synaptic signaling in advance to hypoxia and oxidative stress conditions, possibly to reduce energy expenditure and the build-up of deleterious reactive oxygen species (ROS). Thus, a high expression of CLU isoforms and S100B is likely beneficial during hypoxic conditions.

Introduction

The hooded seal (*Cystophora cristata*) is an excellent breath-hold diver, performing dives for up to 1 h, while diving over 1 km deep (Folkow and Blix 1999; Vacquie-Garcia et al. 2017). Physiological adaptations, such as increased oxygen stores (hemoglobin, myoglobin), a decreased heart rate (bradycardia) and a redirection of blood flow to vital organs (selective peripheral vasoconstriction) have evolved to facilitate this diving lifestyle (Folkow and Blix 2010; Ponganis 2011; Scholander 1940; Blix et al. 1983; Blix 2018; Ponganis 2019). However, during repetitive diving bouts oxygen partial pressure may drop dramatically, as shown in other deep-diving seals (Meir et al. 2009; Qvist et al. 1986), and would lead to neuronal damage in humans (Lutz 2002). Neurons from the hooded seal have an intrinsic hypoxia tolerance that cannot be explained by these physiological adaptations. Isolated hooded seal brain slices maintained their membrane potential during hypoxic treatment, while those of mice lost their functional integrity (Folkow et al. 2008). The molecular basis of this intrinsic hypoxia tolerance is not well understood. In a comparative transcriptomics analysis, the calcium-binding protein S100B and the molecular chaperone clusterin (CLU) emerged as highly expressed in the hooded seal visual cortex, when compared to the ferret (*Mustela putorius furo*). More precisely, S100B expression was 38-fold higher in the hooded seal than in the ferret (Fabrizius et al. 2016). CLU exhibited the highest mRNA levels in the hooded seal cortex, with a 4-fold increase compared to the ferret (Fabrizius et al. 2016). The remarkably enhanced transcription of S100B was confirmed in laser-excised hooded seal neurons, in which S100B was 82-fold more highly expressed than in neurons of mice (*Mus musculus*) (Geßner et al. 2022). The observed overexpression suggests that both genes might contribute to the hypoxia tolerance of the hooded seal brain (Fabrizius et al. 2016; Geßner et al. 2022). Both, S100B and CLU, are associated with many neurological disorders such as Alzheimer's disease and Parkinson's disease in humans that involve hypoxia and oxidative stress (Foster et al. 2019; Michetti et al. 2019). However, their role and molecular mechanisms in these conditions are controversial and ambiguous.

The S100 proteins are appreciably conserved among different species (Geßner et al. 2020; Fanò et al. 1995), which may indicate crucially conserved biological roles. S100B is a calcium-binding protein that is involved in a broad range of Ca^{2+}-dependent pathways (Michetti et al. 2021). Human and rodent studies demonstrated S100B's dual role, acting as an intracellular regulator on the one hand and as an extracellular signal substance on the other hand (Donato et al. 2009). Intracellular S100B is involved in many processes such as proliferation, differentiation and survival (Michetti et al. 2021). For instance, in melanoma cells S100B leads to improved tumor survival, preventing p53-mediated apoptosis (Lin et al. 2004; Lin et al. 2010). Although mainly present in astrocytes (Michetti et al. 2019), S100B was also found to be located in neurons (Rickmann and Wolff 1995), in which it reduced apoptosis and nerve growth factor (NGF)-induced differentiation (Arcuri et al. 2005). S100B may be secreted from

astrocytes and neurons in conditions of metabolic stress and other external stimuli (Gerlach et al. 2006; Ellis et al. 2007), where its role depends on its concentration (Michetti et al. 2021). When released into the extracellular microenvironment, S100B acts as a damage-associated molecular pattern (DAMP) protein through its interaction with the receptor for advanced glycation end products (RAGE) (Cristóvão and Gomes 2019; Sorci et al. 2010). RAGE is a multi-ligand receptor of the immunoglobulin superfamily which is mainly expressed by neurons and microglia and which mediates inflammatory responses by activating multiple signaling pathways (Angelopoulou et al. 2018; Jiang et al. 2018). At nanomolar concentrations, S100B demonstrates neurotrophic effects, promoting neurite extension and neuron survival, modulating long-term potentiation and counteracting neurotoxicants like reactive oxygen species (ROS) (Michetti et al. 2019). Neuron survival may be facilitated by different RAGE-dependent pathways (Leclerc et al. 2007; Huttunen et al. 2000; Donato et al. 2009). By contrast, persistent activation of RAGE by micromolar concentrations of S100B produces increased amounts of ROS, leading to lipid peroxidation and consequently induction of apoptosis (Vincent et al. 2007). However, studies report varying results at what concentration S100B exerts neurotrophic or neurotoxic effects (Donato et al. 2009). In neuronal disorders such as acute brain injury and neurodegenerative diseases, S100B has been found at high levels serving as a biomarker of disease progression (Michetti et al. 2019). Nevertheless, in proteinopathies like Alzheimers's and Parkinson's disease, S100B might also be involved in clearance of detrimental protein aggregates (Michetti et al. 2021).

CLU, a multifunctional glycoprotein, is a constitutively secreted chaperone in its predominant form (soluble CLU, sCLU), but truncated forms localized to the nucleus (nuclear CLU, nCLU) have also been found (Jones 2002b; Herring et al. 2019). The different isoforms of CLU target distinct cellular or subcellular localizations in the rat and human brain, where they demonstrate different functions (Herring et al. 2019). The sCLU isoform is translated as a pre-protein of 36 – 39 kDa, which contains an N-terminal endoplasmic reticulum (ER)-signaling peptide and two nuclear localization sequences. After removal of the signaling peptide, the pre-protein is phosphorylated and glycosylated in the ER and Golgi body. Cleavage of the intermediate glycoprotein results in two subunits linked by disulfide-bonds. The resulting mature antiparallel, heterodimeric glycoprotein [70 – 75 kDa], commonly referred to as sCLU, is then secreted (Burkey et al. 1991). In contrast, nCLU is a truncated isoform of 45 - 50 kDa, lacking the ER signaling peptide and is primarily detected in the cytosol and nucleus (Prochnow et al. 2013; Leskov et al. 2003). Other CLU forms targeted to the mitochondria have also been described, where they may function as antiapoptotic proteins during stress conditions or facilitate mitochondrial respiration (Rodríguez-Rivera et al. 2021; Herring et al. 2019; Zhang et al. 2005). Although some studies question the relevance and existence of CLU isoforms (Satapathy and Wilson 2021), it has been demonstrated that sCLU and nCLU exhibit distinct functions and that they regulate

certain cellular processes in opposite manners (Herring et al. 2019). CLU function and expression is regulated by a wide variety of signals including growth and transcription factors, as well as several stress conditions (Foster et al. 2019). For instance, during oxidative stress conditions, intracellular CLU promotes cardiomyocyte survival (Jun et al. 2011). Due to its stress-increased expression and extracellular chaperone activity CLU has been compared to heat shock proteins (Foster et al. 2019). Indeed, CLU might mediate neuroprotection by preventing stress-induced precipitation and aggregation of proteins, by mediating clearance of extracellular misfolded proteins and aggregates, and by promoting their cellular uptake (Wyatt et al. 2013). Additionally, cytosolic CLU might have an important role in intracellular protein homeostasis (proteostasis), by transporting misfolded proteins to the proteasome and/or autophagy for degradation (Gregory et al. 2017; Zhang et al. 2014; Materia et al. 2012). Similar to S100B, in proteinopathies like Alzheimer's and Parkinson's disease, CLU has been found to associate with protein aggregates and might be involved in their clearance (Lenzi et al. 2020; Foster et al. 2019). However, in advanced disease stages CLU has been found to promote neurotoxicity (Yerbury et al. 2007). Its concentration in peripheral blood was identified as a potential biomarker for neurodegenerative diseases, like Alzheimer's disease (Baig et al. 2012). Still, CLU's downstream pathways and molecular mechanisms are not well characterized. Different cell-types, varying levels of model complexity, and conditions that represent distinct physiological situations might lead to differing conclusions (Foster et al. 2019). Furthermore, lack of discrimination between different CLU isoforms as well as structural differences between these proteins (e.g., glycosylation levels) may be key in explaining the variability in CLU effects in apoptosis and cell death pathways.

Remarkably, the protective effects of S100B and CLU could be demonstrated in cell culture experiments (Geßner et al. 2020). Murine neuronal cell cultures (HN33) that were transfected with S100B, sCLU and nCLU demonstrated elevated viability when exposed to hypoxia (Geßner et al. 2020). Furthermore, overexpression of S100B, sCLU and, to a lesser degree, nCLU, led to a reduction of ROS and lipid peroxidation (Geßner et al. 2020). While these findings confirmed neuroprotective roles of S100B and CLU in hypoxia and oxidative stress, their molecular mechanisms remained obscure. In order to improve our understanding of the roles of these proteins in cell metabolism, we analyzed the transcriptomes of neuronal cell cultures transfected with S100B, nCLU and sCLU and then exposed to normoxia, hypoxia and oxidative stress, with the aim to identify possible molecular targets and pathways of S100B and CLU at different oxygen regimes.

Results & Discussion

Overexpression of transfected genes in HN33 cell lines

Transfected HN33 cell lines demonstrated stable mRNA overexpression of the S100B, sCLU and nCLU transgenes compared to the endogenous expression levels measured in mock-transfected cells. Overexpression in qPCR experiments ranged from 712-fold for S100B to 9230 – 9723-fold for nCLU and sCLU, respectively (Fig. S2.1). Expression of transfected genes was also observed in the RNA-Seq transcriptome data, when mapped to the mouse reference genome with added transgenic sequences (Fig. S2.2).

Viability of HN33 cell lines

Cell lines exhibited significant differences in ATP amounts, as shown by the CTG cell viability assay after exposure to normoxia, hypoxia and oxidative stress (275 uM H_2O_2) for 24h (Fig. 2.1). Cells transfected with sCLU and S100B were more viable at normoxic conditions than the mock and nCLU cell lines (sCLU: false discovery rate (p_{FDR}) < 0.001; S100B: p_{FDR} < 0.001). At hypoxic conditions, only sCLU demonstrated significantly elevated ATP levels compared to mock cells (p_{FDR} < 0.01). Viability of nCLU and S100B cell lines was with 85 % insignificantly higher than that of mock cells with 84 %. When exposed to oxidative stress, ATP levels of the sCLU and S100B cell lines were significantly higher than in the mock cell line (sCLU: p_{FDR} < 0.01; S100B: p_{FDR} < 0.01), while the nCLU cell line exhibited a similar ATP concentration as did the mock cell line.

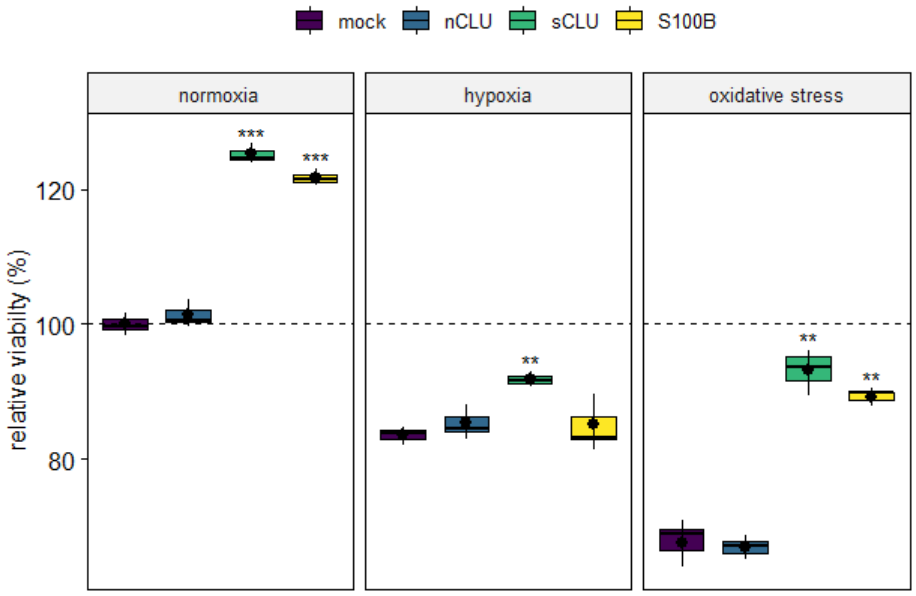

Fig. 2.1: Relative viability (%) of transfected cell lines compared to a mock cell line at the respective stress conditions. *After exposure to normoxia, hypoxia and oxidative stress for 24 h, cell viability was measured by CellTiter-Glo® assay. Viability of transfected cells (n = 3) was compared to the mock cell line, at each respective stress condition. The dashed line indicates viability of the mock cell line at normoxia. **** p_{FDR} < 0.0001, *** p_{FDR} < 0.001, ** p_{FDR} < 0.01, * p_{FDR} < 0.05.*

Transcriptome sequencing of transfected cell lines

Three replicates per cell line and condition were sequenced, with the exception of the mock cell line at oxidative stress conditions with two replicates. An average of 51 million RNA-Seq reads per sample were generated, with a minimum of 27 million and a maximum of 82 million reads per sample. Around 75% of all reads mapped to the GRCm39 mouse reference genome (Table S2.1) across all cell lines. Cells were compared to the mock cell line at the respective stress condition, to identify differentially expressed genes (DEGs). Principal component analysis of DEGs revealed that cells clustered according to stress conditions (Fig. 2.2). Hypoxia and oxidative stress elicited very distinct responses that were well-distinguishable. Still, within stress conditions, differences in gene expression for transfected cell lines could be determined (Fig. 2.3).

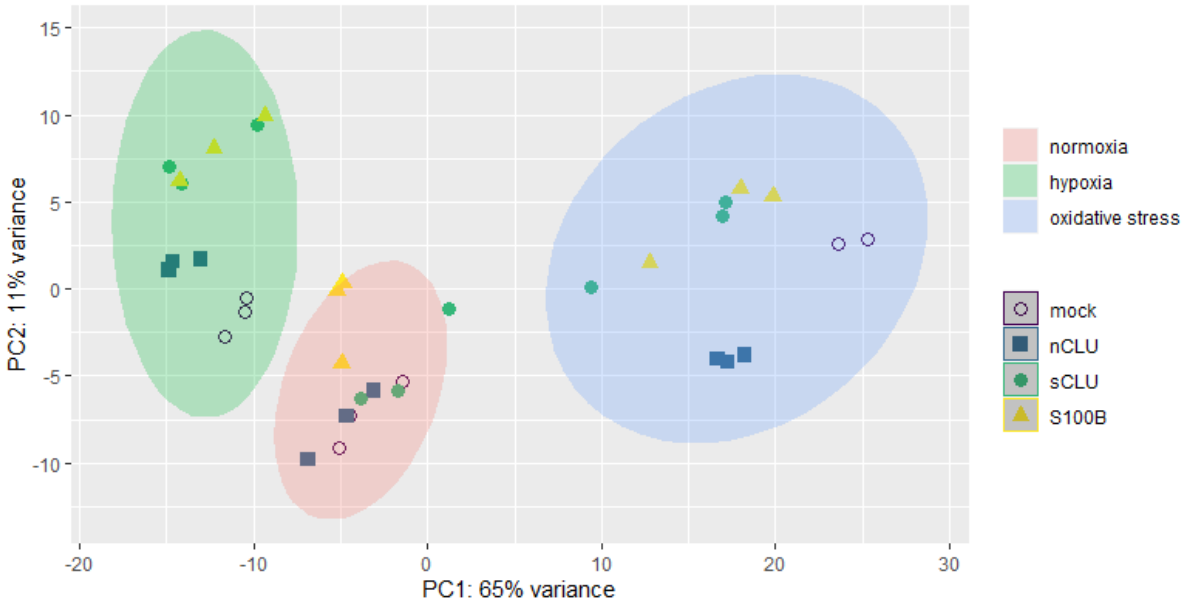

Fig. 2.2: Principal component analysis of transcriptomes from transfected cell lines. *Obtained reads from transfected cell lines were mapped against the mouse reference genome (GRCm39) and read counts analyzed using DESeq2. Gene expressions mostly clustered according to oxygen conditions (normoxia, hypoxia, oxidative stress).*

At normoxia, the nCLU cell line demonstrated the least variable DEGs ($p < 0.05$, TPM > 1), with only 69 DEGs, while the sCLU and S100B cell lines exhibited 676 and 1484 DEGs, respectively (Fig. 2.3). At hypoxia, numbers were more similar across cell lines, with 1018, 2316 and 2003 DEGs for nCLU, sCLU and S100B cell lines, respectively. Proportions shifted, when at oxidative stress the nCLU cell line displayed 5556 DEGs whereas sCLU and S100B cells only had 143 and 156 DEGs. The sCLU and S100B cell lines shared a substantial amount of DEGs at normoxia (142 up- and 201 downregulated genes), while the nCLU cell line only contributed few genes to the shared DEG pool of all cell lines (9 up- and 8 downregulated genes). The overlap of DEGs between cell lines was larger at hypoxia (192 up- and 135 downregulated genes), but was almost non-existent at oxidative stress (21 upregulated genes).

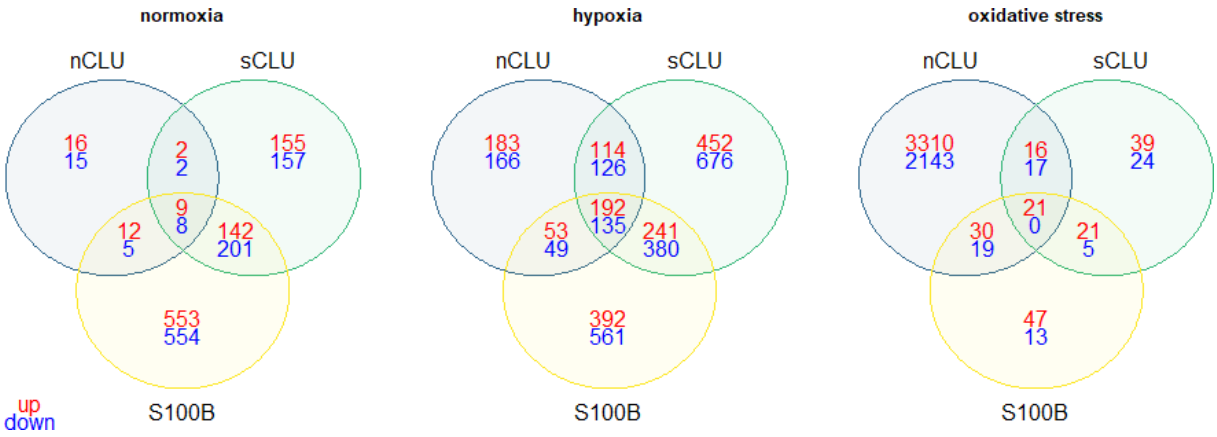

Fig. 2.3: Venn diagrams of differentially expressed genes in transfected cell lines. *Illustrated are the significantly upregulated (black, binary logarithm of fold change (log2FC) > 0) and downregulated (grey, log2FC < 0) genes, with transcripts per million (TPM) > 1 in transfected cell lines for each stress condition, compared to the mock cell line at the respective condition.*

Transcriptome response of the nCLU-transfected cell line

The nCLU-transfected cells exhibit minor gene expression differences at normoxic conditions

In normoxia, the nCLU cell line demonstrated the least differentially expressed genes (DEGs) in comparison to the mock cell line. The only enriched pathway was the inhibited *neuropathic pain signaling in dorsal horn neurons* (z-score (z) = -1, -log(p) = 2.9) (Fig. 2.4) with an upregulated potassium channel (KCNN3) within this pathway (binary logarithm of fold change (log2FC) = 1.19). Some developmental genes also showed high expression, demonstrated by activation of upstream regulator eomesodermin (EOMES, z = 2.0, p < 0.0001). Homozygous silencing of EOMES leads to neurodevelopmental disorders such as microcephaly in the human brain (Baala et al. 2007) and full knockout leads to embryonic lethality in mice (Russ et al. 2000). One of EOMES' targets, semaphorin receptor plexin A4 (PLXNA4, (log2FC = 1.01), as well as another gene involved in axon guidance, ephrin type-A receptor 8 (EPHA8) exhibited high expression levels (log2FC = 2.16). Axon guidance may be an important process for development of the nervous system (Jongbloets and Pasterkamp 2014). In contrast, the expression of opioid receptor delta 1 (OPRD1) was decreased in nCLU cells after normoxia (log2FC = -1.49). In mouse astrocyte cell culture, activation of the delta opioid receptor increased expression of excitatory amino acid transporters, suggesting a role in glutamate uptake and prevention of glutamate-induced neuroexcitotoxicity (Liang et al. 2014). Similar neuroprotection by delta opioid receptor activation has been found in mouse neuronal cell culture, which attenuated neuronal injury in normoxic and hypoxic conditions (Zhang et al. 2002; He et al. 2013). Downregulation of OPRD1 may therefore indicate reduced capacity of nCLU-transfected cells to respond to stress conditions.

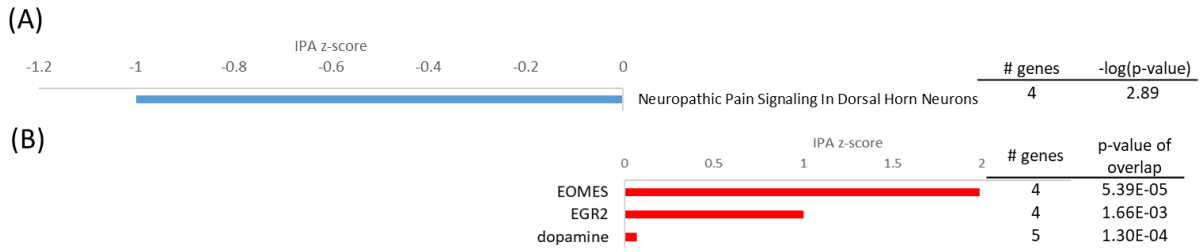

Fig. 2.4: Top pathways and upstream regulators for the nCLU cell line at normoxia. *(A) Top IPA canonical pathways activated (red, positive z-score) and inhibited (blue, negative z-score); (B) Top upstream regulators activated (red, positive z-score) and inhibited (blue, negative z-score) in the nCLU cell line at normoxia in comparison to the mock cell line.*

The nCLU-transfected cells demonstrate elevated hypoxia response

When exposed to hypoxia, the nCLU-transfected neuronal cells demonstrated elevated hypoxia response pathways in comparison to the mock cells (Fig. 2.5). Nevertheless, the mock cells displayed a hypoxia response as well. When comparing its gene expression in hypoxic conditions to normoxic conditions, *cellular response to hypoxia* was among top 10 enriched pathways (FE = 15.89, $p_{FDR} < 0.05$). Even when only looking at highly differentially expressed genes (log2fc>1 or log2fc<-1) *cellular response to hypoxia* was among top 10 enriched pathways (FE > 100, $p_{FDR} < 0.05$). However, hypoxia response of the nCLU-transfected cells appeared to be even stronger in comparison to mock cells.

In hypoxia, most eukaryotic cells can shift their primary metabolic strategy from predominantly mitochondrial respiration towards increased glycolysis (Kierans and Taylor 2021). However, it is not clear if neurons are able to undergo such a shift in metabolism (Dienel 2019). GO term *glycolytic process* (fold enrichment (FE) = 9.8, false discovery rate (p_{FDR}) < 0.01), as well as IPA pathways *glycolysis I* (z = 2.6, -log(p) = 4.1) and *gluconeogenesis* (z = 1.6, -log(p) = 3.1) were enhanced in nCLU-transfected cells. Additionally, GO term *glycogen biosynthetic process* (FE = 14.0, $p_{FDR} < 0.05$) and IPA pathway *glycogen biosynthesis* (-log(p) = 3.0) were increased in the nCLU-transfected cells, which is a common response to hypoxia (Pelletier et al. 2012). Thus, enzymes for glycogen metabolism which mainly promote glycogen accumulation (e.g., glucan phosphatase EPM2A, log2FC = 1.03) (Raththagala et al. 2015) were upregulated in the nCLU-transfected cell lines. Glycogen has been demonstrated to protect cerebellar and cortical mouse neurons from hypoxic stress-induced cell death in cell culture (Saez et al. 2014) and glycogen storage is increased in the seal brain (Kerem et al. 1973; Czech-Damal et al. 2014), which illustrates its significance in dealing with hypoxia. In a transcriptome analysis, glycogenolysis-associated genes were, thus, found to be upregulated in hooded seal neurons compared to neurons of mice (Geßner et al. 2022). In general, energy metabolism through glycogen biosynthesis and glycolysis were enhanced in the nCLU-transfected cells in hypoxic conditions.

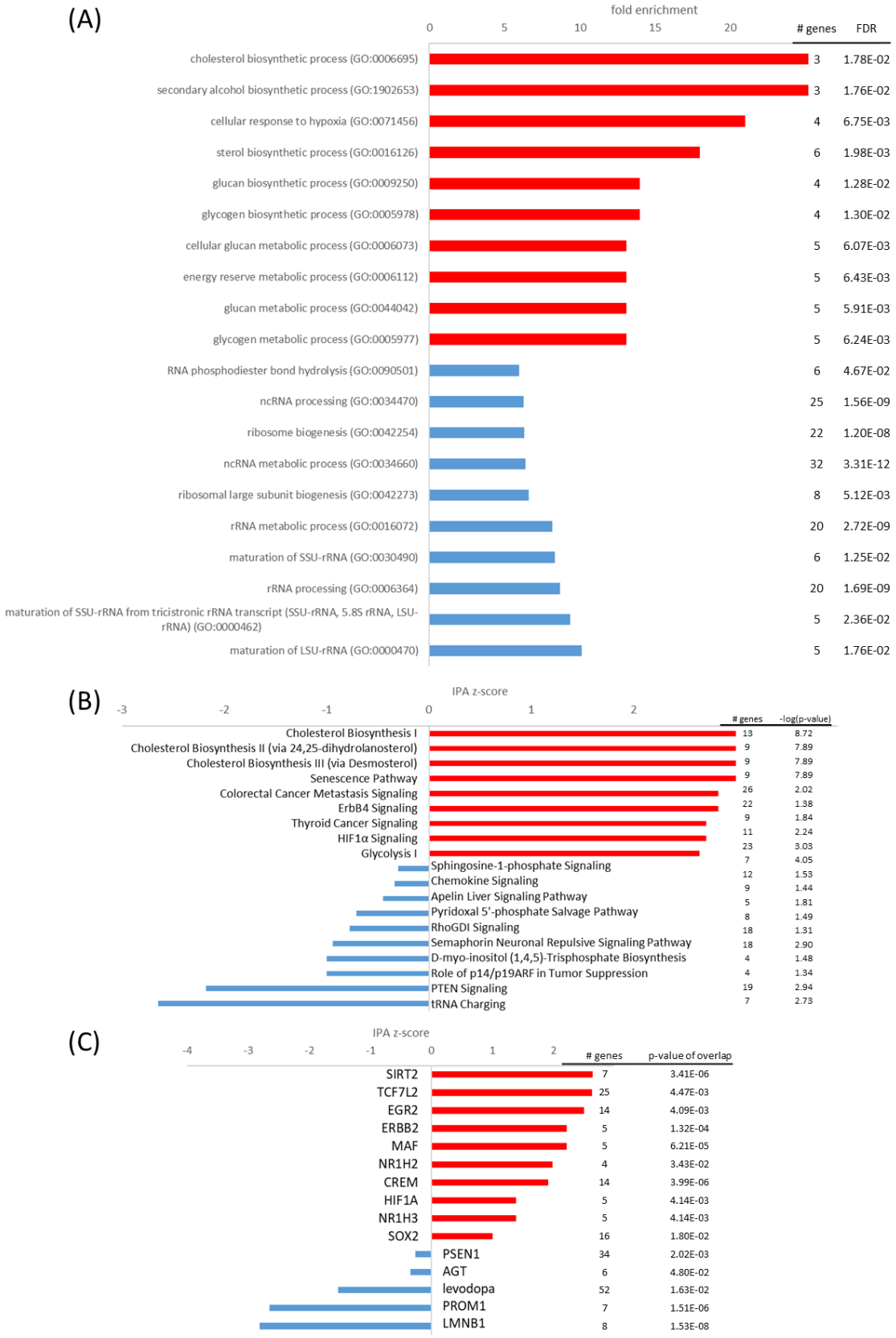

Fig. 2.5: Top pathways and upstream regulators for the nCLU cell line at hypoxia. *(A) Top GO terms enriched in upregulated (red) and downregulated (blue) genes; (B) Top IPA canonical pathways activated (red, positive z-score) and inhibited (blue, negative z-score); (C) Top upstream regulators activated (red, positive z-score) and inhibited (blue, negative z-score) in the nCLU cell line at hypoxia in comparison to the mock cell line.*

Response to hypoxia is substantially mediated by the hypoxia-inducible factor (HIF1), which is a master regulator that activates the transcription of many genes involved in energy metabolism, apoptosis and oxygen delivery. In the present study, nCLU transfected cell lines increased *HIF1A signaling* (z = 2.7, -log(p) = 3.0), while HIF1A was also found to be an upstream regulator (z = 1.4, $p < 0.01$). Additionally, in GO analyses, *cellular response to hypoxia* was enhanced in the nCLU cell line (FE = 21.0, $p_{FDR} < 0.01$). However, as in normoxic conditions, OPRD1 demonstrated low expression in the nCLU cell line (log2FC = -1.32), which might be disadvantageous in dealing with hypoxic conditions.

The oxidative stress response of the nCLU cell line is characterized by mitochondrial dysregulation

Oxidative stress is an inevitable by-product of oxidative metabolism and reflects a state of imbalance between reactive oxygen species (ROS) and substances that are involved in their detoxification, which may cause damage to proteins, lipids and DNA. Diving mammals may counteract oxidative stress through elevated antioxidant levels in its brain (Geßner et al. 2022; Fabrizius et al. 2016). At oxidative stress conditions, antioxidants, such as the glutathione S-transferase alpha 4 (GSTA4, log2FC = 1.80), thioredoxin 1 (TXN1, log2FC = 1.40), peroxiredoxin 3 (PRDX3, log2FC = 1.40), selenoprotein F (SELENOF, log2FC = 1.27) and the putative glutathione peroxidase 8 (GPX8, log2FC =1.00) were increased in the nCLU cell line, which may partly be ascribed to activation of nuclear factor, erythroid 2 like 2 (NFE2l2, also abbreviated as NRF2, z = 2.2, $p < 0.05$) as upstream regulator. The transcription factor NRF2 plays a pivotal role controlling the expression of antioxidant genes that exert neuroprotective functions (Saha et al. 2020). Nevertheless, the nCLU cell line exhibited a profound *response to oxidative stress* (FE = 2.8, $p_{FDR} < 0.05$), characterized by *mitochondrial dysfunction* (-log(p) = 8.1), enhanced *oxidative phosphorylation* (z = 6.6, -log(p) = 4.3) and *TCA cycle* (z = 4.0, -log(p) = 5.9) (Fig. 2.6). Mitochondrial complexes such as cytochrome c oxidase subunits COX7A2 (log2FC = 1.91), COX4I1 (log2FC = 1.28), COX5B (log2FC = 1.10), COX7C (log2FC = 1.09), NADH:ubiquinone oxidoreductase subunits NDUFB1 (log2FC = 1.37), NDUFC2 (log2FC = 1.36), NDUFB9 (log2FC = 1.34), NDUFV2 (log2FC = 1.20), NDUFA7 (log2FC = 1.12), NDUFS4 (log2FC =1.06), NDUFA9 (log2FC = 1.03), isocitrate dehydrogenases IDH3A (log2FC = 1.08), IDH1 (log2FC = 1.05) and succinate dehydrogenase subunit SDHB (log2FC =1.09) exhibited high expression levels. Dysregulated aerobic respiration may have led to *apoptotic mitochondrial changes* (FE = 4.3, $p_{FDR} < 0.05$), increased *proteasome assembly* (FE = 6.0, $p_{FDR} < 0.05$) and *autophagy* (z = 3.3, -log(p) = 1.7), which might serve to clear cells from dysfunctional mitochondria. Important genes involved in autophagy processes such as BCL2 interacting protein 3 (BNIP3, log2FC = 1.11), VPS35 retromer complex component (VPS35, log2FC = 1.01), as well as FUN14 domain containing 1 (FUNDC1, log2FC = 1.76) were upregulated in the oxidative-stress-challenged nCLU cell line.

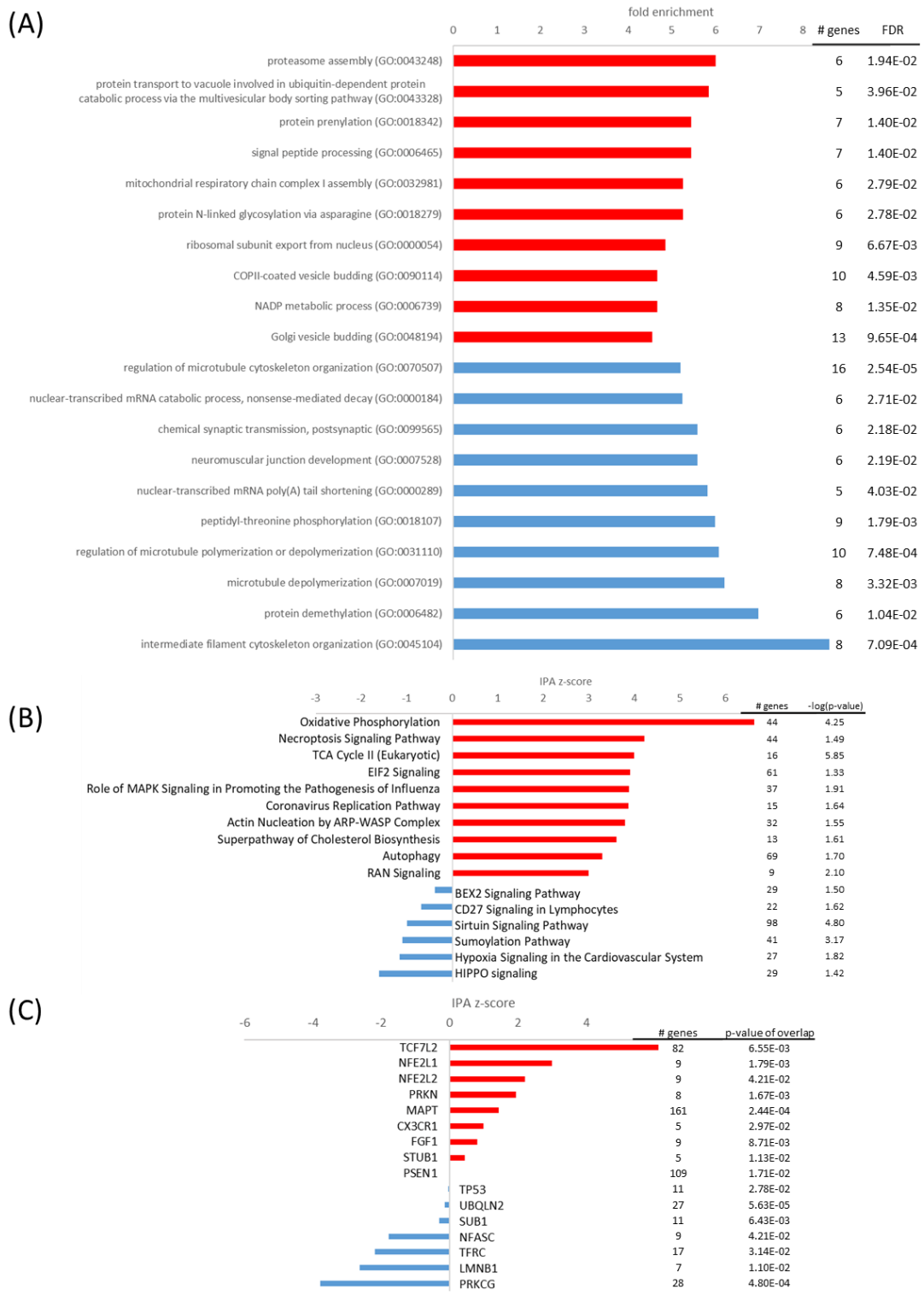

Fig. 2.6: Top pathways and upstream regulators for the nCLU cell line at oxidative stress. *(A) Top GO terms enriched in upregulated (red) and downregulated (blue) genes; (B) Top IPA canonical pathways activated (red, positive z-score) and inhibited (blue, negative z-score); (C) Top upstream regulators activated (red, positive z-score) and inhibited (blue, negative z-score) in the nCLU cell line at oxidative stress in comparison to the mock cell line.*

Ultimately, autophagy processes and redox imbalance may have induced *ferroptosis* (z = 1.2, -log(p) = 1.9), which is an iron-dependent form of non-apoptotic cell death (Tang et al. 2021) and *necroptosis signaling pathway* (z = 4.2, -log(p) = 1.5), another form of non-apoptotic cell death (Newton and Manning 2016). In accordance, low expression of glial cell line derived neurotrophic factor (GDNF, log2FC = -1.45) may reduce survival pathways (Cintrón-Colón et al. 2020). In summary, the nCLU-transfected cells attempted to counter the deleterious effects of dysregulated mitochondrial aerobic respiration by increasing antioxidant expression, but ultimately experienced elevated cell death at oxidative stress conditions.

Transcriptome response of the sCLU-transfected cell line

The sCLU-transfected cells promote glycolytic capacity and protein folding at normoxia

In contrast to the nCLU cell line, the sCLU-transfected cells already demonstrated substantial differences in gene expression at normoxic conditions, which included energy metabolism and autophagy processes. Adenosine triphosphate (ATP) provides the energy necessary to drive all energy-demanding processes in living cells. Elevated ATP levels of sCLU-transfected cells have already been demonstrated in cell viability assays (Geßner et al. 2020) and were confirmed in this study. At aerobic conditions, the main ATP production usually takes place at the mitochondrial electron transport chain. However, this process is also associated with the generation of ROS, which can be detrimental in high concentrations. The high expression of pyruvate dehydrogenase kinase 1 (PDK1, log2FC = 1.20) in sCLU cells might inactivate pyruvate dehydrogenase and consequently inhibit the first step of the citric acid cycle. In carcinoma and fibroblast cell cultures, overexpression of PDK1 shifted ATP production from mitochondrial respiration to glycolysis, thereby attenuating hypoxic ROS generation and rescuing cells from hypoxia-induced apoptosis (Papandreou et al. 2006; Kim et al. 2006). Additionally, low expression of myeloid translocation gene 16 product (MTG16, also abbreviated as CBFA2T3, log2FC = -1.14) was observed in the sCLU cell line. MTG16 reduced the expression of PDK1 and genes involved in glycolysis in lymphoma cells (Kumar et al. 2013), and reduced levels of MTG16 might therefore indicate enhanced glycolytic capacity. Consistent with this, sCLU expression correlated with high expression of the monocarboxylate transporter 4 (MCT4, also abbreviated as SLC16A3, log2FC = 1.20). MCT4 has an important role in tissues reliant on glycolysis (Halestrap and Wilson 2012), by facilitating lactate efflux and preventing pyruvate efflux, thereby enabling conversion of pyruvate to lactate and regeneration of NADH for glycolysis (Halestrap and Wilson 2012). MCT4 was also upregulated in hooded seal brain slices that were exposed to hypoxia and reoxygenation *in vitro* (Hoff et al. 2017) and MCT4 was more highly expressed in hooded seal than in mouse neurons (Geßner et al. 2022). Exported lactate by MCT4 might be further metabolized by neighboring astrocytes in the hooded seal brain that exhibit high levels of lactate dehydrogenase b (LDHB) (Hoff et al. 2016), as suggested by the 'reverse lactate shuttle' hypothesis, first presented by Mitz et al. (2009). Additionally, aerobic metabolism was found to be

decreased in the visual cortices of hooded seals compared to ferrets (Fabrizius et al. 2016). In contrast, Geßner et al. (2022) concluded that mitochondrial function and numbers may have been enhanced, while glycolytic capacity was slightly lower, in neurons of the hooded seal compared to mice. Arguably, these differences might be related to the choice of the non-diving model organism, i.e., ferrets vs mice, which are known to maintain quite different basal metabolic rates (Geßner et al. 2022). Further, we here consider the effect of particular genes, whereas Geßner et al. (2022) analyzed the neuronal transcriptome as a whole. In summary, alterations of pathways by sCLU during normoxia may indicate a preparation or pre-adaptation of hooded seals to upcoming diving-associated stress conditions, such as low oxygen levels or ROS production. To prepare for these conditions, capacity for aerobic respiration might be decreased and capacity for anaerobic glycolysis might be increased.

Cellular stress responses comprise mechanisms that minimize acute damage and promote cell survival. Oxidative stress might denature proteins, thereby disrupting protein homeostasis (proteostasis) necessary for biological function and cell metabolism (Chaplot et al. 2020). Chaperones can help defend the cell against damage by facilitating protein folding, ensuring that proteins assume their necessary shape. Misfolded proteins may be degraded by proteasomes or autophagy, to remove potentially toxic aggregates. Clusterin (CLU) may play an important role as stress-induced secreted chaperone protein, mediating proteasomal degradation of misfolded proteins (Satapathy and Wilson 2021; Jones 2002b), and CLU is known to protect neuronal cells against intracellular protein aggregation and cytotoxicity (Gregory et al. 2017). Interestingly, in IPA analyses the *endoplasmic reticulum stress pathway* (z = 0.4, -log(p) = 5.23) and *unfolded protein response* (z = 0.3, -log(p) = 2.84) were slightly activated in the normoxic sCLU-transfected cells, suggesting the contribution of CLU to protein homeostasis in the hooded seal brain. In addition, the chaperone peptidylprolyl isomerase C (PPIC, log2FC= 1.15) was upregulated in sCLU cells, which may also be important for coping with oxidative stress (Kumawat et al. 2020; Malesević et al. 2010). Additionally, *autophagy* (z = 0.2, -log(p) = 2.51), which promotes degradation of damaged proteins was slightly activated in the sCLU-transfected cell line. In particular, BNIP3, which is necessary for clearing dysfunctional mitochondria with low membrane potential and reducing the buildup of ROS to promote cell survival (O'Sullivan et al. 2015), was observed to be more highly expressed in the sCLU cell line (log2FC = 1.33). Furthermore, *NRF2 mediated oxidative stress response* (z = -2.7, -log(p) = 1.5) (Fig. 2.7), which coordinates the basal and stress-inducible activation of a vast array of cytoprotective genes, like antioxidants (Saha et al. 2020), was downregulated in sCLU cells. A reduction of this pathway may imply decreased stress and reduced necessity to detoxify ROS. In accordance with our results, Geßner et al. (2020) found no increased caspase activity and ROS amount for sCLU-transfected HN33 cells at normoxia, indicating no increased stress. In conclusion, sCLU might contribute to the stress tolerance of the hooded seal brain by improving autophagy and protein folding pathways as well as glycolytic capacity.

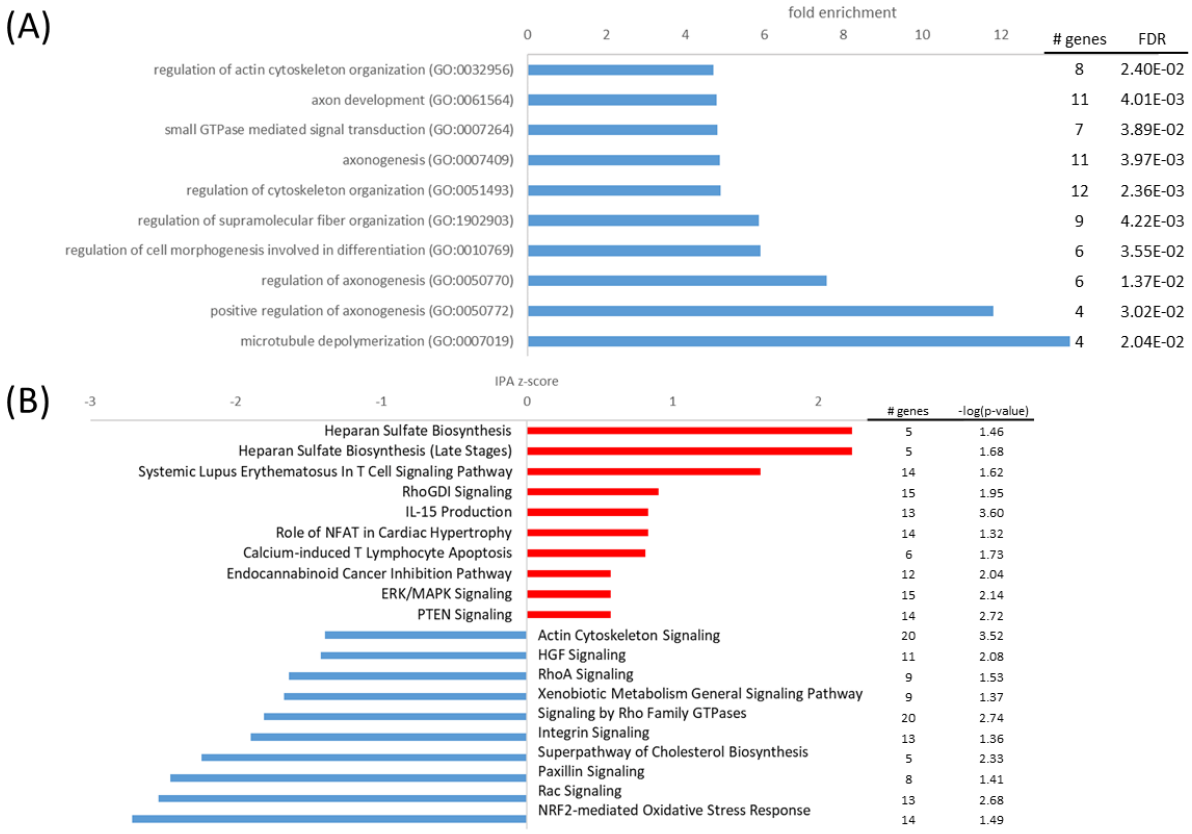

Fig. 2.7: Top pathways and upstream regulators for the sCLU cell line at normoxia. *(A) Top GO terms enriched in upregulated (red) and downregulated (blue) genes; (B) Top IPA canonical pathways activated (red, positive z-score) and inhibited (blue, negative z-score) in the sCLU cell line at normoxia in comparison to the mock cell line.*

The sCLU cell line exhibits elevated hypoxia response

When exposed to hypoxic stress, the sCLU cell line exhibited a similar transcriptome response to the nCLU-transfected cells. IPA pathways *glycolysis I* (z = 3.0, -log(p) = 3.4), *gluconeogenesis* (z = 2.1, -log(p) = 2.7) and *glycogen biosynthesis* (-log(p) = 2.0) and GO terms *glycolytic process* (FE = 5.7, $p_{FDR} < 0.05$) and *glycogen biosynthetic process* (FE = 8.1, $p_{FDR} < 0.05$) were enhanced (Fig. 2.8). The related glycogen storing enzyme EPM2A, important for accurate accumulation of glycogen (Raththagala et al. 2015), also demonstrated increased transcription (log2FC = 2.07). On the other hand, *aerobic respiration* (FE = 3.3, $p_{FDR} < 0.05$) was decreased in sCLU-transfected cells. Aerobic respiration may have been reduced by high expression of PDK1 (log2FC = 1.01) and low expression of MTG16 (log2FC = -0.46) in sCLU-transfected cells, which inhibit the first step of the TCA cycle and improve glycolytic capacity (Kim et al. 2006; Kumar et al. 2013; Papandreou et al. 2006). However, regulation of PDK1 and MTG16 genes was not as strong as at normoxia. This was probably related to that mock cells to some extent also downregulated aerobic respiration at hypoxia and the difference between these cell lines may have become less distinct.

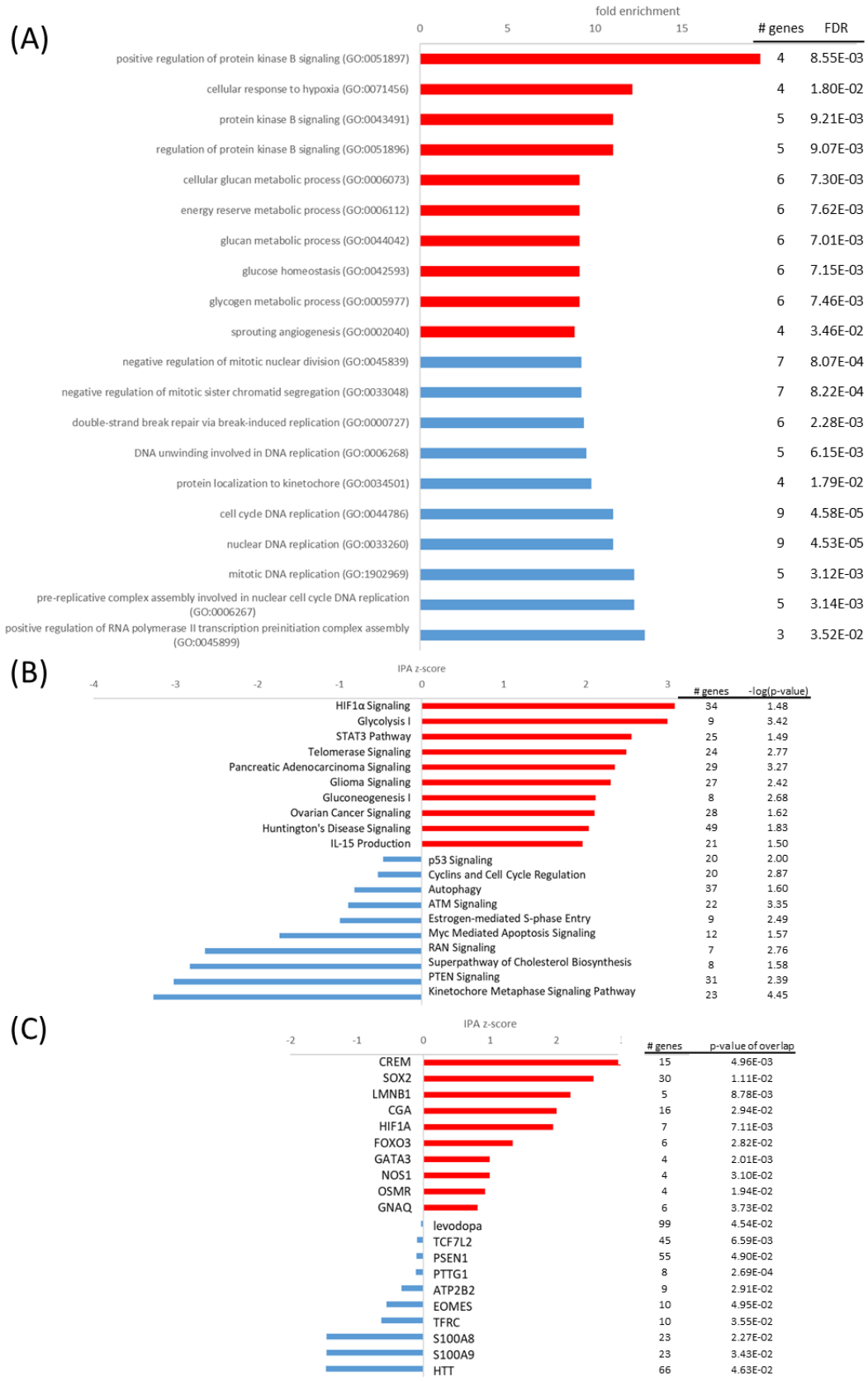

Fig. 2.8: Top pathways and upstream regulators for the sCLU cell line at hypoxia. *(A) Top GO terms enriched in upregulated (red) and downregulated (blue) genes; (B) Top IPA canonical pathways activated (red, positive z-score) and inhibited (blue, negative z-score); (C) Top upstream regulators activated (red, positive z-score) and inhibited (blue, negative z-score) in the sCLU cell line at hypoxia in comparison to the mock cell line.*

GO term *cellular response to hypoxia* (FE = 21.0, $p_{FDR} < 0.05$) in the sCLU cell line may have also been mediated by HIF1A as upstream regulator (z = 2.0, p < 0.01) and *HIF1A signaling* (z = 3.1, -log(p) = 1.5). Furthermore, egl-9 family hypoxia-inducible factor 1 (EGLN1) was highly expressed (log2FC = 1.06), which hydroxylates HIF proteins and thereby targets them for degradation (Fong and Takeda 2008). However, the hydroxylation reaction might have been attenuated by limited oxygen availability. In addition to high expression of BNIP3 (log2FC = 1.36), HIF1-upregulated mitochondria-localized glutamic acid rich protein (MGARP, log2FC = 1.33) was highly expressed in sCLU cells and might further support mitophagy (Jia et al. 2014), which may reduce deleterious ROS by clearance of dysfunctional mitochondria. Additionally, upregulation of PPIC (log2FC = 2.06) may have further improved protein folding and reduced ER stress in the sCLU-transfected cell line (Kumawat et al. 2020; Malesević et al. 2010). According to described neurotrophic functions, *intrinsic apoptotic signaling* (FE = 3.6, $p_{FDR} < 0.05$) as well as *MYC mediated apoptosis* (z = -1.7, -log(p) = 1.6) were found to be downregulated in the sCLU cell line. Decreased apoptosis is in line with previous findings, e.g. as reflected by decreased caspase activity and phosphatidylserine exposure in transfected cells (Geßner et al. 2020). Overall, sCLU cells might enhance stress resistance and reduce apoptosis in response to hypoxia.

The sCLU-transfected cells show limited transcriptome response at oxidative stress despite elevated viability

When applying oxidative stress, the sCLU cell line exhibited a limited DEG response. This seems counterintuitive, since sCLU cells had a significantly higher viability in oxidative stress than nCLU and mock cells (Geßner et al. 2020). Normoxic (i.e., constitutional) differences in gene expression might therefore already have prepared sCLU-transfected cells for oxidative stress, indicating a pre-adaptive response to upcoming stress conditions.

Nevertheless, the upregulation of some genes might assist sCLU in protein folding such as cAMP responsive element binding protein 3-like 2 (CREB3L2, log2FC = 1.26) and PPIC (log2FC = 2.17). CREB3L2 protected cells from ER stress-induced death in a neuroblastoma cell line (Kondo et al. 2007), while the chaperone PPIC might have further promoted protein folding and reduce oxidative stress (Malesević et al. 2010). Additionally, pathways involved in synaptic signaling were elevated in the sCLU cell line at oxidative stress such as *calcium signaling* (z = 2.5, -log(p) = 1.8), *semaphorin neuronal repulsive signaling* (z = 1.3, -log(p) = 1.9) and *synaptic long term depression* (z = 1.9, -log(p) = 2.8) (Fig. 2.9). High expression of voltage-dependent calcium channels CACNA1G (log2FC = 1.48) and CACNA1I (log2FC = 1.32) may have facilitated calcium flux and subsequent binding of calcium to synaptotagmin I (SYT1, log2FC = 1.33), which may have triggered neurotransmitter release at the synapse (Fernández-Chacón et al. 2001). Especially serotonin may have functioned as neurotransmitter in the oxidative stress-exposed sCLU cell line. Tryptophan hydroxylase 2 (TPH2,

log2FC = 1.74), which catalyzes the first rate-limiting step in serotonin biosynthesis (Höglund et al. 2019), as well as the serotonin receptor HTR3A (log2FC = 1.43) demonstrated increased expression. Binding of serotonin to HTR3A causes fast, depolarizing responses in neurons (Barnes et al. 2009), but may also regulate the development of the mammalian central nervous system (Engel et al. 2013). Described genes might support observed decrease in lipid peroxidation and caspase activity in a previous study (Geßner et al. 2020) and protect sCLU-transfected cells from oxidative stress induced cell death. The majority of preventive measures in sCLU cells though may have already been taken at normoxic conditions.

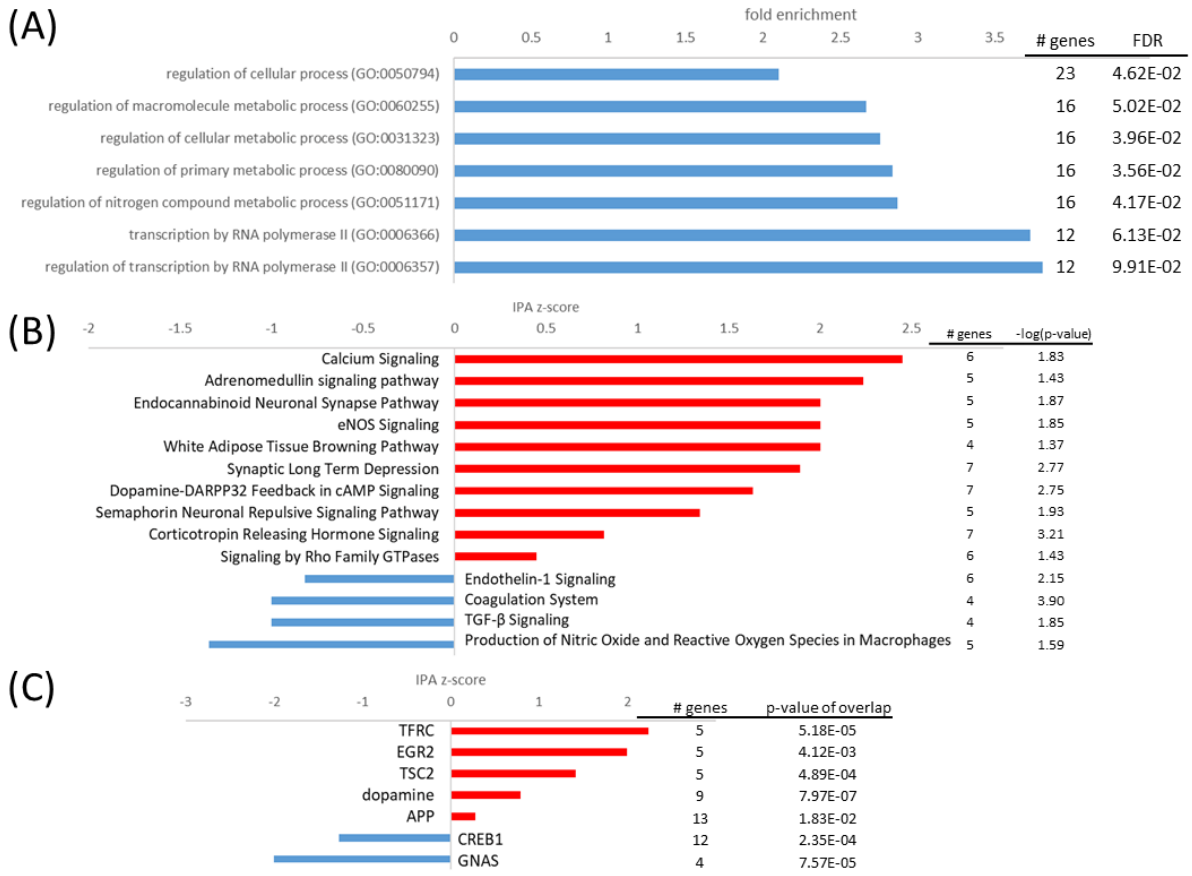

Fig. 2.9: Top pathways and upstream regulators for the sCLU cell line at oxidative stress. *(A) Top GO terms enriched in upregulated (red) and downregulated (blue) genes; (B) Top IPA canonical pathways activated (red, positive z-score) and inhibited (blue, negative z-score); (C) Top upstream regulators activated (red, positive z-score) and inhibited (blue, negative z-score) in the sCLU cell line at oxidative stress in comparison to the mock cell line.*

Transcriptome response of the S100B-transfected cell line

The S100B-transfected cells reduce synaptic signaling pathways at normoxia

Similar to the sCLU cell line, the S100B-transfected cells exhibited elevated ATP levels at normoxic conditions, which is in accordance to a previous study (Geßner et al. 2020). Likewise, *glycolytic process* (FE = 6.6, $p_{FDR} < 0.05$) and MCT4 expression (log2FC = 1.87) were elevated in the S100B cells at

normoxia, while the TCA cycle may have been inhibited by high expression of PDK1 (log2FC = 1.14). Consequently, capacity for glycolytic metabolism may have been increased and aerobic respiration decreased in the S100B cell line at normoxic conditions.

Furthermore, S100B may play a role in neurodegeneration or neuroprotection (Foster et al. 2019). Although genes associated with the GO term *neuron development* (FE = 2.3, $p_{FDR} < 0.05$) demonstrated reduced expression in S100B-transfected cells, increased expression of neurotrophic factors such as growth-associated protein 43 (GAP43, log2FC = 1.52) and brain-derived neurotrophic factor (BDNF, log2FC = 0.83) might enhance neuron growth and survival. GAP43 may regulate synaptic plasticity and neurite outgrowth (Sheu et al. 1994) and is also an important mediator of the neuroprotective effects of BDNF in connection with excitotoxicity (Gupta et al. 2009). The growth factor BDNF is one of the most widely distributed and extensively studied neurotrophins in the mammalian brain (Kowiański et al. 2018), and is associated with neuronal maintenance, survival, plasticity, and neurotransmitter regulation (Giacobbo et al. 2019). Furthermore, the neurotrophic growth factor pleiotrophin (PTN, log2FC = 0.37) and its receptor anaplastic lymphoma kinase (ALK, log2FC = 1.20) were upregulated in S100B-transfected cells (Kalamatianos et al. 2018). Loss of PTN in pericyte-ablated mice has been linked to a rapid neurodegeneration cascade (Nikolakopoulou et al. 2019), which illustrates its role in neuroprotection. Additionally, tissue-type plasminogen activator (PLAT, log2FC = 1.03) and a PLAT inhibitor (SERPINI1, log2FC = 1.07), which are involved in synaptic plasticity (Calabresi et al. 2000) and have been reported to facilitate neuron survival depending on concentration and isoform (Chevilley et al. 2015), were upregulated in S100B cells. In summary, although most genes involved in neuron development were slightly downregulated in normoxic S100B cells, highly upregulated important neurotrophic factors may have promoted neuronal plasticity and survival.

During synaptic signaling, the presynaptic neuron membrane at the synapse depolarizes, causing influx of calcium ions and release of neurotransmitters. Reestablishing the resting membrane potential, calcium gradient and neurotransmitter levels, are all highly energy-intensive processes in the brain. S100B is involved in calcium homeostasis and thereby presumably also in regulating synaptic plasticity (Donato et al. 2013). It has been suggested that its high expression in marine mammals may help prevent excitotoxicity by reducing free intracellular Ca^{2+} and thereby attenuate continued release of glutamate and other neurotransmitters (Geiseler et al. 2016). In the S100B-transfected cells neurotransmitter release might be reduced by activation of *opioid signaling* (z = 1.2, -log(p) = 2.1) (Fig. 2.10), which can prevent calcium ion influx and facilitate potassium ion efflux, thereby causing membrane hyperpolarization and a reduced neurotransmitter release (Gopalakrishnan et al. 2021). The upregulated OPRD1 (log2FC = 0.80) may have facilitated clearance of neurotransmitters from the synaptic cleft and prevent neuroexcitotoxicity (He et al. 2013).

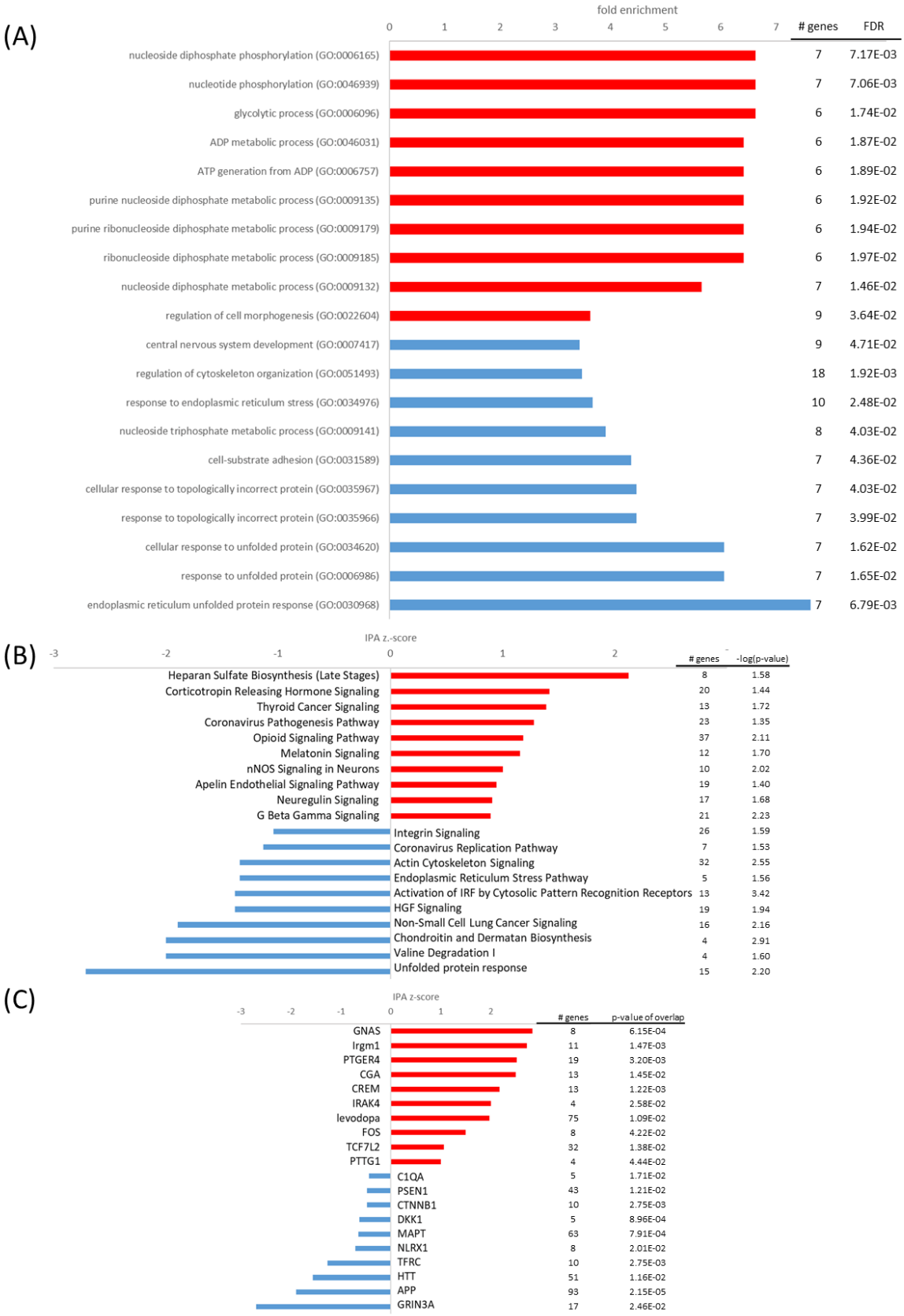

Fig. 2.10: Top pathways and upstream regulators for the S100B cell line at normoxia. *(A) Top GO terms enriched in upregulated (red) and downregulated (blue) genes; (B) Top IPA canonical pathways activated (red, positive z-score) and inhibited (blue, negative z-score); (C) Top upstream regulators activated (red, positive z-score) and inhibited (blue, negative z-score) in the S100B cell line at normoxia in comparison to the mock cell line.*

Furthermore, levels of purkinje cell protein 4 (PCP4) were decreased in S100B cells (log2FC = -1.96). PCP4 is a small calmodulin-binding protein that promotes calcium exchange and neurotransmitter release (Renelt et al. 2014). Its downregulation might further support a reduction of neurotransmitter levels in S100B cells. A previous study that compared the transcriptomes of hooded seal and mouse neurons also indicated reduced glutamatergic transmission in the seal, by reduced expression of glutamate receptors, while glutamate uptake was increased (Geßner et al. 2022). Noh et al. (2022) stated that glutaminergic synapse function might have been commonly positively selected in pinnipeds, indicating its importance for the adaptation to the marine environment. In summary, S100B may contribute to the neuronal hypoxia tolerance by reducing neurotransmission and thus, our findings support the observations of Geiseler et al. (2016) and Geßner et al. (2022). A reduction in neurotransmission might ultimately serve to reduce energy consumption and thereby the oxygen needs of neuronal cells.

The S100B cell line exhibits elevated hypoxia response

In analogy to the other transfected cell lines, hypoxia response of the S100B cell line might have been mediated by activated *HIF1A signaling* (z = 3.1, -log(p) = 1.4) (Fig. 2.11). GO terms *tricarboxylic acid cycle* (FE = 6.37, $p_{FDR} < 0.05$), *oxidative phosphorylation* (FE = 6.11, $p_{FDR} < 0.01$) and *aerobic respiration* (FE = 5.4, $p_{FDR} < 0.01$) as well as IPA pathway *TCA cycle* (z = -2.6, -log(p) = 2.1) were decreased in S100B-transfected cells, but PDK1 upregulation (log2FC = 0.65) was not as prominent in inhibiting the first step of TCA cycle as in normoxic conditions. In accordance with the putative function of S100B GO term *calcium-ion regulated exocytosis* (FE = 6.1, $p_{FDR} < 0.05$) was enriched in upregulated genes of the S100B-transfected cells. Furthermore, *opioid signaling* (z = 1.9, -log(p) = 1.9) and *synaptogenesis signaling pathway* (z = 1.6, -log(p) = 1.4) were enhanced in the S100B-transfected cells when subjected to hypoxia. As mentioned before, high expression of OPRD1 (log2FC = 0.99) and low expression of PCP4 (log2FC = -1.89) may reduce neurotransmitter levels and protect cells from hypoxia-induced excitotoxicity (He et al. 2013; Renelt et al. 2014). Additionally, GAP43 (log2FC = 1.45) and BDNF (log2FC = 1.17) may facilitate neuron survival (Gupta et al. 2009; Giacobbo et al. 2019). According to described neurotrophic functions, *intrinsic apoptotic signaling* (FE = 4.8, $p_{FDR} < 0.01$) was enriched in downregulated genes of S100B-transfected cells at hypoxic conditions. Therefore, in addition to decreasing aerobic respiration, S100B may facilitate neuroprotection of neuronal cells by downregulating synaptic signaling and upregulating neurotrophic factors at hypoxic conditions.

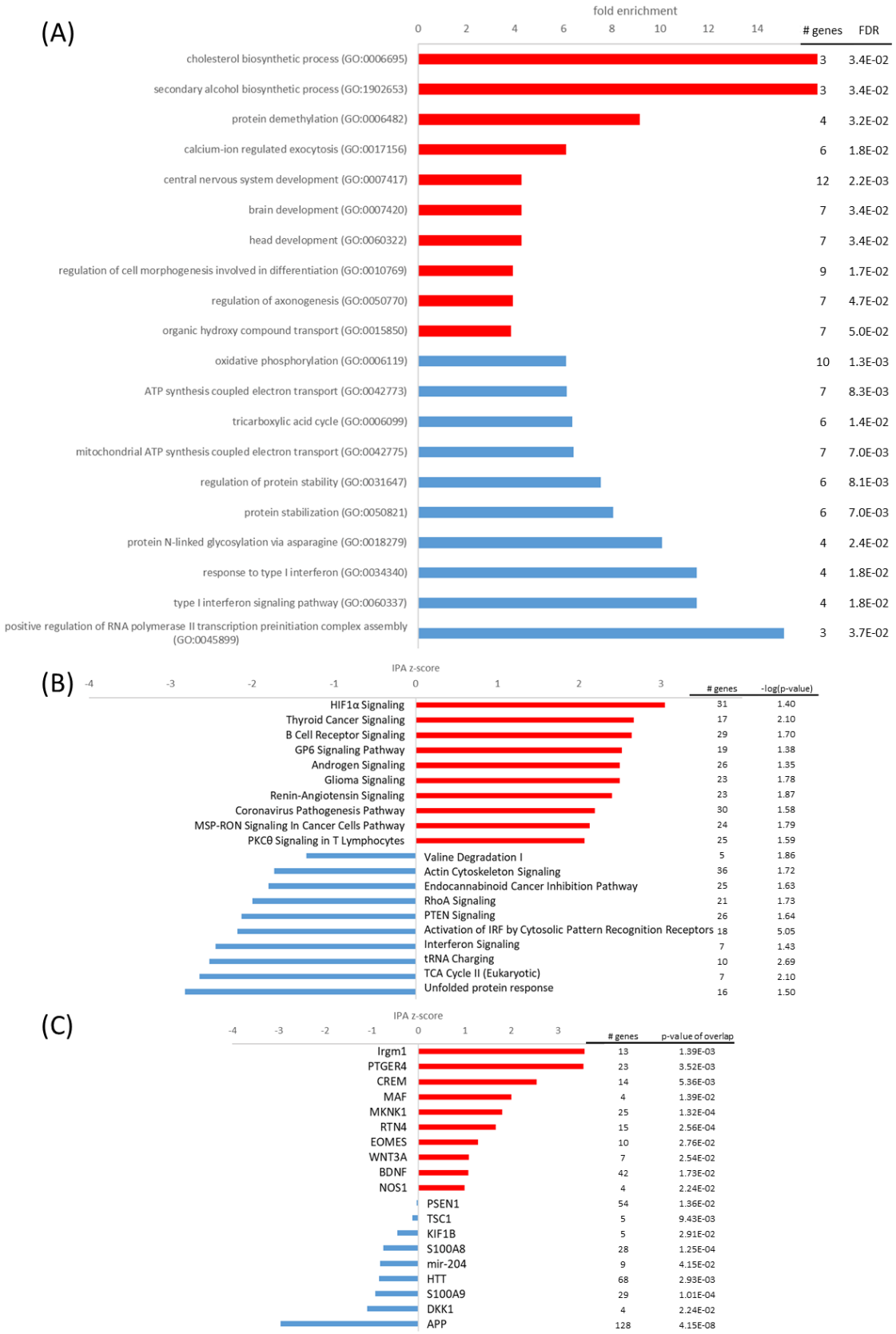

Fig. 2.11: Top pathways and upstream regulators for the S100B cell line at hypoxia. *(A) Top GO terms enriched in upregulated (red) and downregulated (blue) genes; (B) Top IPA canonical pathways activated (red, positive z-score) and inhibited (blue, negative z-score); (C) Top upstream regulators activated (red, positive z-score) and inhibited (blue, negative z-score) in the S100B cell line at hypoxia in comparison to the mock cell line.*

The S100B cell line demonstrates limited transcriptome response at oxidative stress despite elevated viability

Similar to the sCLU-transfected cells, the S100B cell line did not exhibit a diverse DEG response at oxidative stress. However, elevated viability (Geßner et al. 2020) may point to pre-adaptive mechanisms already carried out at normoxia. When exposed to oxidative stress, the only two activated pathways in IPA analysis were *semaphorin neuronal repulsive signaling pathway* (z = 1.9, -log(p) = 3.07) and *IL-15 production* (z = 1, -log(p) = 1.51) (Fig. 2.12). The former already demonstrated activation at normoxia (z = 0.8, -log(p) = 2.98). Semaphorin such as SEMA6D (log2FC = 1.35) and the semaphorin co-receptor neuropilin 1 (NRP1, log2FC = 1.02) may have played an essential role in *axonal guidance signaling* (-log(p) = 2.4) and thereby overall nervous system development at oxidative stress conditions (Jongbloets and Pasterkamp 2014). Additionally, high expression of OPRD1 (log2FC = 1.06) and low expression of PCP4 (log2FC = -1.86) may have facilitated neuroprotection by reduction of neurotransmitter levels as mentioned before (He et al. 2013; Renelt et al. 2014). These mechanisms may aid in protecting S100B-transfected cells from oxidative stress induced cell death. However, metabolic alterations at normoxia may have already prepared cells for imminent stress conditions.

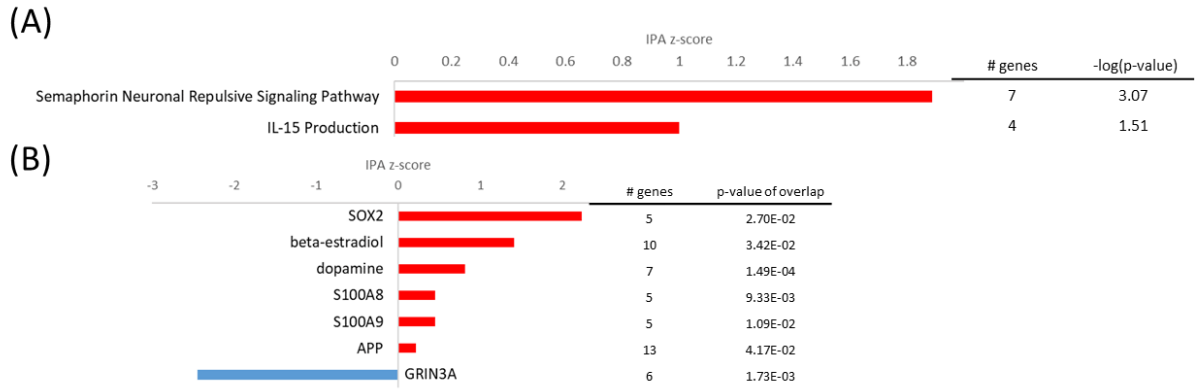

Fig. 2.12: Top pathways and upstream regulators for the S100B cell line at oxidative stress. *(A) Top IPA canonical pathways activated (red, positive z-score) and inhibited (blue, negative z-score); (B) Top upstream regulators activated (red, positive z-score) and inhibited (blue, negative z-score) in the S100B cell line at oxidative stress in comparison to the mock cell line.*

Conclusion

Clusterin (CLU) and S100B are highly expressed in the hooded seal brain and probably represent two of numerous factors that contribute to its intrinsic hypoxia tolerance. In order to investigate their potential roles, we transfected HN33 cells with soluble clusterin (sCLU), nucleus clusterin (nCLU) and S100B, subjected these cell lines to three challenges; normoxia, hypoxia and oxidative stress, and studied viability and differential gene expression (DEG) responses (Tables 2.1-2.3). We found that aerobic metabolism was reduced in the sCLU and S100B cell lines, and that synaptic signaling pathways were reduced in S100B-transfected cells, at normoxic conditions. These transcriptomic responses might reduce production of reactive oxygen species (ROS), while also reducing the energy consumption of neuronal cells. Additionally, autophagy processes appeared to be important for cellular homeostasis in sCLU-transfected cells, which might ultimately protect cells from apoptosis. When oxidatively stressed, sCLU- and S100B-transfected cells did not mount similar gene regulatory responses, but nevertheless demonstrated improved viability compared to mock-transfected cells, presumably due to a pre-adaptive (constitutional) response, seen already under normoxic conditions, in preparation for upcoming stress conditions. In contrast to this effect, the nCLU cell line exhibited elevated stress and apoptosis pathways in response to oxidative stress, which suggests a reduced basal protection against oxidative damage in this cell line. Furthermore, known hypoxia response genes and pathways, such as HIF1A signaling and glycogen metabolism, were enhanced in transfected cells when exposed to hypoxic conditions. While the roles of CLU and S100B in neurodegenerative diseases are being debated, we found evidence for the upregulation of neuroprotective effects in cell lines overexpressing these genes, in response to hypoxia and oxidative stress.

The findings of the present study have been demonstrated in a cell culture model and effects would still need to be confirmed *in vivo*. Unfortunately, it is not feasible to obtain samples from naturally diving hooded seals that experience hypoxia. Alternatively, fresh brain slices exposed to hypoxia *in vitro* could mimic more closely natural conditions than cell culture. However, capturing hooded seals and performing experiments on fresh tissue requires great effort and have only been done on rare occasions (Czech-Damal et al. 2014; Hoff et al. 2017). Cell culture experiments therefore represent a great possibility to mimic hypoxic conditions.

In this study, we highlighted pathways and targets of hypoxia tolerance that may provide clues to tackle neurodegenerative diseases such as Alzheimer's disease and Parkinson's disease. While the cell culture experiments indicated neuroprotective effects of CLU and S100B at hypoxia and oxidative stress, these results yet require confirmation in *in vivo* studies.

Table 2.1: Selection of significant GO terms enriched in transfected cell lines compared to mock cell line.

	Normoxia			Hypoxia			Oxidative stress		
	nCLU	sCLU	S100B	nCLU	sCLU	S100B	nCLU	sCLU	S100B
(A) Energy metabolism									
glycolytic process (GO:0006096)			6.6	9.8	5.7				
aerobic respiration (GO:0009060)					3.4	5.4	3.8		
glycogen biosynthetic process (GO:0005978)				14.0	8.1				
(B) Neuron development									
neuron development (GO:0048666)		4.0	2.3	2.9	2.2		2.0		
mitotic cell cycle (GO:0000278)			3.1		3.6	2.0	1.8		
ribosome biogenesis (GO:0042254)				6.3	4.6	2.5	2.5		
(C) Synaptic signaling									
chemical synaptic transmission, postsynaptic (GO:0099565)							5.6		
calcium-ion regulated exocytosis (GO:0017156)						6.1			
(D) Stress response									
cellular response to hypoxia (GO:0071456)				21.0	12.2				
intrinsic apoptotic signaling pathway (GO:0097193)					3.6	4.8			
apoptotic mitochondrial changes (GO:0008637)							4.3		
response to oxidative stress (GO:0006979)							2.8		
Other									
cholesterol biosynthetic process (GO:0006695)				25.2		16.5			

Significant GO terms related to (A) energy metabolism, (B) neuron development, (C) synaptic signaling and (D) stress response, were selected that were enriched in upregulated (red) and downregulated genes (blue) for each cell line and treatment, when compared to the mock cell line at each respective condition. Displayed are fold enrichments of pathways.

Table 2.2: Selection of significant IPA canonical pathways for transfected cell lines compared to mock cell line.

	Normoxia			Hypoxia			Oxidative stress		
	nCLU	sCLU	S100B	nCLU	sCLU	S100B	nCLU	sCLU	S100B
(A) Energy metabolism									
Gluconeogenesis I				1.6	2.1				
Glycolysis I				2.6	3.0				
Oxidative Phosphorylation							6.6		
TCA Cycle II (Eukaryotic)						-2.6	4.0		
(B) Neuron development									
NGF Signaling				1.3		1.3	2.5		
PTEN Signaling		0.6		-2.2	-3.0	-2.1			
Reelin Signaling in Neurons				1.1	1.6	0.4	1.4		
Semaphorin Neuronal Repulsive Signaling Pathway		0.5	0.8	-0.9		-0.4		1.3	1.9
(C) Synaptic signaling									
Calcium Signaling								2.4	
Endocannabinoid Neuronal Synapse Pathway								2.0	
nNOS Signaling in Neurons			1.0						
Opioid Signaling Pathway			1.2			1.9			
Synaptic Long Term Depression								1.9	
Synaptic Long Term Potentiation							1.4		
Synaptogenesis Signaling Pathway						1.6			
(D) Stress response									
Autophagy		0.2			-0.8	0.2	3.3		
Endoplasmic Reticulum Stress Pathway		0.4	-1.3						
Ferroptosis Signaling Pathway		-0.5	-0.9	-0.3		0.2	1.2		
HIF1α Signaling				2.7	3.1	3.1			
Myc Mediated Apoptosis Signaling				0.4	-1.7				
NF-κB Signaling				2.5					
NRF2-mediated Oxidative Stress Response		-2.7	-0.9			-0.7			
SAPK/JNK Signaling		-0.3		1.7		0.9			
Unfolded protein response		0.3	-2.7			-2.8			
Other									
Superpathway of Cholesterol Biosynthesis		-2.2		3.6	-2.8		3.6		

Significant IPA canonical pathways related to (A) energy metabolism, (B) neuron development, (C) synaptic signaling and (D) stress response. Activation/inhibition of pathways are indicated by positive (red)/negative (blue) IPA z-score values.

Table 2.3: Selection of interesting upstream regulators for transfected cell lines, when compared to mock cell line.

	Normoxia			Hypoxia			Oxidative stress		
	nCLU	**sCLU**	**S100B**	**nCLU**	**sCLU**	**S100B**	**nCLU**	**sCLU**	**S100B**
APP		-0.5	-1.9	0.7	0.5	-3.0		0.3	0.2
BDNF		0.6	0.5	0.7		1.1			
DKK1			-0.6			-1.1			
EOMES	2.0	0.1			-0.6	1.3			
GRIN3A			-2.7		-2.7	-3.4			-2.4*
HIF1A				1.4	2.0				
MAPT			-0.7		0.6		1.4		
NFE2L2							2.2		
NOS1			0.4		1.0	1.0			
S100A8		-1.0	-0.2		-1.5	-0.8			0.4
S100A9		-1.0	-0.2		-1.5	-0.9			0.4
TCF7L2		0.1	1.1	2.6	-0.1	0.2	6.1*		

*Interesting upstream regulators were selected as 'activated' (red)/'inhibited' (blue) in comparison to mock cell line, by use of the IPA Activation z-score. *regulation bias, implying that X-fold change of upstream regulator does not match expected regulation of targets in its network*

Methods

Cell culture

HN33 cells (murine hippocampal neurons x neuroblastoma) (Lee et al. 1990) (American Type Culture Collection, Rockville, MO) had been stably transfected with each candidate gene (nuclear clusterin (nCLU), soluble clusterin (sCLU) and S100B) and an empty vector (mock), respectively (Geßner et al. 2020). The four cell lines were cultivated in Dulbecco's Modified Eagle Medium (DMEM) (Biowest, Darmstadt) containing 10% fetal calf serum (FCS) (Biowest, Darmstadt, Germany) and 1% of a mixture of penicillin and streptomycin (PAA, Pasching, Austria) at 37 °C in a humidified atmosphere and 5% CO_2. The medium of the transfected cells was supplemented with 700 µg/ml geniticin (PAA, Pasching, Austria).

Quantitative real-time PCR

The successful overexpression of target genes was verified before and after experiments by qRT-PCR as described in Geßner et al. (2020). For that purpose, RNA was extracted from cells using the Crystal RNA Mini Kit (BiolabProducts, Gödenstorf, Germany) including an on-column DNA digestion with RNase-free DNase (Qiagen, Germany). First-strand cDNA was synthesized from 1 µg of isolated RNA with Oligo(dT)18 primer using the Fermentas RevertAid H Minus First Strand cDNA Synthesis Kit (Thermo Scientific, Schwerte, Germany). The qPCR was performed with a 7500 Fast Real-Time PCR System and the Power SYBR Green master mix (Applied Biosystems, Darmstadt, Germany) using a

standard PCR protocol (step 1-2: 50 °C 2 min, 95 °C 10 min; 40 cycles step 3-5: 95 °C for 15 s, 60 °C for 30 s, 72 °C for 30 s) including melting curve analysis. Absolute mRNA copies were calculated with the 7500 System Sequence Detection Software 2.0.6 (Applied Biosystems) using recombinant plasmid dilutions of 10^2 – 10^8 as standard curve, and then normalized to 1 µg of total RNA.

Normoxia, hypoxia and oxidative stress treatment

Experiments were conducted in 96-well plates containing 3.75 x 104 cells per well diluted in 50 µl DMEM medium (10% FCS, 1% Penicillin/Streptomycin) of each transfected cell line at passage 38, including a cell line transfected with an empty vector (mock cell line). Cells were exposed to normoxia (21% O_2, 5% CO_2, 37 °C), hypoxia (1.2% O_2, 5% CO_2, 93.8% N_2, 37 °C) and oxidative stress (275 µM H_2O_2 in 50 µl DMEM per well, 21% O_2, 5% CO_2, 37 °C) for 24h, respectively. After trypsinization every 6 wells were pooled and used as one replicate, generating four replicates per cell line and treatment. Samples were centrifuged at 180 x g for 5 min, supernatant removed and pellets stored at -20 °C until further processing.

We note that we considered 21% as normoxic condition. The HN33-cells used in this study were cultured at 21% O_2 since their dissociation and somatic cell fusion with neuroblastoma cells (Lee et al. 1990). In these conditions, the cells displayed expression of neurofilaments and electrophysiological behavior typical of hippocampal neurons (Lee et al. 1990). While other hippocampal neurons may experience 21% O_2 as hyperoxic, the HN33-cells have been exposed to 21% O_2 over many generations and hence arguably perceive this condition as normoxic. Related studies (Koch and Burmester 2016; Koch et al. 2016; Geßner et al. 2020) also considered 21% as normoxia.

Cell viability assay

Cell viability was assessed by CellTiter-Glo® (CTG) Luminescent Cell Viability Assay Kit (Promega, Mannheim, Germany) according to the manufacturer's instructions. The assay determines the ATP content of the cells and serves as reliable indicator of the number of healthy, metabolically active cells (Noah et al. 2007). After incubation at normoxia, hypoxia and oxidative stress, as mentioned above, CTG reagent was added and luminescence measured by a DTX 880 Multimode Detector (Beckmann Coulter, Krefeld, Germany). Statistical analysis was conducted in R version 4.1.2 (R Core Team 2021). Robust triplicates were determined and intensities normalized to the mock cell line at normoxic conditions. Pairwise t-test and false discovery rate (FDR) multiple correction testing was performed using the compare_means function of ggpubr package, with the mock cell line as reference group at each respective condition (Kassambara 2020).

RNA preparation and RNA-Seq

Total RNA of frozen cell pellets was extracted with the Crystal RNA Mini Kit (BiolabProducts, Gödenstorf, Germany) after the manufacturer's instructions, including an on-column DNA digestion with RNase-free DNase (Qiagen, Germany). RNA integrity and quantity were assessed with the Agilent 4200 TapeStation system (Agilent Technology, Santa Clara, USA) and triplicates determined for sequencing. The cDNA libraries were generated with 500 ng of total RNA after rRNA depletion, and sequenced on a NovaSeq platform with a setting of 150 bp paired-end reads and an estimated output of 50 million reads (GeneWiz, Leipzig, Germany). The raw transcriptome files are available from the NCBI Sequence Read Archive (SRA) from cell lines transfected with mock vector, nCLU, sCLU and S100B at normoxic, hypoxic and oxidative stress conditions (Table S1).

Transcriptome analysis

Sequencing files were uploaded to a Galaxy platform in fastq.gz format for further analysis. A sequencing quality report was generated using FastQC (Galaxy Version 0.72) and MultiQC (Galaxy Version 1.7). Since read quality was good (average Phred score > 35, Table S1), no further read trimming was performed. Reads were mapped against the mouse reference genome GRCm39 (www.ncbi.nlm.nih.gov/assembly/GCF_000001635.27/, genomic FASTA and GTF) with Bowtie2 (Galaxy Version 2.3.4.2) with the very sensitive end-to-end preset setting (--very-sensitive). Mapped reads from generated genome BAM files were filtered by a minimum mapping quality of 10 and determined with featureCounts (Galaxy Version 1.6.3+galaxy2), counting aligned fragments (even when only one paired read mapped) and excluding chimeric fragments. Reads were allowed to contribute to one feature only. Differentially expressed genes (DEGs) were determined from count tables using DESeq2 (Galaxy Version 2.11.40.6), performing pairwise comparisons with the mock cell line at the respective condition as reference. Only genes with a corrected FDR p-value < 0.05 were considered significant. Principal component analysis (PCA) was performed on count tables from all cell lines and treatments with DESeq2 (Version 1.32.0) in R (Version 4.1.0). Gene Ontology (GO) analysis was performed using PANTHER Overrepresentation Test (Protein Analysis Through Evolutionary Relationships, http://go.pantherdb.org/, GO Ontology database DOI: 10.5281/zenodo.5228828 Released 2021-08-18) (Mi et al. 2021). The annotated mouse genes in the PANTHER DB were used as a reference list, and overrepresentation was tested in GO and GO Slim terms and Reactome pathways with Fisher's Exact Test with FDR multiple testing correction. Only categories with corrected p-values < 0.05 were considered significant. Enrichment in Canonical Pathways and Upstream Regulator Analysis were performed with Qiagen's Ingenuity Pathway Analysis (IPA, Qiagen, Hilden, Germany) Core analysis tool.

Declarations

Ethics approval and consent to participate

Not applicable.

Consent for publication

Not applicable.

Availability of data and materials

Sequence data that support the findings of this study have been deposited in the Sequence Read Archive (SRA) with the primary accession code PRJNA86312, available at: https://www.ncbi.nlm.nih.gov/sra/?term=PRJNA862312.

Competing interests

The authors declare that they have no competing interests.

Funding

This work was supported by the Deutsche Forschungsgemeinschaft (Bu956/22).

Authors' contributions

TB conceived the research idea and received the funding. GM and CG acquired the experimental data. GM carried out the data analysis. CO and TH assisted with Ingenuity Pathway Analysis and interpretation of results. GM and CG wrote the manuscript with input from all authors. All authors have read and approved the final manuscript.

Acknowledgements

Thanks are due to Prof. Dr. Lars P. Folkow for suggestions and assistance in writing the manuscript.

8 Chapter III

Elevated antioxidant defence in the brain of deep-diving pinnipeds

Gerrit A. Martens[1], Lars P. Folkow[2], Thorsten Burmester[1], Cornelia Geßner[1]*

[1] Institute of Cell and Systems Biology of Animals, University of Hamburg, Hamburg, Germany

[2] Department of Arctic and Marine Biology, UiT The Arctic University of Norway, Tromsø, Norway

*Correspondence: Cornelia Geßner

cornelia.gessner@hotmail.de

Keywords: marine mammals, pinniped, hypoxia, brain, antioxidants, seal, diving mammals

Published: 16 December 2022 in *Frontiers in Physiology*

Martens, Gerrit A.; Folkow, Lars P.; Burmester, Thorsten; Geßner, Cornelia (2022): Elevated antioxidant defence in the brain of deep-diving pinnipeds. In *Frontiers in Physiology*. 13, Article 1064476. DOI: 10.3389/fphys.2022.1064476.

Abstract

While foraging, marine mammals undertake repetitive diving bouts. When the animal surfaces, reperfusion makes oxygen readily available for the electron transport chain, which leads to increased production of reactive oxygen species and risk of oxidative damage. In blood and several tissues, such as heart, lung, muscle and kidney, marine mammals generally exhibit an elevated antioxidant defence. However, the brain, whose functional integrity is critical to survival, has received little attention. We previously observed an enhanced expression of several antioxidant genes in cortical neurons of hooded seals (*Cystophora cristata*). Here, we studied antioxidant gene expression and enzymatic activity in the visual cortex, cerebellum and hippocampus of harp seals (*Pagophilus groenlandicus*) and hooded seals. Moreover, we tested several genes for positive selection. We found that antioxidants in the first line of defence, such as superoxide dismutase (SOD), glutathione peroxidase (GPX) and glutathione (GSH) were constitutively enhanced in the seal brain compared to mice (*Mus musculus*), whereas the glutaredoxin and thioredoxin systems were not. Possibly, the activity of the latter systems is stress-induced rather than constitutively elevated. Further, some, but not all members, of the glutathione-s-transferase (GST) family appear more highly expressed. We found no signatures of positive selection, indicating that sequence and function of the studied antioxidants are conserved in pinnipeds.

Introduction

Marine mammals have undergone a fascinating transition from a terrestrial to a marine habitat and evolved various adaptations to aquatic life. One of the major challenges is the supply of oxygen while foraging at depth. During diving, breathing, and consequently the intake of oxygen, stops. Marine mammals have adapted by evolving a high capacity for oxygen storage, e.g., high levels of muscle myoglobin and an elevated blood volume with a high content of hemoglobin (e.g., Ponganis 2011; Blix 2018). Additionally, bradycardia and peripheral vasoconstriction during dives contribute to an efficient use of stored oxygen (Scholander 1940; Ponganis 2011; Blix 2018). In spite of these preventive adaptations, deep-diving seals can experience very low blood oxygen tensions. During long, voluntary dives the deep-diving Weddell (*Leptonychotes weddellii*) and northern elephant (*Mirounga angustirostris*) seals endure arterial oxygen tensions well below 20mmHg (Qvist et al. 1986; Meir et al. 2009).

In addition to the limited availability of oxygen when submerged, transformation of oxygen into reactive oxygen species (ROS) also represents a major challenge. ROS are radical or non-radical oxygen species produced by the partial reduction of oxygen. Mitochondria have been recognized as an important intracellular source of ROS, which can arise during oxidative phosphorylation that produces energy in the form of ATP. ATP production is accomplished by a tetravalent reduction of oxygen. In

normal physiological conditions, 1–4% of the oxygen is incompletely reduced and leaks from the electron transport chain (ETC) in the form of superoxide radical ($O_2^{\bullet-}$) (Kevin et al. 2005). However, ROS are also produced in the endoplasmatic reticulum, peroxisomes, lysosomes and others (Milkovic et al. 2019). ROS play an important role as redox signaling messengers contributing, amongst others, to cell proliferation and survival and thus, are part of the normal functioning of cells. However, when ROS are produced in excess, signaling ability is lost and macromolecules are unspecifically damaged promoting several pathologies such as neurodegenerative diseases, atherosclerosis, diabetes and cancer (Ray et al. 2012; Milkovic et al. 2019). Acknowledging both the importance and potential risks of ROS, physiological levels of ROS can be termed oxidative eustress, while excessive oxidant challenge may be considered as oxidant distress (Sies et al. 2017; Sies 2017).

Diving bouts of marine mammals lead to recurrent phases in which the availability of oxygen is limited, followed by reoxygenation upon resurfacing. When the animal surfaces, all tissues are reperfused with oxygenated blood (e.g., Blix 2018). It is known that cellular hypoxia leads to a reduced activity of complex IV (cytochrome oxidase) in the ETC and that re-introduction of oxygen causes an accelerated leakage of radicals from more proximal complexes and the production of $O_2^{\bullet-}$ is increased (Kevin et al. 2005). In terrestrial organisms, ischemia/reperfusion increases ROS production and the potential for oxidative damage (Halliwell and Gutteridge 2015). In marine mammals, reoxygenation upon resurfacing replenishes oxygen stores and boosts aerobic ATP production, but it may also generate ROS and oxidative stress can occur (Fridovich 1998). Evidence exist to indicate that marine mammals and terrestrial, hibernating species, such as some bats and ground squirrels, display adaptations to fast reoxygenation that prevent reperfusion injury (Hermes-Lima et al. 2015). In ringed seals, ischemia and subsequent reoxygenation occurring during and after a dive increased ROS production, but not the oxidative stress (Zenteno-Savín and Elsner 1998, 2000).

To prevent oxidative stress, organisms have evolved an antioxidant defence consisting of enzymes and non-enzymatic antioxidants, such as glutathione (GSH), uric acid, melatonin, vitamins C and E and others (Milkovic et al. 2019). Prominent examples of antioxidant enzymes that were analyzed in this study are the superoxide dismutase (SOD) converting $O_2^{\bullet-}$ into hydrogen peroxide (H_2O_2), and glutathione peroxidase (GPX) transforming H_2O_2 into H_2O and limiting the hydroxyl radical ($OH^{\bullet}$) formation. Glutathione-S-transferase (GST) binds toxic products to glutathione and the resulting glutathione conjugates can then be removed from the organism (Cooper and Kristal 1997). Moreover, we studied representatives of the glutaredoxin and thioredoxin systems that play a key role in antioxidant defence and redox state of a cell. Amongst others, these systems remove ROS or activate oxidative-sensitive transcription factors (Lu and Holmgren 2014).

Considering the diving behavior of marine mammals, one might expect these species to have a constitutively higher antioxidant defence system in adaptation to an elevated risk of ROS exposure. Indeed, previous studies in some pinnipeds, the manatee (*Trichechus manatus*) and several cetacean species, have generally revealed higher antioxidant levels in diving compared to non-diving mammals (Elsner et al. 1998; Wilhelm Filho et al. 2002; Zenteno-Savín et al. 2002; Vázquez-Medina et al. 2006; Vázquez-Medina et al. 2012). In these studies, blood samples, but also samples from heart, lung, kidney, liver and skeletal muscle, were studied. To the best of our knowledge, with exception of a study in the bottlenose dolphin (*Tursiops truncatus*) and the dwarf sperm whale (*Kogia sima*) (Cantú-Medellín et al. 2011), the antioxidant status of the diving brain has not previously been studied. Since the functional integrity of the brain is essential to the survival of an organism, we expect marine mammals to have an elevated cerebral antioxidant defence to prevent oxidative stress. In a comparative transcriptomic analysis of neurons of the visual cortex in hooded seals (*Cystophora cristata*) and mice (*Mus musculus*), we previously observed a significantly higher expression of antioxidant genes in hooded seals (Geßner et al. 2022). Similarly, in the visual cortex of whales, we found a high expression of transcripts related to the detoxification of ROS when compared to cattle (*Bos taurus*) (Krüger et al. 2020).

In this study, we extend the results of Geßner et al. (2022) and aim to identify whether elevated antioxidant levels found in neurons of the visual cortex are unique to this brain region or if they are present in other regions and could, thus, possibly be representative for the whole brain. Further, we studied antioxidant levels in harp seals (*Pagophilus groenlandicus*), to investigate whether an increased antioxidant defence of the brain might be relevant in pinniped species other than the hooded seal. We studied antioxidant gene expression in the visual cortex, cerebellum and hippocampus of hooded seals, harp seals and mice. Further, we determined the enzymatic activity of SOD, GST, GPX and glutathione reductase (GSR) and the concentration of reduced glutathione (GSH) in these brain regions. We further tested a set of antioxidant genes in seven pinniped species for positive selection, to test whether selection pressure has favoured changes in gene sequences that might also lead to functional changes.

Methods

Antioxidant gene expression in neurons of the visual cortex

Transcriptomes of mouse and hooded seal neurons that were separated via laser-capture microdissection of the visual cortex were available from Geßner et al. (2022). The expression analysis via RNA-seq and the differential expression analysis were performed as described in Geßner et al. (2022), using the CLC workbench v.10.0.1. Briefly, quality-trimmed reads (Phred score >35, removal of first 20 5'-terminal nucleotides, with less than two ambiguous bases and reads >30 nucleotides in length) were mapped against the human genome (assembly GRCh38. p13) that served as a reference genome. Only reads that matched 75% of the read length and 75% of the nucleotides to the reference genome were included in the mapping. Gene expression is presented as TPM (Transcripts Per Kilobase Million mapped reads), whereby only reads that mapped uniquely in the genome were included in the calculation of TPM values. p-values of differentially expressed genes were corrected for multiple testing using the false discovery rate (FDR) (Benjamini and Hochberg 1995). Only genes with a $p_{FDR} \leq 0.05$, TPM-value ≥1 in either species and a fold change (FC) ≥ 2 or ≤−2 were considered as significantly differentially expressed genes (DEGs). From these DEGs, genes of the GO terms "antioxidant activity" (GO:0016209) were taken from Geßner et al. (2022). For this study, we additionally extracted genes of "glutathione metabolic process" (GO:0006749) (http://www.informatics.jax.org) and a list of human antioxidant genes (Gelain et al. 2009). Additionally, we included heme oxygenase 2 (HMOX2) and Paraoxonase 2 (PON2), which are both known to be involved in the antioxidant defence (Barañano et al. 2002; Ng et al. 2006).

Animals

Hooded seals (*Cystophora cristata*; n = 4 adult females, March 2019) and harp seals (*Pagophilus groenlandicus*; n = 3 adult females in March 2018; n = 1 adult female in March 2019, no hippocampus available for latter individual) were captured in the pack ice of the Greenland Sea under permits from relevant Norwegian and Greenland authorities. The hooded seals were euthanized immediately following live-capture, by sedation with an intramuscular injection of zolazepam/tiletamine (1.5–2.0 mg per kg of body mass), followed by catheterization of the extradural intravertebral vein and i. v. injection of an overdose of pentobarbital (Euthasol vet. Le Vet B.V. Netherlands; ∼30 mg per kg of body mass). The harp seals were all shot to the head and bled, after which brain tissue was immediately sampled from intact brain regions. For the repetition of the GST and GSH/GSSG assays that were performed at a later point in time, hooded seal tissues (from n = 3 adult females) were collected in March 2021, using the same procedure as described above for this species. All animal handling was in accordance with the Norwegian Animal Welfare Act and with approvals from the Norwegian Food Safety Authority (permits no. 12268 and 22451). Adult female mice (C57BL/6, n = 20, whereby n = 4

were used per assay and qPCR) were a gift by Prof. Dr. Christian Lohr (University of Hamburg, Hamburg, Germany) and were anaesthetized with 1 ml isoflurane (Forene, Abbott, Germany) in a chamber (1,000 ml) and decapitated. All animals were handled according to the EU Directive 63 (Directive 2010/63/EU). This mouse strain has served as model organism in studies investigating oxidative stress, e.g., during aging (Jeong et al. 2018) or when exposed to ethanol during brain development (Kumral et al. 2005). C57BL/6 mice were also used in a previous comparative study with diving mammals (Geßner et al. 2022). While mouse strains and their hybrids differ in susceptibility to hypoxia, C57BL/6 appear to be an intermediate type, neither particularly sensitive nor tolerant to hypoxia (Sheldon et al. 1998). Fresh tissue of the visual cortex, cerebellum and hippocampus was frozen in liquid nitrogen and later transferred to -80°C for storage until subsequent use.

Quantitative real-time reverse transcription polymerase chain reaction (qPCR)

For expression analyses using qPCR, we selected essential antioxidant genes (GPX3, SOD1, GSTK1, GSTO1) or genes that represent a component of important antioxidant systems (TXNRD3, GLRX2). Only genes with a $p_{FDR} \leq 0.05$, TPM-value ≥1 in either species and a fold change (FC) ≥ 3 or ≤−3 in the transcriptomic data were considered for qPCR. Since we aim to determine the antioxidant defence of neurons, we used RBFOX3 as a neuronal marker to account for different numbers of neurons in every tissue sample. Primer sequences (Supplementary Table S3.1A) for the mouse were designed based on sequences retrieved from GenBank (https://www.ncbi.nlm.nih.gov/genbank/) and hooded seal sequences were extracted from Geßner et al. (2022). Since there are no harp seal data available on GenBank, primer from the hooded seal were used and primer specificity verified via gel electrophoresis and/or sequencing.

Total RNA from frozen tissue samples of the visual cortex, cerebellum and hippocampus of hooded seals, harp seals and mice were extracted using the Crystal RNA Mini Kit (BiolabProducts, Gödenstorf, Germany) according to the manufacturer's instructions, including an on-column DNA digestion with RNase-free DNase (Qiagen, Germany). The quantity and integrity of the isolated total RNA were assessed using the Agilent 4,200 TapeStation System and RNA ScreenTape Assay (Agilent Technology, Santa Clara, United States). First-strand cDNA was synthesized from 1 µg of total RNA with Oligo (dT)18 primer using the RevertAid H Minus First Strand cDNA Synthesis Kit (Thermo Scientific, Germany). The qPCR was performed with a 7,500 Fast Real-Time PCR System and the Power SYBR Green master mix (Applied Biosystems, Darmstadt, Germany) using a standard PCR protocol (step 1–2: 50°C for 2 min, 95°C for 10 min, step 3–5: 95°C for 30 s, 58°C for 30 s, and 72°C for 30 s; 40 cycles step 3–5). Primer efficiencies (Supplementary Table S3.1B) were assessed with serial dilutions of pooled cDNA samples from each brain region and species, respectively. For relative comparisons of gene expression, a 1:25 dilution of the cDNA (equivalent to 40 ng RNA) was used per reaction. The experiments, including

negative controls, were carried out as triplicates. To account for variations between runs, identical interrun calibrators were added on each microtiter qPCR plate, with pooled cDNA from visual cortex of each species, respectively. Dissociation curve analyses were used to validate the specificity of the amplifications. Raw Ct-values were calculated with the 7,500 System Sequence Detection Software 2.0.6 (Applied Biosystems) and adjusted according to interrun calibrators. The dCt values were obtained by normalizing the Ct-values to the widely used neuronal marker RBFOX3 encoding NeuN protein (Duan et al. 2016). Fold changes (FC) for harp and hooded seals were calculated with mouse samples as reference using the ddCt method. Statistical analysis was performed on dCt values using the statistical program R version 4.1.2 (R Core Team 2021) and the Tukey_hsd function of the rstatix_0.7.0 package (Kassambara 2021). Fold changes were visualized with the ggpubr package (Kassambara 2020).

Enzymatic activity assays

For all assays, ~20 mg of tissue from every brain region was washed twice in phosphate buffered saline (PBS) (140 mM NaCl, 2.7 mM KCl, 8.1 mM Na_2HPO_4, 1.5 mM KH_2PO_4, pH7.4) to remove blood before assay-specific buffers were used for homogenization.

Glutathione peroxidase (GPX) activity

Total GPX activity was determined using the Glutathione Peroxidase Assay Kit (Cayman Chemical, item no. 703102). Tissue samples (20 mg) were homogenized in 75 µL cold buffer (50 mM Tris-HCl, pH7.5, 5 mM EDTA and 1 mM DTT) according to the manufacturer's instructions. Total protein contents were measured with the Bradford assay (Carl Roth, Karlsruhe, Germany) and adjusted with homogenization buffer to the sample with the lowest concentration (17.94 mg/ml). Of all adjusted samples a 1:5 dilution was prepared and used in the assay. Absorbance was read every minute at 340 nm using a DTX 880 Multimode Detector (Beckmann Coulter, Krefeld, Germany). The decrease in absorbance was measured for 25 min. The decrease was linear up until minute 10 and thus, the first 10 data points were used for statistical analysis and to calculate the GPX-activities (nmol/min/ml) according to the manufacturer's instructions.

Superoxide dismutase (SOD) and glutathione-S-transferase (GST) activity

The tissues samples (20 mg) were homogenized in 100 µL of cold 20 mM HEPES buffer (1 mM EDTA, 210 mM mannitol and 70 mM sucrose, pH 7.2). Total protein concentration was measured with the Bradford assay (Carl Roth, Karlsruhe, Germany) and adjusted with HEPES buffer to the sample with the lowest concentration (1.97 mg/ml).

SOD activity

All samples were further diluted 1:300 in HEPES buffer. The total SOD activity was measured with the Superoxide Dismutase Assay Kit (Cayman Chemical, item no. 706002) according to the manufacturer's instructions. The absorbance was determined at 450 nm and SOD activities are expressed as U/ml.

GST activity

All samples were diluted 1:5 in HEPES buffer. The total GST activity was determined using the Glutathione S-Transferase Assay Kit (Cayman Chemical, item no. 703302) according to the manufacturer's instructions. The absorbance was recorded every minute at 340 nm for 60 min and the linear range from minute 1 to 9 was used for calculation of the GST activities (nmol/min/ml). Measurement of the GST activity was repeated using a different GST assay kit (Abcam, ab65325) and newly sampled hooded seal tissues (March 2021). The tissue was homogenized in Assay buffer and the concentration of all samples was adjusted to 3.9 mg/ml. The assay was performed according to the manufacturer's instruction using a 1:5 dilution of the samples.

Glutathione reductase (GSR) activity

The tissues samples (20 mg) were homogenized in 100 µL of cold buffer (50 mM potassium phosphate, pH 7.5, 1 mM EDTA). Total protein concentration was measured with the Bradford assay (Carl Roth, Karlsruhe, Germany) and adjusted with Sample buffer (Cayman Chemical, item no. 703202) to the sample with the lowest concentration (2.3 mg/ml). The GSR activity was measured according to the manufacturer's instructions using the Glutathione Reductase Assay kit (Cayman Chemical, item no.703202). The absorbance was read at 340 nm once every minute for 6 min and GSR activity was calculated in nmol/min/ml.

GSH/GSSG ratio

The ratio of reduced glutathione (GSH) and oxidized glutathione (GSSG) was determined using the Amplite Fluorometric Glutathione GSH/GSSG Ratio Assay Kit Green Fluorescence (Biomol, Catalog number 10056). Tissues were homogenized in HEPES buffer, protein concentrations adjusted to 5.2 mg/ml and diluted 1:50 in Assay buffer. The assay was run according to manufacturer's instructions. The results were verified at a later point in time using a different assay, the GSH/GSSG Ratio Detection Assay Kit (Abcam, ab138881), and newly sampled hooded seal tissues from March 2021. Tissues were homogenized in 1xPBS (pH = 6) with 0.5% NP40 (Abcam, ab142227). Protein concentrations were adjusted to 3 mg/ml and samples were diluted 1:50 in Assay buffer. Before both assays were run, samples were deproteinized with the ReadiUse™ TCA Deproteinization Sample Preparation Kit (Biomol, ABD-19501).

Statistical analysis of enzymatic activity assays

The statistical analyses were carried out in the R v. 3.5.1 statistics program (R Core Team 2021). Significant differences in the means of our species and brain regions were identified with an ANOVA, since the residuals of all assays were normally distributed. We employed the Levene test included in the Rcmdr package (Fox et al. 2019; Fox 2005) to test for variance homogeneity. Then, the Tukey-Kramer test of the DTK package (Lau 2013) was used to test for significant differences between species and brain regions. To correct for type I errors, p-values were corrected with the False Discovery Rate (Benjamini and Hochberg 1995) using the p. adjust ()-function in R. Results are presented as mean values ± SEM.

Inferring positive selection

We tested for positive selection in all genes explored via qPCR, that is GPX3, SOD1, GSTK1 GSTO1, TXNRD3, GLRX2 and additionally GSR. We explored selection pressures in seven pinnipeds and in five terrestrial carnivores that served as non-diving relatives. Among pinnipeds, the deep diving hooded seal (*Cystophora cristata*), the Weddell seal (*Leptonychotes weddelli*), the southern elephant seal (*Mirounga leonina*), the Hawaiian monk seal (*Neomonachus schauinslandi*), the gray seal (*Halichoerus grypus*), the harbour seal (*Phoca vitulina*) and the walrus (*Odobenus rosmarus divergens*) were compared with the dog (*Canis lupus familiaris*), ferret (*Mustela putorius furo*), giant panda (*Ailuropoda melanoleuca*), grizzly bear (*Ursus arctos horribilis*) and the polar bear (*Ursus maritimus*). The nucleotide sequences were retrieved from GenBank (Supplementary Table S3.3 for accession numbers) except for the sequences of the hooded seal, that were extracted from Geßner et al. (2022). For each gene, nucleotide sequences were aligned using TranslatorX (http://translatorx.co.uk, 21.01.2022) providing a peptide alignment generated in MAFFT (Katoh and Standley 2013) to ensure alignment quality. Selection pressure was assessed by estimating the non-synonymous to synonymous rate ratio using the Branch-wide Unrestricted Statistical Test for Episodic Diversification (BUSTED) (Murrell et al. 2015) and the adaptive Branch-Site Random Effects Likelihood (aBSREL) model (Smith et al. 2015) on the Datamonkey server (https://www.datamonkey.org, 21.01.2022) (Pond and Frost 2005). In both models, pinnipeds were denoted as foreground branches in which some sites might be positively selected, whereas non-diving mammals served as background branches in which positive selection is absent. BUSTED assesses whether a gene has experienced positive selection in at least one site in at least one of the branches tested, while aBSREL estimates for every foreground branch whether a proportion of sites has undergone positive selection. Only genes for which positive selection was inferred by both methods were considered positively selected.

Results

Antioxidant gene expression in neurons of hooded seals and mice

We extracted the antioxidant gene expression values from the cell-type specific transcriptome of visual cortex neurons in hooded seals and mice (Geßner et al. 2022). We found a total of 49 differentially expressed antioxidant genes (DEGs), i.e. genes with $p_{FDR} \leq 0.05$, a TPM-value ≥1 in either species and a fold change (FC) ≥ 2 or ≤−2. Table 3.1 lists genes that were further analyzed by e.g. qPCR in this study. Please see Supplementary Table S3.2 for a complete list of all 49 genes.

Table 3.1. *Antioxidant gene expression in visual cortex neurons of hooded seals (Cystophora cristata), expressed in relation to gene expression in mice (Mus musculus), with a $p_{FDR} \leq 0.05$, TPM-value ≥1 and a fold change ≥2 or ≤ -2. p_{FDR} represents the p-value corrected for multiple testing using the False Discovery Rate (FDR), while Transcripts Per Kilobase Million mapped reads (TPM) represent normalized expression values. Only genes analyzed in qPCR, and/or for which enzyme activity assays were available, are presented. For a complete list, please see Supplementary Table S3.2.*

Annotated Term	Gene symbol	Fold change	FDR	TPM mouse	TPM hooded seal
antioxidant activity (GO:0016209) adapted from Geßner et al (2022)					
glutathione peroxidase activity	*GPX1*	2.2	$2.52 \cdot 10^{-5}$	65.4	140.2
	GPX3	8.6	$1.47 \cdot 10^{-11}$	4.0	34.2
	GSTK1	26.9	$6.76 \cdot 10^{-72}$	0.7	19.1
	GSTO1	15.1	$2.30 \cdot 10^{-30}$	3.6	53.9
	GSTO2	9.9	$2.12 \cdot 10^{-7}$	0.1	1.1
antioxidant activity	*SOD1*	9.1	$7.29 \cdot 10^{-59}$	52.8	481.0
glutathione-disulfide reductase (NADPH) activity	*GSR*	2.0	$1.50 \cdot 10^{-2}$	6.5	12.8
thioredoxin-disulfide reductase activity	*TXNRD3*	4.7	$6.03 \cdot 10^{-7}$	1.3	5.9
Human antioxidant genes (Gelain et al 2009)					
Thiol redox	*GLRX2*	-3.3	$1.09 \cdot 10^{-8}$	3.8	1.1

Of the 49 genes, 28 were more highly expressed in hooded seal compared to mouse neurons. The annotated GO term “glutathione peroxidase activity” was represented by eight of these 28 genes and thus, was the most frequently represented term. For example, genes assigned to this function were the glutathione peroxidase 1 (GPX1, FC = 2.2) and 3 (GPX3, FC = 8.6) and the glutathione-S-transferase kappa 1 (GSTK1, FC = 26.9), omega 1 (GSTO1, FC = 15.1), omega 2 (GSTO2, FC = 9.9) and the microsomal glutathione-S-transferase 1 (MGST1, FC = 13.7).

The GO term “antioxidant activity” was represented by six genes and all of them were more highly expressed in neurons of hooded seals compared to mice. Among these genes were S100 calcium binding protein A9 (S100A9, FC = 99.7, but we note that TPM values were relatively low in both species), superoxide dismutase 1 (SOD1, FC = 9.1), peroxiredoxin-like 2 A (PRXL2A, FC = 3.5),

peroxiredoxin 2 (PRDX2, FC = 3.4) and selenoprotein W (SELENOW, FC = 2). Further, within antioxidant genes, SOD1 was among the top five genes with the highest TPM value (TPM = 481) in hooded seal neurons, followed by PRDX2 (TPM = 388), GPX1 (TPM = 140), heme oxygenase 2 (HMOX2, TPM = 99) and glyoxalase 1 (GL O 1, TPM = 70). Even when all genes (not only antioxidants) in the transcriptome were considered, SOD1 had a high expression, being the gene with the 22nd highest TPM value. Antioxidant genes with the top five F C were S100A9 (FC = 99.7), GSTK1 (FC = 26.9), arachidonate 5-lipoxygenase activating protein (ALOX5AP, FC = 21.5), selenoprotein T (SELENOT, FC = 17.6) and GSTO1 (FC = 15.1).

Antioxidant gene expression in brain regions of seals and mice via qPCR

In order to test whether elevated antioxidant gene expression is also present in other brain regions and in diving mammals other than the hooded seal, we performed qPCR analyses in the visual cortex, the cerebellum and the hippocampus of hooded seals and harp seals, and compared results to mice (Fig. 3.1).

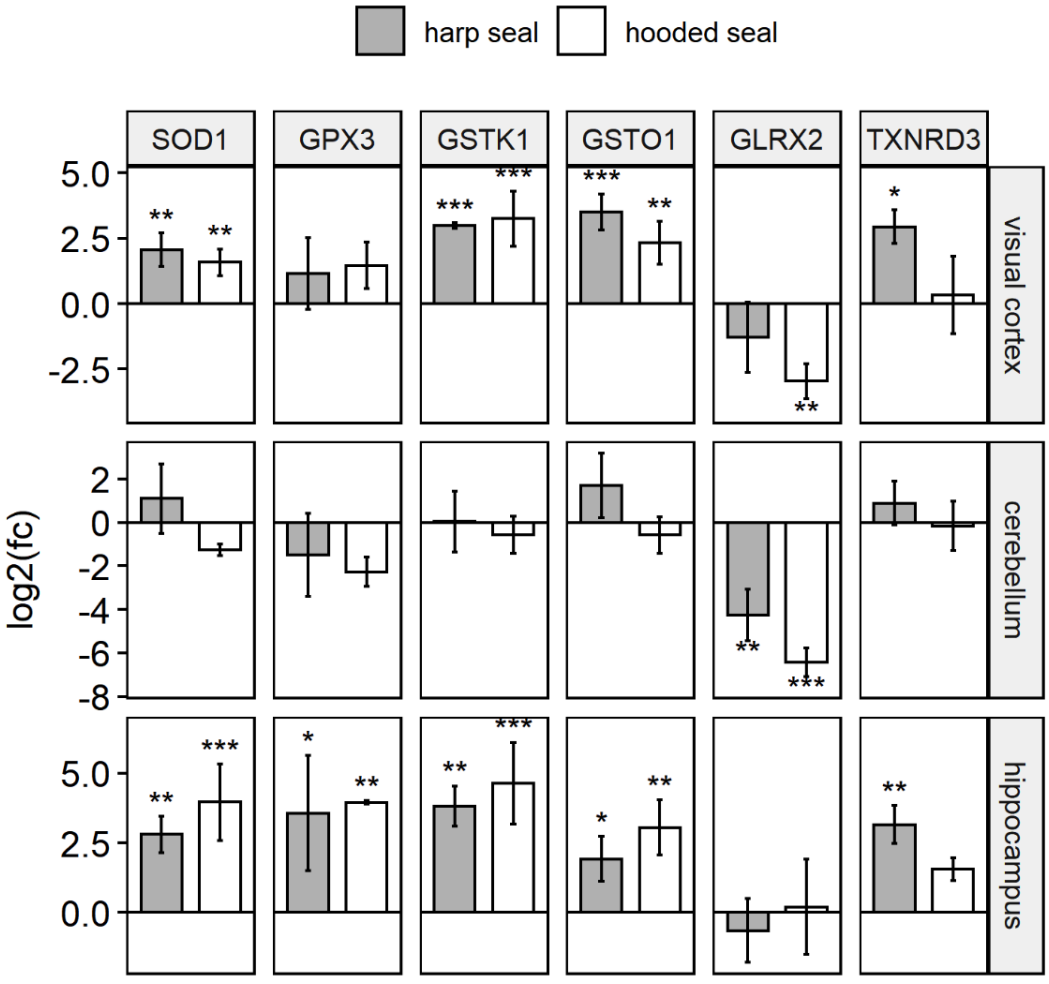

Fig. 3.1. *Antioxidant gene expression of hooded seals and harp seals, when compared to mice, as determined using qPCR. Relative gene expression is presented in log2 fold changes [log2 (fc)], whereby positive/negative values represent higher/lower expression in seals as compared to mice. Significance is expressed by asterisks (p ≤ 0.05 (*), p ≤ 0.01 (**), p ≤ 0.01 (***).*

In the visual cortex, expression of all six antioxidants confirmed the transcriptomic data, i.e. the expression was higher in hooded seals than in mice (pGSTK1 = 0.0003, pGSTO1 = 0.0033, pSOD1 = 0.0038), although the difference in expression was not always significant (GPX3 and TXNRD3). As in the transcriptomic data, GLRX2, was less expressed in hooded seals than in mice (pGLRX2 = 0.002). Similarly, expression in harp seals was significantly (pGSTO1 = 0.0004, pSOD1 = 0.0011, pTXNRD3 = 0.0112) or insignificantly higher (GPX3, GSTK1) and insignificantly lower for GLRX2.

In the cerebellum, GLRX2 was less expressed in hooded seals (p = 0.0008) and harp seals (p = 0.0087) than in mice. There were no significant differences in the expression of the other antioxidants between species.

In the hippocampus, we observed no difference in GLRX2 expression. However, the other antioxidants were all significantly more highly expressed in hooded seals (pGPX3 = 0.0092, pGSTK1 = 0.0008, pGSTO1 = 0.0019, pSOD1 = 0.0002) and harp seals (pGPX3 = 0.0155, pGSTK1 = 0.0025, pGSTO1 = 0.0221, pSOD1 = 0.0071, pTXNRD3 = 0.0051) with exception of an insignificantly higher expression of TXNRD3 in hooded seals.

Enzymatic activity assays

Elevated SOD activities in pinniped brains compared to mice

In all three brain regions tested (visual cortex, cerebellum, hippocampus), SOD activity was significantly higher in hooded seals and harp seals than in mice (Table 3.2; Fig. 3.2). In the visual cortex, we observed similar mean rates of 48.4 ± 1.7 U/ml (p = 0.003) and 45.9 ± 1.6 U/ml (p = 0.006) in the harp and hooded seal, respectively, while mice showed a mean activity of 37.3 ± 1.1 U/ml. The cerebellum exhibited SOD activities similar to the visual cortex, with harp and hooded seals reaching 47 ± 2.1 U/ml (p = 0.006) and 47.7 ± 3 U/ml (p = 0.003) compared to mice, which showed a mean activity of 37.6 ± 1.2 U/ml. The hippocampus displayed the overall lowest SOD activity levels, with 46.4 ± 2.4 U/ml (p ≤ 0.001) and 40.4 ± 2.6 U/ml (p = 0.007) in harp and hooded seals, respectively, and 32.3 ± 0.6 U/ml in mice.

Table 3.2. Summary of results from the neuronal transcriptome of hooded seals and mice, the gene expression of harp seals (Pgr), hooded seals (Ccr) whole brain tissue normalized to a neuronal marker, as measured using qPCR, the enzymatic activity or concentration levels (for GSH), and the results from tests to infer positive selection. Fold changes (FC) and log2(FC) provide a measure of the difference between pinnipeds and mice, whereby positive values indicate a higher expression/activity/concentration in seals compared to mice. Enzymatic activity of SOD was measured in U/ml, GPX, GST, and GSR in nmol/min/ml and GSH in µM and the difference is presented in the respective unit.

	transcriptome	**gene expression (qPCR, log2(FC))**						**Enzymatic activity (difference to mice)**						**pos. selection**
	Fold change (FC)	visual cortex		cerebellum		hippocampus		visual cortex		cerebellum		hippocampus		
		Pgr	**Ccr**	**Pgr**	**Ccr**	**Pgr**	**Ccr**	**Pgr**	**Ccr**	**Pgr**	**Ccr**	**Pgr**	**Ccr**	
superoxide dismutase														
SOD1	9.1	2.06	1.58	1.12	-1.26	2.81	4	11.6	8.6	9.5	11.5	14.1	8.1	no
glutathione peroxidase														
GPX3	8.6	1.16	1.46	-1.5	-2.28	3.58	4	148	145	225	119	214	146.4	no
glutathione-s-transferases														
GSTK1	26.9	1.16	3.26	-1.5	-0.57	3.58	4.7	-67.8	-71.3	-97.4	-92.7	-65.3	-77.3	no
GSTO1	15.1	3.51	2.34	1.71	-0.58	1.93	3.1							no
glutaredoxin system														
GLRX2	-3.3	-1.29	-3	-4.3	-6.45	-0.65	0.2							no
thioredoxin system														
TXNRD3	4.7	2.95	0.33	0.89	-0.16	3.17	1.6							no
glutathione cycle														
GSR	2							9.25	-10	-65.1	86.1	-0.53	-16.6	no
GSH								62.3	69.2	74.1	64.2	56	69.8	

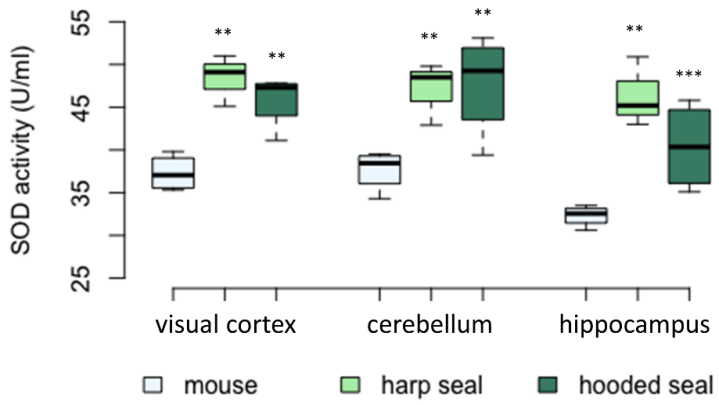

***Fig. 3.2**. Superoxide dismutase (SOD) activity (U/ml) in mice, harp seals and hooded seals. Significance levels refer to differences compared to mice in the respective brain region and are represented by asterisks (p ≤ 0.05 (*), p ≤ 0.01 (**), p ≤ 0.01 (***).*

Higher GPX activities in pinniped brains compared to mice

The total GPX activity was significantly higher in hooded seals and harp seals than in mice across brain regions (Fig. 3.3; Table 3.2). Thus, while the GPX activity in the visual cortex of mice was 207 ± 10.7 nmol/min/ml, hooded and harp seals had similarly higher activities of 351 ± 13.9 nmol/min/ml (p = < 0.001) and 355 ± 37.2 nmol/min/ml (p = < 0.001), respectively. Across species, the cerebellum displayed the highest GPX activity, with mice reaching 385 ± 22.1 nmol/min/ml, while hooded seals displayed a significantly higher activity of 504 ± 37.1 nmol/min/ml (p = 0.003) whereas the highest activity of 610 ± 17 nmol/min/ml was noted in the harp seal cerebellum (p < 0.001). In contrast, the hippocampus showed the overall lowest GPX activity, where mice had a lower rate (162 ± 11.2 nmol/min/ml) than either the hooded seal or the harp seal (309 ± 22.2 nmol/min/ml (p = < 0.001) and 376 ± 39.4 nmol/min/ml (p = 0.001), respectively). With exception of the visual cortex, harp seals displayed the overall highest GPX activity levels, even compared to hooded seals, in both the cerebellum (p = 0.007) and the hippocampus (p = 0.023).

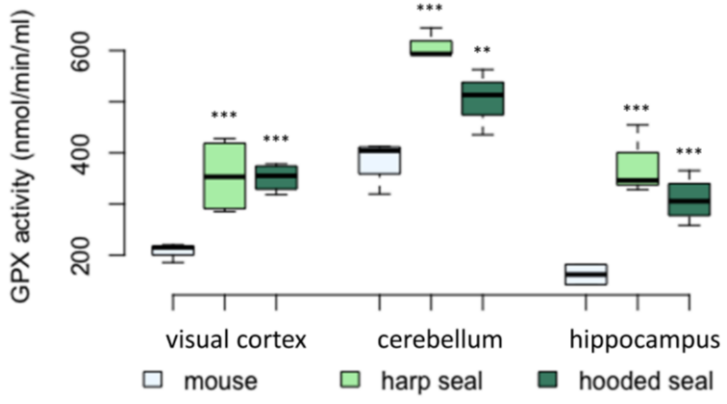

***Fig. 3.3**. Glutathione peroxidase (GPX) activity (nmol/min/ml) in mice, harp seals and hooded seals. Significance levels refer to differences compared to mice in the respective brain region and are represented by asterisks (p ≤ 0.05 (*), p ≤ 0.01 (**), p ≤ 0.01 (***).*

GSR and GST enzyme activities were not higher in pinnipeds than in mice

The results of the GSR enzymatic activity assay were mixed, but overall pinnipeds displayed a lower activity than mice (Fig. 3.4A; Table 3.2). Enzyme activity was higher in the visual cortex of harp seals (73 ± 8 nmol/min/ml, p = 0.03), while hooded seals showed significantly lower activity (54 ± 4.1 nmol/min/ml, p = 0.03), compared to mice (64 ± 3.1 nmol/min/ml). In the cerebellum, harp seals (85 ± 2 nmol/min/ml, p < 0.001) and hooded seals (64 ± 2.9 nmol/min/ml, p < 0.001), had significantly lower enzyme activities than mice (150 ± 1.6 nmol/min/ml). In the hippocampus, we found no difference between harp seals (65 ± 7 nmol/min/ml) and mice (65 ± 0.6 nmol/min/ml), while hooded seals showed significantly lower GSR activities (49 ± 1.1 nmol/min/ml, p = 0.01).

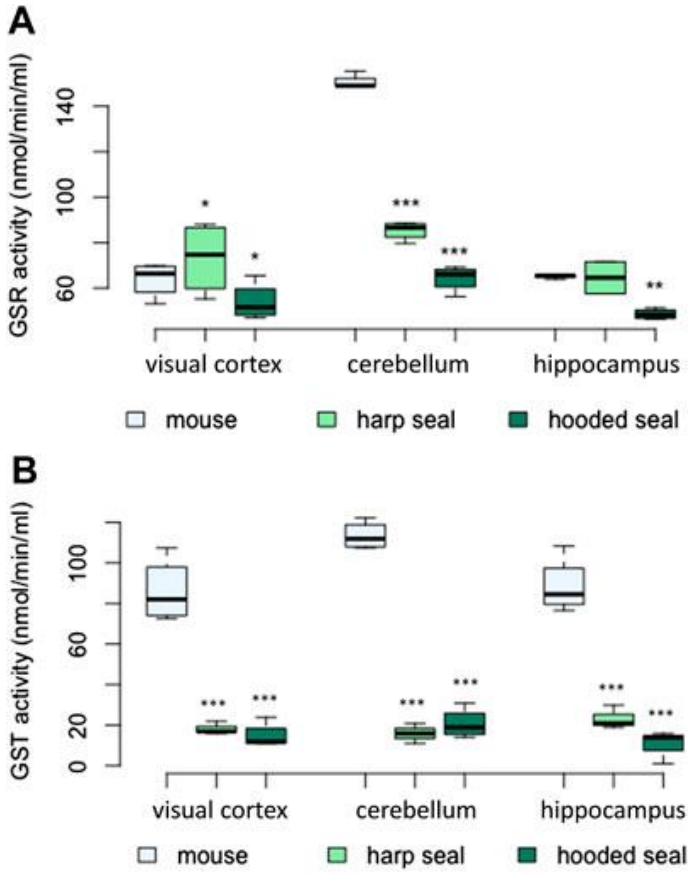

***Fig. 3.4**. **(A)** Glutathione-disulfide reductase (GSR) activity (nmol/min/ml) and **(B)** glutathione-S-transferase (GST) activity (nmol/min/ml) in mice, harp seals and hooded seals. Significance levels refer to differences compared to mice in the respective brain region and are represented by asterisks (p ≤ 0.05 (*), p ≤ 0.01 (**), p ≤ 0.01 (***).*

The GST activity was measured using two assays. The results were similar and thus, only the results of the Glutathione S-Transferase Assay Kit (Cayman Chemical) are presented. Total GST activity did not confirm the significantly higher expression of GST observed in the neuronal transcriptomic data (Fig. 3.4B). Across brain regions, harp and hooded seals exhibited a significantly lower GST activity compared to mice. While mice had GST activities of 86 ± 7.9, 113 ± 3.5 and 88 ± 6.9 nmol/min/ml in the visual cortex, cerebellum and hippocampus, respectively, we found enzyme activities to be as low

as 18 ± 1.8, 16 ± 2.9, and 23 ± 3.4 nmol/min/ml, respectively, in harp seals. Similarly, hooded seals displayed GST activities of 15 ± 3.1, 21 ± 3.7, and 11 ± 3.4 nmol/min/ml in the same brain regions.

Higher GSH-levels in pinnipeds compared to mice

The results of two different assays were similar and thus, only the results of the Amplite Fluorometric Glutathione GSH/GSSG Ratio Assay are presented. In order to calculate the GSH/GSSG ratio, both the amounts of reduced glutathione (GSH) and total glutathione (GSH + GSSG) must be determined, whereby the concentration of total glutathione is expected to be equal to or higher than the GSH amount. However, total glutathione levels (GSH + GSSG) of both assays were lower than GSH concentrations, in spite of repeated trials with different sample preparation and different individuals used. Therefore, GSSG determination failed and the specific GSH/GSSG ratio could not be calculated.

As for GSH, both seal species exhibited significantly elevated levels compared to mice (Fig. 3.5; Table 3.2). The visual cortex had the overall highest GSH concentrations, with 96 ± 7.2 µM ($p < 0.001$) in harp seals and 103 ± 8.3 µM ($p < 0.001$) in hooded seals, compared to only 34 ± 2.9 µM in mice. Further, while harp seals and hooded seals had cerebellar GSH concentrations of 90 ± 10.1 µM ($p < 0.001$) and 80 ± 3.2 µM ($p < 0.001$), respectively, mice had only 16 ± 0.4 µM. Similarly, the hippocampi of harp and hooded seals had GSH levels of 86 ± 17.7 µM ($p < 0.001$) and 100 ± 5.5 µM ($p < 0.001$), while mice had 30 ± 1.5 µM.

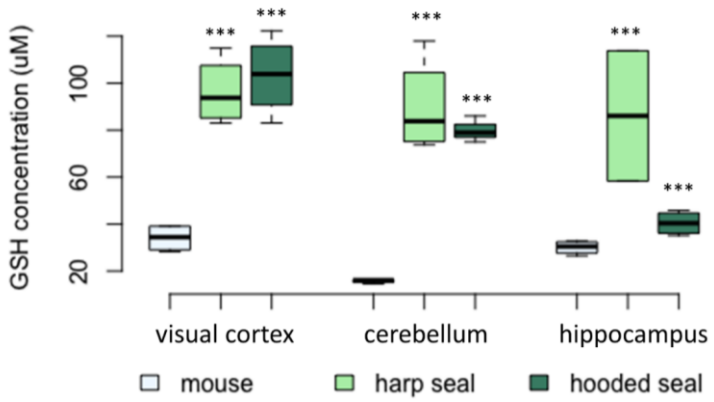

***Fig. 3.5**. The concentration of reduced glutathione (GSH, µM) in mice, harp seals and hooded seals. Significance levels refer to differences compared to mice in the respective brain region and are represented by asterisks (p ≤ 0.05 (*), p ≤ 0.01 (**), p ≤ 0.01 (***).*

Positive selection

To explore whether positive selection was acting on genes coding for antioxidants in the pinniped lineages, we selected seven pinnipeds and five terrestrial carnivores and fitted two branch-site models (BUSTED and aBSREL). We found no genes for which any positive selection pressure was indicated, for either seal species (Supplementary Table S3.4).

Discussion

Elevated antioxidant gene expression in hooded seal neurons

We here extend the work of Geßner et al. (2022) by investigating the expression levels of all antioxidant genes from the neuron-specific transcriptomes of hooded seals and mice. The majority of differentially expressed genes were more highly expressed in seal neurons (Supplementary Table S3.2) and thus, our data indicate an overall higher expression of antioxidant genes in hooded seal neurons than in mice, regardless of brain region studied. For example, the S100 calcium-binding protein A9 (S100A9) (Supplmentary Table S3.2), which plays an important role in the regulation of inflammatory processes and the immune response (Ryckman et al. 2003), was 99.7-fold more highly expressed in the seal compared to the mouse. The expression of S100A9 in neutrophiles and activated macrophages, cells that produce large amounts of ROS during inflammation, suggests that it protects tissues from oxidative damage (Srikrishna 2012). In murine neutrophils, S100A9 alters mitochondrial homeostasis. Neutrophils lacking S100A9 produce increased levels of mitochondrial $O_2^{\bullet -}$ when challenged with bacteria (Monteith et al. 2021). In the seal brain, S100A9 may possibly have similar roles in ROS defence and mitochondrial balance, which could explain its high expression in hooded seal neurons.

Another example was selenoprotein T (SELENOT, FC = 17.6, Supplementary Table S3.2), which possesses a potent oxidoreductase activity and protects dopaminergic neurons in mice from oxidative stress and cell death (Boukhzar et al. 2016).

Two more interesting candidates that were more highly expressed in seal than in mouse neurons, although with less margin, are heme oxygenase 2 (HMOX2, FC = 2.5) and paraoxonase 2 (PON2, FC = 4, Supplementary Table S3.2). HMOX2 is a constitutively expressed enzyme involved in heme catabolism, by cleaving heme to biliverdin which is then metabolized to bilirubin. Free cellular heme, if not cleaved, can lead to ROS production and membrane lipid peroxidation (Belcher et al. 2010). Both, biliverdin and bilirubin, are potent antioxidants (Barañano et al. 2002). Consequently, HMOX2 activity has an important role in heme homeostasis and cytoprotection. In contrast to the well-studied isoform HMOX1, HMOX2 is more highly expressed in neuronal cells in the forebrain, cerebellum, hippocampus and other brain regions in rats and has functions in cytoprotection and oxygen sensing (Muñoz-Sánchez and Chánez-Cárdenas 2014). Several studies have shown that HMOX2 gene expression is activated by oxidative stress, while hypoxia can regulate gene expression and translation (Muñoz-Sánchez and Chánez-Cárdenas 2014 for a review). Interestingly, while HMOX1 expression in skeletal muscle of northern elephant seals is associated with the expression of other antioxidants, correlates with age and was highest in adult females, HMOX2 expression did not vary with age or sex (Piotrowski et al. 2021). Adult females are thought to dive beyond their calculated aerobic dive limit (Hassrick et al. 2007) and thus, the observed elevated expression may be needed to protect them from a more

severe risk of oxidative damage (Piotrowski et al. 2021). These results show that the precise interplay of antioxidants may vary with species, age and sex.

PON2 is mainly localized in the mitochondria, where it scavenges ROS. Its expression is highest in dopaminergic regions, such as the striata, where it is more highly expressed in astrocytes than in neurons (Costa et al. 2014). PON2 knockdown mice and mice with reduced PON2 levels were more susceptible to oxidative stress than wild type mice (Ng et al. 2006). This indicates that the constitutively high PON2 levels in hooded seals might prevent cellular damage in phases of oxidative stress.

Antioxidant expression in the cerebellum

While the differential expression found in the neuronal transcriptomes of hooded seals and mice was mostly confirmed using qPCR and enzymatic acitivity assays, the qPCR data of the cerebellum was an exception. For example, SOD1 expression (transcriptome) in hooded seal neurons from the visual cortex was higher than in corresponding cells from mice (Table 3.1). Concordantly, SOD enzymatic activity was higher in all three brain regions of both seal species than in mice (Fig. 3.2). SOD1 expression (qPCR) confirmed these data in the visual cortex and hippocampus, while the expression of the cerebellum was different across most of the genes studied (Fig. 3.1). Consequently, while activity assays suggested that the cerebellum of seals has an antioxidative capacity similar to other brain regions, the qPCR implies that it was lower. This difference is possibly due to activity assays detecting all isoforms of an enzyme, while the qPCR specifically detects the isoform of interest. Thus, we cannot fully exclude that the cerebellum might have an overall lower antioxidant capacity than the other studied brain regions. Future expression studies could analyze all isoforms of a particular enzyme in the cerebellum and compare a larger number of genes in different brain regions to clarify this observation.

High SOD levels in the pinniped brain

One of the most common ROS is the highly reactive superoxide anion radical ($O_2^{\bullet-}$), which is the primary free oxygen radical produced in mitochondria (Murphy 2009). Superoxide dismutase (SOD) is in the first line of defence against ROS. SOD converts $O_2^{\bullet-}$ to the more stable hydrogen peroxide (H_2O_2) (McCord and Fridovich 1969). SOD1 was found to be more highly expressed in neurons of the visual cortex in hooded seals than in mouse neurons (Geßner et al. 2022). Even when all transcripts (not only antioxidant genes) were considered, SOD1 was among the top 10 most strongly expressed genes in hooded seal neurons and it was among the top 10 with the highest fold change compared to neurons of mice, which implies its high importance for seal neurons. SOD1 qPCR expression analyses (except for cerebellum) and enzymatic activity assays indicated that constitutively elevated SOD levels might be an important adaptation to diving in pinnipeds and could be relevant in different brain regions.

Mitochondrial energy metabolism is quantitatively the most relevant source of ROS in eukaryotic cells (Kowaltowski et al. 2009). Earlier transcriptome studies of hooded seal neurons and whale brains (whole tissue) have revealed an elevated expression of genes involved in mitochondrial function and oxidative phosphorylation (Krüger et al. 2020; Geßner et al. 2022). However, a study in which only enriched gene ontology terms were considered, but without detailed study of mitochondrial genes, did not find this (Fabrizius et al. 2016). Geßner et al. (2022) suggested that an elevated mitochondrial function, i.e., an elevated aerobic capacity, is important to efficiently use oxygen as far as it is available. However, it might also lead to phases of higher ROS production, especially upon reperfusion as the animal surfaces after a dive, which might necessitate constitutively higher SOD levels in order to prevent ROS leakage from mitochondria.

Our results are in line with previous studies in diving mammals: Blood, heart, kidney and lung tissue of several cetacean, pinniped and manatee species have generally higher SOD activities as compared to domestic pigs and/or other non-diving mammals (Elsner et al. 1998; Wilhelm Filho et al. 2002; Vázquez-Medina et al. 2006). Among diving mammals, SOD activity was positively correlated with dive duration data for the involved species (Righetti et al. 2014), although that does not hold true for all species comparisons (Cantú-Medellín et al. 2011).

Elevated GPX expression and activity in pinnipeds

After the conversion of $O_2^{\bullet-}$ by SODs to hydrogen peroxide (H_2O_2), H_2O_2 can be reduced to water by glutathione peroxidase (GPX) (Lubos et al. 2011). GPX also reduces lipid peroxides and organic hydroperoxides (Esworthy et al. 1991). GPX1, and GPX3 in particular, were more highly expressed in hooded seal neurons compared to mouse neurons. Similar to SOD1, GPX3 was among the top 10 most highly expressed genes and among the top 10 genes with the highest-fold changes compared to neurons of mice, indicating its importance in hooded seal neurons of the visual cortex. Enzymatic activity assays detecting all GPX forms showed increased activity in hooded and harp seals in all brain regions studied. GPX3 expression (qPCR) was only elevated in the visual cortex (and insignificantly increased in the hippocampus) of both seal species compared to mice. Our data suggest that GPX is a relevant component of the antioxidant defence system of diving mammals. Possibly, high conversion rates of $O_2^{\bullet-}$ to H_2O_2 via SOD necessitates further processing of H_2O_2 by high GPX activity. Our results supplement previous observations of high GPX levels in other tissues than brain, showing that heart, lung and muscle tissue of ringed seals (*Phoca hispida*) has elevated GPX activity compared to domestic pig tissues (*Sus scrofa domesticus*) (Vázquez-Medina et al. 2006). Blood of several cetacean species also showed elevated GPX activities compared to terrestrial mammals (Wilhelm Filho et al. 2002). Similar to SOD, some authors found higher GPX activities in blood from species with longer

submergence times (Righetti et al. 2014), while other studies did not find such a correlation when heart, brain, lung, kidney and muscle tissues were analyzed (Cantú-Medellín et al. 2011).

The conversion of H_2O_2 to water by GPX goes along with the oxidation of the reduced glutathione (GSH) to glutathione disulphide (GSSG) (Lauterburg et al. 1984). The glutathione system, thus, plays a central role in antioxidant defence. For that reason, we studied it in greater detail.

The glutathione system: GSH and GSR levels, and GSH biosynthesis

GSH is a non-enzymatic antioxidant that functions as scavenger of free radicals (e.g., Jiménez and Speisky 2000), as a substrate in GPX reactions, in reactions catalyzed by glutathione-S-transferases (GST) possessing peroxidase function and by phospholipide hydroperoxide glutathione peroxidase, and in reactions with α-tocopherol (vitamin E) protecting lipids from ROS damage (Meister 1983). All these processes lead to the oxidation of GSH to glutathione disulfide (GSSG). Consequently, the organism depends on a GSH concentration that is sufficient to facilitate these reactions. We expected elevated GSH levels in the pinniped brain compared to mice and our data confirmed this hypothesis. Our results are in line with elevated GSH levels in several tissues of ringed seals compared to domestic pigs (Vázquez-Medina et al. 2007) and in blood from several cetaceans and one semiaquatic species (neotropical otter (*Lontra longicaudis annectens*)) compared to terrestrial mammals (Wilhelm Filho et al. 2002; García-Castañeda et al. 2017).

We were unable to correctly measure total glutathione levels (GSH + GSSG) and thus, could not calculate the GSH/GSSG ratio in spite of using two different assays, varying preparation of samples, and testing different individuals of seals and mice. In mice, the expected GSSG concentration should be ~0.7% of the GSH concentration, as was found in the cerebral cortex, cerebellum and brain stem in mice (Folbergrová et al. 1979). Wilhelm Filho et al. (2002) found no difference in blood total glutathione content (ratio was not calculated) between cetaceans and terrestrial species. García-Castañeda et al. (2017) calculated the GSSG/total glutathione ratio, which was lower in diving species than in non-diving mammals, ascribing diving species a higher capacity for GSH-dependent reactions.

Often, the GSH/GSSG ratio is considered an indicator of the redox state and, thus, the wellbeing of a cell. Drastic changes in this ratio indicate that there is an imbalance in the redox metabolism. However, enzymatic reactions involving GSH depend on the GSH-concentration, not on GSSG, as predicted by the Nernst equation, and are typically not affected by GSSG (Flohé 2013). Even though our dataset is partially incomplete, given the missing data on total glutathione levels, this missing value might not compromise our overall findings.

Glutathione reductase (GSR) mediates the transition of GSSG to GSH that is necessary for the recovery of the GSH pool (Fig. 3.6). Since GSH levels were high in seals, we expected similarly elevated GSR

levels. GSR expression was only moderately, but yet significantly, elevated in hooded seal neurons. However, the GSR activity was found to be similar, or even lower, in seals than in mice. This is surprising, since blood samples from cetaceans showed elevated GSR activities compared with terrestrial mammals (Wilhelm Filho et al. 2002). Blood from seals and brain tissue from mice can be sampled easier and faster than brain tissue of seals. Given that GSR gene expression was high and that enzymes differ in stability, we cannot exclude that GSR possibly degraded during the 10 min it took to sample and preserve seal brain tissues. However, since GSR activity increases in response to rising GSSG levels during oxidative stress, it is possible that significant increases in GSR activity are a characteristic of tissue in acute oxidative stress rather than a constitutive measure (Jones 2002a).

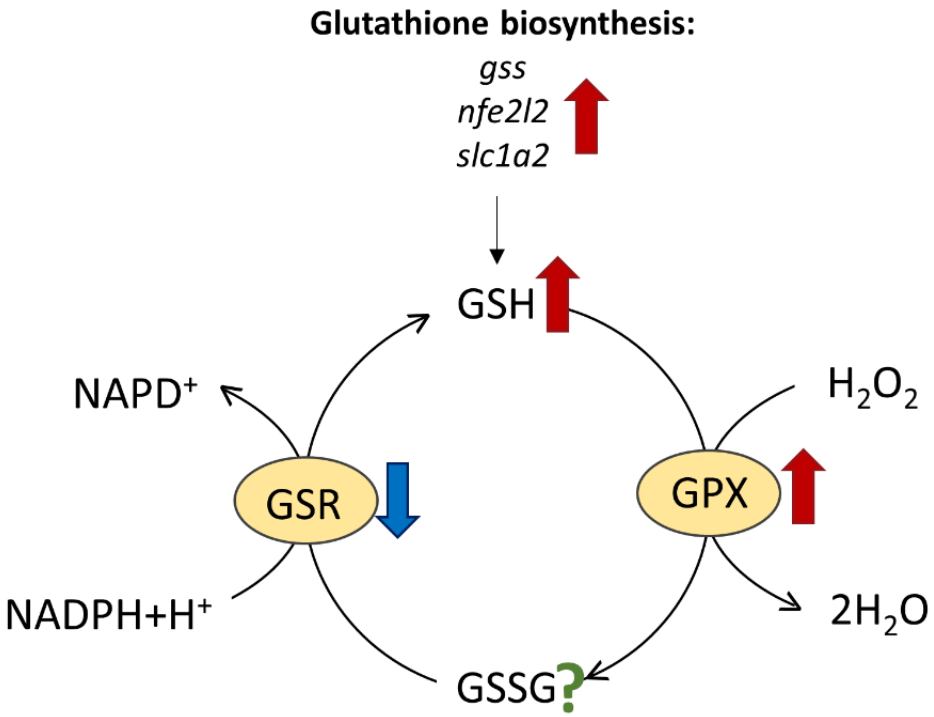

***Fig. 3.6**. Reactions involving reduced glutathione (GSH), such as the conversion of H_2O_2 to water by glutathione peroxidase (GPX), oxidize GSH to glutathione disulphide (GSSG), which is then re-cycled to GSH by glutathione reductase (GSR). Results of elevated expression/enzymatic activity in harp and/or hooded seals vs. mice are indicated by red arrows and reduced activity by blue arrows, while the question mark signifies unknown activity change.*

Apart from GSR, other enzymes and factors also contribute to the GSH level. Since GST conjugates GSH to electrophilic compounds, a reduced activity of GSTs - as found in pinnipeds - might draw relatively less GSH from the GSH pool, although to the best of our knowledge we do not know the effect size of GST activity on GSH concentration. In hooded seal neurons, glutathione synthase (GSS, EC 6.3.2.3), nuclear factor erythroid 2-related Factor 2 (NFE2L2), a transcription factor activating glutathione biosynthesis and the expression of other antioxidants (Cullinan and Diehl 2004; Eggler et al. 2009), and solute carrier family 1 member 2 (SLC1A2, EAAT2), were all more highly expressed than in mice (Supplementary Table S3.2). SLC1A2 is a membrane-bound transporter mediating neuronal uptake of

amino-acids, which, among other things, is responsible for clearing glutamate from the synaptic cleft (e.g., Arriza et al. 1994). Additionally, mouse cortical neuron culture studies show that SLC1A2 and SLC1A3 also facilitate the uptake of cysteine, which is a rate-limiting factor in glutathione synthesis (Chen and Swanson 2003). Taken together, our data suggest that elevated levels of GSH in the seal brain are, at least in part, explained by elevated GSH biosynthesis.

High expression of specific GSTs, but overall reduced GST activity in the pinniped brain

The glutathione-S-transferases (GSTs) are enzymes that conjugate GSH to electrophilic reactive compounds that would otherwise bind to proteins or nucleic acid, leading to cellular damage. Some GSTs are also able to detoxify hydroperoxides (Cooper and Kristal 1997; Sherratt and Hayes 2001) and certain cytosolic GSTs also catalyze GSH-dependent reduction of lipid peroxides (Cooper and Kristal 1997). We found GSTK1, GSTO1 and GSTO2 to have a noticeably elevated expression in hooded seal neurons compared to mice (Table 3.1). We selected GSTK1 and GSTO1 for qPCR analysis that confirmed a higher pinniped expression in the brain regions studied (except for the cerebellum, Fig. 3.1). Surprisingly, the GST assay, detecting all GSTs, showed a clearly lower GST activity in both seal species. We therefore extracted gene expression values for all GSTs present in our neuronal transcriptome (Supplementary Table S3.5) and found that other GSTs, such as GSTM1 and GSTM3, are markedly less expressed in neurons of the hooded seal than in mice, which caused the overall GST expression to be similar between the species. The broad and partly overlapping substrate specificity of GSTs (Wätjen and Fritsche 2010) makes it difficult to explain why some GSTs might be more, or less, expressed in the seal brain. However, these data suggest that GSTs in general might not be a crucial component in the antioxidant defence system of the seal brain.

Previous studies on GST activities in tissues from diving mammals also reveal mixed results. GST activities were higher in the blood of southern elephant seals (*Mirounga leonina*), marine manatee (*Trichechus manatus*) and 3 dolphin species, when compared to terrestrial mammals (Wilhelm Filho et al. 2002). In ringed seal tissues, GST activity was higher and lower in heart and liver, respectively, compared to domestic pigs, but similar in lung, kidney and muscle (Vázquez-Medina et al. 2006). GST activity does not appear to correlate positively with diving capacity/behaviour, since GST activities of short-duration/shallow divers versus deep/long-duration divers were similar in seven tissues studied (Cantú-Medellín et al. 2011). Only in blood, GST activity appears to increase with diving ability in seals (Righetti et al. 2014). Interestingly, cetaceans have undergone a reduction of the GST gene family, with bowhead whales (*Balaena mysticetus*) having 16 GSTs, while mice have 30 copies and Weddell seals have an intermediate number of 22 GSTs (Tian et al. 2019). The hypoxia tolerant naked mole rat (*Heterocephalus glaber*) has a high number of the cytosolic mu subclass of GSTs responsible for cellular detoxification (10 copies). Further, some GSTs have signatures of positive selection (GSTP2) in five

mammalian lineages, while others (GSTP1) are conserved across mammals (Tian et al. 2019). We did not find GSTO1 to be positively selected in seals. To summarize, a detailed study of the orchestra of expansion/reduction, expression and functional changes of certain GST subclasses, rather than a measurement of the overall GST activity alone, would better explain the adaptation to differently adverse environments.

The glutaredoxin and thioredoxin systems

In mammalian cells, the cytosolic and mitochondrial thioredoxin systems and the glutathione-glutaredoxin system have a key role in antioxidant defence and have a great impact on the cellular redox state (Lu and Holmgren 2014). We here examine a representative of each system.

Mixed GLRX2 expression in the pínniped brain

Glutaredoxin 2 (GLRX2) is an antioxidant enzyme belonging to the glutaredoxin family, which consists of small redox proteins of the thioredoxin superfamily. It catalyzes the transfer of electrons from GSH to disulfides (Holmgren 1989), which maintains the intracellular redox homeostasis in the face of oxidative stress (Jung and Thomas 1996). GLRX2 is expressed in a range of tissues, including neurons of the mammalian brain (e.g., Padilla et al. 1992; García-Pardo et al. 1999; Karunakaran et al. 2007; Mailloux et al. 2014; Upadhyaya et al. 2015). GLRX2 is an interesting candidate when studying the antioxidant defence of diving mammals since it protects mouse cardiomyocytes from hypoxia-/reoxygenation-induced oxidative stress, apoptosis and inflammation (Li et al. 2021). GLRX2 facilitates mitochondrial redox homeostasis and thus, contributes to the functional integrity of mitochondria (Karunakaran et al. 2007). Since whale brains (Krüger et al. 2020) and hooded seal neurons (Geßner et al. 2022) appear to have a high capacity for oxidative phosphorylation and possibly an abundant number of mitochondria based on a high expression of components of the mitochondrial envelope in hooded seal neurons (but see Mitz et al. 2009), we could perhaps have anticipated an elevated expression of GLRX2. Instead, we found GLRX2 to be less expressed in hooded seal neurons than in mice and tested whether this trend is true for other brain regions, as well. Indeed, GLRX2 expression in harp seals and hooded seals was lower or similar compared to mice. Further, GLRX and GLRX3 were also less expressed in hooded seal neurons than in mice (Supplementary Table S3.2).

Since other essential components of the antioxidant system, such as SOD and GPX, appear to be constitutively more highly expressed in seals, it might not be necessary for the glutaredoxin system to be constitutively more active. Instead, upregulation of GLRX2 might be triggered by oxidative stress, as observed in mouse cardiomyocytes upon hypoxia/reoxygenation treatment (Li et al. 2021). Further support comes from diving-induced upregulation of GLRX2 in the blood of bottlenose dolphins (Blawas et al. 2021).

TXNRD3 expression was higher (harp seal) or similar (hooded seal) to mice

Thioredoxin reductase 3 (TXNRD3) is a representative of the thioredoxin system. Among the three thioredoxin reductase isoenzymes known in mammals, TXNRD3 is the only one that contains an additional N-terminal glutaredoxin domain, which enables this isoenzyme to be involved in both the thioredoxin and the glutaredoxin systems (Arnér 2009). TXNRD3 reduces thioredoxin. The thioredoxin system provides electrons to thiol-dependent peroxidases, to detoxify reactive oxygen and nitrogen species (Lu and Holmgren 2014). TXNRD1 and TXNRD3 were both more highly expressed in hooded seal neurons compared to mice (Supplementary Table S3.2), while thioredoxin was not differentially expressed (data not shown). Expression data in other brain regions were mixed, with TXNRD3 being more highly expressed in harp seals (except for cerebellum), while being similarly expressed in hooded seals compared to mice. To the best of our knowledge, the thioredoxin system has not been studied in hypoxia-tolerant species. However, Alzheimer's disease (AD) is characterized by hypoxia and oxidative damage and - similar to our findings–increased TXNRD levels, but decreased thioredoxin levels were found in AD brains. The increased TXNRD levels alone were interpreted as insufficiently protective (Lovell et al. 2000). Similar to the glutaredoxin system, thioredoxins may, thus, not belong to the constitutively increased antioxidative defence system of the pinniped brain.

Antioxidant genes appear to be conserved in pinnipeds

We found that none of the here studied antioxidant genes (GPX3, SOD1, GSTK1 GSTO1, TXNRD3, GLRX2 and GSR) have been subject to positive selection in pinnipeds when compared to non-diving carnivores (Supplementary Table S3.4). Since we found elevated expression and enzymatic activity levels in several of these antioxidants, the results suggest that selection might have favoured increased levels, whereas gene sequence and function were conserved in pinnipeds. There is, however, evidence that positive selection is relevant in the adaptation to the aquatic life in general and to hypoxia in particular. For instance, genes for oxygen transport (hemoglobin-α and -β, myoglobin) and genes regulating vasoconstriction show positive selection in cetaceans (Tian et al. 2016). Further, GSR was positively selected in the bottlenose dolphin (*Tursiops truncatus*) and both GSR and GPX2 show cetacean-specific amino-acid substitution (Yim et al. 2014). Interestingly, there are three pinniped-specific amino-acid changes in GSR (Supplementary Fig. S3.1) and BUSTED found evidence for diversifying selection, i.e., at least one site in at least one branch has undergone positive selection. However, aBSREL failed to identify one or more branches. Consequently, GSR might not truly be positively selected in pinnipeds, but it might be carefully interpreted as weak signals of positive selection that are not beyond the threshold of being clearly characterized as positive selection.

In this study, pinniped antioxidant capacity was compared to that of mice. While mice are a well-accepted organism for scientific purposes with clear advantages in availability and handling, it would

be ideal to compare pinnipeds to non-diving mammals of similar body size, since metabolic rate correlates with body mass (e.g., Gillooly et al. 2001) which might also affect ROS production and, thus, antioxidant capacity. Previous studies compared antioxidants in ringed seals with domestic pigs and found a similar trend as in this study, i.e., a generally elevated antioxidant capacity in ringed seals.

Conclusion

We conclude that the brains of harp and hooded seals have an overall constitutively enhanced antioxidant defence system, as has been generally found in other tissues of diving mammals. We found that not the antioxidant system as a whole, but some of its essential components, such as SOD and GPX, were constitutively elevated, whereas others, like the glutaredoxin and thioredoxin systems, were not enhanced (Table 3.2 for a summary). These systems and possibly other antioxidants are likely activated as needed, and may be further boosted by diving-induced mechanisms, as observed for GLRX2 in bottlenose dolphins (Blawas et al. 2021). Since we studied two pinniped species, our findings might generally be similar in other pinnipeds. However, the precise orchestra of protective mechanisms, including antioxidant capacity, might vary with species based on their life history traits, with age and with sex. For instance, the muscle expression of several antioxidant genes increased with age and diving ability in northern elephant seals and hooded seals (Vázquez-Medina et al. 2011b; Piotrowski et al. 2021) and some antioxidants were observed to be higher in northern elephant females than in males (Piotrowski et al. 2021).

Data availability statement

The original contributions presented in the study are included in the article/Supplementary Material, further inquiries can be directed to the corresponding author.

Ethics statement

The animal study was reviewed and approved by Norwegian Animal Welfare Act and with approvals from the National Animal Research Authority of Norway (Norwegian Food Safety Authority permits no. 12268 and 22451).

Author contributions

CG conceived the research idea, CG and GM conducted the experiments and analyzed the data, LF sampled the hooded seal and harp seal tissues, TB received the funding, CG wrote the manuscript with input from all authors.

Funding

This work was supported by the Deutsche Forschungsgemeinschaft (Bu956/22).

Conflict of interest

The authors declare that the research was conducted in the absence of any commercial or financial relationships that could be construed as a potential conflict of interest.

9 Discussion

Marine mammals demonstrate a fascinating adaptation to their aquatic environment. Their diving lifestyle involves recurrent low oxygen conditions, which may have put evolutionary pressure on specific genetic components (Hindle 2020). Thus, studies investigating gene selection may elucidate adaptive mechanisms in marine mammals. For instance, altered evolutionary rates for genes involved in oxygen transport (e.g., hemoglobin subunits alpha and beta and myoglobin), vasoconstriction (e.g., endothelin pathway genes) and cell protection (e.g., detoxification of reactive oxygen species (ROS)) have been demonstrated in cetacean species (Tian et al. 2016; Tian et al. 2019; Yim et al. 2014). Other studies also revealed that genes with nervous system functions were positively selected in genomes of cetaceans (bottlenose dolphin (*Tursiops truncatus*), Yangtze river dolphin (*Lipotes vexillifer*)) (McGowen et al. 2012; Zhou et al. 2013). Although the genomes of marine mammals demonstrate substantial convergent evolution, it does not always link to convergent phenotypes in cetaceans and pinnipeds (Foote et al. 2015; Thomas et al. 2017). Noh et al. (2022) took a closer look at the genomes of a phocid seal, the Weddell seal (*Leptonychotes weddellii*), and the walrus (*Odobenus rosmarus divergens*) and identified regions of accelerated divergence compared to 57 other placental mammals. Those regions were especially enriched in genes involved in lipid metabolism and hypoxia regulation, but also neurologic functions such as axonal guidance signaling and glutamatergic synapse signaling (Noh et al. 2022). These findings link cerebral adaptations of marine mammals to their extraordinary diving lifestyle, involving recurrent low oxygen conditions. Despite being among the most sensitive organs to low tissue oxygen levels (hypoxia), the hooded seal (*Cystophora cristata*) brain survives extended periods of severe hypoxia, while neurons from other mammals lose their functional integrity (Folkow et al. 2008; Ramirez et al. 2011; Geiseler et al. 2016). However, this intrinsic hypoxia tolerance of the hooded seal brain is not well understood. Therefore, different molecular targets were investigated in this study such as (i) brain lipids and polar metabolites, (ii) the neuroprotective genes Clusterin (CLU) and S100B in transfected neuronal cell cultures, and (iii) the antioxidant expression and activity in the hooded seal and harp seal (*Pagophilus groenlandicus*) brain. The obtained results further uncovered molecular pathways that may be altered in the pinniped brain, namely neurotransmission (Chapter 9.1), energy metabolism (Chapter 9.2), and protection against oxidative stress (Chapter 9.3), which will be discussed in the following sections.

9.1 Reduced neurotransmission in the pinniped brain

The mammalian brain has a very high demand for energy, which it mainly needs for the maintenance of ion gradients, membrane potentials and neurotransmitter levels (Attwell and Laughlin 2001; Alle et al. 2009). Especially glutamatergic synaptic signaling is a highly energy-intensive process, making it very sensitive to conditions, when energy supply becomes scarce (Sibson et al. 1998; Andersen et al. 2021).

Thus, failure to remove glutamate from the synaptic cleft during hypoxia is a major contributor to neurotoxic cell death due to overstimulation of receptors, excessive calcium influx and neuronal depolarization (Choi and Rothman 1990; Belov Kirdajova et al. 2020). A previous study in our lab compared the transcriptomes of excised neurons from the visual cortex of hooded seals and mice (*Mus musculus*) and observed that neurotransmission and especially glutamatergic processes may be reduced in the hooded seal neurons (Geßner et al. 2022). In detail, expression of glutaminase and glutamate receptors was decreased, reducing the supply of glutamate and glutamatergic signal transduction, while a glutamate transporter was more highly expressed, facilitating glutamate uptake and thus its clearance from the synaptic cleft and termination of its action (Geßner et al. 2022). Reduced neurotransmission may ultimately decrease the energy expenditure in the hooded seal brain and protect against hypoxia, when oxygen and thereby energy supply is limited.

In the present study, specific polar metabolites in the brain of deep-diving pinnipeds, the hooded seal and harp seal, were analyzed and determined that their glutamine and glutamate pool is constitutively reduced compared to mice (Martens et al. 2023). In conditions of hypoxia and reoxygenation it might decrease even further (Martens et al. 2023). In hypoxia-tolerant species such as the naked mole rat (*Heterocephalus glaber*) hypoxia also leads to a reduction of glutamine and glutamate in its brain, while in mice only glutamine decreases (Cheng et al. 2022). A reduction in glutamate and glutamine may serve to reduce neurotoxic effects and an overall decreased neurotransmitter pool may therefore be beneficial to deal with hypoxic conditions. Interestingly, glutamate is also decreased in the brain of hypoxia-preconditioned mice (Liao et al. 2018). Thus, hypoxia-tolerant species such as marine mammals may develop this feature due to their lifestyle with recurrent hypoxic conditions along with their diving capacity (Geiseler et al. 2013; Noren 2020). However, hypoxia preconditioning also led to an increase of inhibitory neurotransmitters such as γ-aminobutyric acid (GABA) in the mouse brain (Liao et al. 2018). Geßner et al. (2022) observed a decreased GABAergic neurotransmission in hooded seal neurons compared to mice, arguing that the downregulation of its predecessor glutamate might have also led to a reduction in GABA. Thus, GABA might not be as important for metabolic depression and neuroprotection in the hooded seal brain as in other hypoxia-tolerant species (e.g., Nilsson et al. 1991; Lutz 2002).

S100B has been found to be highly expressed in the hooded seal brain and may contribute to the observed reduction in neurotransmission. Specifically, its expression was 38-fold higher in the hooded seal visual cortex compared to the ferret (*Mustela putorius furo*) and 82-fold higher in laser-excised hooded seal neurons than in neurons of mice (Fabrizius et al. 2016; Geßner et al. 2022). Because of its calcium-binding capacity, S100B has been suggested to play a role in buffering excessive calcium influx during hypoxic conditions and dysregulation of ion homeostasis in hooded seal brain slices (Geiseler et al. 2016). It is also associated with neurodegenerative diseases, where it may play a neuroprotective

or neurotoxic role depending on its concentration and subcellular localization (Michetti et al. 2021). Recently, cell culture experiments have shown that overexpression of S100B is protective at hypoxia and oxidative stress conditions (Geßner et al. 2020). However, its exact molecular mechanisms and targets remain controversial and ambiguous (Michetti et al. 2021; Satapathy and Wilson 2021). In this study, the transcriptomes of S100B-transfected neuronal cell lines were analyzed that were exposed to normoxia, hypoxia and oxidative stress *in vitro* (Martens et al. 2022b). Gene expression of transfected cells was already different at normoxic conditions, which may display a preparatory response to upcoming stress conditions (Martens et al. 2022b). The o*pioid signaling pathway* was among the top ten activated IPA pathways, which may prevent calcium ion influx and neurotransmitter release (Gopalakrishnan et al. 2021). Especially the upregulated opioid receptor delta 1 (OPRD1) and the downregulated purkinje cell protein 4 (PCP4) may contribute to reduced neurotransmission (Martens et al. 2022b). OPRD1 mainly facilitates neuroprotection by maintaining ion homeostasis, inhibiting excitatory neurotransmitter release and attenuating disrupted neuronal transmission (He et al. 2013; Sheng et al. 2018). Accordingly, it was demonstrated that OPRD1 prevents hypoxia-induced excitotoxicity in neuron and astrocyte cell cultures (Zhang et al. 2002; He et al. 2013; Liang et al. 2014). However, OPRD1 also promotes other neuroprotective mechanisms such as upregulation of brain-derived neurotrophic factor (BDNF) (Tian et al. 2013; Sheng et al. 2018), mitophagy (Xu et al. 2020) and microRNAs (Chen et al. 2020b). In contrast to OPRD1, PCP4 has been demonstrated to induce Ca^{2+} and neurotransmitter release (Renelt et al. 2014). Its downregulation in the S100B-transfected neuronal cells may further support a reduction of neurotransmission (Martens et al. 2022b). Upregulation of OPRD1 and downregulation of PCP4 was also observed when the transfected cells were exposed to hypoxia and oxidative stress (Martens et al. 2022b). Since the cell line demonstrates an increased viability at these conditions, a reduction of neurotransmission may be beneficial for cell survival (Geßner et al. 2020; Martens et al. 2022b).

In order to maintain normal brain function and compensate reduced neurotransmission, the hooded seal may rely on other processes to support synaptic activity. Sphingolipids, especially sphingomyelins, are part of the myelin sheath surrounding axons and thus play a critical role in supporting efficient signal transduction in the brain (Hartline 2008). In neurodegenerative diseases such as Alzheimer's disease, Parkinson's disease and traumatic brain injury, studies mainly observed increased levels of sphingomyelins (Kao et al. 2020; Ojo et al. 2019; Xicoy et al. 2019). This has been suggested to indicate the strong necessity for myelin repair due to axonal damage (Ojo et al. 2019). Especially long-chain sphingomyelin species may be up-regulated in Alzheimer's disease (Chan et al. 2012). Here, an untargeted lipidomics study revealed very-long-chain sphingomyelin species to be elevated in the brain of the hooded seal and harp seal compared to terrestrial relatives, the ferret and the mouse (Martens et al. 2023). This increase in sphingomyelin levels may have different functions. On the one

hand, the increased sphingomyelin concentrations may be used for remyelination of hypoxia and oxidative stress damaged axons, equivalent to neurodegenerative diseases (Ojo et al. 2019). On the other hand, increased levels of sphingomyelins may lead to a thicker myelin layer and a stronger sheathing of axons, which would enhance conduction speed and reduce ion flux (Hartline 2008). A more efficient signal transduction may be beneficial to further reduce energy expenditure as preparation for upcoming stress conditions. Interestingly, sphingomyelin species were generally elevated in the adult hooded seal and harp seal brain, while juvenile hooded seals did not show a collective increase (Martens et al. 2023). Thus, increased levels of sphingomyelin may develop postnatally with diving activity.

Our studies confirm that the hooded seal brain may exhibit a reduced neurotransmission to decrease energy expenditure and prevent neurotoxic events when energy becomes scarce. Diving mammals may cope with hypoxic conditions by a 'partial shutdown' of neuronal activity during diving (Ramirez et al. 2007). In other hypoxia-tolerant species, a lower basal expression of synaptic proteins and the ability to decrease their function may lead to a 'synaptic arrest' during low oxygen conditions (Buck and Pamenter 2018). Regardless of the mechanism, reducing energy-intensive neurotransmission appears to be beneficial for surviving low oxygen and energy conditions and thus likely contributes to the hypoxia tolerance of the hooded seal brain.

9.2 Altered energy metabolism in the pinniped brain

Because of its high energy demand, the mammalian brain mostly relies on oxidative metabolism, which generates substantially more energy in the form of adenosine triphosphate (ATP) than anaerobic metabolism (Bélanger et al. 2011). Oxygen is the terminal electron acceptor during oxidative phosphorylation of ATP, taking place in the mitochondrial respiratory chain. Marine mammals, which are routinely exposed to low oxygen conditions, may therefore exhibit mechanisms to efficiently use available oxygen and/or reduce oxygen consumption. Two transcriptomics studies in our lab produced contrasting results on whether oxidative metabolism is enhanced or reduced in the hooded seal visual cortex depending on depth of analysis and reference organism (Fabrizius et al. 2016; Geßner et al. 2022). In whole brain tissue of the hooded seal compared to the ferret, aerobic metabolism was found to be decreased (Fabrizius et al. 2016), while in laser-excised neurons of the hooded seal compared to the mouse, mitochondrial function and number appears enhanced (Geßner et al. 2022). Another transcriptomics study investigated the gene expression of various whale species in comparison to cattle (*Bos taurus*). The results included an elevated aerobic capacity in the cetacean brain (Krüger et al. 2020), illustrating the range of hypoxia coping strategies in marine mammals. In the present comparative lipidomics study, increased levels of very-long-chain sphingomyelins were found in the hooded seal and harp seal visual cortex compared to the ferret and mouse (Martens et al. 2023). The

sphingomyelins may be converted to very-long-chain ceramides, which may trigger mitophagy and consequently reduce mitochondrial aerobic respiration (Kolesnick 1994; Law et al. 2018). Transcriptome analyses of transfected neuronal cells demonstrated that the constitutively secreted chaperone 'soluble clusterin' (sCLU) and S100B may reduce aerobic metabolism at normoxic conditions (Martens et al. 2022b). However, a final conclusion on the aerobic capacity of the hooded seal brain is complicated because of the opposing results obtained by previous studies.

A reduction in oxygen consumption may also be achieved through an enhanced anaerobic metabolism (i.e., glycolysis), which may be beneficial for the hooded seal brain in order to survive oxygen shortage during extended diving bouts (Larson et al. 2014). However, previous transcriptomics studies of the visual cortex found little evidence for an increased glycolytic rate compared to ferrets and mice at resting conditions (Fabrizius et al. 2016; Geßner et al. 2022) as well as in cortical slices exposed to hypoxia and reoxygenation *in vitro* (Hoff et al. 2017). In contrast, the present study showed that overexpression of sCLU and S100B appears to promote glycolytic metabolism at normoxic conditions, at least in our transfected neuronal cell lines (Martens et al. 2022b). Additionally, increased glucose and lactate concentrations were found in the hooded and harp seal brain compared to mice, which might further support an enhanced capacity for anaerobic glycolysis (Martens et al. 2023). Because the pinnipeds and terrestrial relatives have been examined at resting state, the differences we observed may indicate a preparatory adaptation of the seal brain to expected low oxygen conditions during diving. In addition to glucose, the brain may also utilize lactate as energy source, which is usually produced in astrocytes by glycolysis and can subsequently be oxidized in neurons (Bélanger et al. 2011). However, this 'astrocyte-neuron lactate shuttle' hypothesis proposed by Pellerin and Magistretti (1994) may not apply to all species. In the hooded seal brain cytochrome c, neuroglobin and lactate dehydrogenase b are localized predominantly in astrocytes rather than in neurons (Mitz et al. 2009; Hoff et al. 2016). Thus, in normoxic conditions lactate may be shuttled from glycolytic neurons to astrocytes, which may perform consecutive oxidation of lactate, put forward as 'reverse lactate shuttle' hypothesis by Mitz et al. (2009). While further studies need to confirm the theory's validity in this system, shifting oxidative metabolism to astrocytes may protect vulnerable neurons from oxidative stress.

Additionally, most eukaryotic cells are able to switch from mainly aerobic respiration, when oxygen availability is sufficient, towards increasingly anaerobic glycolysis during conditions, when oxygen supply becomes limited (Kierans and Taylor 2021). However, if neurons in the mammalian brain can undergo such a metabolic shift is debated (Herrero-Mendez et al. 2009; Dienel 2019). In agreement, Hoff et al. (2017) did not observe substantial metabolic changes in hypoxia- and reoxygenation-treated hooded seal brain slices *in vitro*. Interestingly, an overall increase in glycolytic metabolism and decrease in mitochondrial metabolism has been observed in the hypoxia-tolerant naked mole rat

(*Heterocephalus glaber*) brain (Pamenter 2022). The present results suggest that the glycolytic end product lactate may be decreased in the hooded seal brain, when exposed to hypoxia and reoxygenation *in vitro* (Martens et al. 2023). This could either indicate decreased glycolytic activity and increased oxidative lactate metabolism or efficient lactate transport out of the hooded seal brain, when oxygen supply is limited. Robergs et al. (2018) argue that lactate production supports glycolytic flux and allows the removal of lactate from metabolically active tissues by monocarboxylate transporters (MCTs). Accordingly, the monocarboxylate transporter 4 (MCT4), which facilitates lactate efflux, has been demonstrated to be highly expressed in hooded seal neurons compared to mouse neurons and was further upregulated in hooded seal brain slices in response to *in vitro* hypoxia and reoxygenation (Geßner et al. 2022; Hoff et al. 2017; Halestrap and Wilson 2012). Yet, glucose levels were maintained through *in vitro* hypoxia- and reoxygenation treatment of hooded seal brain samples in this study (Martens et al. 2023). The elevated glycogen stores of the hooded seal brain may aid in preserving glucose levels and promoting glycolytic metabolism (Czech-Damal et al. 2014), which is important for neuronal survival (Swanson and Choi 1993; Choi and Gruetter 2003). In agreement, Geßner et al. (2022) found that genes associated with glycogenolysis were increased in hooded seal neurons compared to mouse neurons. At least after extensive diving bouts, increased lactate levels were observed in the cerebral venous effluent of harbor seals (*Phoca vitulina*), which may reflect enhanced glycolysis and lactate efflux (Kerem and Elsner 1973). Rogatzki et al. (2015) support the concept of lactate accumulation and increased lactate efflux, when oxidative metabolism is inhibited due to low oxygen concentrations. Exported lactate may be subsequently detoxified by tissues with high buffering capacities (Castellini and Somero 1981; Boutilier et al. 1993). Thus, a high glycolytic capacity and removal of lactate from the brain may be beneficial during frequently experienced low oxygen conditions and may contribute to the hypoxia tolerance of the hooded seal brain.

Cellular hypoxia response is primarily mediated by the hypoxia-inducible factor 1 (HIF1), which is a heterodimeric transcription factor, usually consisting of an alpha subunit (HIF1A) and a beta subunit (HIF1B) (Kierans and Taylor 2021). In hypoxia-tolerant mammals, including cetaceans, high altitude ungulates and subterranean rodents, Zhu et al. (2018) detected convergent amino acid substitutions for genes in the HIF pathway including changes in the oxygen-dependent degradation domain of HIF1A. Thus, the HIF pathway may be crucial for the adaptation to environments characterized by low oxygen conditions (Allen and Vázquez-Medina 2019). A comparison of deep- to shallow-diving cetaceans demonstrated that HIF1A sequence differences influence its stability and activity in changing oxygen conditions and may have implications for diving behavior (Bi et al. 2015). However, in the ringed seal (*Phoca hispida*), the HIF1A sequence appears to be similar to terrestrial mammals, but exhibits several amino acid differences in the oxygen-dependent degradation domain (Johnson et al. 2005). Activation of HIF1 during low oxygen conditions may enhance oxygen delivery and reduce oxidative metabolism,

thereby improving cell survival (Lee et al. 2020; Choudhry and Harris 2018). In agreement, hypoxia upregulates several neuroprotective pathways, including HIF1A in the hypoxia-tolerant naked mole rat brain (Pamenter 2022). Expression of HIF1A develops along with diving capacity of northern elephant seals (*Mirounga angustirostris*) and thus likely plays an important role in their hypoxia tolerance (Vázquez-Medina et al. 2011d). Accordingly, HIF1A expression correlated with reduced oxidative damage in ringed seal tissues (Johnson et al. 2004). Here, an enhanced cellular response to hypoxia was observed in neuronal cell lines transfected with two isoforms of clusterin (CLU), namely nuclear CLU (nCLU) and soluble CLU (sCLU), as well as S100B, which may have been mediated by HIF1A (Martens et al. 2022b). In general, transfected cell lines exhibited increased glycolytic processes, which is a common metabolic strategy when oxygen availability is limited (Kierans and Taylor 2021). Additionally, elevated glycogen biosynthetic processes may have been mediated by HIF1 (Pelletier et al. 2012) and high levels of the glucan phosphatase EPM2A may have promoted glycogen accumulation (Raththagala et al. 2015). As mentioned before increased glycogen stores in the hooded seal brain may protect neurons from hypoxia-induced cell death (Czech-Damal et al. 2014; Saez et al. 2014). Conversely, the transfected neuronal cells in this study demonstrated decreased aerobic respiration, possibly by high expression of pyruvate dehydrogenase kinase 1 (PDK1) (Martens et al. 2022b). PDK1 obstructs aerobic metabolism by inhibiting pyruvate dehydrogenase, which otherwise catalyzes the first rate-limiting step of the TCA cycle (Kim et al. 2006; Papandreou et al. 2006). Geßner et al. (2020) demonstrated that transfection of neuronal cells with nCLU, sCLU and S100B promotes survival of cell lines at hypoxic conditions. However, elevated expression of genes in the HIF pathway was neither observed in the hooded seal brain compared to ferrets and mice (Fabrizius et al. 2016; Geßner et al. 2022) nor in brain slices exposed to hypoxia and reoxygenation *in vitro* (Hoff et al. 2017). Thus, upregulation of the HIF pathway by CLU and S100B appears to support neuron survival in cell culture but may not be as important *in vivo*.

9.3 Elevated antioxidant capacity in the pinniped brain

Marine mammals are challenged with an increased generation of reactive oxygen species (ROS), when surfacing after extensive diving bouts (Zenteno-Savín et al. 2002). To prevent oxidative damage and detoxify emerging oxidants, they are generally equipped with an elevated antioxidant capacity (Vázquez-Medina et al. 2012). In blood and several tissues such as heart, muscle, kidney and lung, increased levels of antioxidant molecules, especially those involved in the glutathione system, have been observed (Wilhelm Filho et al. 2002; Vázquez-Medina et al. 2006, 2007). Although the brain is among the organs most sensitive to oxidative stress due to its high oxidative metabolism and oxygen demand, little is known about its antioxidant capacity in marine mammals (Zielke et al. 2009; Bouzier-Sore et al. 2006). Only one previous study directly compared antioxidant levels of the brain in the deep-diving dwarf sperm whale (*Kogia sima*) and pygmy sperm whale (*Kogia breviceps*) to the shallow-diving

bottlenose dolphin (*Tursiops truncatus*) (Cantú-Medellín et al. 2011). However, Geßner et al. (2022) at least demonstrated a higher expression of antioxidant genes in hooded seal neurons (compared to mice) and Krüger et al. (2020) found higher expression of genes associated with ROS detoxification in the cetacean brain (compared to cattle). The antioxidant system of phocid seals such as the hooded seal and northern elephant seal appears to develop during maturation and buildup of diving ability and thus likely plays an important role in their hypoxia tolerance (Vázquez-Medina et al. 2011b; Vázquez-Medina et al. 2011c). In the present study, the antioxidant system in the brain of deep-diving pinnipeds has been further investigated (Martens et al. 2022a).

Concisely, the expression and activity of selected antioxidants in the visual cortex, hippocampus and cerebellum of the hooded seal and harp seal were compared to the respective mouse brain regions (Martens et al. 2022a). Antioxidative enzymes involved in ROS detoxification and in the glutathione system generally exhibited an increased expression and activity in both pinniped brains, ideally equipping them to deal with excessive ROS generation (Martens et al. 2022a). For instance, the expression of superoxide dismutase 1 (SOD1) and overall SOD activity was elevated in the pinniped brains (Martens et al. 2022a). SOD reduces superoxide radicals ($O_2^{\bullet-}$), which arise during mitochondrial aerobic respiration (Valko et al. 2007), to less reactive hydrogen peroxide (H_2O_2) (McCord and Fridovich 1969). As discussed in the previous chapter (Chapter 9.2), the hooded seal brain may exhibit an elevated aerobic capacity. Geßner et al. (2022) argued that increased mitochondrial function, as indicated by a high expression of mitochondrial genes, might be necessary for efficient utilization of oxygen, but may also result in increased ROS generation. Marine mammals may therefore exhibit increased SOD activities for $O_2^{\bullet-}$ detoxification, as shown in several tissues of cetacean, pinniped and manatee species (Elsner et al. 1998; Wilhelm Filho et al. 2002; Vázquez-Medina et al. 2006). However, high antioxidant capacity may not apply to all brain regions. While our observations appear to be generally true for the visual cortex and hippocampus, the cerebellum may represent an exception. The activity of antioxidative enzymes also appears elevated in the pinniped cerebellum, but the expression of specific genes was not higher than in the mouse cerebellum (Martens et al. 2022a). The observed discrepancy may be explained by enzyme assays determining the activity of all isoforms of an enzyme, while expression was only determined for a specific isoform. Thus, supplemental work on all isoforms of these enzymes may resolve this issue. In addition, the present lipidomics analysis revealed increased levels of lipid plasmalogen species in the pinniped brain (Martens et al. 2023), which may further increase its antioxidant capacity (Dean and Lodhi 2018). In the following sections, the expression and activity of enzymes from the glutathione system (Chapter 9.3.1) and the thioredoxin system (Chapter 9.3.2) will be discussed and how protein homeostasis (proteostasis) (Chapter 9.3.3) and mitochondrial autophagy (mitophagy) (Chapter 9.3.4) may prevent oxidative stress.

9.3.1 Glutathione system

Glutathione is the central redox agent in most aerobic organisms and is able to detoxify a wide variety of electrophilic substrates (Deponte 2013). During this process reduced glutathione (GSH) is oxidized to the dimeric glutathione disulfide (GSSG) (Lauterburg et al. 1984). Enzymes such as glutathione peroxidase (GPX) and glutathione-S-transferase (GST) also utilize the non-enzymatic GSH for catalyzing redox reactions (Meister 1983). A higher amount of GSH is therefore beneficial for antagonizing ROS generation. Consequently, elevated GSH levels have been found in several tissues and blood of diving mammals (Vázquez-Medina et al. 2007; Wilhelm Filho et al. 2002; García-Castañeda et al. 2017). Total GSH levels have also been demonstrated to be higher in the brain of deep-diving dwarf sperm whales (*Kogia sima*) and pygmy sperm whales (*Kogia breviceps*) compared to shallow-diving bottlenose dolphins (*Tursiops truncatus*) (Cantú-Medellín et al. 2011). In parallel, the present antioxidant assays revealed higher GSH concentrations in the hooded seal and harp seal brain compared to mice (Martens et al. 2022a). However, GSSG levels were not determined and therefore the GSH/GSSG ratio could not be calculated, which is commonly used to describe the redox state of a cell. In diving mammals, the ratio may be higher than in non-diving species, resulting in a higher capacity for GSH-dependent reactions (García-Castañeda et al. 2017).

Furthermore, elevated expression of enzymes utilizing GSH for redox reactions such as GPX and GST were also determined (Martens et al. 2022a). GPX catalyzes the GSH-dependent conversion of H_2O_2 to water, as well as the reduction of lipid peroxides and organic hydroperoxides (Lubos et al. 2011; Esworthy et al. 1991). Especially, high expression of GPX3 and overall increased GPX activity has been demonstrated in the hooded seal and harp seal brain (Martens et al. 2022a). High activity of SOD and GPX may collaborate in the overall detoxification of deleterious $O_2^{\bullet-}$ to harmless water. Higher SOD and GPX activities may correlate with diving ability in pinnipeds (Righetti et al. 2014), but not in cetacean species (Cantú-Medellín et al. 2011). Elevated GPX activity has also been observed in other tissues and blood of marine mammals compared to terrestrial mammals (Vázquez-Medina et al. 2006; Wilhelm Filho et al. 2002). While GPX may therefore play a critical role in the antioxidant system of diving mammals, the present results for GST expression and activity are ambiguous. GSTs essentially conjugate GSH to reactive electrophilic substrates, preventing them to cause cellular damage. However, some GST isoenzymes may also reduce hydroperoxides or lipid peroxides (Cooper and Kristal 1997; Sherratt and Hayes 2001). Higher expression of GSTK1 and GSTO1 was determined in the brain of hooded seals and harp seals (Martens et al. 2022a), which confirms previous findings in hooded seal neurons compared to mice (Geßner et al. 2022). Contrary, combined activity of all GSTs was markedly lower in the pinniped brain compared to the mouse brain (Martens et al. 2022a). A closer look at the differential expression of all GST isoenzymes revealed that some GSTs such as GSTM1 and GSTM3 are substantially less expressed in hooded seal neurons compared to mice, resulting in an overall similar

expression of GSTs (Geßner et al. 2022; Martens et al. 2022a). Why some GSTs are upregulated, while others are downregulated remains debatable. GST isoenzymes demonstrate overlapping conjugation activity on a wide variety of substrates, rendering explanations a daring task (Kulinsky and Kolesnichenko 2009; Deponte 2013). However, reduced activity in the hooded seal and harp seal brain suggests that GSTs may not be as crucial in the antioxidant defence as other components.

Another investigated antioxidant enzyme, glutaredoxin 2 (GLRX2), also utilizes GSH for electron transfers to disulfides (Holmgren 1989; Jung and Thomas 1996). GLRX2 has been demonstrated to protect mouse cardiomyocytes from hypoxia-/reoxygenation-induced oxidative stress, apoptosis and inflammation (Li et al. 2021). GLRX2 is also expressed in the mammalian brain, where it contributes to the maintenance of mitochondrial redox homeostasis und thus mitochondrial integrity (Padilla et al. 1992; Karunakaran et al. 2007). Because of the potentially higher aerobic capacity of hooded seal neurons (Geßner et al. 2022), high expression of GLRX2 may be beneficial for mitochondrial function. However, expression of GLRX2 appears to be reduced in the harp seal and hooded seal brain compared to mice (Martens et al. 2022a). Additionally, GLRX2 and GLRX3 expression was also lower in hooded seal neurons compared to mouse neurons (Geßner et al. 2022). Thus, glutaredoxin may not be as crucial for the constitutive action of the glutathione system in pinnipeds as SOD and GPX. Conversely, GLRX2 may facilitate a response induced by acute stress. Elevated expression of GLRX2 has been shown in response to oxidative stress in mouse cardiomyocytes (Li et al. 2021) and diving-related hypoxic stress in the blood of bottlenose dolphins (Blawas et al. 2021).

Replenishment of the GSH pool for following redox reactions occurs through reduction of GSSG by the enzyme glutathione reductase (GSR). Sufficient availability of GSH for GSH-dependent redox reactions is elementary for the antioxidative function of the glutathione system. In agreement, GSR expression was found to be significantly, but only moderately, enhanced in hooded seal neurons compared to mice (Geßner et al. 2022). Therefore, GSR activity was also expected to be increased in the pinniped brain, but instead similar or even lower activity compared to mice was observed (Martens et al. 2022a). Other mechanisms may therefore contribute to the elevated GSH pool. For instance, GSR activity increases in response to rising GSSG levels during oxidative stress and may thus not represent a constitutive measure but an induced mechanism at conditions of acute oxidative stress (Jones 2002a). Accordingly, a rapid recovery of glutathione levels has been observed after dives of the Weddell seal (Murphy and Hochachka 1981). Additionally, high expression of genes such as glutathione synthase (GSS), nuclear factor erythroid 2-related factor 2 (NFE2L2) and solute carrier family 2 member 2 (SLC1A2, EAAT2) may contribute to increased glutathione biosynthesis (Geßner et al. 2022). NFE2L2 is a transcription factor, promoting antioxidant expression as well as glutathione biosynthesis (Cullinan and Diehl 2004; Eggler et al. 2009), while SLC1A2 facilitates the uptake of amino acids such as glutamate from the synaptic cleft (Arriza et al. 1994), but also of cysteine, which is a critical component

in glutathione biosynthesis (Chen and Swanson 2003). In summary, the increased GSH pool in the hooded seal and harp seal brain may partially originate from increased glutathione biosynthesis.

9.3.2 Thioredoxin system

In addition to the glutathione system, the thioredoxin system supports the maintenance of the redox environment in mammalian cells (Lu and Holmgren 2014). For this purpose, thioredoxin reductases (TXNRD) reduce thioredoxin, which is used in subsequent redox reactions of reactive oxygen and nitrogen species by thiol-dependent peroxidases (Lu and Holmgren 2014). However, the investigated TXNRD3 may also operate in the glutaredoxin system (Arnér 2009). Here, increased expression of TXNRD3 in the harp seal hippocampus and visual cortex was observed, while it was overall similarly expressed in the hooded seal brain (Martens et al. 2022a). TXNRD1 and TXNRD3 were also both more highly expressed in hooded seal neurons compared to mouse neurons, but thioredoxin did not exhibit differences in gene expression (Geßner et al. 2022). Elevated levels of TXNRD have also been measured in the brain of patients with Alzheimer's disease (Lovell et al. 2000). Because of the simultaneously decreased levels of thioredoxin, an increase of TXNRD alone was not considered to offer protection against oxidative stress (Lovell et al. 2000). To the best of our knowledge, the thioredoxin system has not been studied in other hypoxia-tolerant species, but our findings suggest that it may at least not be crucial for the constitutive antioxidant defence in the pinniped brain.

9.3.3 Protein homeostasis (proteostasis)

In addition to directly countering excessive ROS generation by high antioxidant expression and activity, other processes may also be important to prevent oxidative stress in the pinniped brain. For instance, a disruption in protein homeostasis (proteostasis) by environmental stressors can lead to endoplasmic reticulum (ER) stress and/or oxidative stress (Chaplot et al. 2020). Chaperones such as CLU aid in maintaining proteostasis by promoting proper protein folding and preventing protein aggregation (Jones 2002b; Chaplot et al. 2020). CLU expression is increased in response to stress conditions and thus resembles heat shock proteins (Foster et al. 2019). Indeed, CLU mediates the degradation of misfolded proteins and aggregates by autophagy (Zhang et al. 2014). Consequently, CLU promotes cardiomyocyte survival during oxidative stress (Jun et al. 2011) as well as protects neurons against protein aggregation and cytotoxicity during ER stress (Gregory et al. 2017). In the investigated neuronal cells transfected with the CLU isoform sCLU, a slight activation of pathways related to proteostasis and autophagy was observed, as well as additional chaperones at normoxic conditions, which may prepare and protect cells from subsequent stress conditions (Martens et al. 2022b). In agreement, sCLU-transfected cells displayed a higher viability as well as reduced amounts of ROS and lipid peroxidation than control cells when exposed to oxidative stress (Geßner et al. 2020). Contrary, nuclear CLU (nCLU) did not alter gene expression of neuronal cells at normoxic conditions and thus, nCLU-transfected cells

did not perform better than control cells when challenged with oxidative stress (Geßner et al. 2020; Martens et al. 2022b). Instead, their response to oxidative stress was characterized by mitochondrial dysfunction and increased cell death (Martens et al. 2022b). Hypoxia-tolerant species may therefore exhibit an increased capacity for maintaining proteostasis. For example, the naked mole rat demonstrates less urea-induced protein unfolding, less protein ubiquitination, and higher proteasome activity compared to mice (Pérez et al. 2009). Maintaining protein function is especially important for the naked mole rat because of its decreased protein synthesis at hypoxic conditions (Pamenter 2022). While most organisms, regardless of their tolerance to hypoxia, appear to generally increase expression of heat shock proteins during hypoxic exposure (Pamenter 2022), the naked mole rat specifically increases expression of ATP-independent heat shock proteins in order to minimize energy expenditure (Nguyen et al. 2019). Hypoxia also activates the unfolded protein and DNA damage response in human cell lines (Bolland et al. 2021). Additionally, dysfunctional proteostasis and concomitant defective synaptic homeostasis may precede neuronal loss in neurodegenerative diseases (Decet and Verstreken 2021). In the hooded seal brain, the remarkably high expression of CLU may also support mechanisms for maintaining protein homeostasis (Fabrizius et al. 2016). However, an induced expression in response to hypoxia and reoxygenation has not been observed (Hoff et al. 2017). Therefore, constitutive actions of CLU as shown in neuronal cell culture at normoxic conditions may prepare the hooded seal brain for upcoming oxidative stress conditions (Martens et al. 2022b).

9.3.4 Mitochondrial autophagy (mitophagy)

Another essential mechanism for maintaining cellular health is the selective autophagy of mitochondria (mitophagy), which can effectively remove damaged or stressed mitochondria (Wang et al. 2019). Dysregulation of mitophagy may cause excessive ROS generation and thus has been implicated in several neurodegenerative diseases (Swerdlow and Wilkins 2020). Consequently, clearance of damaged mitochondria may rescue mitochondrial and synaptic dysfunctions in Alzheimer's disease (Du et al. 2017). An important gene mediating mitophagy is the BCL2 interacting protein 3 (BNIP3) (O'Sullivan et al. 2015). BNIP3-induced mitophagy was demonstrated to play a protective role during hypoxic conditions in cancer cells (Ma et al. 2017) and during myocardial ischaemia-reperfusion injury in rats (*Rattus norvegicus domestica*) and heart-derived cells (Zhang et al. 2019). Especially in the sCLU-transfected neuronal cells, genes mediating mitophagy demonstrated increased expression compared to control cells (Martens et al. 2022b). BNIP3 levels were already enhanced at normoxic conditions, while at hypoxic conditions additional upregulation of mitochondria-localized glutamic acid rich protein (MGARP) was found, which may also trigger mitophagy (Martens et al. 2022b; Jia et al. 2014). Expression of these mitophagy inducing genes may support increased viability of this cell line, when oxygen supply is reduced or ROS levels are increased, as demonstrated by Geßner et al. (2020). Both, BNIP3 and MGARP, are induced by HIF1 and thus may

play an important role in dealing with hypoxic conditions (Zhang et al. 2019; Li et al. 2009). Expression of HIF1A was suggested to protect against oxidative damage in tissues of ringed seals (*Phoca hispida*), but the exact mechanism has not been described (Johnson et al. 2004). Mitophagy may be also induced by other mechanisms such as activation of opioid receptor delta (OPRD) (Xu et al. 2020). Interestingly, S100B-transfected cells demonstrated high expression of OPRD1 and increased viability at oxidative stress (Martens et al. 2022b; Geßner et al. 2020). Thus, mitophagy may also play a protective role in this cell line. Additionally, elevated levels of very-long-chain sphingomyelin species were observed in the brains of deep-diving pinnipeds, which may be transformed into very-long-chain ceramides (Martens et al. 2023, Kolesnick 1994). These ceramides may further support protective mitochondrial autophagy processes (Law et al. 2018). Further studies may shed light on mitophagy mechanisms and their contribution to the hypoxia tolerance of the hooded seal brain. However, monitoring mitophagy in animal cells is a challenging task (Klionsky et al. 2021).

Summarizing, the pinniped brain is ideally equipped with an overall enhanced antioxidant capacity to detoxify ROS and consequently deal with oxidative stress, when surfacing after extensive diving bouts. Elevated activity of specific antioxidant enzymes such as SOD and GPX as well as increased levels of GSH support an important role of the glutathione system in the antioxidant defence of the pinniped brain. Additionally, cellular adaptations such as increased levels of plasmalogen lipid species may scavenge ROS. Contrary, components such as thioredoxin and glutaredoxin appear to be not as crucial in avoiding oxidative stress. Other mechanisms such as proteostasis and mitophagy may operate synergistically in maintaining mitochondrial function and thus preventing mitochondrial dysregulation and ROS generation.

10 Conclusions and perspectives

In this study, molecular mechanisms were unveiled that support the intrinsic hypoxia tolerance of the hooded seal brain. In particular, (i) a reduced capacity for neurotransmission, (ii) an altered energy metabolism and (iii) an elevated capacity for detoxification of reactive oxygen species (ROS), as well as maintenance of cellular homeostasis may play a crucial role (summarized in Fig. 8).

The present results directly tie to the study of Geßner et al. (2022), who determined reduced expression of genes associated with glutamatergic synapse signaling. Here, this knowledge was expanded and a reduced pool of the neurotransmitter glutamate could be determined (Martens et al. 2023). In part, the reduction in neurotransmission may be facilitated by high expression of S100B, which may act through the *opioid signaling pathway* (Martens et al. 2022b). To compensate for reduced glutamatergic signaling, the hooded seal brain may depend on efficient signal transduction by increasing the sphingomyelin levels and thus myelin sheath formation (Martens et al. 2023). These mechanisms may help constitutively decrease the energy expenditure of the hooded seal brain, which may prepare for conditions of low oxygen and thus energy availability. Since hypoxia-preconditioning of mice led to a reduction in hippocampal glutamate (Liao et al. 2018), a decrease of glutamate and increase of sphingomyelin in the hooded seal brain may also depend on external stimuli. Other characteristics such as oxygen stores and the antioxidant system of the hooded seal already demonstrate a development along with its diving ability (Burns et al. 2007; Burns et al. 2010; Geiseler et al. 2013; Lestyk et al. 2009; Vázquez-Medina et al. 2011a; Vázquez-Medina et al. 2011b). Future studies may explore, how neuronal signaling systems in the hooded seal brain develop during postnatal maturation and possibly, how these components are regulated by transcription factors and microRNAs (Penso-Dolfin et al. 2020).

The exact mechanism of energy metabolism in the hooded seal brain remains ambiguous but may exhibit distinct modifications. The observed elevated glucose and lactate levels may point to a constitutively increased glycolytic capacity in the pinniped brain (Martens et al. 2023). Further, activation of HIF1 in Clusterin (CLU)- and S100B-transfected neuronal cell culture may indicate a switch from aerobic to anaerobic metabolism during hypoxic conditions (Martens et al. 2022b). The most fascinating adaptation of the hooded seal brain, may be explained by the ‘reverse lactate shuttle’ hypothesis (Mitz et al. 2009; Schneuer et al. 2012; Hoff et al. 2016). A shift of oxidative metabolism from neurons to astrocytes may protect neurons from oxidative stress. Thus, future studies of neuronal and astrocytic processes separately, as well as their interaction, could shed light on the alterations of energy metabolism in the hooded seal brain. Monitoring metabolic flux and energy balance of neurons and astrocytes may be achieved in primary cell culture systems, which are an emerging technology in marine mammal research (Yim et al. 2014; Hindle et al. 2018; Lam et al. 2020).

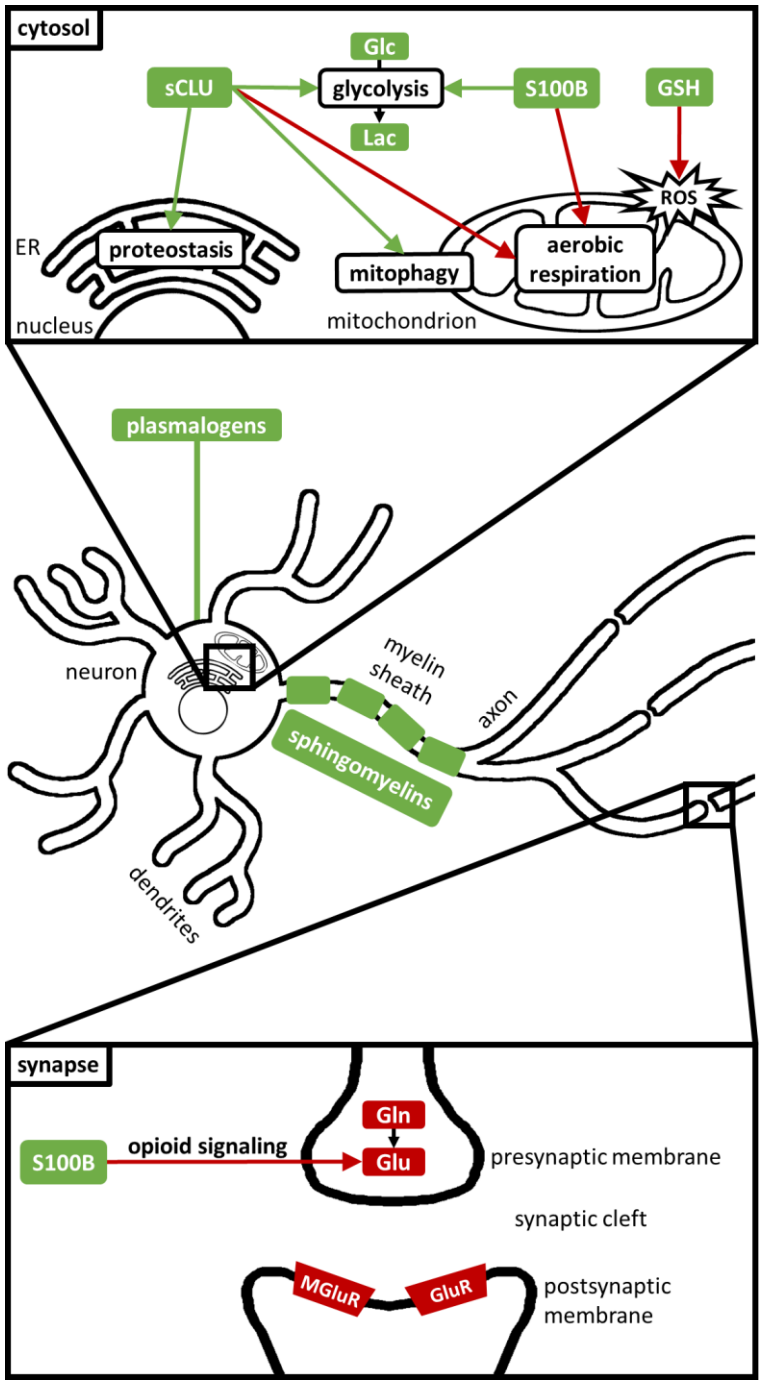

Fig. 8: Schematic overview of adaptations in the phocid seal brain, identified in this study (increased/decreased). *Neurons in the phocid seal brain demonstrate elevated levels of plasmalogen species in their membranes, which exhibit antioxidative functions. An increase of sphingomyelins may strenghten the axon enwrapping myelin sheath and support efficient neurotransmission. In the cell, overexpression of soluble Clusterin (sCLU) promotes protein homeostasis (proteostasis), mainly occurring in the endoplasmic reticulum (ER), as well as glycolysis and mitochondrial autophagy (mitophagy), but inhibits aerobic respiration. S100B also supports glycolysis, but suppresses aerobic respiration. High glucose (Glc) and lactate (Lac) concentrations may indicate enhanced glycolytic activity. Elevated levels of glutathione (GSH), as well as other components in the glutathione system scavenge reactive oxygen species (ROS), primarily originating from the mitochondrion. At the synapse, S100B inhibits neurotransmission by glutamate (Glu) through the opioid signaling pathway, assisted by low glutamine (Gln) and Glu concentrations. Reduced expression of metabotropic (MGluR) and ionotropic glutamate receptors (GluR) in hooded seal neurons were previously determined by Geßner et al. (2022). High expression of CLU and S100B in the hooded seal brain has been demonstrated by Fabrizius et al. (2016) and Geßner et al. (2022).*

Additional mechanisms such as proteostasis and mitophagy may contribute to the hypoxia tolerance of the hooded seal brain by maintaining cellular homeostasis (Martens et al. 2022b). While it is still discussed whether CLU suppresses or enhances neurodegeneration (Yuste-Checa et al. 2022), it has been demonstrated in this study that especially the sCLU (soluble CLU) isoform may facilitate proteostasis and mitophagy and improve neuron survival in conditions of hypoxia and oxidative stress (Martens et al. 2022b). Luckily, monitoring of proteostatic and mitophagic processes receives increasing attention and available methods are continuously improved (Kaushik and Cuervo 2015; Klionsky et al. 2021), making this an excellent area for future research. While maintaining cellular homeostasis may help to reduce ROS generation, mechanisms to detoxify ROS appear constitutively upregulated in the hooded seal brain (Martens et al. 2022a). Particularly, the glutathione system supports the high antioxidative capacity, which may have an important role when the seal surfaces after extensive diving bouts (Martens et al. 2022a).

Improving our understanding of the hypoxia tolerance of pinnipeds and marine mammals in general, sheds light on their adaptation to an aquatic environment. Marine mammals are especially vulnerable to a range of natural and anthropogenic disturbances and thus, these findings aid in the conservational efforts in marine ecosystems (Evans et al. 2014). Insights into molecular mechanisms preventing hypoxia- and oxidative stress-associated damage in the mammalian brain advances therapeutic human medicine, as recently demonstrated for ischaemic insults by Vrselja et al. (2019).

11 References

Alle, Henrik; Roth, Arnd; Geiger, Jörg R. P. (2009): Energy-efficient action potentials in hippocampal mossy fibers. In *Science (New York, N.Y.)* 325 (5946), pp. 1405–1408. DOI: 10.1126/science.1174331.

Allen, Kaitlin N.; Vázquez-Medina, José Pablo (2019): Natural tolerance to ischemia and hypoxemia in diving mammals: a review. In *Frontiers in Physiology* 10, p. 1199. DOI: 10.3389/fphys.2019.01199.

Almeida, A.; Almeida, J.; Bolaños, J. P.; Moncada, S. (2001): Different responses of astrocytes and neurons to nitric oxide: the role of glycolytically generated ATP in astrocyte protection. In *Proceedings of the National Academy of Sciences of the United States of America* 98 (26), pp. 15294–15299. DOI: 10.1073/pnas.261560998.

Almeida, Angeles; Moncada, Salvador; Bolaños, Juan P. (2004): Nitric oxide switches on glycolysis through the AMP protein kinase and 6-phosphofructo-2-kinase pathway. In *Nature Cell Biology* 6 (1), pp. 45–51. DOI: 10.1038/ncb1080.

Andersen, Jens V.; Markussen, Kia H.; Jakobsen, Emil; Schousboe, Arne; Waagepetersen, Helle S.; Rosenberg, Paul A.; Aldana, Blanca I. (2021): Glutamate metabolism and recycling at the excitatory synapse in health and neurodegeneration. In *Neuropharmacology* 196, p. 108719. DOI: 10.1016/j.neuropharm.2021.108719.

Andersen, Julie M.; Skern-Mauritzen, Mette; Boehme, Lars; Wiersma, Yolanda F.; Rosing-Asvid, Aqqalu; Hammill, Mike O.; Stenson, Garry B. (2013): Investigating annual diving behaviour by hooded seals (*Cystophora cristata*) within the Northwest Atlantic Ocean. In *PLoS One* 8 (11), e80438. DOI: 10.1371/journal.pone.0080438.

Angelopoulou, Efthalia; Piperi, Christina; Papavassiliou, Athanasios G. (2018): High-mobility group box 1 in Parkinson's disease: from pathogenesis to therapeutic approaches. In *Journal of Neurochemistry* 146 (3), pp. 211–218. DOI: 10.1111/jnc.14450.

Arcuri, Cataldo; Bianchi, Roberta; Brozzi, Flora; Donato, Rosario (2005): S100B increases proliferation in PC12 neuronal cells and reduces their responsiveness to nerve growth factor via Akt activation. In *Journal of Biological Chemistry* 280 (6), pp. 4402–4414. DOI: 10.1074/jbc.M406440200.

Arnér, Elias S. J. (2009): Focus on mammalian thioredoxin reductases--important selenoproteins with versatile functions. In *Biochimica et Biophysica Acta* 1790 (6), pp. 495–526. DOI: 10.1016/j.bbagen.2009.01.014.

Arriza, J. L.; Fairman, W. A.; Wadiche, J. I.; Murdoch, G. H.; Kavanaugh, M. P.; Amara, S. G. (1994): Functional comparisons of three glutamate transporter subtypes cloned from human motor cortex. In *The Journal of Neuroscience* 14 (9), pp. 5559–5569. DOI: 10.1523/JNEUROSCI.14-09-05559.1994.

Attwell, D.; Laughlin, S. B. (2001): An energy budget for signaling in the grey matter of the brain. In *Journal of Cerebral Blood Flow and Metabolism* 21 (10), pp. 1133–1145. DOI: 10.1097/00004647-200110000-00001.

Baala, Lekbir; Briault, Sylvain; Etchevers, Heather C.; Laumonnier, Frédéric; Natiq, Abdelhafid; Amiel, Jeanne et al. (2007): Homozygous silencing of T-box transcription factor EOMES leads to microcephaly with polymicrogyria and corpus callosum agenesis. In *Nature Genetics* 39 (4), pp. 454–456. DOI: 10.1038/ng1993.

Badan, D. (1986): Diet of the house mouse (*Mus musculus* L.) in two pine and a kauri forest. In *New Zealand Journal of Ecology* 9, pp. 137–141. Available online at http://www.jstor.org/stable/24052774, checked on 12/20/2022.

Baig, Shabnam; Palmer, Laura E.; Owen, Michael J.; Williams, Julie; Kehoe, Patrick G.; Love, Seth (2012): Clusterin mRNA and protein in Alzheimer's disease. In *Journal of Alzheimer's disease* 28 (2), pp. 337–344. DOI: 10.3233/JAD-2011-110473.

Ballard, Karen Ann; Kovacs, Kit M. (1995): The acoustic repertoire of hooded seals (*Cystophora cristata*). In *Canadian Journal of Zoology* 73 (7), pp. 1362–1374. DOI: 10.1139/z95-159.

Barañano, David E.; Rao, Mahil; Ferris, Christopher D.; Snyder, Solomon H. (2002): Biliverdin reductase: a major physiologic cytoprotectant. In *Proceedings of the National Academy of Sciences* 99 (25), pp. 16093–16098. DOI: 10.1073/pnas.252626999.

Barnes, Nicholas M.; Hales, Tim G.; Lummis, Sarah C. R.; Peters, John A. (2009): The 5-HT3 receptor--the relationship between structure and function. In *Neuropharmacology* 56 (1), pp. 273–284. DOI: 10.1016/j.neuropharm.2008.08.003.

Barnette, Alan R.; Neil, Jeffery J.; Kroenke, Christopher D.; Griffith, Jennifer L.; Epstein, Adrian A.; Bayly, Philip V. et al. (2009): Characterization of brain development in the ferret via MRI. In *Pediatric Research* 66 (1), pp. 80–84. DOI: 10.1203/PDR.0b013e3181a291d9.

Bazan, Nicolas G. (2005): Neuroprotectin D1 (NPD1): a DHA-derived mediator that protects brain and retina against cell injury-induced oxidative stress. In *Brain Pathology (Zurich, Switzerland)* 15 (2), pp. 159–166. DOI: 10.1111/j.1750-3639.2005.tb00513.x.

Bazinet, Richard P.; Layé, Sophie (2014): Polyunsaturated fatty acids and their metabolites in brain function and disease. In *Nature Reviews Neuroscience* 15 (12), pp. 771–785. DOI: 10.1038/nrn3820.

Bélanger, Mireille; Allaman, Igor; Magistretti, Pierre J. (2011): Brain energy metabolism: focus on astrocyte-neuron metabolic cooperation. In *Cell Metabolism* 14 (6), pp. 724–738. DOI: 10.1016/j.cmet.2011.08.016.

Bélanger, Mireille; Magistretti, Pierre J. (2009): The role of astroglia in neuroprotection. In *Dialogues in Clinical Neuroscience* 11 (3), pp. 281–295. DOI: 10.31887/DCNS.2009.11.3/mbelanger.

Belcher, John D.; Beckman, Joan D.; Balla, Gyorgy; Balla, Jozsef; Vercellotti, Gregory (2010): Heme degradation and vascular injury. In *Antioxidants & Redox Signaling* 12 (2), pp. 233–248. DOI: 10.1089/ars.2009.2822.

Bellmund, Jacob L. S.; Gärdenfors, Peter; Moser, Edvard I.; Doeller, Christian F. (2018): Navigating cognition: spatial codes for human thinking. In *Science (New York, N.Y.)* 362 (6415). DOI: 10.1126/science.aat6766.

Belov Kirdajova, Denisa; Kriska, Jan; Tureckova, Jana; Anderova, Miroslava (2020): Ischemia-triggered glutamate excitotoxicity from the perspective of glial cells. In *Frontiers in Cellular Neuroscience* 14, p. 51. DOI: 10.3389/fncel.2020.00051.

Benjamini, Yoav; Hochberg, Yosef (1995): Controlling the false discovery rate: a practical and powerful approach to multiple testing. In *Journal of the Royal Statistical Society: Series B (Methodological)* 57 (1), pp. 289–300. DOI: 10.1111/j.2517-6161.1995.tb02031.x.

Bernier-Graveline, Alexandre; Lesage, Véronique; Cabrol, Jory; Lair, Stéphane; Michaud, Robert; Rosabal, Maikel; Verreault, Jonathan (2021): Lipid metabolites as indicators of body condition in highly contaminant-exposed belugas from the endangered St. Lawrence Estuary population (Canada). In *Environmental Research* 192, p. 110272. DOI: 10.1016/j.envres.2020.110272.

Berry, R. J.; Jakobson, M. E. (1975): Adaptation and adaptability in wild-living house mice (*Mus musculus*). In *Journal of Zoology* 176 (3), pp. 391–402. DOI: 10.1111/j.1469-7998.1975.tb03210.x.

Berta, Annalisa; Churchill, Morgan; Boessenecker, Robert W. (2022): The origin of phocid seals and evolution of key behavioral character traits: Springer, Cham, pp. 3–30. DOI: 10.1007/978-3-030-88923-4_1.

Berta, Annalisa; Sumich, James L.; Kovacs, Kit M. (2015): Marine mammals. Evolutionary biology. Third edition. London, UK: Elsevier Academic Press.

Bi, Jianling; Hu, Bo; Zheng, Jinsong; Wang, Jingzhen; Xiao, Wuhan; Wang, Ding (2015): Characterization of the hypoxia-inducible factor 1 alpha gene in the sperm whale, beluga whale, and Yangtze finless porpoise. In *Marine Biology* 162 (6), pp. 1201–1213. DOI: 10.1007/s00227-015-2662-4.

Bininda-Emonds, Olaf R. P. (2000): Pinniped brain sizes. In *Marine Mammal Science* 16 (2), pp. 469–481. DOI: 10.1111/j.1748-7692.2000.tb00939.x.

Bittner, Carla X.; Loaiza, Anitsi; Ruminot, Iván; Larenas, Valeria; Sotelo-Hitschfeld, Tamara; Gutiérrez, Robin et al. (2010): High resolution measurement of the glycolytic rate. In *Frontiers in Neuroenergetics* 2, p. 26. DOI: 10.3389/fnene.2010.00026.

Blawas, Ashley M.; Ware, Kathryn E.; Schmaltz, Emma; Zheng, Larry; Spruance, Jacob; Allen, Austin S. et al. (2021): An integrated comparative physiology and molecular approach pinpoints mediators of breath-hold capacity in dolphins. In *Evolution, Medicine, and Public Health* 9 (1), pp. 420–430. DOI: 10.1093/emph/eoab036.

Bligh, E. G.; Dyer, W. J. (1959): A rapid method of total lipid extraction and purification. In *Canadian Journal of Biochemistry and Physiology* 37 (8), pp. 911–917. DOI: 10.1139/o59-099.

Blix, A. S.; Elsner, R.; Kjekshus, J. K. (1983): Cardiac output and its distribution through capillaries and A-V shunts in diving seals. In *Acta Physiologica Scandinavica* 118 (2), pp. 109–116. DOI: 10.1111/j.1748-1716.1983.tb07250.x.

Blix, Arnoldus Schytte (2018): Adaptations to deep and prolonged diving in phocid seals. In *The Journal of Experimental Biology* 221 (Pt 12). DOI: 10.1242/jeb.182972.

Blix, Arnoldus Schytte; Walløe, Lars; Messelt, Edward B.; Folkow, Lars P. (2010): Selective brain cooling and its vascular basis in diving seals. In *The Journal of Experimental Biology* 213 (Pt 15), pp. 2610–2616. DOI: 10.1242/jeb.040345.

Bolland, Hannah; Ma, Tiffany S.; Ramlee, Syafiq; Ramadan, Kristijan; Hammond, Ester M. (2021): Links between the unfolded protein response and the DNA damage response in hypoxia: a systematic review. In *Biochemical Society Transactions* 49 (3), pp. 1251–1263. DOI: 10.1042/BST20200861.

Bories, Pierre; Rikardsen, Audun H.; Leonards, Pim; Fisk, Aaron T.; Tartu, Sabrina; Vogel, Emma F. et al. (2021): A deep dive into fat: Investigating blubber lipidomic fingerprint of killer whales and humpback whales in northern Norway. In *Ecology and Evolution* 11 (11), pp. 6716–6729. DOI: 10.1002/ece3.7523.

Boukhzar, Loubna; Hamieh, Abdallah; Cartier, Dorthe; Tanguy, Yannick; Alsharif, Ifat; Castex, Matthieu et al. (2016): Selenoprotein T exerts an essential oxidoreductase activity that protects dopaminergic neurons in mouse models of Parkinson's disease. In *Antioxidants & Redox Signaling* 24 (11), pp. 557–574. DOI: 10.1089/ars.2015.6478.

Bouma, Hjalmar R.; Carey, Hannah V.; Kroese, Frans G. M. (2010): Hibernation: the immune system at rest? In *Journal of Leukocyte Biology* 88 (4), pp. 619–624. DOI: 10.1189/jlb.0310174.

Boutilier, R. G.; Nikinmaa, M.; Tufts, B. L. (1993): Relationship between blood buffering properties, erythrocyte pH and water content, in gray seals (*Halichoerus grypus*). In *Acta Physiologica Scandinavica* 147 (2), pp. 241–247. DOI: 10.1111/j.1748-1716.1993.tb09495.x.

Bouzier-Sore, Anne-Karine; Voisin, Pierre; Bouchaud, Véronique; Bezancon, Eric; Franconi, Jean-Michel; Pellerin, Luc (2006): Competition between glucose and lactate as oxidative energy substrates in both neurons and astrocytes: a comparative NMR study. In *The European Journal of Neuroscience* 24 (6), pp. 1687–1694. DOI: 10.1111/j.1460-9568.2006.05056.x.

Bowen, W. D.; Oftedal, O. T.; Boness, D. J. (1985): Birth to weaning in 4 days: remarkable growth in the hooded seal, *Cystophora cristata*. In *Canadian Journal of Zoology* 63 (12), pp. 2841–2846. DOI: 10.1139/z85-424.

Braverman, Nancy E.; Moser, Ann B. (2012): Functions of plasmalogen lipids in health and disease. In *Biochimica et Biophysica Acta* 1822 (9), pp. 1442–1452. DOI: 10.1016/j.bbadis.2012.05.008.

Briga, Michael; Verhulst, Simon (2015): What can long-lived mutants tell us about mechanisms causing aging and lifespan variation in natural environments? In *Experimental Gerontology* 71, pp. 21–26. DOI: 10.1016/j.exger.2015.09.002.

Brown, Angus M.; Ransom, Bruce R. (2007): Astrocyte glycogen and brain energy metabolism. In *Glia* 55 (12), pp. 1263–1271. DOI: 10.1002/glia.20557.

Brown, James H.; Lasiewski, Robert C. (1972): Metabolism of weasels: the cost of being long and thin. In *Ecology* 53 (5), pp. 939–943. DOI: 10.2307/1934312.

Brown, Robert Zanes (1953): Social behavior, reproduction, and population changes in the house mouse (*Mus musculus* L.). In *Ecological Monographs* 23 (3), pp. 217–240. DOI: 10.2307/1943592.

Buccellato, Francesca Romana; D'Anca, Marianna; Fenoglio, Chiara; Scarpini, Elio; Galimberti, Daniela (2021): Role of oxidative damage in Alzheimer's disease and neurodegeneration: from pathogenic mechanisms to biomarker discovery. In *Antioxidants (Basel, Switzerland)* 10 (9). DOI: 10.3390/antiox10091353.

Buck, Leslie T.; Pamenter, Matthew E. (2018): The hypoxia-tolerant vertebrate brain: arresting synaptic activity. In *Comparative Biochemistry and Physiology Part B: Biochemistry & Molecular Biology* 224, pp. 61–70. DOI: 10.1016/j.cbpb.2017.11.015.

Burkey, B. F.; deSilva, H. V.; Harmony, J. A. (1991): Intracellular processing of apolipoprotein J precursor to the mature heterodimer. In *Journal of Lipid Research* 32 (6), pp. 1039–1048. DOI: 10.1016/S0022-2275(20)42000-0.

Burns, J. M.; Lestyk, K. C.; Folkow, L. P.; Hammill, M. O.; Blix, A. S. (2007): Size and distribution of oxygen stores in harp and hooded seals from birth to maturity. In *Journal of Comparative Physiology B: Biochemical, Systemic, and Environmental Physiology* 177 (6), pp. 687–700. DOI: 10.1007/s00360-007-0167-2.

Burns, J. M.; Skomp, N.; Bishop, N.; Lestyk, K.; Hammill, M. (2010): Development of aerobic and anaerobic metabolism in cardiac and skeletal muscles from harp and hooded seals. In *The Journal of Experimental Biology* 213 (5), pp. 740–748. DOI: 10.1242/jeb.037929.

Cabanac, A.; Folkow, L. P.; Blix, A. S. (1997): Volume capacity and contraction control of the seal spleen. In *Journal of Applied Physiology (Bethesda, Md. : 1985)* 82 (6), pp. 1989–1994. DOI: 10.1152/jappl.1997.82.6.1989.

Calabresi, P.; Napolitano, M.; Centonze, D.; Marfia, G. A.; Gubellini, P.; Teule, M. A. et al. (2000): Tissue plasminogen activator controls multiple forms of synaptic plasticity and memory. In *The European Journal of Neuroscience* 12 (3), pp. 1002–1012. DOI: 10.1046/j.1460-9568.2000.00991.x.

Cantú-Medellín, Nadiezhda; Byrd, Barbie; Hohn, Aleta; Vázquez-Medina, José Pablo; Zenteno-Savín, Tania (2011): Differential antioxidant protection in tissues from marine mammals with distinct diving capacities. Shallow/short vs. deep/long divers. In *Comparative Biochemistry and Physiology Part A: Molecular & Integrative Physiology* 158 (4), pp. 438–443. DOI: 10.1016/j.cbpa.2010.11.029.

Carlitz, Esther H. D.; Runge, Jan-Niklas; König, Barbara; Winkler, Lennart; Kirschbaum, Clemens; Gao, Wei; Lindholm, Anna K. (2019): Steroid hormones in hair reveal sexual maturity and competition in wild house mice (*Mus musculus domesticus*). In *Scientific Reports* 9 (1), p. 16925. DOI: 10.1038/s41598-019-53362-4.

Casey, Timothy M.; Casey, Kathleen K. (1979): Thermoregulation of arctic weasels. In *Physiological Zoology* 52 (2), pp. 153–164. DOI: 10.1086/physzool.52.2.30152560.

Castellanos, Daniel Báez; Martín-Jiménez, Cynthia A.; Rojas-Rodríguez, Felipe; Barreto, George E.; González, Janneth (2021): Brain lipidomics as a rising field in neurodegenerative contexts: perspectives with machine learning approaches. In *Frontiers in Neuroendocrinology* 61, p. 100899. DOI: 10.1016/j.yfrne.2021.100899.

Castellini, Michael A.; Somero, George N. (1981): Buffering capacity of vertebrate muscle: correlations with potentials for anaerobic function. In *Journal of Comparative Physiology B: Biochemical, Systemic, and Environmental Physiology* 143 (2), pp. 191–198. DOI: 10.1007/BF00797698.

Champagne, Cory D.; Crocker, Daniel E.; Fowler, Melinda A.; Houser, Dorian S. (2012): Fasting physiology of the pinnipeds: the challenges of fasting while maintaining high energy expenditure and nutrient delivery for lactation: Springer, Berlin, Heidelberg, 309–336. DOI: 10.1007/978-3-642-29056-5_19.

Chan, Robin B.; Oliveira, Tiago G.; Cortes, Etty P.; Honig, Lawrence S.; Duff, Karen E.; Small, Scott A. et al. (2012): Comparative lipidomic analysis of mouse and human brain with Alzheimer disease. In *The Journal of Biological Chemistry* 287 (4), pp. 2678–2688. DOI: 10.1074/jbc.M111.274142.

Chaplot, Kriti; Jarvela, Timothy S.; Lindberg, Iris (2020): Secreted chaperones in neurodegeneration. In *Frontiers in Aging Neuroscience* 12, p. 268. DOI: 10.3389/fnagi.2020.00268.

Chaudhry, Farrukh A.; Schmitz, Dietmar; Reimer, Richard J.; Larsson, Peter; Gray, Andrew T.; Nicoll, Roger et al. (2002): Glutamine uptake by neurons: interaction of protons with system a transporters. In *The Journal of Neuroscience* 22 (1), pp. 62–72. DOI: 10.1523/JNEUROSCI.22-01-00062.2002.

Chen, Chuck T.; Haven, Sophie; Lecaj, Lea; Borgstrom, Mark; Torabi, Mohammad; SanGiovanni, John Paul; Hibbeln, Joseph R. (2020a): Brain PUFA concentrations are differentially affected by interactions of diet, sex, brain regions, and phospholipid pools in mice. In *The Journal of Nutrition* 150 (12), pp. 3123–3132. DOI: 10.1093/jn/nxaa307.

Chen, Yi-Meng; He, Xiao-Zhou; Wang, Shu-Ming; Xia, Ying (2020b): δ-opioid receptors, microRNAs, and neuroinflammation in cerebral ischemia/hypoxia. In *Frontiers in Immunology* 11, p. 421. DOI: 10.3389/fimmu.2020.00421.

Chen, Yongmei; Swanson, Raymond A. (2003): The glutamate transporters EAAT2 and EAAT3 mediate cysteine uptake in cortical neuron cultures. In *Journal of Neurochemistry* 84 (6), pp. 1332–1339. DOI: 10.1046/j.1471-4159.2003.01630.x.

Cheng, Hang; Qin, Yiming Amy; Dhillon, Rashpal; Dowell, James; Denu, John M.; Pamenter, Matthew E. (2022): Metabolomic analysis of carbohydrate and amino acid changes induced by hypoxia in naked mole-rat brain and liver. In *Metabolites* 12 (1). DOI: 10.3390/metabo12010056.

Chevilley, Arnaud; Lesept, Flavie; Lenoir, Sophie; Ali, Carine; Parcq, Jérôme; Vivien, Denis (2015): Impacts of tissue-type plasminogen activator (tPA) on neuronal survival. In *Frontiers in Cellular Neuroscience* 9, p. 415. DOI: 10.3389/fncel.2015.00415.

Choi, D. W.; Rothman, S. M. (1990): The role of glutamate neurotoxicity in hypoxic-ischemic neuronal death. In *Annual Review of Neuroscience* 13, pp. 171–182. DOI: 10.1146/annurev.ne.13.030190.001131.

Choi, In-Young; Gruetter, Rolf (2003): In vivo 13C NMR assessment of brain glycogen concentration and turnover in the awake rat. In *Neurochemistry International* 43 (4-5), pp. 317–322. DOI: 10.1016/S0197-0186(03)00018-4.

Choi, Jaewoo; Yin, Tai; Shinozaki, Koichiro; Lampe, Joshua W.; Stevens, Jan F.; Becker, Lance B.; Kim, Junhwan (2018): Comprehensive analysis of phospholipids in the brain, heart, kidney, and liver: brain phospholipids are least enriched with polyunsaturated fatty acids. In *Molecular and Cellular Biochemistry* 442 (1-2), pp. 187–201. DOI: 10.1007/s11010-017-3203-x.

Chong, Jasmine; Wishart, David S.; Xia, Jianguo (2019): Using MetaboAnalyst 4.0 for comprehensive and integrative metabolomics data analysis. In *Current Protocols in Bioinformatics* 68 (1), p. 86. DOI: 10.1002/cpbi.86.

Choudhry, Hani; Harris, Adrian L. (2018): Advances in hypoxia-inducible factor biology. In *Cell Metabolism* 27 (2), pp. 281–298. DOI: 10.1016/j.cmet.2017.10.005.

Chuquet, Julien; Quilichini, Pascale; Nimchinsky, Esther A.; Buzsáki, György (2010): Predominant enhancement of glucose uptake in astrocytes versus neurons during activation of the somatosensory cortex. In *The Journal of Neuroscience* 30 (45), pp. 15298–15303. DOI: 10.1523/JNEUROSCI.0762-10.2010.

Cintrón-Colón, Alberto F.; Almeida-Alves, Gabriel; Boynton, Alicia M.; Spitsbergen, John M. (2020): GDNF synthesis, signaling, and retrograde transport in motor neurons. In *Cell and Tissue Research* 382 (1), pp. 47–56. DOI: 10.1007/s00441-020-03287-6.

Cobley, James Nathan; Fiorello, Maria Luisa; Bailey, Damian Miles (2018): 13 reasons why the brain is susceptible to oxidative stress. In *Redox Biology* 15, pp. 490–503. DOI: 10.1016/j.redox.2018.01.008.

Cook, Peter F.; Berns, Gregory (2022): Volumetric and connectivity assessment of the caudate nucleus in California sea lions and coyotes. In *Animal Cognition* 25 (5), pp. 1231–1240. DOI: 10.1007/s10071-022-01685-7.

Cooper, Arthur J. L.; Kristal, B. (1997): Multiple roles of glutathione in the central nervous system. In *Biological Chemistry*, 378(8):793-802. PMID: 9377474.

Corry, Kylie A.; White, Olivia R.; Shearlock, AnnaMarie E.; Moralejo, Daniel H.; Law, Janessa B.; Snyder, Jessica M. et al. (2021): Evaluating neuroprotective effects of uridine, erythropoietin, and therapeutic hypothermia in a ferret model of inflammation-sensitized hypoxic-ischemic encephalopathy. In *International Journal of Molecular Sciences* 22 (18). DOI: 10.3390/ijms22189841.

Costa, Lucio G.; Laat, Rian de; Dao, Khoi; Pellacani, Claudia; Cole, Toby B.; Furlong, Clement E. (2014): Paraoxonase-2 (PON2) in brain and its potential role in neuroprotection. In *Neurotoxicology* 43, pp. 3–9. DOI: 10.1016/j.neuro.2013.08.011.

Creydt, Marina; Hudzik, Daria; Rurik, Marc; Kohlbacher, Oliver; Fischer, Markus (2018): Food authentication: small-molecule profiling as a tool for the geographic discrimination of German white asparagus. In *Journal of Agricultural and Food Chemistry* 66 (50), pp. 13328–13339. DOI: 10.1021/acs.jafc.8b05791.

Cristóvão, Joana S.; Gomes, Cláudio M. (2019): S100 proteins in Alzheimer's disease. In *Frontiers in Neuroscience* 13, p. 463. DOI: 10.3389/fnins.2019.00463.

Cullinan, Sara B.; Diehl, J. Alan (2004): PERK-dependent activation of Nrf2 contributes to redox homeostasis and cell survival following endoplasmic reticulum stress. In *Journal of Biological Chemistry* 279 (19), pp. 20108–20117. DOI: 10.1074/jbc.M314219200.

Czech-Damal, N. U.; Geiseler, S. J.; Hoff, M. L. M.; Schliep, R.; Ramirez, J-M; Folkow, L. P.; Burmester, T. (2014): The role of glycogen, glucose and lactate in neuronal activity during hypoxia in the hooded seal (*Cystophora cristata*) brain. In *Neuroscience* 275, pp. 374–383. DOI: 10.1016/j.neuroscience.2014.06.024.

Czubowicz, Kinga; Jęśko, Henryk; Wencel, Przemysław; Lukiw, Walter J.; Strosznajder, Robert P. (2019): The role of ceramide and sphingosine-1-phosphate in Alzheimer's disease and other neurodegenerative disorders. In *Molecular Neurobiology* 56 (8), pp. 5436–5455. DOI: 10.1007/s12035-018-1448-3.

Dadsena, Shashank; Bockelmann, Svenja; Mina, John G. M.; Hassan, Dina G.; Korneev, Sergei; Razzera, Guilherme et al. (2019): Ceramides bind VDAC2 to trigger mitochondrial apoptosis. In *Nature Communications* 10 (1), p. 1832. DOI: 10.1038/s41467-019-09654-4.

Dannenberger, Dirk; Möller, Ramona; Westphal, Linda; Moritz, Timo; Dähne, Michael; Grunow, Bianka (2020): Fatty acid composition in blubber, liver, and muscle of marine mammals in the southern Baltic Sea. In *Animals: an open access journal from MDPI* 10 (9). DOI: 10.3390/ani10091509.

Davis, Randall W. (2014): A review of the multi-level adaptations for maximizing aerobic dive duration in marine mammals: from biochemistry to behavior. In *Journal of Comparative Physiology B: Biochemical, Systemic, and Environmental Physiology* 184 (1), pp. 23–53. DOI: 10.1007/s00360-013-0782-z.

Davis, Randall W. (2019): Physiological adaptations for breath-hold diving: Springer, Cham, pp. 133–175. DOI: 10.1007/978-3-319-98280-9_6.

Davison, A.; Birks, J.D.S; Griffiths, H.I; Kitchener, A.C; Biggins, D.; Butlin, R.K (1999): Hybridization and the phylogenetic relationship between polecats and domestic ferrets in Britain. In *Biological Conservation* 87 (2), pp. 155–161. DOI: 10.1016/S0006-3207(98)00067-6.

de Wit, H.; Metz, J.; Wagner, N.; Cooper, M. (1991): Effects of diazepam on cerebral metabolism and mood in normal volunteers. In *Neuropsychopharmacology* 5 (1), pp. 33–41. PMID: 1930609.

Dean, John M.; Lodhi, Irfan J. (2018): Structural and functional roles of ether lipids. In *Protein & Cell* 9 (2), pp. 196–206. DOI: 10.1007/s13238-017-0423-5.

Decet, Marianna; Verstreken, Patrik (2021): Presynaptic autophagy and the connection with neurotransmission. In *Frontiers in Cell and Developmental Biology* 9, p. 790721. DOI: 10.3389/fcell.2021.790721.

Deponte, Marcel (2013): Glutathione catalysis and the reaction mechanisms of glutathione-dependent enzymes. In *Biochimica et Biophysica Acta* 1830 (5), pp. 3217–3266. DOI: 10.1016/j.bbagen.2012.09.018.

Di Paola, M.; Cocco, T.; Lorusso, M. (2000): Ceramide interaction with the respiratory chain of heart mitochondria. In *Biochemistry* 39 (22), pp. 6660–6668. DOI: 10.1021/bi9924415.

Di Paolo, Gilbert; Camilli, Pietro de (2006): Phosphoinositides in cell regulation and membrane dynamics. In *Nature* 443 (7112), pp. 651–657. DOI: 10.1038/nature05185.

Dienel, Gerald A. (2019): Brain glucose metabolism: integration of energetics with function. In *Physiological Reviews* 99 (1), pp. 949–1045. DOI: 10.1152/physrev.00062.2017.

Donato, R.; Cannon, B. R.; Sorci, G.; Riuzzi, F.; Hsu, K.; Weber, D. J.; Geczy, C. L. (2013): Functions of S100 Proteins. In *Current Molecular Medicine* 13 (1), pp. 24–57. DOI: 10.2174/156652413804486214.

Donato, Rosario; Sorci, Guglielmo; Riuzzi, Francesca; Arcuri, Cataldo; Bianchi, Roberta; Brozzi, Flora et al. (2009): S100B's double life: intracellular regulator and extracellular signal. In *Biochimica et Biophysica Acta* 1793 (6), pp. 1008–1022. DOI: 10.1016/j.bbamcr.2008.11.009.

Drew, K. L.; Rice, M. E.; Kuhn, T. B.; Smith, M. A. (2001): Neuroprotective adaptations in hibernation: therapeutic implications for ischemia-reperfusion, traumatic brain injury and neurodegenerative diseases. In *Free Radical Biology and Medicine* 31 (5), pp. 563–573. DOI: 10.1016/s0891-5849(01)00628-1.

Dringen, R. (2000): Metabolism and functions of glutathione in brain. In *Progress in Neurobiology* 62 (6), pp. 649–671. DOI: 10.1016/S0301-0082(99)00060-X.

Dröge, Wulf (2002): Free radicals in the physiological control of cell function. In *Physiological Reviews* 82 (1), pp. 47–95. DOI: 10.1152/physrev.00018.2001.

Du, Fang; Yu, Qing; Yan, Shijun; Hu, Gang; Lue, Lih-Fen; Walker, Douglas G. et al. (2017): PINK1 signalling rescues amyloid pathology and mitochondrial dysfunction in Alzheimer's disease. In *Brain: a Journal of Neurology* 140 (12), pp. 3233–3251. DOI: 10.1093/brain/awx258.

Duan, Wei; Zhang, Yu-Ping; Hou, Zhi; Huang, Chen; Zhu, He; Zhang, Chun-Qing; Yin, Qing (2016): Novel insights into NeuN: from neuronal marker to splicing regulator. In *Molecular Neurobiology* 53 (3), pp. 1637–1647. DOI: 10.1007/s12035-015-9122-5.

Eggler, Aimee L.; Small, Evan; Hannink, Mark; Mesecar, Andrew D. (2009): Cul3-mediated Nrf2 ubiquitination and antioxidant response element (ARE) activation are dependent on the partial molar volume at position 151 of Keap1. In *The Biochemical Journal* 422 (1), pp. 171–180. DOI: 10.1042/BJ20090471.

Eisen, E. J.; Legates, J. E. (1966): Genotype-sex interaction and the genetic correlation between the sexes for body weight in *Mus musculus*. In *Genetics* 54 (2), pp. 611–623. DOI: 10.1093/genetics/54.2.611.

Eisert, Regina; Potter, Charles W.; Oftedal, Olav T. (2014): Brain size in neonatal and adult Weddell seals: costs and consequences of having a large brain. In *Marine Mammal Science* 30 (1), pp. 184–205. DOI: 10.1111/mms.12033.

Ellis, Earl F.; Willoughby, Karen A.; Sparks, Sallie A.; Chen, Tao (2007): S100B protein is released from rat neonatal neurons, astrocytes, and microglia by in vitro trauma and anti-S100 increases trauma-induced delayed neuronal injury and negates the protective effect of exogenous S100B on neurons. In *Journal of Neurochemistry* 101 (6), pp. 1463–1470. DOI: 10.1111/j.1471-4159.2007.04515.x.

Ellis, Justin K.; Sorrells, Shawn F.; Mikhailova, Sasha; Chavali, Manideep; Chang, Sandra; Sabeur, Khalida et al. (2019): Ferret brain possesses young interneuron collections equivalent to human postnatal migratory streams. In *The Journal of Comparative Neurology* 527 (17), pp. 2843–2859. DOI: 10.1002/cne.24711.

Elsner, R.; Oyasaeter, S.; Almaas, R.; Saugstad, O. D. (1998): Diving seals, ischemia-reperfusion and oxygen radicals. In *Comparative Biochemistry and Physiology Part A: Molecular & Integrative Physiology* 119 (4), pp. 975–980. DOI: 10.1016/S1095-6433(98)00012-9.

Elsner, Robert; Surley, Jay T.; Hammond, Douglas D.; Brooks, Robert E. (1970): Cerebral tolerance to hypoxemia in asphyxiated Weddell seals. In *Respiration Physiology* 9 (2), pp. 287–297. DOI: 10.1016/0034-5687(70)90077-0.

Empie, Kristen; Rangarajan, Vijayeta; Juul, Sandra E. (2015): Is the ferret a suitable species for studying perinatal brain injury? In *International Journal of Developmental Neuroscience* 45, pp. 2–10. DOI: 10.1016/j.ijdevneu.2015.06.005.

Endo, Yoshinori; Kamei, Ken-Ichiro; Inoue-Murayama, Miho (2018): Genetic signatures of lipid metabolism evolution in cetacea since the divergence from terrestrial ancestor. In *Journal of Evolutionary Biology* 31 (11), pp. 1655–1665. DOI: 10.1111/jeb.13361.

Engel, Mareen; Smidt, Marten P.; van Hooft, Johannes A. (2013): The serotonin 5-HT3 receptor: a novel neurodevelopmental target. In *Frontiers in Cellular Neuroscience* 7, p. 76. DOI: 10.3389/fncel.2013.00076.

Enoksen, Solveig; Haug, Tore; Lindstrøm, Ulf; Nilssen, Kjell Tormod (2017): Recent summer diet of hooded *Cystophora cristata* and harp *Pagophilus groenlandicus* seals in the drift ice of the Greenland Sea. In *Polar Biology* 40 (4), pp. 931–937. DOI: 10.1007/s00300-016-2002-2.

Erecińska, Maria; Silver, Ian A. (2001): Tissue oxygen tension and brain sensitivity to hypoxia. In *Respiration Physiology* 128 (3), pp. 263–276. DOI: 10.1016/S0034-5687(01)00306-1.

Esworthy, R. S.; Chu, F. F.; Paxton, R. J.; Akman, S.; Doroshow, J. H. (1991): Characterization and partial amino acid sequence of human plasma glutathione peroxidase. In *Archives of Biochemistry and Biophysics* 286 (2), pp. 330–336. DOI: 10.1016/0003-9861(91)90048-N.

Evans, Peter G.H.; Anderwald, Pia; Wright, Andrew J. (2014): Marine mammal research: its relationship to other scientific disciplines and to wider society. In *Journal of the Marine Biological Association of the United Kingdom* 94 (06), pp. 1073–1077. DOI:10.1017/S0025315414000848.

Fabrizius, Andrej; Hoff, Mariana Leivas Müller; Engler, Gerhard; Folkow, Lars P.; Burmester, Thorsten (2016): When the brain goes diving: transcriptome analysis reveals a reduced aerobic energy metabolism and increased stress proteins in the seal brain. In *BMC Genomics* 17, p. 583. DOI: 10.1186/s12864-016-2892-y.

Falke, K. J.; Hill, R. D.; Qvist, J.; Schneider, R. C.; Guppy, M.; Liggins, G. C. et al. (1985): Seal lungs collapse during free diving: evidence from arterial nitrogen tensions. In *Science (New York, N.Y.)* 229 (4713), pp. 556–558. DOI: 10.1126/science.4023700.

Fanò, Giorgio; Biocca, Silvia; Fulle, Stefania; Mariggiò, Maria A.; Belia, Silvia; Calissano, Pietro (1995): The S-100: a protein family in search of a function. In *Progress in Neurobiology* 46 (1), pp. 71–82. DOI: 10.1016/0301-0082(94)00062-M.

Farhat, Elie; Cheng, Hang; Romestaing, Caroline; Pamenter, Matthew; Weber, Jean-Michel (2021a): Goldfish response to chronic hypoxia: mitochondrial respiration, fuel preference and energy metabolism. In *Metabolites* 11 (3). DOI: 10.3390/metabo11030187.

Farhat, Elie; Devereaux, Maiah E. M.; Cheng, Hang; Weber, Jean-Michel; Pamenter, Matthew E. (2021b): Na+/K+-ATPase activity is regionally regulated by acute hypoxia in naked mole-rat brain. In *Neuroscience Letters* 764, p. 136244. DOI: 10.1016/j.neulet.2021.136244.

Farhat, Elie; Devereaux, Maiah E. M.; Pamenter, Matthew E.; Weber, Jean-Michel (2020): Naked mole-rats suppress energy metabolism and modulate membrane cholesterol in chronic hypoxia. In *American Journal of Physiology: Regulatory, Integrative and Comparative Physiology* 319 (2), R148-R155. DOI: 10.1152/ajpregu.00057.2020.

Farhat, Elie; Turenne, Eric D.; Choi, Kevin; Weber, Jean-Michel (2019): Hypoxia-induced remodelling of goldfish membranes. In *Comparative Biochemistry and Physiology Part B: Biochemistry & Molecular Biology* 237, p. 110326. DOI: 10.1016/j.cbpb.2019.110326.

Farhat, Elie; Weber, Jean-Michel (2021): Hypometabolic responses to chronic hypoxia: a potential role for membrane lipids. In *Metabolites* 11 (8). DOI: 10.3390/metabo11080503.

Fernández-Chacón, R.; Königstorfer, A.; Gerber, S. H.; García, J.; Matos, M. F.; Stevens, C. F. et al. (2001): Synaptotagmin I functions as a calcium regulator of release probability. In *Nature* 410 (6824), pp. 41–49. DOI: 10.1038/35065004.

Fisher, Peter G. (2006): Ferret behavior. In Teresa Bradley Bays, Teresa Lightfoot, Jörg Mayer (Eds.): Exotic pet behavior. Birds, reptiles, and small mammals. St. Louis, Mo: Saunders Elsevier, pp. 163–205. DOI: 10.1016/B978-1-4160-0009-9.50011-6.

Fitzner, Dirk; Bader, Jakob M.; Penkert, Horst; Bergner, Caroline G.; Su, Minhui; Weil, Marie-Theres et al. (2020): Cell-type- and brain-region-resolved mouse brain lipidome. In *Cell Reports* 32 (11), p. 108132. DOI: 10.1016/j.celrep.2020.108132.

Flohé, Leopold (2013): The fairytale of the GSSG/GSH redox potential. In *Biochimica et Biophysica Acta* 1830 (5), pp. 3139–3142. DOI: 10.1016/j.bbagen.2012.10.020.

Folbergrová, J.; Rehncrona, S.; Siesjö, B. K. (1979): Oxidized and reduced glutathione in the rat brain under normoxic and hypoxic conditions. In *Journal of Neurochemistry* 32 (6), pp. 1621–1627. DOI: 10.1111/j.1471-4159.1979.tb02271.x.

Folkow, Lars P.; Blix, Arnoldus S. (2010): Air breathers under water: diving mammals and birds. In Göran E. Nilsson (Ed.): Respiratory physiology of vertebrates. Life with and without oxygen. Cambridge: Cambridge University Press, pp. 222–264. DOI: 10.1017/CBO9780511845178.008.

Folkow, Lars P.; Blix, Arnoldus Schytte (1999): Diving behaviour of hooded seals (*Cystophora cristata*) in the Greenland and Norwegian Seas. In *Polar Biology* 22 (1), pp. 61–74. DOI: 10.1007/s003000050391.

Folkow, Lars P.; Mårtensson, Per-Erik; Blix, Arnoldus Schytte (1996): Annual distribution of hooded seals (*Cystophora cristata*) in the Greenland and Norwegian seas. In *Polar Biology* 16 (3), pp. 179–189. DOI: 10.1007/BF02329206.

Folkow, Lars P.; Nordøy, Erling S.; Blix, Arnoldus S. (2004): Distribution and diving behaviour of harp seals (*Pagophilus groenlandicus*) from the Greenland Sea stock. In *Polar Biology* 27 (5), pp. 281–298. DOI: 10.1007/s00300-004-0591-7.

Folkow, Lars P.; Ramirez, Jan-Marino; Ludvigsen, Stian; Ramirez, Nicolo; Blix, Arnoldus S. (2008): Remarkable neuronal hypoxia tolerance in the deep-diving adult hooded seal (*Cystophora cristata*). In *Neuroscience Letters* 446 (2-3), pp. 147–150. DOI: 10.1016/j.neulet.2008.09.040.

Fong, G-H; Takeda, K. (2008): Role and regulation of prolyl hydroxylase domain proteins. In *Cell Death and Differentiation* 15 (4), pp. 635–641. DOI: 10.1038/cdd.2008.10.

Foote, Andrew D.; Liu, Yue; Thomas, Gregg W. C.; Vinař, Tomáš; Alföldi, Jessica; Deng, Jixin et al. (2015): Convergent evolution of the genomes of marine mammals. In *Nature Genetics* 47 (3), pp. 272–275. DOI: 10.1038/ng.3198.

Foster, Evangeline M.; Dangla-Valls, Adrià; Lovestone, Simon; Ribe, Elena M.; Buckley, Noel J. (2019): Clusterin in Alzheimer's disease: mechanisms, genetics, and lessons from other pathologies. In *Frontiers in Neuroscience* 13, p. 164. DOI: 10.3389/fnins.2019.00164.

Fowler, Melinda; Champagne, Cory; Crocker, Daniel (2018): Adiposity and fat metabolism during combined fasting and lactation in elephant seals. In *The Journal of Experimental Biology* 221 (Pt Suppl 1). DOI: 10.1242/jeb.161554.

Fox, J.; Bouchet-Valat, M.; Andronic, L.; Ash, M.; Boye, T.; Calza, S. (2019): Package 'Rcmdr'. Available online at https://CRAN.R-project.org/package=Rcmdr.

Fox, John (2005): The R commander: a basic-statistics graphical user interface to R. In *Journal of Statistical Software* 14 (9), pp. 1–42. DOI: 10.18637/jss.v014.i09.

Fridovich, I. (1998): Oxygen toxicity: a radical explanation. In *The Journal of Experimental Biology* 201 (Pt 8), pp. 1203–1209. DOI: 10.1242/jeb.201.8.1203.

Frouin-Mouy, Héloïse C.; Hammill, Mike O. (2021): In-air and underwater sounds of hooded seals during the breeding season in the Gulf of St. Lawrence. In *The Journal of the Acoustical Society of America* 150 (1), p. 281. DOI: 10.1121/10.0005478.

Fugio, Lais Brigliadori; Coeli-Lacchini, Fernanda B.; Leopoldino, Andréia Machado (2020): Sphingolipids and mitochondrial dynamic. In *Cells* 9 (3), p. 581. DOI: 10.3390/cells9030581.

Garcia Párraga, Daniel; Moore, Michael; Fahlman, Andreas (2018): Pulmonary ventilation-perfusion mismatch: a novel hypothesis for how diving vertebrates may avoid the bends. In *Proceedings: Biological Sciences* 285 (1877). DOI: 10.1098/rspb.2018.0482.

García-Castañeda, Omar; Gaxiola-Robles, Ramón; Kanatous, Shane; Zenteno-Savín, Tania (2017): Circulating glutathione concentrations in marine, semiaquatic, and terrestrial mammals. In *Marine Mammal Science* 33 (3), pp. 738–747. DOI: 10.1111/mms.12391.

García-Pardo, L.; Granados, M. D.; Gaytán, F.; Padilla, C. A.; Martínez-Galisteo, E.; Morales, C. et al. (1999): Immunolocalization of glutaredoxin in the human corpus luteum. In *Molecular Human Reproduction* 5 (10), pp. 914–919. DOI: 10.1093/molehr/5.10.914.

Geiseler, Samuel J.; Blix, Arnoldus S.; Burns, Jennifer M.; Folkow, Lars P. (2013): Rapid postnatal development of myoglobin from large liver iron stores in hooded seals. In *The Journal of Experimental Biology* 216 (Pt 10), pp. 1793–1798. DOI: 10.1242/jeb.082099.

Geiseler, Samuel J.; Larson, John; Folkow, Lars P. (2016): Synaptic transmission despite severe hypoxia in hippocampal slices of the deep-diving hooded seal. In *Neuroscience* 334, pp. 39–46. DOI: 10.1016/j.neuroscience.2016.07.034.

Gelain, Daniel P.; Dalmolin, Rodrigo J. S.; Belau, Vanessa L.; Moreira, Jose C. F.; Klamt, Fabio; Castro, Mauro A. A. (2009): A systematic review of human antioxidant genes. In *Frontiers in Bioscience (Landmark edition)* 14 (12), pp. 4457–4463. DOI: 10.2741/3541.

Genoud, Christel; Quairiaux, Charles; Steiner, Pascal; Hirling, Harald; Welker, Egbert; Knott, Graham W. (2006): Plasticity of astrocytic coverage and glutamate transporter expression in adult mouse cortex. In *PLoS Biology* 4 (11), e343. DOI: 10.1371/journal.pbio.0040343.

Gerlach, R.; Demel, G.; König, H-G; Gross, U.; Prehn, J. H. M.; Raabe, A. et al. (2006): Active secretion of S100B from astrocytes during metabolic stress. In *Neuroscience* 141 (4), pp. 1697–1701. DOI: 10.1016/j.neuroscience.2006.05.008.

Geßner, Cornelia; Krüger, Alena; Folkow, Lars P.; Fehrle, Wilfrid; Mikkelsen, Bjarni; Burmester, Thorsten (2022): Transcriptomes suggest that pinniped and cetacean brains have a high capacity for aerobic metabolism while reducing energy-intensive processes such as synaptic transmission. In *Frontiers in Molecular Neuroscience* 15, Article 877349. DOI: 10.3389/fnmol.2022.877349.

Geßner, Cornelia; Stillger, Maren Nicole; Mölders, Naomi; Fabrizius, Andrej; Folkow, Lars P.; Burmester, Thorsten (2020): Cell culture experiments reveal that high S100B and clusterin levels may convey hypoxia-tolerance to the hooded seal (*Cystophora cristata*) brain. In *Neuroscience* 451, pp. 226–239. DOI: 10.1016/j.neuroscience.2020.09.039.

Ghafourifar, P.; Klein, S. D.; Schucht, O.; Schenk, U.; Pruschy, M.; Rocha, S.; Richter, C. (1999): Ceramide induces cytochrome c release from isolated mitochondria. Importance of mitochondrial redox state. In *Journal of Biological Chemistry* 274 (10), pp. 6080–6084. DOI: 10.1074/jbc.274.10.6080.

Giacobbo, Bruno Lima; Doorduin, Janine; Klein, Hans C.; Dierckx, Rudi A. J. O.; Bromberg, Elke; Vries, Erik F. J. de (2019): Brain-derived neurotrophic factor in brain disorders: focus on neuroinflammation. In *Molecular Neurobiology* 56 (5), pp. 3295–3312. DOI: 10.1007/s12035-018-1283-6.

Gilardi, Carlotta; Kalebic, Nereo (2021): The ferret as a model system for neocortex development and evolution. In *Frontiers in Cell and Developmental Biology* 9, p. 661759. DOI: 10.3389/fcell.2021.661759.

Gillooly, J. F.; Brown, J. H.; West, G. B.; Savage, V. M.; Charnov, E. L. (2001): Effects of size and temperature on metabolic rate. In *Science (New York, N.Y.)* 293 (5538), pp. 2248–2251. DOI: 10.1126/science.1061967.

Glandon, Hillary L.; Loh, Ai Ning; McLellan, William A.; Pabst, D. Ann; Westgate, Andrew J.; Koopman, Heather N. (2021): Lipid signature of neural tissues of marine and terrestrial mammals: consistency across species and habitats. In *Journal of Comparative Physiology B: Biochemical, Systemic, and Environmental Physiology* 191 (4), pp. 815–829. DOI: 10.1007/s00360-021-01373-x.

Gonzalez-Riano, Carolina; León-Espinosa, Gonzalo; Regalado-Reyes, Mamen; García, Antonia; DeFelipe, Javier; Barbas, Coral (2019): Metabolomic study of hibernating Syrian hamster brains: in search of neuroprotective agents. In *Journal of Proteome Research* 18 (3), pp. 1175–1190. DOI: 10.1021/acs.jproteome.8b00816.

Goodman, DeWitt S. (1988): Report of the national cholesterol education program expert panel on detection, evaluation, and treatment of high blood cholesterol in adults. In *Archives of Internal Medicine* 148 (1), p. 36. DOI: 10.1001/archinte.1988.00380010040006.

Gopalakrishnan, Lathika; Chatterjee, Oishi; Ravishankar, Namitha; Suresh, Sneha; Raju, Rajesh; Mahadevan, Anita; Prasad, T. S. Keshava (2021): Opioid receptors signaling network. In *Journal of Cell Communication and Signaling*, pp. 1–9. DOI: 10.1007/s12079-021-00653-z.

Gregory, Jenna M.; Whiten, Daniel R.; Brown, Rebecca A.; Barros, Teresa P.; Kumita, Janet R.; Yerbury, Justin J. et al. (2017): Clusterin protects neurons against intracellular proteotoxicity. In *Acta Neuropathologica Communications* 5 (1), p. 81. DOI: 10.1186/s40478-017-0481-1.

Grill-Spector, Kalanit; Weiner, Kevin S. (2014): The functional architecture of the ventral temporal cortex and its role in categorization. In *Nature Reviews Neuroscience* 15 (8), pp. 536–548. DOI: 10.1038/nrn3747.

Gudz, T. I.; Tserng, K. Y.; Hoppel, C. L. (1997): Direct inhibition of mitochondrial respiratory chain complex III by cell-permeable ceramide. In *Journal of Biological Chemistry* 272 (39), pp. 24154–24158. DOI: 10.1074/jbc.272.39.24154.

Gupta, S. K.; Mishra, R.; Kusum, S.; Spedding, M.; Meiri, K. F.; Gressens, P.; Mani, S. (2009): GAP-43 is essential for the neurotrophic effects of BDNF and positive AMPA receptor modulator S18986. In *Cell Death and Differentiation* 16 (4), pp. 624–637. DOI: 10.1038/cdd.2008.188.

Guyton, G. P.; Stanek, K. S.; Schneider, R. C.; Hochachka, P. W.; Hurford, W. E.; Zapol, D. G. et al. (1995): Myoglobin saturation in free-diving Weddell seals. In *Journal of Applied Physiology (Bethesda, Md. : 1985)* 79 (4), pp. 1148–1155. DOI: 10.1152/jappl.1995.79.4.1148.

Halestrap, Andrew P.; Wilson, Marieangela C. (2012): The monocarboxylate transporter family--role and regulation. In *IUBMB Life* 64 (2), pp. 109–119. DOI: 10.1002/iub.572.

Halliwell, Barry; Gutteridge, John M. C. (2015): Free radicals in biology and medicine. 5. Ed. Oxford: Oxford University Press. DOI: 10.1093/acprof:oso/9780198717478.001.0001.

Han, X.; Holtzman, D. M.; McKeel, D. W. (2001): Plasmalogen deficiency in early Alzheimer's disease subjects and in animal models: molecular characterization using electrospray ionization mass spectrometry. In *Journal of Neurochemistry* 77 (4), pp. 1168–1180. DOI: 10.1046/j.1471-4159.2001.00332.x.

Hannun, Yusuf A.; Obeid, Lina M. (2018): Sphingolipids and their metabolism in physiology and disease. In *Nature Reviews Molecular Cell Biology* 19 (3), pp. 175–191. DOI: 10.1038/nrm.2017.107.

Harrington, Lauren A.; Biggins, Dean E.; Alldredge, A. William (2003): Basal metabolism of the black-footed ferret (*Mustela nigripes*) and the Siberian polecat (*M. eversmannii*). In *Journal of Mammalogy* 84 (2), pp. 497–504. DOI: 10.1644/1545-1542(2003)084<0497:BMOTBF>2.0.CO;2.

Hartline, Daniel K. (2008): What is myelin? In *Neuron Glia Biology* 4 (2), pp. 153–163. DOI: 10.1017/S1740925X09990263.

Hassrick, Jason L.; Crocker, Daniel E.; Zeno, Ramona L.; Blackwell, Susanna B.; Costa, Daniel P.; Le Boeuf, Burney J. (2007): Swimming speed and foraging strategies of northern elephant seals. In *Deep Sea Research Part II: Topical Studies in Oceanography* 54 (3-4), pp. 369–383. DOI: 10.1016/j.dsr2.2006.12.001.

Haug, Tore; Tormod Nilssen, Kjell; Lindblom, Lotta; Lindstrøm, Ulf (2007): Diets of hooded seals (*Cystophora cristata*) in coastal waters and drift ice waters along the east coast of Greenland. In *Marine Biology Research* 3 (3), pp. 123–133. DOI: 10.1080/17451000701358531.

Hazel, J. (1990): The role of alterations in membrane lipid composition in enabling physiological adaptation of organisms to their physical environment. In *Progress in Lipid Research* 29 (3), pp. 167–227. DOI: 10.1016/0163-7827(90)90002-3.

He, Xiaozhou; Sandhu, Harleen K.; Yang, Yilin; Hua, Fei; Belser, Nathalee; Kim, Dong H.; Xia, Ying (2013): Neuroprotection against hypoxia/ischemia: δ-opioid receptor-mediated cellular/molecular events. In *Cellular and Molecular Life Sciences* 70 (13), pp. 2291–2303. DOI: 10.1007/s00018-012-1167-2.

Heit, Bradley S.; Dykas, Patricia; Chu, Alex; Sane, Abhay; Larson, John (2021): Synaptic and network contributions to anoxic depolarization in mouse hippocampal slices. In *Neuroscience* 461, pp. 102–117. DOI: 10.1016/j.neuroscience.2021.02.021.

Herberstein, Marie E.; McLean, Donald James; Lowe, Elizabeth; Wolff, Jonas O.; Khan, Md Kawsar; Smith, Kaitlyn et al. (2022): AnimalTraits - a curated animal trait database for body mass, metabolic rate and brain size. In *Scientific Data* 9 (1), p. 265. DOI: 10.1038/s41597-022-01364-9.

Hermes-Lima, Marcelo; Moreira, Daniel C.; Rivera-Ingraham, Georgina A.; Giraud-Billoud, Maximiliano; Genaro-Mattos, Thiago C.; Campos, Élida G. (2015): Preparation for oxidative stress under hypoxia and metabolic depression: Revisiting the proposal two decades later. In *Free Radical Biology and Medicine* 89, pp. 1122–1143. DOI: 10.1016/j.freeradbiomed.2015.07.156.

Herrero-Mendez, Angel; Almeida, Angeles; Fernández, Emilio; Maestre, Carolina; Moncada, Salvador; Bolaños, Juan P. (2009): The bioenergetic and antioxidant status of neurons is controlled by continuous degradation of a key glycolytic enzyme by APC/C-Cdh1. In *Nature Cell Biology* 11 (6), pp. 747–752. DOI: 10.1038/ncb1881.

Herring, Sarah K.; Moon, Hee-Jung; Rawal, Punam; Chhibber, Anindit; Zhao, Liqin (2019): Brain clusterin protein isoforms and mitochondrial localization. In *eLife* 8. DOI: 10.7554/eLife.48255.

Hill, R. D.; Schneider, R. C.; Liggins, G. C.; Schuette, A. H.; Elliott, R. L.; Guppy, M. et al. (1987): Heart rate and body temperature during free diving of Weddell seals. In *The American Journal of Physiology* 253 (2 Pt 2), R344-51. DOI: 10.1152/ajpregu.1987.253.2.R344.

Hindle, Allyson; Allen, Kaitlin; Batten, Annabelle; Wareham, Lauren; Buys, Emmanuel; Zapol, Warren (2018): From field to lab: asking questions about hypoxia regulation of vascular tone in cell culture systems. In *The FASEB Journal* 31, 1075.1-1075.1. DOI: 10.1096/fasebj.31.1_supplement.1075.1.

Hindle, Allyson G. (2020): Diving deep: understanding the genetic components of hypoxia tolerance in marine mammals. In *Journal of Applied Physiology (Bethesda, Md. : 1985)* 128 (5), pp. 1439–1446. DOI: 10.1152/japplphysiol.00846.2019.

Hoeksema, Nienke; Verga, Laura; Mengede, Janine; van Roessel, Corné; Villanueva, Stella; Salazar-Casals, Anna et al. (2021): Neuroanatomy of the grey seal brain: bringing pinnipeds into the neurobiological study of vocal learning. In *Philosophical Transactions of the Royal Society of London Series B: Biological Sciences* 376 (1836), p. 20200252. DOI: 10.1098/rstb.2020.0252.

Hoff, Mariana Leivas Müller; Fabrizius, Andrej; Czech-Damal, Nicole U.; Folkow, Lars P.; Burmester, Thorsten (2017): Transcriptome analysis identifies key metabolic changes in the hooded seal (*Cystophora cristata*) brain in response to hypoxia and reoxygenation. In *PLoS One* 12 (1), e0169366. DOI: 10.1371/journal.pone.0169366.

Hoff, Mariana Leivas Müller; Fabrizius, Andrej; Folkow, Lars P.; Burmester, Thorsten (2016): An atypical distribution of lactate dehydrogenase isoenzymes in the hooded seal (*Cystophora cristata*) brain may reflect a biochemical adaptation to diving. In *Journal of Comparative Physiology B: Biochemical, Systemic, and Environmental Physiology* 186 (3), pp. 373–386. DOI: 10.1007/s00360-015-0956-y.

Höglund, Erik; Øverli, Øyvind; Winberg, Svante (2019): Tryptophan metabolic pathways and brain serotonergic activity: a comparative review. In *Frontiers in Endocrinology* 10, p. 158. DOI: 10.3389/fendo.2019.00158.

Holmgren, A. (1989): Thioredoxin and glutaredoxin systems. In *Journal of Biological Chemistry* 264 (24), pp. 13963–13966. DOI: 10.1016/S0021-9258(18)71625-6.

Hunter, John (1787): XXXVIII. Observations on the structure and oeconomy of whales. By John Hunter, Esq. F. R. S. communicated by Sir Joseph Banks, Bart. F. R. S. In *Philosophical Transactions of the Royal Society of London* 77, pp. 371–450. DOI: 10.1098/rstl.1787.0038.

Huttunen, H. J.; Kuja-Panula, J.; Sorci, G.; Agneletti, A. L.; Donato, R.; Rauvala, H. (2000): Coregulation of neurite outgrowth and cell survival by amphoterin and S100 proteins through receptor for advanced glycation end products (RAGE) activation. In *Journal of Biological Chemistry* 275 (51), pp. 40096–40105. DOI: 10.1074/jbc.M006993200.

Hylland, Patrick; Milton, Sarah; Pek, Marta; Nilsson, Göran E.; L. Lutz, Peter (1997): Brain Na+/K+-ATPase activity in two anoxia tolerant vertebrates: crucian carp and freshwater turtle. In *Neuroscience Letters* 235 (1-2), pp. 89–92. DOI: 10.1016/S0304-3940(97)00727-1.

Innis, S. M. (2005): Chapter 10 Essential fatty acid metabolism during early development. In *Biology of Growing Animals* 3, pp. 235–274. DOI: 10.1016/S1877-1823(09)70017-7.

Irving, Laurence; Hart, J. S. (1957): The metabolism and insulation of seals as bare-skinned mammals in cold water. In *Canadian Journal of Zoology* 35 (4), pp. 497–511. DOI: 10.1139/z57-041.

Jefferson, Thomas A.; Pitman, Robert L.; Webber, Marc A. (Eds.) (2015): Marine mammals of the world. A comprehensive guide to their identification. With assistance of Uko Gorter. Second edition. Amsterdam, Boston, Heidelberg: Elsevier/Academic Press. DOI: 10.1016/C2012-0-06919-0.

Jeong, Ye Ji; Son, Yeonghoon; Han, Na-Kyung; Choi, Hyung-Do; Pack, Jeong-Ki; Kim, Nam et al. (2018): Impact of long-term RF-EMF on oxidative stress and neuroinflammation in aging brains of C57BL/6 mice. In *International Journal of Molecular Sciences* 19 (7). DOI: 10.3390/ijms19072103.

Jia, Liyun; Liang, Tong; Yu, Xiaoyan; Ma, Chao; Zhang, Shuping (2014): MGARP regulates mouse neocortical development via mitochondrial positioning. In *Molecular Neurobiology* 49 (3), pp. 1293–1308. DOI: 10.1007/s12035-013-8602-8.

Jiang, Xiuli; Wang, Xiaoli; Tuo, Miao; Ma, Jiangnan; Xie, Anmu (2018): RAGE and its emerging role in the pathogenesis of Parkinson's disease. In *Neuroscience Letters* 672, pp. 65–69. DOI: 10.1016/j.neulet.2018.02.049.

Jiménez, I.; Speisky, H. (2000): Effects of copper ions on the free radical-scavenging properties of reduced gluthathione: implications of a complex formation. In *Journal of Trace Elements in Medicine and Biology* 14 (3), pp. 161–167. DOI: 10.1016/S0946-672X(00)80005-X.

Jin, Junfei; Hou, Qi; Mullen, Thomas D.; Zeidan, Youssef H.; Bielawski, Jacek; Kraveka, Jacqueline M. et al. (2008): Ceramide generated by sphingomyelin hydrolysis and the salvage pathway is involved in hypoxia/reoxygenation-induced Bax redistribution to mitochondria in NT-2 cells. In *Journal of Biological Chemistry* 283 (39), pp. 26509–26517. DOI: 10.1074/jbc.M801597200.

Johnson, Peter; Elsner, Robert; Zenteno-Savín, Tania (2004): Hypoxia-Inducible Factor in ringed seal (Phoca hispida) tissues. In *Free Radical Research* 38 (8), pp. 847–854. DOI: 10.1080/10715760410001725526.

Johnson, Peter; Elsner, Robert; Zenteno-Savín, Tania (2005): Hypoxia-inducible factor 1 proteomics and diving adaptations in ringed seal. In *Free Radical Biology and Medicine* 39 (2), pp. 205–212. DOI: 10.1016/j.freeradbiomed.2005.03.008.

Johnson, Victoria E.; Meaney, David F.; Cullen, D. Kacy; Smith, Douglas H. (2015): Chapter 8 - Animal models of traumatic brain injury. In Jordan Grafman, Andres M. Salazar (Eds.): Handbook of clinical neurology: traumatic brain injury, part I, vol. 127: Elsevier, pp. 115–128. DOI: 10.1016/B978-0-444-52892-6.00008-8.

Jones, Dean P. (2002a): [11] Redox potential of GSH/GSSG couple: assay and biological significance. In Helmut Sies, Lester Packer (Eds.): Methods in enzymology: protein sensors and reactive oxygen species - part B: thiol enzymes and proteins, vol. 348: Academic Press, pp. 93–112. DOI: 10.1016/S0076-6879(02)48630-2.

Jones, S. (2002b): Clusterin. In *The International Journal of Biochemistry & Cell Biology* 34 (5), pp. 427–431. DOI: 10.1016/S1357-2725(01)00155-8.

Jongbloets, Bart C.; Pasterkamp, R. Jeroen (2014): Semaphorin signalling during development. In *Development (Cambridge, England)* 141 (17), pp. 3292–3297. DOI: 10.1242/dev.105544.

Jun, Hyoung-Oh; Kim, Dong-hun; Lee, Sae-Won; Lee, Hye Shin; Seo, Ji Hae; Kim, Jeong Hun et al. (2011): Clusterin protects H9c2 cardiomyocytes from oxidative stress-induced apoptosis via Akt/GSK-3β signaling pathway. In *Experimental & Molecular Medicine* 43 (1), pp. 53–61. DOI: 10.3858/emm.2011.43.1.006.

Jung, C. H.; Thomas, J. A. (1996): S-glutathiolated hepatocyte proteins and insulin disulfides as substrates for reduction by glutaredoxin, thioredoxin, protein disulfide isomerase, and glutathione. In *Archives of Biochemistry and Biophysics* 335 (1), pp. 61–72. DOI: 10.1006/abbi.1996.0482.

Jurevics, H.; Hostettler, J.; Muse, E. D.; Sammond, D. W.; Matsushima, G. K.; Toews, A. D.; Morell, P. (2001): Cerebroside synthesis as a measure of the rate of remyelination following cuprizone-induced demyelination in brain. In *Journal of Neurochemistry* 77 (4), pp. 1067–1076. DOI: 10.1046/j.1471-4159.2001.00310.x.

Kacem, Kamel; Lacombe, Pierre; Seylaz, Jacques; Bonvento, Gilles (1998): Structural organization of the perivascular astrocyte endfeet and their relationship with the endothelial glucose transporter: a confocal microscopy study. In *Glia* 23 (1), pp. 1–10. DOI: 10.1002/(SICI)1098-1136(199805)23:1<1::AID-GLIA1>3.0.CO;2-B.

Kaczmarek, Jeppe; Reichmuth, Colleen; McDonald, Birgitte I.; Kristensen, Jakob H.; Larson, Josefin; Johansson, Fredrik et al. (2018): Drivers of the dive response in pinnipeds; apnea, submergence or temperature? In *The Journal of Experimental Biology* 221 (Pt 13). DOI: 10.1242/jeb.176545.

Kalamatianos, Theodosis; Denekou, Despoina; Stranjalis, George; Papadimitriou, Evangelia (2018): Anaplastic lymphoma kinase in glioblastoma: detection/diagnostic methods and therapeutic options. In *Recent Patents on Anti-Cancer Drug Discovery* 13 (2), pp. 209–223. DOI: 10.2174/1574892813666180115151554.

Kanatous, Shane B.; Mammen, Pradeep P. A. (2010): Regulation of myoglobin expression. In *The Journal of Experimental Biology* 213 (Pt 16), pp. 2741–2747. DOI: 10.1242/jeb.041442.

Kang, Mi Sun; Ahn, Kyong Hoon; Kim, Seok Kyun; Jeon, Hyung Jun; Ji, Jung Eun; Choi, Jong Min et al. (2010): Hypoxia-induced neuronal apoptosis is mediated by de novo synthesis of ceramide through activation of serine palmitoyltransferase. In *Cellular Signalling* 22 (4), pp. 610–618. DOI: 10.1016/j.cellsig.2009.11.015.

Kao, Yu-Chia; Ho, Pei-Chuan; Tu, Yuan-Kun; Jou, I-Ming; Tsai, Kuen-Jer (2020): Lipids and Alzheimer's Disease. In *International Journal of Molecular Sciences* 21 (4). DOI: 10.3390/ijms21041505.

Karunakaran, Smitha; Saeed, Uzma; Ramakrishnan, Sujanitha; Koumar, Ratnacaram Chandrahaas; Ravindranath, Vijayalakshmi (2007): Constitutive expression and functional characterization of mitochondrial glutaredoxin (Grx2) in mouse and human brain. In *Brain Research* 1185, pp. 8–17. DOI: 10.1016/j.brainres.2007.09.019.

Kasamatsu, Masahiko; Hasegawa, Kazuhiro; Wakabayashi, Ikuo; Seko, Atsushi; Furuta, Masami (2012): Hematology and serum biochemistry values in five captive finless porpoises (*Neophocaena phocaenoides*). In *The Journal of Veterinary Medical Science* 74 (10), pp. 1319–1322. DOI: 10.1292/jvms.11-0407.

Kasamatsu, Masahiko; Kawauchi, Rieko; Tsunokawa, Masatoshi; Ueda, Keiichi; Uchida, Eiji; Oikawa, Shin et al. (2009): Comparison of serum lipid compositions, lipid peroxide, alpha-tocopherol and lipoproteins in captive marine mammals (bottlenose dolphins, spotted seals and West Indian manatees) and terrestrial mammals. In *Research in Veterinary Science* 86 (2), pp. 216–222. DOI: 10.1016/j.rvsc.2008.07.006.

Kassambara, Alboukadel (2020): ggpubr: 'ggplot2' based publication ready plots. R package version 0.4.0. Available online at https://CRAN.R-project.org/package=ggpubr.

Kassambara, Alboukadel (2021): Rstatix: pipe-friendly framework for basic statistical tests. R.package.version.0.7.0. Available online at https://CRAN.R.project.org/package=rstatix.

Katoh, Kazutaka; Standley, Daron M. (2013): MAFFT multiple sequence alignment software version 7: improvements in performance and usability. In *Molecular Biology and Evolution* 30 (4), pp. 772–780. DOI: 10.1093/molbev/mst010.

Kaushik, Susmita; Cuervo, Ana Maria (2015): Proteostasis and aging. In *Nature Medicine* 21 (12), pp. 1406–1415. DOI: 10.1038/nm.4001.

Kelly, P. A.; Ford, I.; McCulloch, J. (1986): The effect of diazepam upon local cerebral glucose use in the conscious rat. In *Neuroscience* 19 (1), pp. 257–265. DOI: 10.1016/0306-4522(86)90019-9.

Kerem, D.; Elsner, R. (1973): Cerebral tolerance to asphyxial hypoxia in the harbor seal. In *Respiration Physiology* 19 (2), pp. 188–200. DOI: 10.1016/0034-5687(73)90077-7.

Kerem, D.; Hammond, D.D; Elsner, R. (1973): Tissue glycogen levels in the Weddell seal, *Leptonychotes weddelli*: a possible adaptation to asphyxial hypoxia. In *Comparative Biochemistry and Physiology Part A: Physiology* 45 (3), pp. 731–736. DOI: 10.1016/0300-9629(73)90076-5.

Kevin, Leo G.; Novalija, Enis; Stowe, David F. (2005): Reactive oxygen species as mediators of cardiac injury and protection: the relevance to anesthesia practice. In *Anesthesia and Analgesia* 101 (5), pp. 1275–1287. DOI: 10.1213/01.ANE.0000180999.81013.D0.

Kierans, S. J.; Taylor, C. T. (2021): Regulation of glycolysis by the hypoxia-inducible factor (HIF): implications for cellular physiology. In *The Journal of Physiology* 599 (1), pp. 23–37. DOI: 10.1113/JP280572.

Kim, J. W.; Tchernyshyov, I.; Semenza, G. L.; Dang, C. V. (2006): HIF-1-mediated expression of pyruvate dehydrogenase kinase: a metabolic switch required for cellular adaptation to hypoxia. In *Cell Metabolism* 3 (3), pp. 177–185. DOI: 10.1016/j.cmet.2006.02.002.

King, C. M. (1982): Age structure and reproduction in feral New Zealand populations of the house mouse (*Mus musculus*), in relation to seedfall of southern beech. In *New Zealand Journal of Zoology* 9 (4), pp. 467–480. DOI: 10.1080/03014223.1982.10423879.

Kjellqwist, S. (1995): Trends in age-composition, growth and reproductive parameters of Barents Sea harp seals, *Phoca groenlandica*. In *ICES Journal of Marine Science* 52 (2), pp. 197–208. DOI: 10.1016/1054-3139(95)80035-2.

Klionsky, Daniel J.; Abdel-Aziz, Amal Kamal; Abdelfatah, Sara; Abdellatif, Mahmoud; Abdoli, Asghar; Abel, Steffen et al. (2021): Guidelines for the use and interpretation of assays for monitoring autophagy (4th edition)1. In *Autophagy* 17 (1), pp. 1–382. DOI: 10.1080/15548627.2020.1797280.

Koch, Jonas; Burmester, Thorsten (2016): Membrane-bound globin X protects the cell from reactive oxygen species. In *Biochemical and Biophysical Research Communications* 469 (2), pp. 275–280. DOI: 10.1016/j.bbrc.2015.11.105.

Koch, Jonas; Lüdemann, Julia; Spies, Rieke; Last, Marco; Amemiya, Chris T.; Burmester, Thorsten (2016): Unusual diversity of myoglobin genes in the lungfish. In *Molecular Biology and Evolution* 33 (12), pp. 3033–3041. DOI: 10.1093/molbev/msw159.

Kohyama, Kaoru; Inoshima, Yasuo (2017): Normal hematology and serum chemistry of northern fur seals (*Callorhinus ursinus*) in captivity. In *Zoo Biology* 36 (5), pp. 345–350. DOI: 10.1002/zoo.21376.

Kolesnick, R. (1994): Signal transduction through the sphingomyelin pathway. In *Molecular and Chemical Neuropathology* 21 (2-3), pp. 287–297. DOI: 10.1007/BF02815356.

Kondo, Shinichi; Saito, Atsushi; Hino, Shin-Ichiro; Murakami, Tomohiko; Ogata, Maiko; Kanemoto, Soshi et al. (2007): BBF2H7, a novel transmembrane bZIP transcription factor, is a new type of endoplasmic reticulum stress transducer. In *Molecular and Cellular Biology* 27 (5), pp. 1716–1729. DOI: 10.1128/MCB.01552-06.

Korhonen, H.; Harri, M.; Asikainen, J. (1983): Thermoregulation of polecat and raccoon dog: a comparative study with stoat, mink and blue fox. In *Comparative Biochemistry and Physiology Part A: Physiology* 74 (2), pp. 225–230. DOI: 10.1016/0300-9629(83)90592-3.

Kowaltowski, Alicia J.; Souza-Pinto, Nadja C. de; Castilho, Roger F.; Vercesi, Anibal E. (2009): Mitochondria and reactive oxygen species. In *Free Radical Biology and Medicine* 47 (4), pp. 333–343. DOI: 10.1016/j.freeradbiomed.2009.05.004.

Kowiański, Przemysław; Lietzau, Grażyna; Czuba, Ewelina; Waśkow, Monika; Steliga, Aleksandra; Moryś, Janusz (2018): BDNF: a key factor with multipotent impact on brain signaling and synaptic plasticity. In *Cellular and Molecular Neurobiology* 38 (3), pp. 579–593. DOI: 10.1007/s10571-017-0510-4.

Krüger, Alena; Fabrizius, Andrej; Mikkelsen, Bjarni; Siebert, Ursula; Folkow, Lars P.; Burmester, Thorsten (2020): Transcriptome analysis reveals a high aerobic capacity in the whale brain. In *Comparative Biochemistry and Physiology Part A: Molecular & Integrative Physiology* 240, p. 110593. DOI: 10.1016/j.cbpa.2019.110593.

Kuhl, Carsten; Tautenhahn, Ralf; Böttcher, Christoph; Larson, Tony R.; Neumann, Steffen (2012): CAMERA: an integrated strategy for compound spectra extraction and annotation of liquid chromatography/mass spectrometry data sets. In *Analytical Chemistry* 84 (1), pp. 283–289. DOI: 10.1021/ac202450g.

Kulinsky, V. I.; Kolesnichenko, L. S. (2009): The glutathione system. I. Synthesis, transport, glutathione transferases, glutathione peroxidases. In *Biochemistry (Moscow) Supplement Series B: Biomedical Chemistry* 3 (2), pp. 129–144. DOI: 10.1134/S1990750809020036.

Kumar, Parveen; Sharoyko, Vladimir V.; Spégel, Peter; Gullberg, Urban; Mulder, Hindrik; Olsson, Inge; Ajore, Ram (2013): The transcriptional co-repressor myeloid translocation gene 16 inhibits glycolysis and stimulates mitochondrial respiration. In *PLoS One* 8 (7), e68502. DOI: 10.1371/journal.pone.0068502.

Kumar, Sudhir; Stecher, Glen; Suleski, Michael; Hedges, S. Blair (2017): TimeTree: a resource for timelines, timetrees, and divergence times. In *Molecular Biology and Evolution* 34 (7), pp. 1812–1819. DOI: 10.1093/molbev/msx116.

Kumawat, Manoj; Singh, Piyush Kumar; Rananaware, Supriya Rajendra; Ahlawat, Sushma (2020): Comparative evaluation of structure and characteristic of peptidyl-prolyl cis-trans isomerase proteins and their function in *Salmonella Typhimurium* stress responses and virulence. In *Folia Microbiologica* 65 (1), pp. 161–171. DOI: 10.1007/s12223-019-00717-z.

Kumral, Abdullah; Tugyan, Kazim; Gonenc, Sevil; Genc, Kursat; Genc, Sermin; Sonmez, Ulker et al. (2005): Protective effects of erythropoietin against ethanol-induced apoptotic neurodegenaration and oxidative stress in the developing C57BL/6 mouse brain. In *Developmental Brain Research* 160 (2), pp. 146–156. DOI: 10.1016/j.devbrainres.2005.08.006.

Laake, J. H.; Slyngstad, T. A.; Haug, F. M.; Ottersen, O. P. (1995): Glutamine from glial cells is essential for the maintenance of the nerve terminal pool of glutamate: immunogold evidence from hippocampal slice cultures. In *Journal of Neurochemistry* 65 (2), pp. 871–881. DOI: 10.1046/j.1471-4159.1995.65020871.x.

Ladiges, Warren; van Remmen, Holly; Strong, Randy; Ikeno, Yuji; Treuting, Piper; Rabinovitch, Peter; Richardson, Arlan (2009): Lifespan extension in genetically modified mice. In *Aging Cell* 8 (4), pp. 346–352. DOI: 10.1111/j.1474-9726.2009.00491.x.

Lam, Emily K.; Allen, Kaitlin N.; Torres-Velarde, Julia María; Vázquez-Medina, José Pablo (2020): Functional studies with primary cells provide a system for genome-to-phenome investigations in marine mammals. In *Integrative and Comparative Biology* 60 (2), pp. 348–360. DOI: 10.1093/icb/icaa065.

Larson, John; Drew, Kelly L.; Folkow, Lars P.; Milton, Sarah L.; Park, Thomas J. (2014): No oxygen? No problem! Intrinsic brain tolerance to hypoxia in vertebrates. In *The Journal of Experimental Biology* 217 (Pt 7), pp. 1024–1039. DOI: 10.1242/jeb.085381.

Lau, M. K. (2013): Dtk: Dunnett-Tukey-Kramer pairwise multiple comparison. Version R. package version 3. Available online at https://cran.r-project.org/package=DTK.

Lauderdale, Lisa K.; Walsh, Michael T.; Mitchell, Kevin A.; Granger, Douglas A.; Mellen, Jill D.; Miller, Lance J. (2021): Health reference intervals and values for common bottlenose dolphins (*Tursiops truncatus*), Indo-Pacific bottlenose dolphins (*Tursiops aduncus*), Pacific white-sided dolphins (*Lagenorhynchus obliquidens*), and beluga whales (*Delphinapterus leucas*). In *PLoS One* 16 (8), e0250332. DOI: 10.1371/journal.pone.0250332.

Lauterburg, B. H.; Smith, C. V.; Hughes, H.; Mitchell, J. R. (1984): Biliary excretion of glutathione and glutathione disulfide in the rat. Regulation and response to oxidative stress. In *The Journal of Clinical Investigation* 73 (1), pp. 124–133. DOI: 10.1172/JCI111182.

Lavigne, David M. (2008): Harp Seal: *Pagophilus groenlandicus*. In J. G.M. Thewissen, William F. Perrin, Bernd Wursig (Eds.): Encyclopedia of marine mammals. 2. Aufl. s.l.: Elsevier professional, pp. 542–546. DOI: 10.1016/B978-0-12-373553-9.00127-9.

Law, Brittany A.; Liao, Xianghai; Moore, Kelsey S.; Southard, Abigail; Roddy, Patrick; Ji, Ruiping et al. (2018): Lipotoxic very-long-chain ceramides cause mitochondrial dysfunction, oxidative stress, and cell death in cardiomyocytes. In *The FASEB Journal* 32 (3), pp. 1403–1416. DOI: 10.1096/fj.201700300R.

Le Roux, V.; J.-L., Chapuis; Y., Frenot; P., Vernon (2002): Diet of the house mouse (*Mus musculus*) on Guillou Island, Kerguelen archipelago, Subantarctic. In *Polar Biology* 25 (1), pp. 49–57. DOI: 10.1007/s003000100310.

Leclerc, Estelle; Fritz, Günter; Weibel, Mirjam; Heizmann, Claus W.; Galichet, Arnaud (2007): S100B and S100A6 differentially modulate cell survival by interacting with distinct RAGE (receptor for advanced glycation end products) immunoglobulin domains. In *Journal of Biological Chemistry* 282 (43), pp. 31317–31331. DOI: 10.1074/jbc.M703951200.

Lee, H. J.; Hammond, D. N.; Large, T. H.; Roback, J. D.; Sim, J. A.; Da Brown et al. (1990): Neuronal properties and trophic activities of immortalized hippocampal cells from embryonic and young adult mice. In *The Journal of Neuroscience* 10 (6), pp. 1779–1787. DOI: 10.1523/JNEUROSCI.10-06-01779.1990.

Lee, Pearl; Chandel, Navdeep S.; Simon, M. Celeste (2020): Cellular adaptation to hypoxia through hypoxia inducible factors and beyond. In *Nature Reviews Molecular Cell Biology* 21 (5), pp. 268–283. DOI: 10.1038/s41580-020-0227-y.

Lehninger, Albert L. (1981): Biochemistry. The molecular basis of cell structure and function. 2. ed., 6. print. New York: Worth Publ.

Lenfant, C.; Elsner, R.; Kooyman, G. L.; Drabek, C. M. (1969): Respiratory function of blood of the adult and fetus Weddell seal *Leptonychotes weddelli*. In *The American Journal of Physiology* 216 (6), pp. 1595–1597. DOI: 10.1152/ajplegacy.1969.216.6.1595.

Lenfant, C.; Johansen, K.; Torrance, J. D. (1970): Gas transport and oxygen storage capacity in some pinnipeds and the sea otter. In *Respiration Physiology* 9 (2), pp. 277–286. DOI: 10.1016/0034-5687(70)90076-9.

Lenzi, Chiara; Ramazzina, Ileana; Russo, Isabella; Filippini, Alice; Bettuzzi, Saverio; Rizzi, Federica (2020): The down-regulation of clusterin expression enhances the αSynuclein aggregation process. In *International Journal of Molecular Sciences* 21 (19). DOI: 10.3390/ijms21197181.

Leskov, Konstantin S.; Klokov, Dmitry Y.; Li, Jing; Kinsella, Timothy J.; Boothman, David A. (2003): Synthesis and functional analyses of nuclear clusterin, a cell death protein. In *Journal of Biological Chemistry* 278 (13), pp. 11590–11600. DOI: 10.1074/jbc.M209233200.

Lestyk, Keri C.; Folkow, L. P.; Blix, A. S.; Hammill, M. O.; Burns, J. M. (2009): Development of myoglobin concentration and acid buffering capacity in harp (*Pagophilus groenlandicus*) and hooded (*Cystophora cristata*) seals from birth to maturity. In

Journal of Comparative Physiology B: Biochemical, Systemic, and Environmental Physiology 179 (8), pp. 985–996. DOI: 10.1007/s00360-009-0378-9.

Li, Chengliang; Xin, Hong; Shi, Yingpeng; Mu, Jianjun (2021): Glutaredoxin 2 protects cardiomyocytes from hypoxia/reoxygenation-induced injury by suppressing apoptosis, oxidative stress, and inflammation via enhancing Nrf2 signaling. In *International Immunopharmacology* 94, p. 107428. DOI: 10.1016/j.intimp.2021.107428.

Li, Yan; Lim, Seung; Hoffman, David; Aspenstrom, Pontus; Federoff, Howard J.; Rempe, David A. (2009): HUMMR, a hypoxia- and HIF-1alpha-inducible protein, alters mitochondrial distribution and transport. In *The Journal of Cell Biology* 185 (6), pp. 1065–1081. DOI: 10.1083/jcb.200811033.

Liang, Jianfeng; Chao, Dongman; Sandhu, Harleen K.; Yu, Yanbing; Zhang, Li; Balboni, Gianfranco et al. (2014): δ-opioid receptors up-regulate excitatory amino acid transporters in mouse astrocytes. In *British Journal of Pharmacology* 171 (23), pp. 5417–5430. DOI: 10.1111/bph.12857.

Liao, Wen-Ting; Liu, Jie; Zhou, Si-Min; Xu, Gang; Gao, Yu-Qi; Liu, Wen-Yuan (2018): UHPLC-QTOFMS-based metabolomic analysis of the hippocampus in hypoxia preconditioned mouse. In *Frontiers in Physiology* 9, p. 1950. DOI: 10.3389/fphys.2018.01950.

Libiseller, Gunnar; Dvorzak, Michaela; Kleb, Ulrike; Gander, Edgar; Eisenberg, Tobias; Madeo, Frank et al. (2015): IPO: a tool for automated optimization of XCMS parameters. In *BMC Bioinformatics* 16 (1), p. 118. DOI: 10.1186/s12859-015-0562-8.

Lin, Jing; Yang, Qingyuan; Wilder, Paul T.; Carrier, France; Weber, David J. (2010): The calcium-binding protein S100B down-regulates p53 and apoptosis in malignant melanoma. In *The Journal of Biological Chemistry* 285 (35), pp. 27487–27498. DOI: 10.1074/jbc.M110.155382.

Lin, Jing; Yang, Qingyuan; Yan, Zhe; Markowitz, Joseph; Wilder, Paul T.; Carrier, France; Weber, David J. (2004): Inhibiting S100B restores p53 levels in primary malignant melanoma cancer cells. In *Journal of Biological Chemistry* 279 (32), pp. 34071–34077. DOI: 10.1074/jbc.M405419200.

Lindeberg, H. (2008): Reproduction of the female ferret (*Mustela putorius furo*). In *Reproduction in Domestic Animals* 43 Suppl 2, pp. 150–156. DOI: 10.1111/j.1439-0531.2008.01155.x.

Lindholm, P.; Lundgren, C. E. G. (2006): Alveolar gas composition before and after maximal breath-holds in competitive divers. In *Undersea & Hyperbaric Medicine* 33 (6), pp. 463–467. PMID: 17274316.

Lindstrøm, Ulf; Nilssen, Kjell T.; Pettersen, Line M. S.; Haug, Tore (2013): Harp seal foraging behaviour during summer around Svalbard in the northern Barents Sea: diet composition and the selection of prey. In *Polar Biology* 36 (3), pp. 305–320. DOI: 10.1007/s00300-012-1260-x.

Liwanag, Heather E. M.; Berta, Annalisa; Costa, Daniel P.; Budge, Suzanne M.; Williams, Terrie M. (2012): Morphological and thermal properties of mammalian insulation: the evolutionary transition to blubber in pinnipeds. In *Biological Journal of the Linnean Society* 107 (4), pp. 774–787. DOI: 10.1111/j.1095-8312.2012.01992.x.

Lode, Thierry (1995): Activity pattern of polecats *Mustela putorius* L. in relation to food habits and prey activity. In *Ethology* 100 (4), pp. 295–308. DOI: 10.1111/j.1439-0310.1995.tb00334.x.

Lodygensky, Gregory A.; Inder, Terrie E.; Neil, Jeffrey J. (2008): Application of magnetic resonance imaging in animal models of perinatal hypoxic-ischemic cerebral injury. In *International Journal of Developmental Neuroscience* 26 (1), pp. 13–25. DOI: 10.1016/j.ijdevneu.2007.08.018.

Long, Ben; Jiang, Tao; Zhang, Jianmin; Chen, Siqi; Jia, Xueyan; Xu, Xiaofeng et al. (2020): Mapping the architecture of ferret brains at single-cell resolution. In *Frontiers in Neuroscience* 14, p. 322. DOI: 10.3389/fnins.2020.00322.

Loomba, Sahil; Straehle, Jakob; Gangadharan, Vijayan; Heike, Natalie; Khalifa, Abdelrahman; Motta, Alessandro et al. (2022): Connectomic comparison of mouse and human cortex. In *Science (New York, N.Y.)* 377 (6602), eabo0924. DOI: 10.1126/science.abo0924.

Lovell, M. A.; Xie, C.; Gabbita, S. P.; Markesbery, W. R. (2000): Decreased thioredoxin and increased thioredoxin reductase levels in Alzheimer's disease brain. In *Free Radical Biology and Medicine* 28 (3), pp. 418–427. DOI: 10.1016/S0891-5849(99)00258-0.

Lu, Jun; Holmgren, Arne (2014): The thioredoxin antioxidant system. In *Free Radical Biology and Medicine* 66, pp. 75–87. DOI: 10.1016/j.freeradbiomed.2013.07.036.

Lubos, Edith; Loscalzo, Joseph; Handy, Diane E. (2011): Glutathione peroxidase-1 in health and disease: from molecular mechanisms to therapeutic opportunities. In *Antioxidants & Redox Signaling* 15 (7), pp. 1957–1997. DOI: 10.1089/ars.2010.3586.

Lutz, P. L. (2002): The brain without oxygen. Causes of Failure-Physiological and Molecular Mechanisms for Survival. With assistance of G. E. Nilsson, H. M. Prentice. 3rd ed. Dordrecht: Springer Netherlands. DOI: 10.1007/0-306-48197-9.

Lutz, Peter L.; Nilsson, Göran E. (2004): Vertebrate brains at the pilot light. In *Respiratory Physiology & Neurobiology* 141 (3), pp. 285–296. DOI: 10.1016/j.resp.2004.03.013.

Lydersen, Christian; Kovacs, Kit M. (1993): Diving behaviour of lactating harp seal, *Phoca groenlandica*, females from the Gulf of St Lawrence, Canada. In *Animal Behaviour* 46 (6), pp. 1213–1221. DOI: 10.1006/anbe.1993.1312.

Ma, Z.; Chen, C.; Tang, P.; Zhang, H.; Yue, J.; Yu, Z. (2017): BNIP3 induces apoptosis and protective autophagy under hypoxia in esophageal squamous cell carcinoma cell lines: BNIP3 regulates cell death. In *Diseases of the Esophagus* 30 (9), pp. 1–8. DOI: 10.1093/dote/dox059.

Magistretti, Pierre J.; Allaman, Igor (2015): A cellular perspective on brain energy metabolism and functional imaging. In *Neuron* 86 (4), pp. 883–901. DOI: 10.1016/j.neuron.2015.03.035.

Mahmoud, Shaimaa; Gharagozloo, Marjan; Simard, Camille; Gris, Denis (2019): Astrocytes maintain glutamate homeostasis in the CNS by controlling the balance between glutamate uptake and release. In *Cells* 8 (2). DOI: 10.3390/cells8020184.

Mailloux, Ryan J.; Xuan, Jian Ying; McBride, Skye; Maharsy, Wael; Thorn, Stephanie; Holterman, Chet E. et al. (2014): Glutaredoxin-2 is required to control oxidative phosphorylation in cardiac muscle by mediating deglutathionylation reactions. In *Journal of Biological Chemistry* 289 (21), pp. 14812–14828. DOI: 10.1074/jbc.M114.550574.

Malesević, Miroslav; Poehlmann, Angela; Hernandez Alvarez, Birte; Diessner, André; Träger, Mario; Rahfeld, Jens-Ulrich et al. (2010): The protein-free IANUS peptide array uncovers interaction sites between *Escherichia coli* parvulin 10 and alkyl hydroperoxide reductase. In *Biochemistry* 49 (39), pp. 8626–8635. DOI: 10.1021/bi101015p.

Manger, Paul R.; Spocter, Muhammad A.; Patzke, Nina (2013): The evolutions of large brain size in mammals: the 'over-700-gram club quartet'. In *Brain, Behavior and Evolution* 82 (1), pp. 68–78. DOI: 10.1159/000352056.

Manier, Sascha K.; Keller, Andreas; Meyer, Markus R. (2019): Automated optimization of XCMS parameters for improved peak picking of liquid chromatography-mass spectrometry data using the coefficient of variation and parameter sweeping for untargeted metabolomics. In *Drug Testing and Analysis* 11 (6), pp. 752–761. DOI: 10.1002/dta.2552.

Martens, Gerrit A.; Folkow, Lars P.; Burmester, Thorsten; Geßner, Cornelia (2022a): Elevated antioxidant defence in the brain of deep-diving pinnipeds. In *Frontiers in Physiology* 13, Article 1064476. DOI: 10.3389/fphys.2022.1064476.

Martens, Gerrit A.; Geßner, Cornelia; Folkow, Lars P.; Creydt, Marina; Fischer, Markus; Burmester, Thorsten (2023): The roles of brain lipids and polar metabolites in the hypoxia tolerance of deep-diving pinnipeds. In *Journal of Experimental Biology*, Article jeb.245355. DOI: 10.1242/jeb.245355.

Martens, Gerrit A.; Geßner, Cornelia; Osterhof, Carina; Hankeln, Thomas; Burmester, Thorsten (2022b): Transcriptomes of clusterin- and S100B-transfected neuronal cells elucidate protective mechanisms against hypoxia and oxidative stress in the hooded seal (*Cystophora cristata*) brain. In *BMC Neuroscience* 23 (1), p. 59. DOI: 10.1186/s12868-022-00744-6.

Martinez-Hernandez, A.; Bell, K. P.; Norenberg, M. D. (1977): Glutamine synthetase: glial localization in brain. In *Science (New York, N.Y.)* 195 (4284), pp. 1356–1358. DOI: 10.1126/science.14400.

Mass, Alla M.; Supin, A. Y. (2003): Retinal topography of the harp seal *Pagophilus groenlandicus*. In *Brain, Behavior and Evolution* 62 (4), pp. 212–222. DOI: 10.1159/000073273.

Materia, Stephanie; Cater, Michael A.; Klomp, Leo W. J.; Mercer, Julian F. B.; La Fontaine, Sharon (2012): Clusterin and COMMD1 independently regulate degradation of the mammalian copper ATPases ATP7A and ATP7B. In *The Journal of Biological Chemistry* 287 (4), pp. 2485–2499. DOI: 10.1074/jbc.M111.302216.

Mazzaro, Lisa M.; Lawrence Dunn, J.; Furr, Harold C.; Clark, Richard M. (2003): Serum Retinol, alpha-tocopherol, and lipids in four species of adult captive pinnipeds. In *Zoo Biology* 22 (1), pp. 83–96. DOI: 10.1002/zoo.10075.

McClelland, Grant B.; Scott, Graham R. (2019): Evolved mechanisms of aerobic performance and hypoxia resistance in high-altitude natives. In *Annual Review of Physiology* 81, pp. 561–583. DOI: 10.1146/annurev-physiol-021317-121527.

McCord, Joe M.; Fridovich, Irwin (1969): Superoxide dismutase: an enzymic function for erythrocuprein (hemocuprein). In *Journal of Biological Chemistry* 244 (22), pp. 6049–6055. DOI: 10.1016/S0021-9258(18)63504-5.

McDonald, Birgitte I.; Ponganis, Paul J. (2013): Insights from venous oxygen profiles: oxygen utilization and management in diving California sea lions. In *The Journal of Experimental Biology* 216 (Pt 17), pp. 3332–3341. DOI: 10.1242/jeb.085985.

McGowen, Michael R.; Grossman, Lawrence I.; Wildman, Derek E. (2012): Dolphin genome provides evidence for adaptive evolution of nervous system genes and a molecular rate slowdown. In *Proceedings: Biological Sciences* 279 (1743), pp. 3643–3651. DOI: 10.1098/rspb.2012.0869.

Meir, Jessica U.; Champagne, Cory D.; Costa, Daniel P.; Williams, Cassondra L.; Ponganis, Paul J. (2009): Extreme hypoxemic tolerance and blood oxygen depletion in diving elephant seals. In *American Journal of Physiology: Regulatory, Integrative and Comparative Physiology* 297 (4), R927-39. DOI: 10.1152/ajpregu.00247.2009.

Meir, Jessica U.; Robinson, Patrick W.; Vilchis, L. Ignacio; Kooyman, Gerald L.; Costa, Daniel P.; Ponganis, Paul J. (2013): Blood oxygen depletion is independent of dive function in a deep diving vertebrate, the northern elephant seal. In *PLoS One* 8 (12), e83248. DOI: 10.1371/journal.pone.0083248.

Meister, A. (1983): Selective modification of glutathione metabolism. In *Science (New York, N.Y.)* 220 (4596), pp. 472–477. DOI: 10.1126/science.6836290.

Meldrum, B. S. (2000): Glutamate as a neurotransmitter in the brain: review of physiology and pathology. In *The Journal of Nutrition* 130 (4S Suppl), 1007S-15S. DOI: 10.1093/jn/130.4.1007S.

Mello, Daniela M. D.; Melo, Fabiana A.; Silva, Vera M. F. (2021): Reference values for serum chemistry of wild Amazon river dolphins (*Inia geoffrensis*) from the central Amazon. In *Marine Mammal Science* 37 (2), pp. 561–576. DOI: 10.1111/mms.12765.

Meyer, Axel; Schloissnig, Siegfried; Franchini, Paolo; Du, Kang; Woltering, Joost M.; Irisarri, Iker et al. (2021): Giant lungfish genome elucidates the conquest of land by vertebrates. In *Nature* 590 (7845), pp. 284–289. DOI: 10.1038/s41586-021-03198-8.

Mi, Huaiyu; Ebert, Dustin; Muruganujan, Anushya; Mills, Caitlin; Albou, Laurent-Philippe; Mushayamaha, Tremayne; Thomas, Paul D. (2021): PANTHER version 16: a revised family classification, tree-based classification tool, enhancer regions and extensive API. In *Nucleic Acids Research* 49 (D1), D394-D403. DOI: 10.1093/nar/gkaa1106.

Michetti, Fabrizio; D'Ambrosi, Nadia; Toesca, Amelia; Puglisi, Maria Ausiliatrice; Serrano, Alessia; Marchese, Elisa et al. (2019): The S100B story: from biomarker to active factor in neural injury. In *Journal of Neurochemistry* 148 (2), pp. 168–187. DOI: 10.1111/jnc.14574.

Michetti, Fabrizio; Di Sante, Gabriele; Clementi, Maria Elisabetta; Sampaolese, Beatrice; Casalbore, Patrizia; Volonté, Cinzia et al. (2021): Growing role of S100B protein as a putative therapeutic target for neurological- and nonneurological-disorders. In *Neuroscience and Biobehavioral Reviews* 127, pp. 446–458. DOI: 10.1016/j.neubiorev.2021.04.035.

Milkovic, Lidija; Cipak Gasparovic, Ana; Cindric, Marina; Mouthuy, Pierre-Alexis; Zarkovic, Neven (2019): Short overview of ROS as cell function regulators and their implications in therapy concepts. In *Cells* 8 (8). DOI: 10.3390/cells8080793.

Miller, Edward H.; Jones, Ian L.; Stenson, Garry B. (1999): Baculum and testes of the hooded seal (*Cystophora cristata*): growth and size-scaling and their relationships to sexual selection. In *Canadian Journal of Zoology* 77 (3), pp. 470–479. DOI: 10.1139/z98-233.

Mills, James D.; Bailes, Julian E.; Sedney, Cara L.; Hutchins, Heather; Sears, Barry (2011): Omega-3 fatty acid supplementation and reduction of traumatic axonal injury in a rodent head injury model. In *Journal of Neurosurgery* 114 (1), pp. 77–84. DOI: 10.3171/2010.5.JNS08914.

Mirceta, Scott; Signore, Anthony V.; Burns, Jennifer M.; Cossins, Andrew R.; Campbell, Kevin L.; Berenbrink, Michael (2013): Evolution of mammalian diving capacity traced by myoglobin net surface charge. In *Science (New York, N.Y.)* 340 (6138), p. 1234192. DOI: 10.1126/science.1234192.

Mitchell, Mark A.; Tully, Thomas N. (Eds.) (2006): Manual of exotic pet practice. St. Louis, Mo.: Saunders Elsevier. DOI: 10.1016/B978-1-4160-0119-5.X5001-X.

Mitz, S. A.; Reuss, S.; Folkow, L. P.; Blix, A. S.; Ramirez, J-M; Hankeln, T.; Burmester, T. (2009): When the brain goes diving: glial oxidative metabolism may confer hypoxia tolerance to the seal brain. In *Neuroscience* 163 (2), pp. 552–560. DOI: 10.1016/j.neuroscience.2009.06.058.

Mohamed, Ahmed; Molendijk, Jeffrey (2022): lipidr: data mining and analysis of lipidomics datasets. Available online at https://github.com/ahmohamed/lipidr.

Monteiro, João P.; Maciel, Elisabete; Maia, Rita; Pereira, Andreia T.; Calado, Ricardo; Domingues, Pedro et al. (2021a): Characterization of the cardiac phospholipidome of small cetaceans provides adaptational insight and a foundation for indirect population health screening. In *Marine Mammal Science* 37 (4), pp. 1406–1427. DOI: 10.1111/mms.12823.

Monteiro, João P.; Maciel, Elisabete; Melo, Tânia; Flanagan, Carla; Urbani, Nuno; Neves, João; Domingues, Maria Rosário (2021b): The plasma phospholipidome of *Tursiops truncatus*: From physiological insight to the design of prospective tools for managed cetacean monitorization. In *Lipids* 56 (5), pp. 461–473. DOI: 10.1002/lipd.12307.

Monteith, Andrew J.; Miller, Jeanette M.; Maxwell, C. Noel; Chazin, Walter J.; Skaar, Eric P. (2021): Neutrophil extracellular traps enhance macrophage killing of bacterial pathogens. In *Science Advances* 7 (37), eabj2101. DOI: 10.1126/sciadv.abj2101.

Muñoz-Sánchez, Jorge; Chánez-Cárdenas, María Elena (2014): A review on hemeoxygenase-2: focus on cellular protection and oxygen response. In *Oxidative Medicine and Cellular Longevity* 2014, p. 604981. DOI: 10.1155/2014/604981.

Murphy, B. J.; Hochachka, P. W. (1981): Free amino acid profiles in blood during diving and recovery in the Antarctic Weddell seal. In *Canadian Journal of Zoology* 59 (3), pp. 455–459. DOI: 10.1139/z81-066.

Murphy, Michael P. (2009): How mitochondria produce reactive oxygen species. In *The Biochemical Journal* 417 (1), pp. 1–13. DOI: 10.1042/BJ20081386.

Murrell, Ben; Weaver, Steven; Smith, Martin D.; Wertheim, Joel O.; Murrell, Sasha; Aylward, Anthony et al. (2015): Gene-wide identification of episodic selection. In *Molecular Biology and Evolution* 32 (5), pp. 1365–1371. DOI: 10.1093/molbev/msv035.

Nabi, Ghulam; Robeck, Todd R.; Hao, Yujiang; Wang, Ding (2019): Hematologic and biochemical reference interval development and the effect of age, sex, season, and location on hematologic analyte concentrations in critically endangered Yangtze finless porpoise (*Neophocaena asiaeorientalis ssp. asiaeorientalis*). In *Frontiers in Physiology* 10, p. 792. DOI: 10.3389/fphys.2019.00792.

Nehlig, Astrid (2004): Brain uptake and metabolism of ketone bodies in animal models. In *Prostaglandins, Leukotrienes and Essential Fatty Acids* 70 (3), pp. 265–275. DOI: 10.1016/j.plefa.2003.07.006.

Ng, Carey J.; Hama, Susan Y.; Bourquard, Noam; Navab, Mohamad; Reddy, Srinivasa T. (2006): Adenovirus mediated expression of human paraoxonase 2 protects against the development of atherosclerosis in apolipoprotein E-deficient mice. In *Molecular Genetics and Metabolism* 89 (4), pp. 368–373. DOI: 10.1016/j.ymgme.2006.07.004.

Ng, Si Yun; Lee, Alan Yiu Wah (2019): Traumatic brain injuries: pathophysiology and potential therapeutic targets. In *Frontiers in Cellular Neuroscience* 13, p. 528. DOI: 10.3389/fncel.2019.00528.

Nguyen, Vu Chau; Deck, Courtney A.; Pamenter, Matthew E. (2019): Naked mole-rats reduce the expression of ATP-dependent but not ATP-independent heat shock proteins in acute hypoxia. In *The Journal of Experimental Biology* 222 (Pt 22). DOI: 10.1242/jeb.211243.

Nikolakopoulou, Angeliki M.; Montagne, Axel; Kisler, Kassandra; Dai, Zhonghua; Wang, Yaoming; Huuskonen, Mikko T. et al. (2019): Pericyte loss leads to circulatory failure and pleiotrophin depletion causing neuron loss. In *Nature Neuroscience* 22 (7), pp. 1089–1098. DOI: 10.1038/s41593-019-0434-z.

Nilsson, Göran E.; Lutz, Peter L.; Jackson, Thomas L. (1991): Neurotransmitters and anoxic survival of the brain: a comparison of anoxia-tolerant and anoxia-intolerant vertebrates. In *Physiological Zoology* 64 (3), pp. 638–652. DOI: 10.1086/physzool.64.3.30158198.

Noah, James W.; Severson, William; Noah, Diana L.; Rasmussen, Lynn; White, E. Lucile; Jonsson, Colleen B. (2007): A cell-based luminescence assay is effective for high-throughput screening of potential influenza antivirals. In *Antiviral Research* 73 (1), pp. 50–59. DOI: 10.1016/j.antiviral.2006.07.006.

Noh, Hyun Ji; Turner-Maier, Jason; Schulberg, S. Anne; Fitzgerald, Michael L.; Johnson, Jeremy; Allen, Kaitlin N. et al. (2022): The Antarctic Weddell seal genome reveals evidence of selection on cardiovascular phenotype and lipid handling. In *Communications Biology* 5 (1), p. 140. DOI: 10.1038/s42003-022-03089-2.

Nollens, Hendrik H.; Haney, Nylah J.; Stacy, Nicole I.; Robeck, Todd R. (2020): Effects of sex, age, and season on the variation of blood analytes in a clinically healthy ex situ population of bottlenose dolphins (*Tursiops spp.*). In *The Veterinary Quarterly* 40 (1), pp. 342–352. DOI: 10.1080/01652176.2020.1845415.

Nollens, Hendrik H.; Robeck, Todd R.; Schmitt, Todd L.; Croft, Lara L.; Osborn, Steve; McBain, James F. (2019): Effect of age, sex, and season on the variation in blood analytes of a clinically normal ex situ population of killer whales (*Orcinus orca*). In *Veterinary Clinical Pathology* 48 (1), pp. 100–113. DOI: 10.1111/vcp.12697.

Nordøy, Erling S.; Aakvaag, Asbjørn; Larsen, Terje S. (1993): Metabolic adaptations to fasting in harp seal pups. In *Physiological Zoology* 66 (6), pp. 926–945. DOI: 10.1086/physzool.66.6.30163747.

Noren, S. R.; Williams, T. M. (2000): Body size and skeletal muscle myoglobin of cetaceans: adaptations for maximizing dive duration. In *Comparative Biochemistry and Physiology Part A: Molecular & Integrative Physiology* 126 (2), pp. 181–191. DOI: 10.1016/s1095-6433(00)00182-3.

Noren, Shawn R. (2020): Postnatal development of diving physiology: implications of anthropogenic disturbance for immature marine mammals. In *The Journal of Experimental Biology* 223 (Pt 17). DOI: 10.1242/jeb.227736.

Norman, Stephanie A.; Beckett, Laurel A.; Miller, Woutrina A.; St Leger, Judy; Hobbs, Roderick C. (2013): Variation in hematologic and serum biochemical values of belugas (*Delphinapterus leucas*) under managed care. In *Journal of Zoo and Wildlife Medicine* 44 (2), pp. 376–388. DOI: 10.1638/2012-0172R.

Novgorodov, Sergei A.; Voltin, Joshua R.; Gooz, Monika A.; Li, Li; Lemasters, John J.; Gudz, Tatyana I. (2018): Acid sphingomyelinase promotes mitochondrial dysfunction due to glutamate-induced regulated necrosis. In *Journal of Lipid Research* 59 (2), pp. 312–329. DOI: 10.1194/jlr.M080374.

Novgorodov, Sergei A.; Voltin, Joshua R.; Wang, Wenxue; Tomlinson, Stephen; Riley, Christopher L.; Gudz, Tatyana I. (2019): Acid sphingomyelinase deficiency protects mitochondria and improves function recovery after brain injury. In *Journal of Lipid Research* 60 (3), pp. 609–623. DOI: 10.1194/jlr.M091132.

O'Sullivan, Timothy E.; Johnson, Lexus R.; Kang, Helen H.; Sun, Joseph C. (2015): BNIP3-and BNIP3L-mediated mitophagy promotes the generation of natural killer cell memory. In *Immunity* 43 (2), pp. 331–342. DOI: 10.1016/j.immuni.2015.07.012.

O'Brien, John S.; Sampson, E. Lois (1965): Lipid composition of the normal human brain: gray matter, white matter, and myelin. In *Journal of Lipid Research* 6 (4), pp. 537–544. DOI: 10.1016/S0022-2275(20)39619-X.

Odden, A.; Folkow, L. P.; Caputa, M.; Hotvedt, R.; Blix, A. S. (1999): Brain cooling in diving seals. In *Acta Physiologica Scandinavica* 166 (1), pp. 77–78. DOI: 10.1046/j.1365-201x.1999.00536.x.

Oftedal, O. T.; Bowen, W. D.; Widdowson, E. M.; Boness, D. J. (1989): Effects of suckling and the postsuckling fast on weights of the body and internal organs of harp and hooded seal pups. In *Biology of the Neonate* 56 (5), pp. 283–300. DOI: 10.1159/000243136.

Ojo, Joseph O.; Algamal, Moustafa; Leary, Paige; Abdullah, Laila; Mouzon, Benoit; Evans, James E. et al. (2019): Converging and differential brain phospholipid dysregulation in the pathogenesis of repetitive mild traumatic brain injury and Alzheimer's disease. In *Frontiers in Neuroscience* 13, p. 103. DOI: 10.3389/fnins.2019.00103.

Oltedal, Leif; Haglerød, Camilla; Furmanek, Tomasz; Davanger, Svend (2008): Vesicular release of glutamate from hippocampal neurons in culture: an immunocytochemical assay. In *Experimental Brain Research* 184 (4), pp. 479–492. DOI: 10.1007/s00221-007-1118-6.

Padilla, C. A.; Martínez-Galisteo, E.; López-Barea, J.; Holmgren, A.; Bárcena, J. A. (1992): Immunolocalization of thioredoxin and glutaredoxin in mammalian hypophysis. In *Molecular and Cellular Endocrinology* 85 (1-2), pp. 1–12. DOI: 10.1016/0303-7207(92)90119-Q.

Pamenter, Matthew E. (2022): Adaptations to a hypoxic lifestyle in naked mole-rats. In *The Journal of Experimental Biology* 225 (4). DOI: 10.1242/jeb.196725.

Pang, Zhiqiang; Chong, Jasmine; Zhou, Guangyan; Lima Morais, David Anderson de; Le Chang; Barrette, Michel et al. (2021): MetaboAnalyst 5.0: narrowing the gap between raw spectra and functional insights. In *Nucleic Acids Research* 49 (W1), W388-W396. DOI: 10.1093/nar/gkab382.

Papandreou, I.; Cairns, R. A.; Fontana, L.; Lim, A. L.; Denko, N. C. (2006): HIF-1 mediates adaptation to hypoxia by actively downregulating mitochondrial oxygen consumption. In *Cell Metabolism* 3 (3), pp. 187–197. DOI: 10.1016/j.cmet.2006.01.012.

Parra, Valentina; Eisner, Veronica; Chiong, Mario; Criollo, Alfredo; Moraga, Francisco; Garcia, Alejandra et al. (2008): Changes in mitochondrial dynamics during ceramide-induced cardiomyocyte early apoptosis. In *Cardiovascular Research* 77 (2), pp. 387–397. DOI: 10.1093/cvr/cvm029.

Patrician, Alexander; Dujić, Željko; Spajić, Boris; Drviš, Ivan; Ainslie, Philip N. (2021): Breath-hold diving – the physiology of diving deep and returning. In *Frontiers in Physiology* 12, Article 639377, p. 582. DOI: 10.3389/fphys.2021.639377.

Pellerin, L.; Magistretti, P. J. (1994): Glutamate uptake into astrocytes stimulates aerobic glycolysis: a mechanism coupling neuronal activity to glucose utilization. In *Proceedings of the National Academy of Sciences of the United States of America* 91 (22), pp. 10625–10629. DOI: 10.1073/pnas.91.22.10625.

Pelletier, Joffrey; Bellot, Grégory; Gounon, Pierre; Lacas-Gervais, Sandra; Pouysségur, Jacques; Mazure, Nathalie M. (2012): Glycogen synthesis is induced in hypoxia by the hypoxia-inducible factor and promotes cancer cell survival. In *Frontiers in Oncology* 2, p. 18. DOI: 10.3389/fonc.2012.00018.

Penso-Dolfin, Luca; Haerty, Wilfried; Hindle, Allyson; Di Palma, Federica (2020): microRNA profiling in the Weddell seal suggests novel regulatory mechanisms contributing to diving adaptation. In *BMC Genomics* 21 (1), p. 303. DOI: 10.1186/s12864-020-6675-0.

Pérez, Viviana I.; Buffenstein, Rochelle; Masamsetti, Venkata; Leonard, Shanique; Salmon, Adam B.; Mele, James et al. (2009): Protein stability and resistance to oxidative stress are determinants of longevity in the longest-living rodent, the naked mole-rat. In *Proceedings of the National Academy of Sciences* 106 (9), pp. 3059–3064. DOI: 10.1073/pnas.0809620106.

Perrin, William F.; Wursig, Bernd; Thewissen, J. G.M. (2009): Encyclopedia of marine mammals. 2. ed. Edited by William F. Perrin. Amsterdam: Academic Press. DOI: 10.1016/C2015-0-00820-6.

Pickles, Sarah; Vigié, Pierre; Youle, Richard J. (2018): Mitophagy and quality control mechanisms in mitochondrial maintenance. In *Current Biology: CB* 28 (4), R170-R185. DOI: 10.1016/j.cub.2018.01.004.

Piomelli, Daniele; Astarita, Giuseppe; Rapaka, Rao (2007): A neuroscientist's guide to lipidomics. In *Nature Reviews Neuroscience* 8 (10), pp. 743–754. DOI: 10.1038/nrn2233.

Piotrowski, Elizabeth R.; Tift, Michael S.; Crocker, Daniel E.; Pearson, Anna B.; Vázquez-Medina, José P.; Keith, Anna D.; Khudyakov, Jane I. (2021): Ontogeny of carbon monoxide-related gene expression in a deep-diving marine mammal. In *Frontiers in Physiology* 12, p. 762102. DOI: 10.3389/fphys.2021.762102.

Pond, Sergei L. Kosakovsky; Frost, Simon D. W. (2005): Datamonkey: rapid detection of selective pressure on individual sites of codon alignments. In *Bioinformatics (Oxford, England)* 21 (10), pp. 2531–2533. DOI: 10.1093/bioinformatics/bti320.

Ponganis, Paul J. (2011): Diving mammals. In *Comprehensive Physiology* 1 (1), pp. 447–465. DOI: 10.1002/cphy.c091003.

Ponganis, Paul J. (2015): Diving physiology of marine mammals and seabirds. Cambridge: Cambridge University Press. DOI: 10.1017/CBO9781139045490.

Ponganis, Paul J. (2019): State of the art review: from the seaside to the bedside: insights from comparative diving physiology into respiratory, sleep and critical care. In *Thorax* 74 (5), pp. 512–518. DOI: 10.1136/thoraxjnl-2018-212136.

Prando, Silvana; Carneiro, Camila de Godoi; Otsuki, Denise Aya; Sapienza, Marcelo Tatit (2019): Effects of ketamine/xylazine and isoflurane on rat brain glucose metabolism measured by 18 F-fluorodeoxyglucose-positron emission tomography. In *The European Journal of Neuroscience* 49 (1), pp. 51–61. DOI: 10.1111/ejn.14252.

Prochnow, Hans; Gollan, Rene; Rohne, Philipp; Hassemer, Matthias; Koch-Brandt, Claudia; Baiersdörfer, Markus (2013): Non-secreted clusterin isoforms are translated in rare amounts from distinct human mRNA variants and do not affect Bax-mediated apoptosis or the NF-κB signaling pathway. In *PLoS One* 8 (9), e75303. DOI: 10.1371/journal.pone.0075303.

Qvist, J.; Hill, R. D.; Schneider, R. C.; Falke, K. J.; Liggins, G. C.; Guppy, M. et al. (1986): Hemoglobin concentrations and blood gas tensions of free-diving Weddell seals. In *Journal of Applied Physiology (Bethesda, Md. : 1985)* 61 (4), pp. 1560–1569. DOI: 10.1152/jappl.1986.61.4.1560.

R Core Team (2021): R: a language and environment for statistical computing. R Foundation for Statistical Computing, Vienna, Austria. Available online at https://www.R-project.org/.

Raju, Chandrasekhar S.; Spatazza, Julien; Stanco, Amelia; Larimer, Phillip; Sorrells, Shawn F.; Kelley, Kevin W. et al. (2018): Secretagogin is expressed by developing neocortical GABAergic neurons in humans but not mice and increases neurite arbor size and complexity. In *Cerebral Cortex (New York, N.Y. : 1991)* 28 (6), pp. 1946–1958. DOI: 10.1093/cercor/bhx101.

Ramirez, Jan-Marino; Folkow, Lars P.; Blix, Arnoldus S. (2007): Hypoxia tolerance in mammals and birds: from the wilderness to the clinic. In *Annual Review of Physiology* 69, pp. 113–143. DOI: 10.1146/annurev.physiol.69.031905.163111.

Ramirez, J-M; Folkow, L. P.; Ludvigsen, S.; Ramirez, P. N.; Blix, A. S. (2011): Slow intrinsic oscillations in thick neocortical slices of hypoxia tolerant deep diving seals. In *Neuroscience* 177, pp. 35–42. DOI: 10.1016/j.neuroscience.2010.12.032.

Raththagala, Madushi; Brewer, M. Kathryn; Parker, Matthew W.; Sherwood, Amanda R.; Wong, Brian K.; Hsu, Simon et al. (2015): Structural mechanism of laforin function in glycogen dephosphorylation and lafora disease. In *Molecular Cell* 57 (2), pp. 261–272. DOI: 10.1016/j.molcel.2014.11.020.

Ray, Paul D.; Huang, Bo-Wen; Tsuji, Yoshiaki (2012): Reactive oxygen species (ROS) homeostasis and redox regulation in cellular signaling. In *Cellular Signalling* 24 (5), pp. 981–990. DOI: 10.1016/j.cellsig.2012.01.008.

Renelt, Maria; Bohlen und Halbach, Viola von; Bohlen und Halbach, Oliver von (2014): Distribution of PCP4 protein in the forebrain of adult mice. In *Acta Histochemica* 116 (6), pp. 1056–1061. DOI: 10.1016/j.acthis.2014.04.012.

Rey, Felisa; Melo, Tânia; Lopes, Diana; Couto, Daniela; Marques, Francisca; Domingues, M. Rosário (2022): Applications of lipidomics in marine organisms: progress, challenges and future perspectives. In *Molecular Omics* 18 (5), pp. 357–386. DOI: 10.1039/D2MO00012A.

Richmond, T. S. (1997): Cerebral resuscitation after global brain ischemia: linking research to practice. In *AACN Clinical Issues* 8 (2), pp. 171–181. DOI: 10.1097/00044067-199705000-00002.

Rickmann, M.; Wolff, J. R. (1995): S100 protein expression in subpopulations of neurons of rat brain. In *Neuroscience* 67 (4), pp. 977–991. DOI: 10.1016/0306-4522(94)00615-C.

Righetti, B. P. H.; Simões-Lopes, P. C.; Uhart, M. M.; Wilhelm Filho, D. (2014): Relating diving behavior and antioxidant status: Insights from oxidative stress biomarkers in the blood of two distinct divers, *Mirounga leonina* and *Arctocephalus australis*. In *Comparative Biochemistry and Physiology Part A: Molecular & Integrative Physiology* 173C, pp. 1–6. DOI: 10.1016/j.cbpa.2014.02.017.

Robergs, Robert A.; McNulty, Craig R.; Minett, Geoffrey M.; Holland, Justin; Trajano, Gabriel (2018): Lactate, not lactic acid, is produced by cellular cytosolic energy catabolism. In *Physiology (Bethesda, Md.)* 33 (1), pp. 10–12. DOI: 10.1152/physiol.00033.2017.

Roboon, Jureepon; Hattori, Tsuyoshi; Nguyen, Dinh Thi; Ishii, Hiroshi; Takarada-Iemata, Mika; Kannon, Takayuki et al. (2022): Isolation of ferret astrocytes reveals their morphological, transcriptional, and functional differences from mouse astrocytes. In *Frontiers in Cellular Neuroscience* 16, p. 877131. DOI: 10.3389/fncel.2022.877131.

Rodríguez-Rivera, Carmen; Garcia, Miguel M.; Molina-Álvarez, Miguel; González-Martín, Carmen; Goicoechea, Carlos (2021): Clusterin: always protecting. Synthesis, function and potential issues. In *Biomedicine & Pharmacotherapy = Biomedecine & Pharmacotherapie* 134, p. 111174. DOI: 10.1016/j.biopha.2020.111174.

Rogatzki, Matthew J.; Ferguson, Brian S.; Goodwin, Matthew L.; Gladden, L. Bruce (2015): Lactate is always the end product of glycolysis. In *Frontiers in Neuroscience* 9, p. 22. DOI: 10.3389/fnins.2015.00022.

Ruiz-Hernández, Ixchel M.; Nouri, Mohammad-Zaman; Kozuch, Marianne; Denslow, Nancy D.; Díaz-Gamboa, Raúl E.; Rodríguez-Canul, Rossanna; Collí-Dulá, Reyna C. (2022): Trace element and lipidomic analysis of bottlenose dolphin blubber from the Yucatan coast: lipid composition relationships. In *Chemosphere* 299, p. 134353. DOI: 10.1016/j.chemosphere.2022.134353.

Russ, A. P.; Wattler, S.; Colledge, W. H.; Aparicio, S. A.; Carlton, M. B.; Pearce, J. J. et al. (2000): Eomesodermin is required for mouse trophoblast development and mesoderm formation. In *Nature* 404 (6773), pp. 95–99. DOI: 10.1038/35003601.

Ryckman, Carle; Vandal, Karen; Rouleau, Pascal; Talbot, Mariève; Tessier, Philippe A. (2003): Proinflammatory activities of S100: proteins S100A8, S100A9, and S100A8/A9 induce neutrophil chemotaxis and adhesion. In *Journal of Immunology (Baltimore, Md. : 1950)* 170 (6), pp. 3233–3242. DOI: 10.4049/jimmunol.170.6.3233.

Saez, Isabel; Duran, Jordi; Sinadinos, Christopher; Beltran, Antoni; Yanes, Oscar; Tevy, María F. et al. (2014): Neurons have an active glycogen metabolism that contributes to tolerance to hypoxia. In *Journal of Cerebral Blood Flow and Metabolism* 34 (6), pp. 945–955. DOI: 10.1038/jcbfm.2014.33.

Saha, Sarmistha; Buttari, Brigitta; Panieri, Emiliano; Profumo, Elisabetta; Saso, Luciano (2020): An overview of Nrf2 signaling pathway and its role in inflammation. In *Molecules (Basel, Switzerland)* 25 (22). DOI: 10.3390/molecules25225474.

Sainsbury, Katherine A.; Shore, Richard F.; Schofield, Henry; Croose, Elizabeth; Hantke, Georg; Kitchener, Andrew C.; McDonald, Robbie A. (2020): Diets of European polecat *Mustela putorius* in Great Britain during fifty years of population recovery. In *Mammal Research* 65 (2), pp. 181–190. DOI: 10.1007/s13364-020-00484-0.

Satapathy, Sandeep; Wilson, Mark R. (2021): The dual roles of clusterin in extracellular and intracellular proteostasis. In *Trends in Biochemical Sciences* 46 (8), pp. 652–660. DOI: 10.1016/j.tibs.2021.01.005.

Sawada, Kazuhiko; Watanabe, Misaki (2012): Development of cerebral sulci and gyri in ferrets (*Mustela putorius*). In *Congenital Anomalies* 52 (3), pp. 168–175. DOI: 10.1111/j.1741-4520.2012.00372.x.

Sawyer, Eva K.; Turner, Emily C.; Kaas, Jon H. (2016): Somatosensory brainstem, thalamus, and cortex of the California sea lion (*Zalophus californianus*). In *The Journal of Comparative Neurology* 524 (9), pp. 1957–1975. DOI: 10.1002/cne.23984.

Schlegel, R. A.; Williamson, P. (2001): Phosphatidylserine, a death knell. In *Cell Death and Differentiation* 8 (6), pp. 551–563. DOI: 10.1038/sj.cdd.4400817.

Schmahmann, Jeremy D.; Guell, Xavier; Stoodley, Catherine J.; Halko, Mark A. (2019): The theory and neuroscience of cerebellar cognition. In *Annual Review of Neuroscience* 42, pp. 337–364. DOI: 10.1146/annurev-neuro-070918-050258.

Schneider, Nora; Hauser, Jonas; Oliveira, Manuel; Cazaubon, Elise; Mottaz, Sara Colombo; O'Neill, Barry V. et al. (2019): Sphingomyelin in brain and cognitive development: preliminary data. In *eNeuro* 6 (4). DOI: 10.1523/ENEURO.0421-18.2019.

Schneuer, M.; Flachsbarth, S.; Czech-Damal, N. U.; Folkow, L. P.; Siebert, U.; Burmester, T. (2012): Neuroglobin of seals and whales: evidence for a divergent role in the diving brain. In *Neuroscience* 223, pp. 35–44. DOI: 10.1016/j.neuroscience.2012.07.052.

Scholander, P.F. (1940): Experimental investigations on the respiratory function in diving mammals and birds. Oslo: Hvalradets Skrifter, Scientific Results of Marine Biological Research.

Schousboe, Arne (1981): Transport and metabolism of glutamate and GABA in neurons and glial cells. In *International Review of Neurobiology* 22, pp. 1–45. DOI: 10.1016/S0074-7742(08)60289-5.

Schousboe, Arne; Waagepetersen, Helle S.; Sonnewald, Ursula (2019): Astrocytic pyruvate carboxylation: status after 35 years. In *Journal of Neuroscience Research* 97 (8), pp. 890–896. DOI: 10.1002/jnr.24402.

Schwerin, Susan C.; Hutchinson, Elizabeth B.; Radomski, Kryslaine L.; Ngalula, Kapinga P.; Pierpaoli, Carlo M.; Juliano, Sharon L. (2017): Establishing the ferret as a gyrencephalic animal model of traumatic brain injury: optimization of controlled cortical impact procedures. In *Journal of Neuroscience Methods* 285, pp. 82–96. DOI: 10.1016/j.jneumeth.2017.05.010.

Sentelle, R. David; Senkal, Can E.; Jiang, Wenhui; Ponnusamy, Suriyan; Gencer, Salih; Selvam, Shanmugam Panneer et al. (2012): Ceramide targets autophagosomes to mitochondria and induces lethal mitophagy. In *Nature Chemical Biology* 8 (10), pp. 831–838. DOI: 10.1038/nchembio.1059.

Sergeant, D. E. (1966): Reproductive rates of harp seals, *Pagophilus groenlandicus* (Erxleben). In *Journal of the Fisheries Research Board of Canada* 23 (5), pp. 757–766. DOI: 10.1139/f66-066.

Shamim, Arshiya; Mahmood, Tarique; Ahsan, Farogh; Kumar, Arun; Bagga, Paramdeep (2018): Lipids: an insight into the neurodegenerative disorders. In *Clinical Nutrition Experimental* 20, pp. 1–19. DOI: 10.1016/j.yclnex.2018.05.001.

Sheldon, R. A.; Sedik, C.; Ferriero, D. M. (1998): Strain-related brain injury in neonatal mice subjected to hypoxia-ischemia. In *Brain Research* 810 (1-2), pp. 114–122. DOI: 10.1016/s0006-8993(98)00892-0.

Sheng, Shiying; Huang, Jingzhong; Ren, Yi; Zhi, Feng; Tian, Xuansong; Wen, Guoqiang et al. (2018): Neuroprotection against hypoxic/ischemic injury: δ-opioid receptors and BDNF-TrkB pathway. In *Cellular Physiology and Biochemistry* 47 (1), pp. 302–315. DOI: 10.1159/000489808.

Sherratt, Philip J.; Hayes, John D. (2001): Glutathione S-transferases. In Costas Ioannides (Ed.): Enzyme systems that metabolise drugs and other xenobiotics. 1st ed. Chichester: John Wiley Sons Ltd (Current toxicology series), pp. 319–352. DOI: 10.1002/0470846305.ch9.

Sheu, F. S.; Azmitia, E. C.; Marshak, D. R.; Parker, P. J.; Routtenberg, A. (1994): Glial-derived S100B protein selectively inhibits recombinant beta-protein kinase-C (PKC) phosphorylation of neuron-specific protein F1/GAP43. In *Molecular Brain Research* 21 (1-2), pp. 62–66. DOI: 10.1016/0169-328X(94)90378-6.

Shimizu, S.; Narita, M.; Tsujimoto, Y. (1999): Bcl-2 family proteins regulate the release of apoptogenic cytochrome c by the mitochondrial channel VDAC. In *Nature* 399 (6735), pp. 483–487. DOI: 10.1038/20959.

Shinmyo, Yohei; Hamabe-Horiike, Toshihide; Saito, Kengo; Kawasaki, Hiroshi (2022): Investigation of the mechanisms underlying the development and evolution of the cerebral cortex using gyrencephalic ferrets. In *Frontiers in Cell and Developmental Biology* 10, p. 847159. DOI: 10.3389/fcell.2022.847159.

Shump, A. U.; Shump, K. A. (1978): Growth and development of the European ferret (*Mustela putorius*). In *Laboratory Animal Science* 28 (1), pp. 89–91. PMID: 633841.

Sibson, N. R.; Shen, J.; Mason, G. F.; Rothman, D. L.; Behar, K. L.; Shulman, R. G. (1998): Functional energy metabolism: in vivo 13C-NMR spectroscopy evidence for coupling of cerebral glucose consumption and glutamatergic neuronalactivity. In *Developmental Neuroscience* 20 (4-5), pp. 321–330. DOI: 10.1159/000017327.

Sies, Helmut (2017): Hydrogen peroxide as a central redox signaling molecule in physiological oxidative stress: oxidative eustress. In *Redox Biology* 11, pp. 613–619. DOI: 10.1016/j.redox.2016.12.035.

Sies, Helmut; Berndt, Carsten; Jones, Dean P. (2017): Oxidative stress. In *Annual Review of Biochemistry* 86, pp. 715–748. DOI: 10.1146/annurev-biochem-061516-045037.

Simond, Antoine E.; Houde, Magali; Lesage, Véronique; Michaud, Robert; Verreault, Jonathan (2020): Metabolomic profiles of the endangered St. Lawrence Estuary beluga population and associations with organohalogen contaminants. In *The Science of the Total Environment* 717, p. 137204. DOI: 10.1016/j.scitotenv.2020.137204.

Simond, Antoine É.; Noël, Marie; Loseto, Lisa; Houde, Magali; Kirk, Jane; Elliott, Ashley; Brown, Tanya M. (2022): A multi-matrix metabolomic approach in ringed seals and beluga whales to evaluate contaminant and climate-related stressors. In *Metabolites* 12 (9). DOI: 10.3390/metabo12090813.

Singh, Anju; Kukreti, Ritushree; Saso, Luciano; Kukreti, Shrikant (2019): Oxidative stress: a key modulator in neurodegenerative diseases. In *Molecules (Basel, Switzerland)* 24 (8). DOI: 10.3390/molecules24081583.

Siskind, Leah J.; Kolesnick, Richard N.; Colombini, Marco (2002): Ceramide channels increase the permeability of the mitochondrial outer membrane to small proteins. In *Journal of Biological Chemistry* 277 (30), pp. 26796–26803. DOI: 10.1074/jbc.M200754200.

Sjöstedt, Evelina; Zhong, Wen; Fagerberg, Linn; Karlsson, Max; Mitsios, Nicholas; Adori, Csaba et al. (2020): An atlas of the protein-coding genes in the human, pig, and mouse brain. In *Science (New York, N.Y.)* 367 (6482). DOI: 10.1126/science.aay5947.

Smith, Colin A.; Want, Elizabeth J.; O'Maille, Grace; Abagyan, Ruben; Siuzdak, Gary (2006): XCMS: processing mass spectrometry data for metabolite profiling using nonlinear peak alignment, matching, and identification. In *Analytical Chemistry* 78 (3), pp. 779–787. DOI: 10.1021/ac051437y.

Smith, Martin D.; Wertheim, Joel O.; Weaver, Steven; Murrell, Ben; Scheffler, Konrad; Kosakovsky Pond, Sergei L. (2015): Less is more: an adaptive branch-site random effects model for efficient detection of episodic diversifying selection. In *Molecular Biology and Evolution* 32 (5), pp. 1342–1353. DOI: 10.1093/molbev/msv022.

Song, Hyun Keun; Hwang, Dae Youn (2017): Use of C57BL/6N mice on the variety of immunological researches. In *Laboratory Animal Research* 33 (2), pp. 119–123. DOI: 10.5625/lar.2017.33.2.119.

Sonnewald, Ursula (2014): Glutamate synthesis has to be matched by its degradation - where do all the carbons go? In *Journal of Neurochemistry* 131 (4), pp. 399–406. DOI: 10.1111/jnc.12812.

Sorci, Guglielmo; Bianchi, Roberta; Riuzzi, Francesca; Tubaro, Claudia; Arcuri, Cataldo; Giambanco, Ileana; Donato, Rosario (2010): S100B protein, a damage-associated molecular pattern protein in the brain and heart, and beyond. In *Cardiovascular Psychiatry and Neurology* 2010. DOI: 10.1155/2010/656481.

Sparling, Carol E.; Fedak, Michael A. (2004): Metabolic rates of captive grey seals during voluntary diving. In *The Journal of Experimental Biology* 207 (Pt 10), pp. 1615–1624. DOI: 10.1242/jeb.00952.

Srikrishna, Geetha (2012): S100A8 and S100A9: new insights into their roles in malignancy. In *Journal of Innate Immunity* 4 (1), pp. 31–40. DOI: 10.1159/000330095.

Steinman, K. J.; Robeck, T. R.; Fetter, G. A.; Schmitt, T. L.; Osborn, S.; DiRocco, S. et al. (2020): Circulating and excreted corticosteroids and metabolites, hematological, and serum chemistry parameters in the killer whale (*Orcinus orca*) before and after a stress response. In *Frontiers in Marine Science* 6, Article 830. DOI: 10.3389/fmars.2019.00830.

Stenson, Garry B.; Perry, Elizabeth A. (1992): Observations on nursing behaviour of hooded seals, *Cystophora cristata*. In *Behaviour* 122 (1-2), pp. 1–10. DOI: 10.1163/156853992X00264.

Storz, Jay F. (2021): High-altitude adaptation: mechanistic insights from integrated genomics and physiology. In *Molecular Biology and Evolution* 38 (7), pp. 2677–2691. DOI: 10.1093/molbev/msab064.

Storz, Jay F.; Cheviron, Zachary A. (2021): Physiological genomics of adaptation to high-altitude hypoxia. In *Annual Review of Animal Biosciences* 9, pp. 149–171. DOI: 10.1146/annurev-animal-072820-102736.

Strand, Andrew D.; Aragaki, Aaron K.; Baquet, Zachary C.; Hodges, Angela; Cunningham, Philip; Holmans, Peter et al. (2007): Conservation of regional gene expression in mouse and human brain. In *PLoS Genetics* 3 (4), e59. DOI: 10.1371/journal.pgen.0030059.

Strandberg, Ursula; Käkelä, Anne; Lydersen, Christian; Kovacs, Kit M.; Grahl-Nielsen, Otto; Hyvärinen, Heikki; Käkelä, Reijo (2008): Stratification, composition, and function of marine mammal blubber: the ecology of fatty acids in marine mammals. In *Physiological and Biochemical Zoology* 81 (4), pp. 473–485. DOI: 10.1086/589108.

Sud, Manish; Fahy, Eoin; Cotter, Dawn; Azam, Kenan; Vadivelu, Ilango; Burant, Charles et al. (2016): Metabolomics Workbench: an international repository for metabolomics data and metadata, metabolite standards, protocols, tutorials and training, and analysis tools. In *Nucleic Acids Research* 44 (D1), D463-70. DOI: 10.1093/nar/gkv1042.

Sun, Ming-Shuo; Jin, Hang; Sun, Xin; Huang, Shuo; Zhang, Fu-Liang; Guo, Zhen-Ni; Yang, Yi (2018): Free radical damage in ischemia-reperfusion injury: an obstacle in acute ischemic stroke after revascularization therapy. In *Oxidative Medicine and Cellular Longevity* 2018, p. 3804979. DOI: 10.1155/2018/3804979.

Swanson, R. A.; Choi, D. W. (1993): Glial glycogen stores affect neuronal survival during glucose deprivation in vitro. In *Journal of Cerebral Blood Flow and Metabolism* 13 (1), pp. 162–169. DOI: 10.1038/jcbfm.1993.19.

Swerdlow, Natalie S.; Wilkins, Heather M. (2020): Mitophagy and the brain. In *International Journal of Molecular Sciences* 21 (24). DOI: 10.3390/ijms21249661.

Tang, Chuan-Ho; Lin, Ching-Yu; Tsai, Yi-Lun; Lee, Shu-Hui; Wang, Wei-Hsien (2018): Lipidomics as a diagnostic tool of the metabolic and physiological state of managed whales: a correlation study of systemic metabolism. In *Zoo Biology* 37 (6), pp. 440–451. DOI: 10.1002/zoo.21452.

Tang, Daolin; Chen, Xin; Kang, Rui; Kroemer, Guido (2021): Ferroptosis: molecular mechanisms and health implications. In *Cell Research* 31 (2), pp. 107–125. DOI: 10.1038/s41422-020-00441-1.

Teppema, Luc J.; Dahan, Albert (2010): The ventilatory response to hypoxia in mammals: mechanisms, measurement, and analysis. In *Physiological Reviews* 90 (2), pp. 675–754. DOI: 10.1152/physrev.00012.2009.

Thomas, Gregg W. C.; Hahn, Matthew W.; Hahn, Yoonsoo (2017): The effects of increasing the number of taxa on inferences of molecular convergence. In *Genome Biology and Evolution* 9 (1), pp. 213–221. DOI: 10.1093/gbe/evw306.

Thompson, D.; Fedak, M. A. (1993): Cardiac responses of grey seals during diving at sea. In *The Journal of Experimental Biology* 174, pp. 139–154. DOI: 10.1242/jeb.174.1.139.

Thordarson, Gudmundur; Vikingsson, Gisli A.; Hersteinsson, Pall (2007): Seasonal variation in body condition of adult male hooded seals (*Cystophora cristata*) in Skjalfandi-Bay, northeast Iceland. In *Polar Biology* 30 (3), pp. 379–386. DOI: 10.1007/s00300-006-0194-6.

Tian, Ran; Seim, Inge; Ren, Wenhua; Xu, Shixia; Yang, Guang (2019): Contraction of the ROS scavenging enzyme glutathione S-transferase gene family in cetaceans. In *G3 (Bethesda, Md.)* 9 (7), pp. 2303–2315. DOI: 10.1534/g3.119.400224.

Tian, Ran; Wang, Zhengfei; Niu, Xu; Zhou, Kaiya; Xu, Shixia; Yang, Guang (2016): Evolutionary genetics of hypoxia tolerance in cetaceans during diving. In *Genome Biology and Evolution* 8 (3), pp. 827–839. DOI: 10.1093/gbe/evw037.

Tian, Xuesong; Guo, Jingchun; Zhu, Min; Li, Minwei; Wu, Gencheng; Xia, Ying (2013): δ-opioid receptor activation rescues the functional TrkB receptor and protects the brain from ischemia-reperfusion injury in the rat. In *PLoS One* 8 (7), e69252. DOI: 10.1371/journal.pone.0069252.

Tift, Michael S.; Houser, Dorian S.; Crocker, Daniel E. (2011): High-density lipoprotein remains elevated despite reductions in total cholesterol in fasting adult male elephant seals (*Mirounga angustirostris*). In *Comparative Biochemistry and Physiology Part B: Biochemistry & Molecular Biology* 159 (4), pp. 214–219. DOI: 10.1016/j.cbpb.2011.04.005.

Trumble, Stephen J.; Noren, Shawn R.; Cornick, Leslie A.; Hawke, Thomas J.; Kanatous, Shane B. (2010): Age-related differences in skeletal muscle lipid profiles of Weddell seals: clues to developmental changes. In *The Journal of Experimental Biology* 213 (Pt 10), pp. 1676–1684. DOI: 10.1242/jeb.040923.

Tsai, Yi-Lun; Chen, Shih-Yu; Lin, Suen-Chuain; Li, Jiun-Yuan (2016): Effects of physiological factors and seasonal variations on hematology and plasma biochemistry of beluga whales (*Delphinapterus leucas*) managed in Pingtung, Taiwan. In *Aquatic Mammals* 42 (4), pp. 494–506. DOI: 10.1578/AM.42.4.2016.494.

Tsujimoto, Y.; Shimizu, S. (2000): VDAC regulation by the Bcl-2 family of proteins. In *Cell Death and Differentiation* 7 (12), pp. 1174–1181. DOI: 10.1038/sj.cdd.4400780.

Tully, Thomas N. (2006): Chapter 12 - mice and rats. In Mark A. Mitchell, Thomas N. Tully (Eds.): Manual of exotic pet practice. St. Louis, Mo.: Saunders Elsevier, pp. 326–344. DOI: 10.1016/B978-141600119-5.50015-9.

Turner, Emily C.; Sawyer, Eva K.; Kaas, Jon H. (2017): Optic nerve, superior colliculus, visual thalamus, and primary visual cortex of the northern elephant seal (*Mirounga angustirostris*) and California sea lion (*Zalophus californianus*). In *The Journal of Comparative Neurology* 525 (9), pp. 2109–2132. DOI: 10.1002/cne.24188.

Uhen, Mark D. (2007): Evolution of marine mammals: back to the sea after 300 million years. In *Anatomical Record (Hoboken, N.J. : 2007)* 290 (6), pp. 514–522. DOI: 10.1002/ar.20545.

Upadhyaya, Bijaya; Tian, Xiaoli; Wu, Hongli; Lou, Marjorie F. (2015): Expression and distribution of thiol-regulating enzyme glutaredoxin 2 (GRX2) in porcine ocular tissues. In *Experimental Eye Research* 130, pp. 58–65. DOI: 10.1016/j.exer.2014.12.004.

Vacquie-Garcia, Jade; Lydersen, Christian; Biuw, Martin; Haug, Tore; Fedak, Mike A.; Kovacs, Kit M. (2017): Hooded seal *Cystophora cristata* foraging areas in the Northeast Atlantic Ocean-investigated using three complementary methods. In *PLoS One* 12 (12), e0187889. DOI: 10.1371/journal.pone.0187889.

Valko, Marian; Leibfritz, Dieter; Moncol, Jan; Cronin, Mark T. D.; Mazur, Milan; Telser, Joshua (2007): Free radicals and antioxidants in normal physiological functions and human disease. In *The International Journal of Biochemistry & Cell Biology* 39 (1), pp. 44–84. DOI: 10.1016/j.biocel.2006.07.001.

van Blitterswijk, Wim J.; van der Luit, Arnold H.; Veldman, Robert Jan; Verheij, Marcel; Borst, Jannie (2003): Ceramide: second messenger or modulator of membrane structure and dynamics? In *The Biochemical Journal* 369 (Pt 2), pp. 199–211. DOI: 10.1042/BJ20021528.

van Hall, Gerrit; Strømstad, Morten; Rasmussen, Peter; Jans, Ole; Zaar, Morten; Gam, Christian et al. (2009): Blood lactate is an important energy source for the human brain. In *Journal of Cerebral Blood Flow and Metabolism* 29 (6), pp. 1121–1129. DOI: 10.1038/jcbfm.2009.35.

van Meer, Gerrit; Voelker, Dennis R.; Feigenson, Gerald W. (2008): Membrane lipids: where they are and how they behave. In *Nature Reviews Molecular Cell Biology* 9 (2), pp. 112–124. DOI: 10.1038/nrm2330.

Vázquez-Medina, J. P.; Olguín-Monroy, N. O.; Maldonado, P. D.; Santamaría, A.; Königsberg, M.; Elsner, R. et al. (2011a): Maturation increases superoxide radical production without increasing oxidative damage in the skeletal muscle of hooded seals (*Cystophora cristata*). In *Canadian Journal of Zoology* 89 (3), pp. 206–212. DOI: 10.1139/Z10-107.

Vázquez-Medina, José Pablo; Soñanez-Organis, José Guadalupe; Burns, Jennifer M.; Zenteno-Savín, Tania; Ortiz, Rudy M. (2011b): Antioxidant capacity develops with maturation in the deep-diving hooded seal. In *The Journal of Experimental Biology* 214 (Pt 17), pp. 2903–2910. DOI: 10.1242/jeb.057935.

Vázquez-Medina, José Pablo; Zenteno-Savín, Tania; Elsner, Robert (2006): Antioxidant enzymes in ringed seal tissues: potential protection against dive-associated ischemia/reperfusion. In *Comparative Biochemistry and Physiology Part C: Toxicology & Pharmacology* 142 (3-4), pp. 198–204. DOI: 10.1016/j.cbpc.2005.09.004.

Vázquez-Medina, José Pablo; Zenteno-Savín, Tania; Elsner, Robert (2007): Glutathione protection against dive-associated ischemia/reperfusion in ringed seal tissues. In *Journal of Experimental Marine Biology and Ecology* 345 (2), pp. 110–118. DOI: 10.1016/j.jembe.2007.02.003.

Vázquez-Medina, José Pablo; Zenteno-Savín, Tania; Elsner, Robert; Ortiz, Rudy M. (2012): Coping with physiological oxidative stress: a review of antioxidant strategies in seals. In *Journal of Comparative Physiology B: Biochemical, Systemic, and Environmental Physiology* 182 (6), pp. 741–750. DOI: 10.1007/s00360-012-0652-0.

Vázquez-Medina, José Pablo; Zenteno-Savín, Tania; Forman, Henry Jay; Crocker, Daniel E.; Ortiz, Rudy M. (2011c): Prolonged fasting increases glutathione biosynthesis in postweaned northern elephant seals. In *The Journal of Experimental Biology* 214 (Pt 8), pp. 1294–1299. DOI: 10.1242/jeb.054320.

Vázquez-Medina, José Pablo; Zenteno-Savín, Tania; Tift, Michael S.; Forman, Henry Jay; Crocker, Daniel E.; Ortiz, Rudy M. (2011d): Apnea stimulates the adaptive response to oxidative stress in elephant seal pups. In *The Journal of Experimental Biology* 214 (Pt 24), pp. 4193–4200. DOI: 10.1242/jeb.063644.

Venn-Watson, Stephanie; Smith, Cynthia R.; Jensen, Eric D. (2008): Assessment of increased serum aminotransferases in a managed Atlantic bottlenose dolphin (*Tursiops truncatus*) population. In *Journal of Wildlife Diseases* 44 (2), pp. 318–330. DOI: 10.7589/0090-3558-44.2.318.

Vincent, Andrea M.; Perrone, Lorena; Sullivan, Kelli A.; Backus, Carey; Sastry, Ann Marie; Lastoskie, Christian; Feldman, Eva L. (2007): Receptor for advanced glycation end products activation injures primary sensory neurons via oxidative stress. In *Endocrinology* 148 (2), pp. 548–558. DOI: 10.1210/en.2006-0073.

Vrselja, Zvonimir; Daniele, Stefano G.; Silbereis, John; Talpo, Francesca; Morozov, Yury M.; Sousa, André M. M. et al. (2019): Restoration of brain circulation and cellular functions hours post-mortem. In *Nature* 568 (7752), pp. 336–343. DOI: 10.1038/s41586-019-1099-1.

Wang, Yan; Liu, Na; Lu, Bingwei (2019): Mechanisms and roles of mitophagy in neurodegenerative diseases. In *CNS Neuroscience & Therapeutics* 25 (7), pp. 859–875. DOI: 10.1111/cns.13140.

Wätjen, W.; Fritsche, E. (2010): Rolle des Fremdstoffmetabolismus in Pharmakologie und Toxikologie: Teil 2: Phase-II-Reaktionen. In *Apothekenmagazin* 9, pp. 6–14.

Watson, David G.; Pomeroy, Patrick P.; Kennedy, Malcolm W. (2021): Atlantic grey seal milk shows continuous changes in key metabolites and indicators of metabolic transition in pups from birth to weaning. In *Frontiers in Marine Science* 7, Article 596904. DOI: 10.3389/fmars.2020.596904.

Wheatley, Kathryn E.; Bradshaw, Corey J. A.; Harcourt, Robert G.; Davis, Lloyd S.; Hindell, Mark A. (2006): Chemical immobilization of adult female Weddell seals with tiletamine and zolazepam: effects of age, condition and stage of lactation. In *BMC Veterinary Research* 2 (1), p. 8. DOI: 10.1186/1746-6148-2-8.

Wheatley, Kathryn E.; Nichols, Peter D.; Hindell, Mark A.; Harcourt, Robert G.; Bradshaw, Corey J. A. (2008): Differential mobilization of blubber fatty acids in lactating Weddell seals: evidence for selective use. In *Physiological and Biochemical Zoology* 81 (5), pp. 651–662. DOI: 10.1086/590397.

Wilhelm Filho, D.; Sell, F.; Ribeiro, L.; Ghislandi, M.; Carrasquedo, F.; Fraga, C. G. et al. (2002): Comparison between the antioxidant status of terrestrial and diving mammals. In *Comparative Biochemistry and Physiology Part A: Molecular & Integrative Physiology* 133 (3), pp. 885–892. DOI: 10.1016/S1095-6433(02)00253-2.

Williams, E. E.; Stewart, B. S.; Beuchat, C. A.; Somero, G. N.; Hazel, J. R. (2001): Hydrostatic-pressure and temperature effects on the molecular order of erythrocyte membranes from deep-, shallow-, and non-diving mammals. In *Canadian Journal of Zoology* 79 (5), pp. 888–894. DOI: 10.1139/cjz-79-5-888.

Witting, Michael; Ruttkies, Christoph; Neumann, Steffen; Schmitt-Kopplin, Philippe (2017): LipidFrag: Improving reliability of in silico fragmentation of lipids and application to the *Caenorhabditis elegans* lipidome. In *PLoS One* 12 (3), e0172311. DOI: 10.1371/journal.pone.0172311.

Wohlert, Dennis; Kröger, Jürgen; Witt, Martin; Schmitt, Oliver; Wree, Andreas; Czech-Damal, Nicole et al. (2016): A comparative morphometric analysis of three cranial nerves in two phocids: the hooded seal (*Cystophora cristata*) and the harbor seal (*Phoca vitulina*). In *Anatomical Record (Hoboken, N.J. : 2007)* 299 (3), pp. 370–378. DOI: 10.1002/ar.23298.

Wolf, Sebastian; Schmidt, Stephan; Müller-Hannemann, Matthias; Neumann, Steffen (2010): In silico fragmentation for computer assisted identification of metabolite mass spectra. In *BMC Bioinformatics* 11 (1), p. 148. DOI: 10.1186/1471-2105-11-148.

Wolf, Tiffany M. (2006): Chapter 13 - ferrets. In Mark A. Mitchell, Thomas N. Tully (Eds.): Manual of exotic pet practice. St. Louis, Mo.: Saunders Elsevier, pp. 345–374. DOI: 10.1016/B978-141600119-5.50016-0.

Wood, Thomas; Moralejo, Daniel; Corry, Kylie; Fisher, Cole; Snyder, Jessica M.; Acuna, Vivienne et al. (2019): A ferret model of inflammation-sensitized late preterm hypoxic-ischemic brain injury. In *Journal of Visualized Experiments: JoVE* (153). DOI: 10.3791/60131.

Wood, Thomas; Moralejo, Daniel; Corry, Kylie; Snyder, Jessica M.; Traudt, Christopher; Curtis, Chad et al. (2018): A ferret model of encephalopathy of prematurity. In *Developmental Neuroscience* 40 (5-6), pp. 475–489. DOI: 10.1159/000498968.

Wood, Thomas R.; Hildahl, Kate; Helmbrecht, Hawley; Corry, Kylie A.; Moralejo, Daniel H.; Kolnik, Sarah E. et al. (2022): A ferret brain slice model of oxygen-glucose deprivation captures regional responses to perinatal injury and treatment associated with specific microglial phenotypes. In *Bioengineering & Translational Medicine* 7 (2), e10265. DOI: 10.1002/btm2.10265.

Worthen, G. L.; Kilgore, D. L. (1981): Metabolic rate of pine marten in relation to air temperature. In *Journal of Mammalogy* 62 (3), pp. 624–628. DOI: 10.2307/1380410.

Wyatt, Amy R.; Yerbury, Justin J.; Ecroyd, Heath; Wilson, Mark R. (2013): Extracellular chaperones and proteostasis. In *Annual Review of Biochemistry* 82, pp. 295–322. DOI: 10.1146/annurev-biochem-072711-163904.

Xia, Jianguo; Psychogios, Nick; Young, Nelson; Wishart, David S. (2009): MetaboAnalyst: a web server for metabolomic data analysis and interpretation. In *Nucleic Acids Research* 37 (Web Server issue), W652-60. DOI: 10.1093/nar/gkp356.

Xicoy, Helena; Wieringa, Bé; Martens, Gerard J. M. (2019): The role of lipids in Parkinson's disease. In *Cells* 8 (1). DOI: 10.3390/cells8010027.

Xu, Yuan; Zhi, Feng; Mao, Jiahao; Peng, Ya; Shao, Naiyuan; Balboni, Gianfranco et al. (2020): δ-opioid receptor activation protects against Parkinson's disease-related mitochondrial dysfunction by enhancing PINK1/Parkin-dependent mitophagy. In *Aging* 12 (24), pp. 25035–25059. DOI: 10.18632/aging.103970.

Yerbury, Justin J.; Poon, Stephen; Meehan, Sarah; Thompson, Brianna; Kumita, Janet R.; Dobson, Christopher M.; Wilson, Mark R. (2007): The extracellular chaperone clusterin influences amyloid formation and toxicity by interacting with prefibrillar structures. In *FASEB Journal* 21 (10), pp. 2312–2322. DOI: 10.1096/fj.06-7986com.

Yim, Hyung-Soon; Cho, Yun Sung; Guang, Xuanmin; Kang, Sung Gyun; Jeong, Jae-Yeon; Cha, Sun-Shin et al. (2014): Minke whale genome and aquatic adaptation in cetaceans. In *Nature Genetics* 46 (1), pp. 88–92. DOI: 10.1038/ng.2835.

Yu, A. C.; Drejer, J.; Hertz, L.; Schousboe, A. (1983): Pyruvate carboxylase activity in primary cultures of astrocytes and neurons. In *Journal of Neurochemistry* 41 (5), pp. 1484–1487. DOI: 10.1111/j.1471-4159.1983.tb00849.x.

Yu, Zai Fang; Nikolova-Karakashian, Mariana; Zhou, Daohong; Cheng, Guanjun; Schuchman, Edward H.; Mattson, Mark P. (2000): Pivotal role for acidic sphingomyelinase in cerebral ischemia-induced ceramide and cytokine production, and neuronal apoptosis. In *Journal of Molecular Neuroscience* 15 (2), pp. 85–98. DOI: 10.1385/JMN:15:2:85.

Yuste-Checa, Patricia; Bracher, Andreas; Hartl, F. Ulrich (2022): The chaperone Clusterin in neurodegeneration-friend or foe? In *BioEssays* 44 (7), e2100287. DOI: 10.1002/bies.202100287.

Zapol, W. M.; Liggins, G. C.; Schneider, R. C.; Qvist, J.; Snider, M. T.; Creasy, R. K.; Hochachka, P. W. (1979): Regional blood flow during simulated diving in the conscious Weddell seal. In *Journal of Applied Physiology: Respiratory, Environmental and Exercise Physiology* 47 (5), pp. 968–973. DOI: 10.1152/jappl.1979.47.5.968.

Zenteno-Savín, T.; Clayton-Hernández, E.; Elsner, R. (2002): Diving seals: are they a model for coping with oxidative stress? In *Comparative Biochemistry and Physiology Part C: Toxicology & Pharmacology* 133 (4), pp. 527–536. DOI: 10.1016/S1532-0456(02)00075-3.

Zenteno-Savín, Tania; Elsner, Robert (1998): Seals and oxidative stress. In *Free Radical Biology and Medicine* 25, S42. DOI: 10.1016/S0891-5849(98)90127-7.

Zenteno-Savín, Tania; Elsner, Robert (2000): Differential oxidative stress in ringed seal tissues. In *Free Radical Biology and Medicine* 29, S139.

Zhang, Fan; Kumano, Masafumi; Beraldi, Eliana; Fazli, Ladan; Du, Caigan; Moore, Susan et al. (2014): Clusterin facilitates stress-induced lipidation of LC3 and autophagosome biogenesis to enhance cancer cell survival. In *Nature Communications* 5 (1), p. 5775. DOI: 10.1038/ncomms6775.

Zhang, Honglai; Kim, Jin Koo; Edwards, Chris A.; Xu, Zhaohui; Taichman, Russell; Wang, Cun-Yu (2005): Clusterin inhibits apoptosis by interacting with activated Bax. In *Nature Cell Biology* 7 (9), pp. 909–915. DOI: 10.1038/ncb1291.

Zhang, Junhui; Gibney, Geoffrey Thomas; Zhao, Peng; Xia, Ying (2002): Neuroprotective role of delta-opioid receptors in cortical neurons. In *American Journal of Physiology: Cell Physiology* 282 (6), C1225-34. DOI: 10.1152/ajpcell.00226.2001.

Zhang, Yanan; Liu, Dawei; Hu, Haijuan; Zhang, Puqiang; Xie, Ruiqin; Cui, Wei (2019): HIF-1α/BNIP3 signaling pathway-induced-autophagy plays protective role during myocardial ischemia-reperfusion injury. In *Biomedicine & Pharmacotherapy = Biomedecine & Pharmacotherapie* 120, p. 109464. DOI: 10.1016/j.biopha.2019.109464.

Zhang, Ye; Sloan, Steven A.; Clarke, Laura E.; Caneda, Christine; Plaza, Colton A.; Blumenthal, Paul D. et al. (2016): Purification and characterization of progenitor and mature human astrocytes reveals transcriptional and functional differences with mouse. In *Neuron* 89 (1), pp. 37–53. DOI: 10.1016/j.neuron.2015.11.013.

Zhao, Yuhai; Calon, Frederic; Julien, Carl; Winkler, Jeremy W.; Petasis, Nicos A.; Lukiw, Walter J.; Bazan, Nicolas G. (2011): Docosahexaenoic acid-derived neuroprotectin D1 induces neuronal survival via secretase- and PPARγ-mediated mechanisms in Alzheimer's disease models. In *PLoS One* 6 (1), e15816. DOI: 10.1371/journal.pone.0015816.

Zhou, F.; Zhu, X.; Castellani, R. J.; Stimmelmayr, R.; Perry, G.; Smith, M. A.; Drew, K. L. (2001): Hibernation, a model of neuroprotection. In *The American Journal of Pathology* 158 (6), pp. 2145–2151. DOI: 10.1016/S0002-9440(10)64686-X.

Zhou, Xuming; Sun, Fengming; Xu, Shixia; Fan, Guangyi; Zhu, Kangli; Liu, Xin et al. (2013): Baiji genomes reveal low genetic variability and new insights into secondary aquatic adaptations. In *Nature Communications* 4 (1), p. 2708. DOI: 10.1038/ncomms3708.

Zhu, Kangli; Ge, Deyan; Wen, Zhixin; Xia, Lin; Yang, Qisen (2018): Evolutionary genetics of hypoxia and cold tolerance in mammals. In *Journal of Molecular Evolution* 86 (9), pp. 618–634. DOI: 10.1007/s00239-018-9870-8.

Zielke, H. Ronald; Zielke, Carol L.; Baab, Peter J. (2009): Direct measurement of oxidative metabolism in the living brain by microdialysis: a review. In *Journal of Neurochemistry* 109 Suppl 1, pp. 24–29. DOI: 10.1111/j.1471-4159.2009.05941.x.

Zurita, Esther; Chagoyen, Mónica; Cantero, Marta; Alonso, Rosario; González-Neira, Anna; López-Jiménez, Alejandro et al. (2011): Genetic polymorphisms among C57BL/6 mouse inbred strains. In *Transgenic Research* 20 (3), pp. 481–489. DOI: 10.1007/s11248-010-9403-8.

12 Appendix

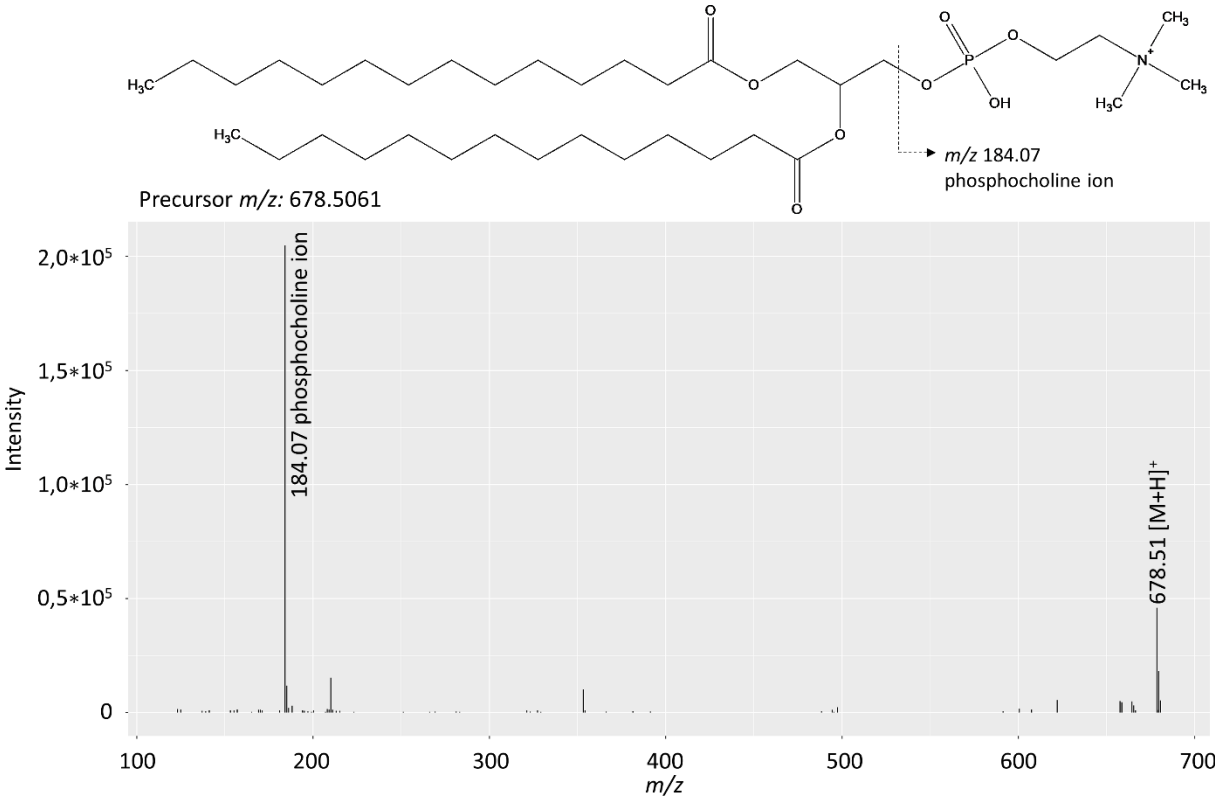

Fig. S1.1: *MS/MS spectrum of Phosphatidylcholine (PC) species PC(28:0) measured in positive ionization mode*

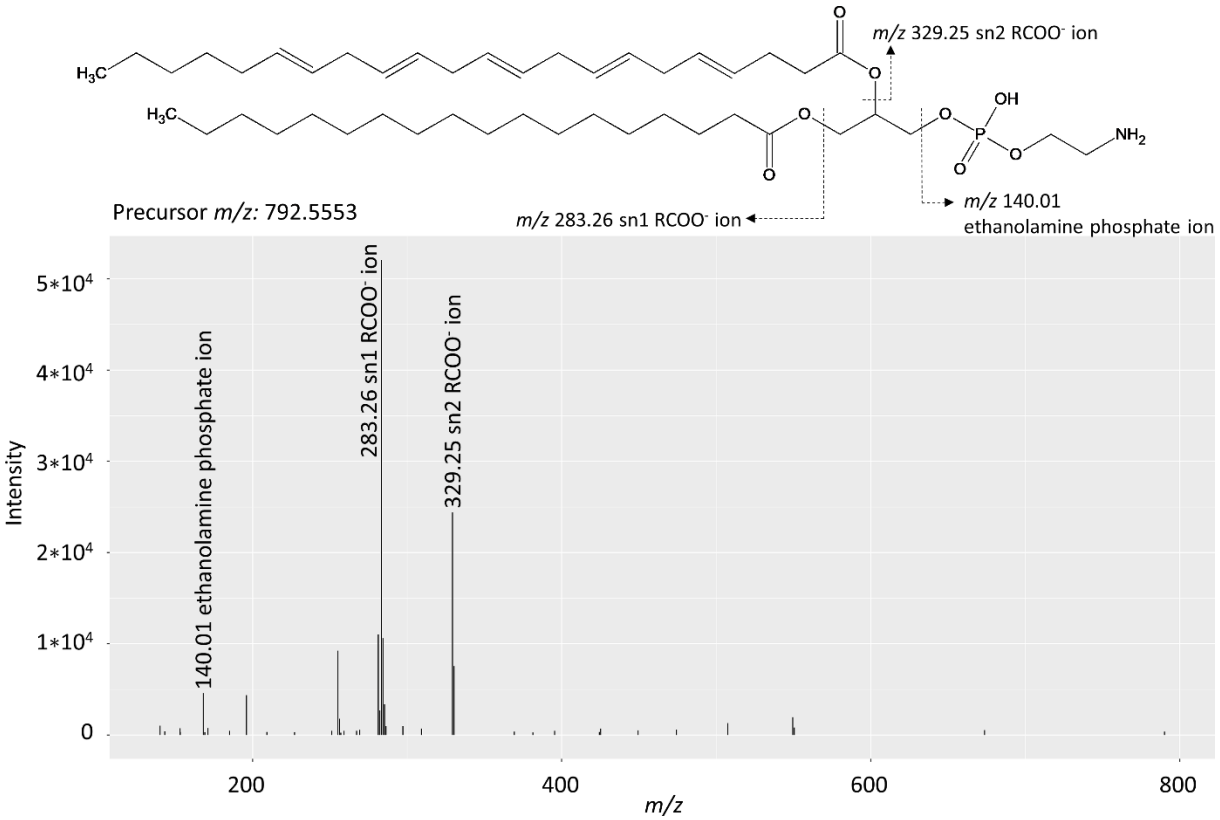

Fig. S1.2: *MS/MS spectrum of Phosphatidylethanolamine (PE) species PE(40:5) measured in negative ionization mode*

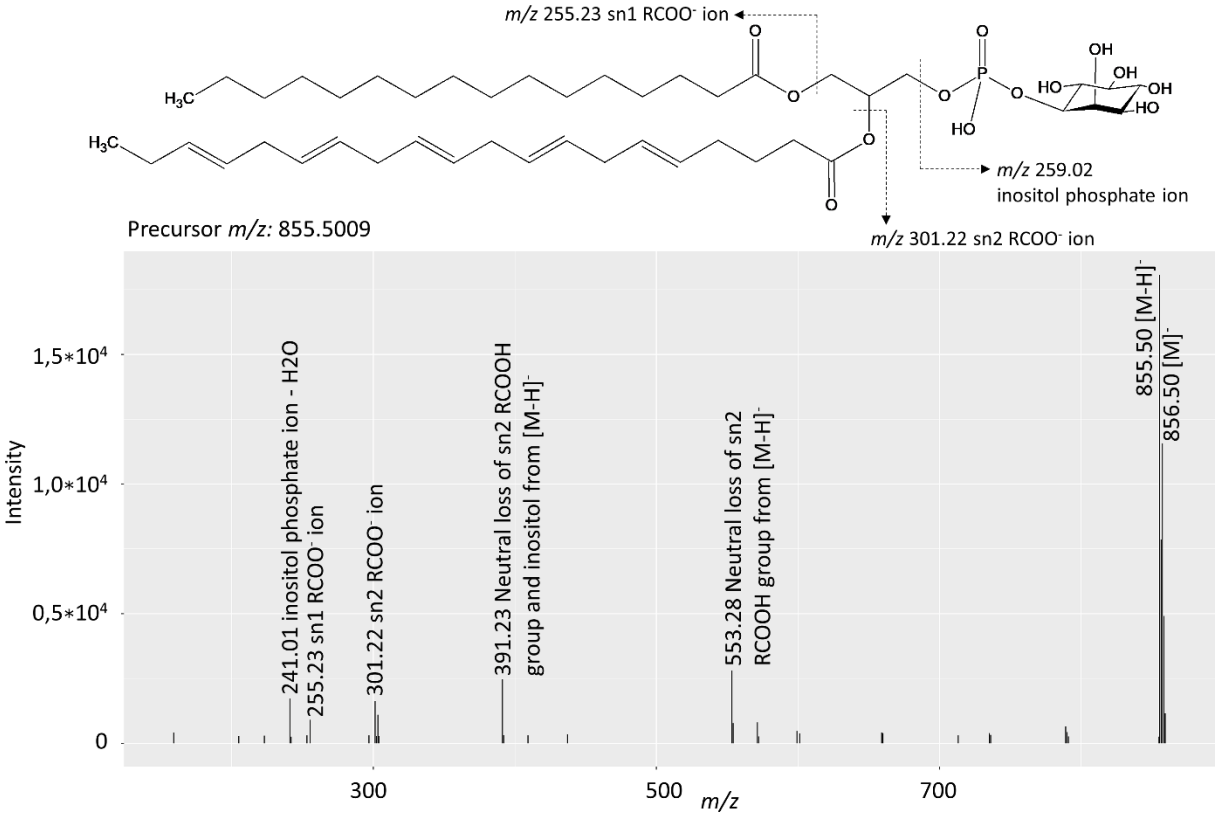

Fig. S1.3: *MS/MS spectrum of Phosphatidylinositol (PI) species PI(36:5) measured in negative ionization mode*

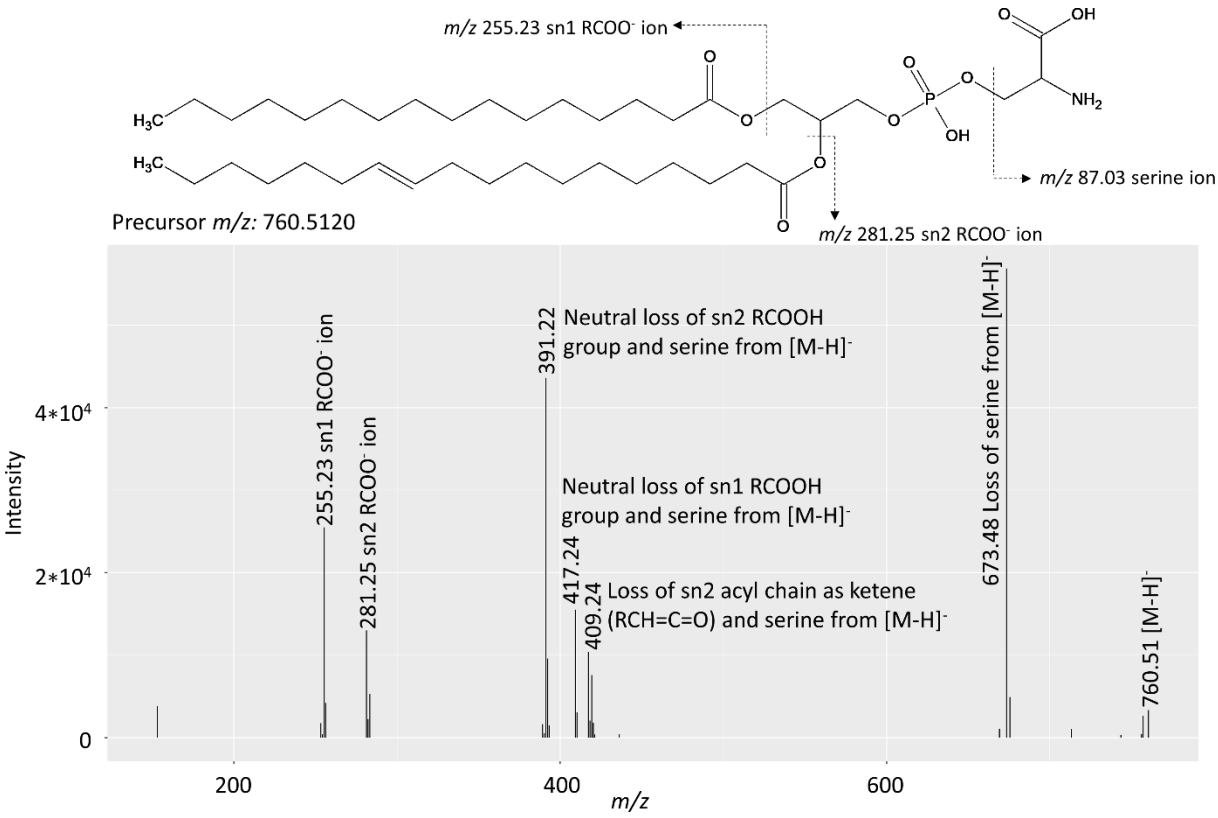

Fig. S1.4: *MS/MS spectrum of Phosphatidylserine (PS) species PS(34:1) measured in negative ionization mode*

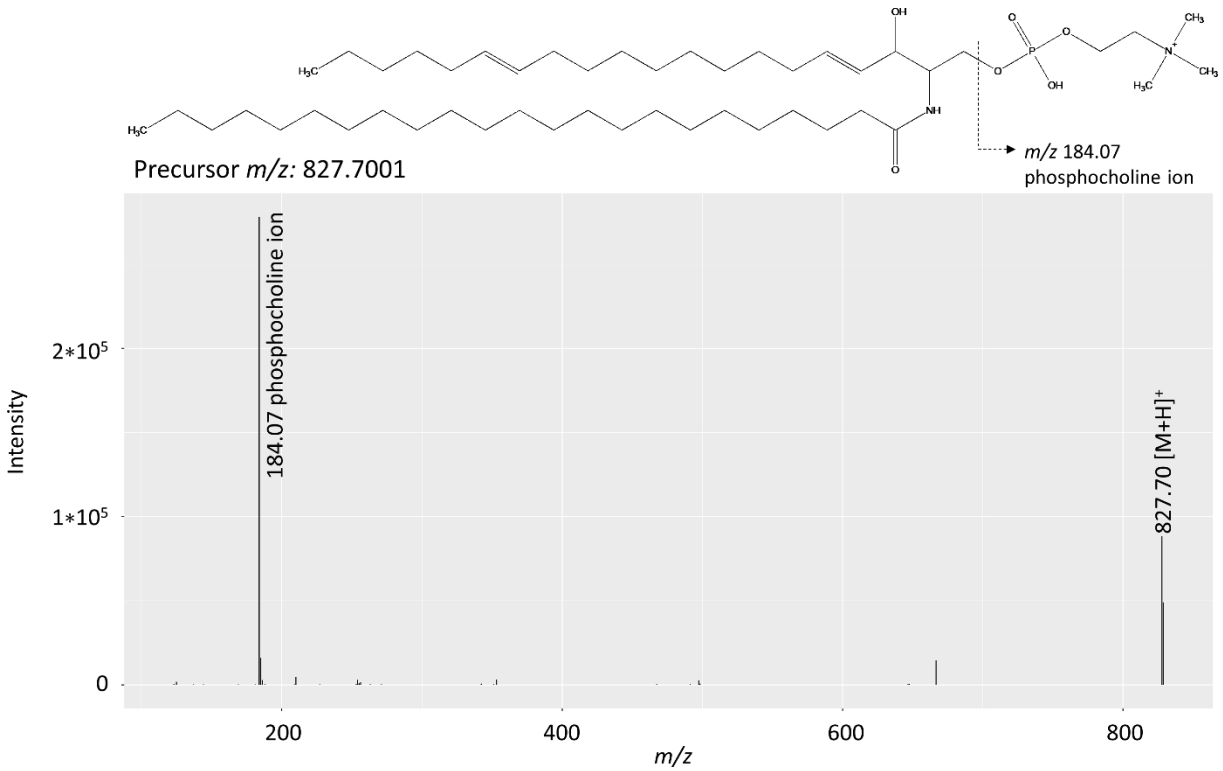

Fig. S1.5: *MS/MS spectrum of Sphingomyelin (SM) species SM(d43:2) measured in positive ionization mode*

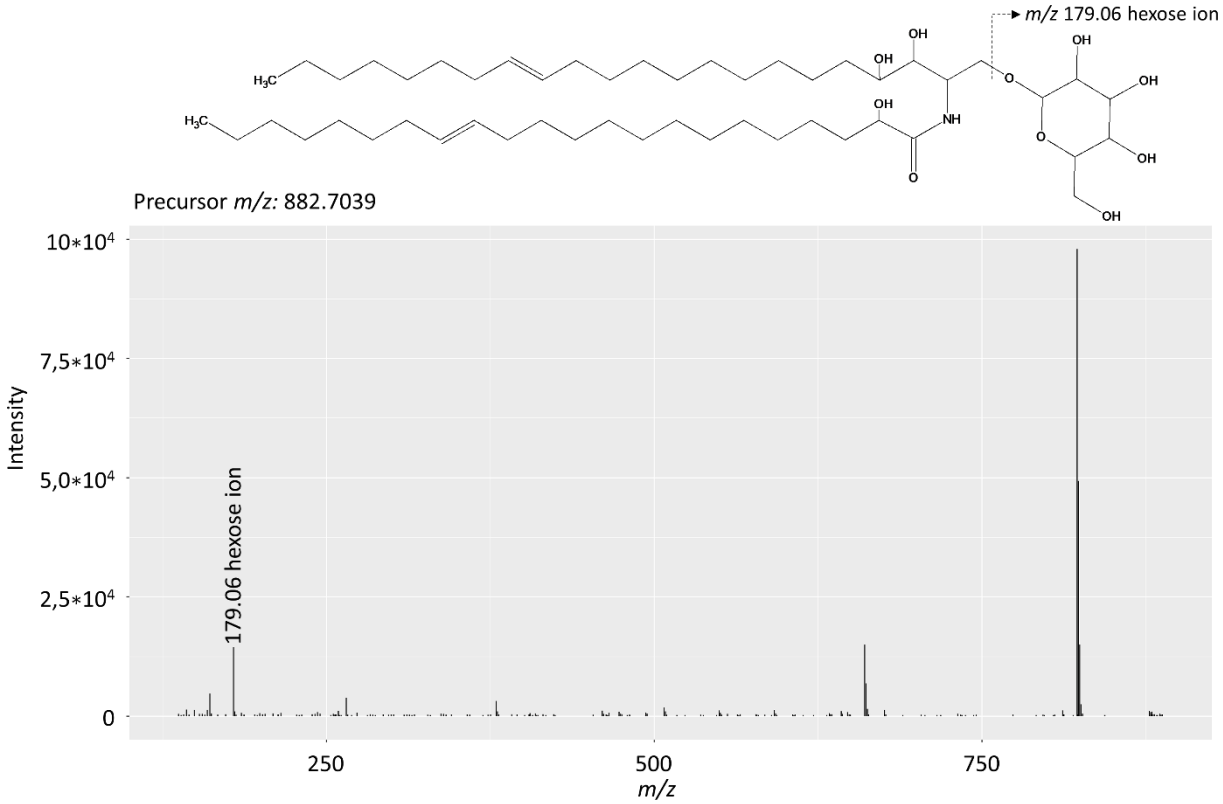

Fig. S1.6: *MS/MS spectrum of cerebroside (HexCer) species HexCer(d44:2) measured in negative ionization mode*

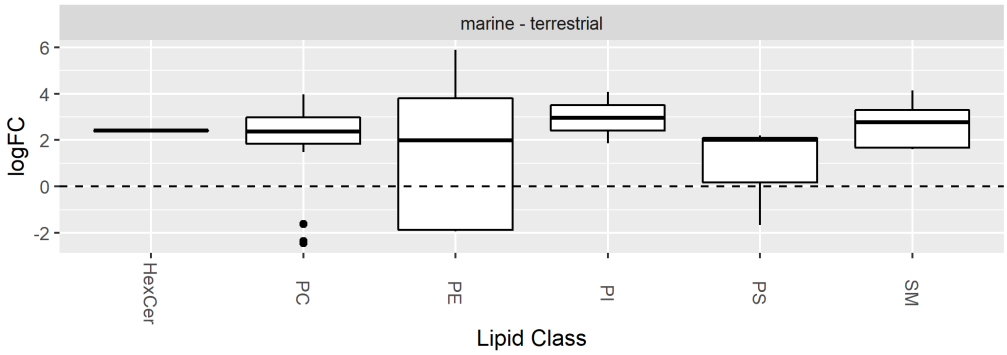

Fig. S1.7: *Fold change of lipid classes between marine and terrestrial mammals. The dashed line indicates the value (logFC = 0), at which lipids are present in equal concentrations in marine and terrestrial mammals. Positive logFC values represent higher abundance in marine mammals, while negative logFC values describe increase in terrestrial mammals. PC: phosphatidylcholine; PE: phosphatidylethanolamine; PI: phospatidylinositol; PS: phosphatidylserine; SM: sphingomylein; HexCer: cerebroside. No significant differences could be determined.*

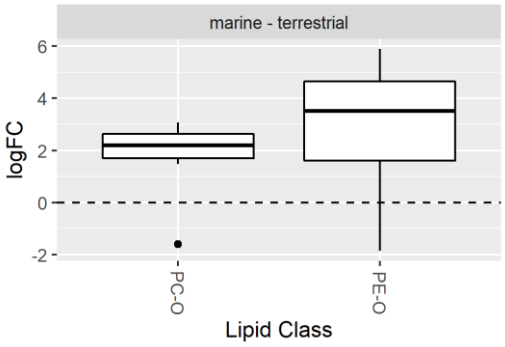

Fig. S1.8: *Fold change of plasmalogen lipid classes between marine and terrestrial mammals. The dashed line indicates the value (logFC = 0), at which lipids are present in equal concentrations in marine and terrestrial mammals. Positive logFC values represent higher abundance in marine mammals, while negative logFC values describe increase in terrestrial mammals. PC-O: phosphatidylcholine plasmalogen; PE-O: phosphatidylethanolamine plasmalogen. No significant differences could be determined.*

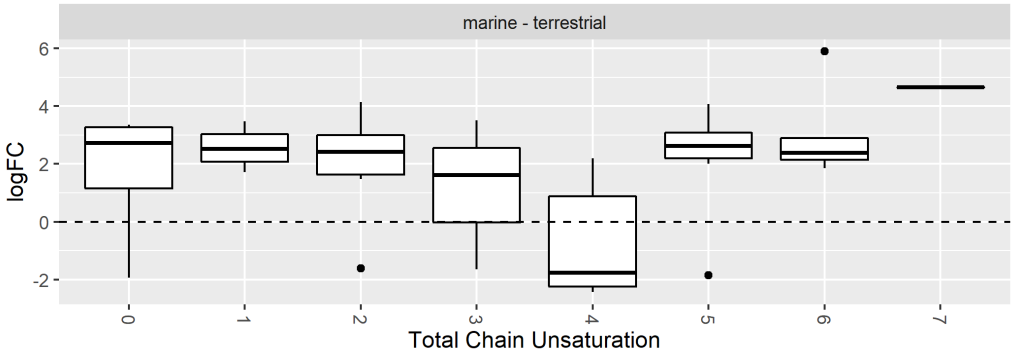

Fig. S1.9: *Fold change of fatty acid unsaturation of identified lipids between marine and terrestrial mammals. The dashed line indicates the value (logFC = 0), at which lipids are present in equal concentrations in marine and terrestrial mammals. Positive logFC values represent higher abundance in marine mammals, while negative logFC values describe increase in terrestrial mammals. No significant differences could be determined.*

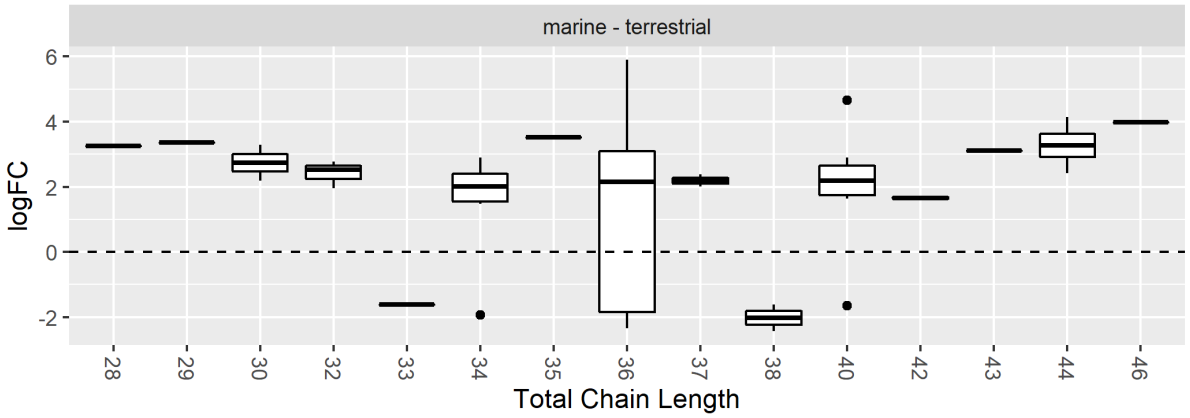

Fig. S1.10: *Fold change of fatty acid chain length of identified lipids between marine and terrestrial mammals. The dashed line indicates the value (logFC = 0), at which lipids are present in equal concentrations in marine and terrestrial mammals. Positive logFC values represent higher abundance in marine mammals, while negative logFC values describe increase in terrestrial mammals. No significant differences could be determined.*

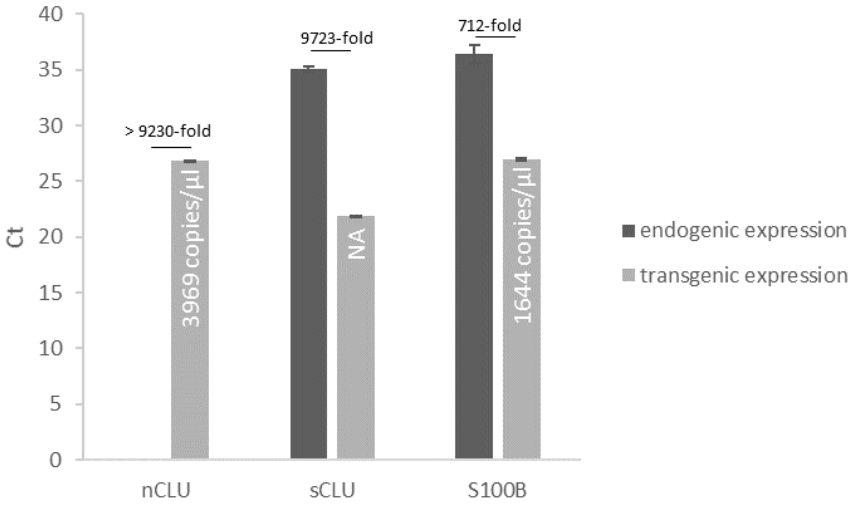

Fig. S2.1: *Expression of endogenic and transgenic CLU and S100B sequences in transfected HN33 cell lines at normoxia, determined by qPCR experiments. Differences in Ct-values between endogenic and transgenic nCLU, sCLU and S100B were 13.17 (with Ct of 40 for endogenic nCLU), 13.25 and 9.48, respectively. The fold-expression difference for nCLU, sCLU and S100B therefore were* $2^{13.17}$, $2^{13.25}$ *and* $2^{9.48}$, *respectively.*

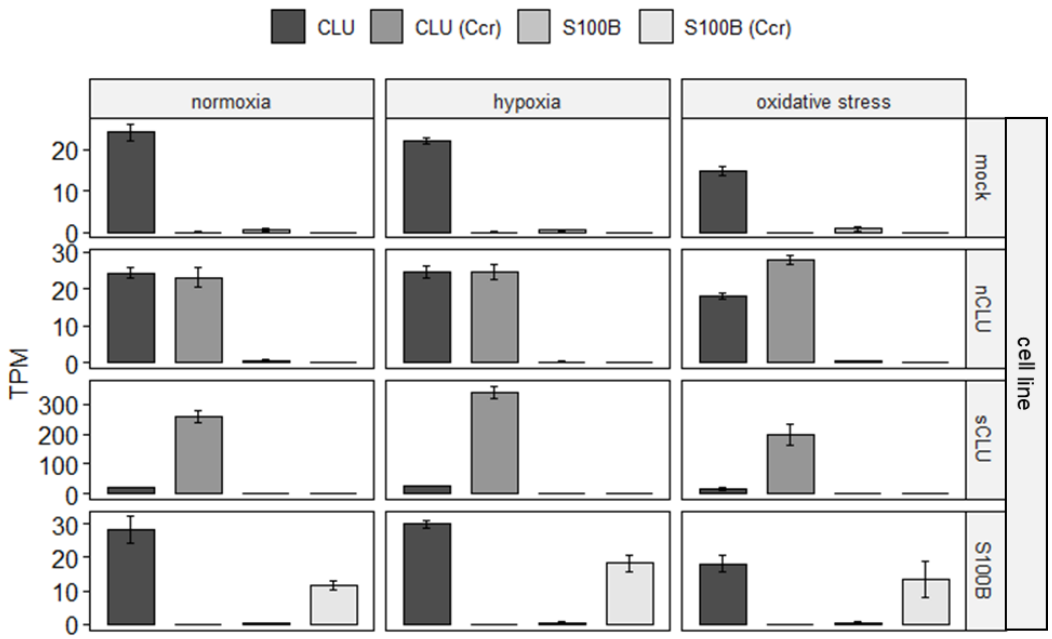

Fig. S2.2: *TPM values of endogenic (CLU, S100B) and transgenic (CLU (Ccr), S100B (Ccr)) sequences in transfected cell lines (mock, nCLU, sCLU, S100B) at normoxia, hypoxia and oxidative stress*

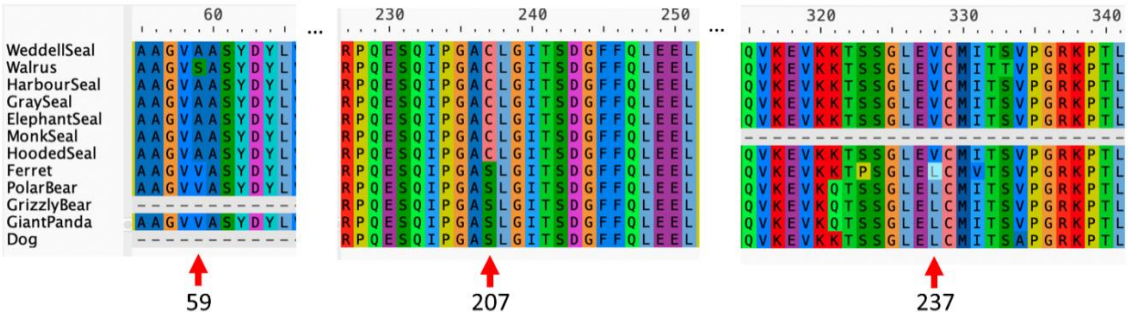

Fig. S3.1: *Glutathione reductase (GSR) amino-acid alignment constructed using MAFFT (Katoh and Standley, 2013) and visualized with AliView (Larsson, 2014). The alignment positions of three pinniped-specific amino-acid substitutions are indicated by red arrows.*

Table S1.1: *Detected lipids with annotation from MS/MS spectra including adduct, mass, MetFrag and LipidFrag scores. Fold change (log2FC) and false discovery rate (FDR) were calculated from MS spectra. Positive log2FC values represent higher abundance in marine mammals (↑), while negative log2FC values describe lower abundance in comparison to the terrestrial mammals (↓). Error between measured, i.e., detected m/z in mass spectrometry, and calculated, i.e., expected m/z from molecular formula, is given in parts per million (ppm). The optimum MetFrag as well as LipidFrag score of 1.0 represents a likely lipid identification, while lower scores indicate weaker annotation confidence. PC: phosphatidylcholine; PE: phosphatidylethanolamine; PI: phospatidylinositol; PS: phosphatidylserine; SM: sphingomylein; HexCer: cerebroside.*

Tentative compound	Proposed formula	Retention time [min]	Adduct	*m/z* measured	*m/z* calculated	Error [ppm]	Relevant fragments	MetFrag Score	LipidFrag Score	log2FC	FDR
Glycerophospholipids											
PC(28:0)	$C_{36}H_{72}NO_8P$	9.3	$[M+H]^+$	678.5065	678.5068	-0.4	184.07: $C_5H_{13}NO_4P$	1.0	0.6	2.9↑	<0.0001
PC(29:0)	$C_{37}H_{74}NO_8P$	9.8	$[M+H]^+$	692.5223	692.5225	-0.3	184.07: $C_5H_{13}NO_4P$	1.0	0.5	3.3↑	<0.0001
PC(30:1)	$C_{38}H_{74}NO_8P$	9.5	$[M+H]^+$	704.5222	704.5225	-0.4	184.07: $C_5H_{13}NO_4P$	1.0	0.6	2.9↑	<0.0001
PC(32:2)	$C_{40}H_{76}NO_8P$	9.7	$[M+H]^+$	730.5378	730.5381	-0.4	184.07: $C_5H_{13}NO_4P$	1.0	0.5	2.0↑	<0.0001
PC(33:4)	$C_{41}H_{74}NO_8P$	11.1	$[M+H]^+$	740.5218	740.5225	-0.9	184.07: $C_5H_{13}NO_4P$	0.5	1.0	-1.5↓	<0.0001
PC(36:4)	$C_{44}H_{80}NO_8P$	10.8	$[M+H]^+$	782.5708	782.5694	1.7	184.07: $C_5H_{13}NO_4P$	1.0	0.5	-1.6↓	0.0122
PC(36:5)	$C_{44}H_{78}NO_8P$	9.9	$[M+H]^+$	780.5535	780.5538	-0.4	184.07: $C_5H_{13}NO_4P$	1.0	0.6	2.8↑	<0.0001
PC(36:5)	$C_{44}H_{78}NO_8P$	10.1	$[M+H]^+$	780.5536	780.5538	-0.3	184.07: $C_5H_{13}NO_4P$	1.0	0.5	3.4↑	<0.0001
PC(36:6)	$C_{44}H_{76}NO_8P$	9.5	$[M+H]^+$	778.5380	778.5381	-0.1	184.07: $C_5H_{13}NO_4P$; 433.3: $C_{22}H_{43}NO_5P$	1.0	0.6	2.4↑	<0.0001
PC(37:5)	$C_{45}H_{80}NO_8P$	12.3	$[M+H]^+$	794.5690	794.5694	-0.5	184.07: $C_5H_{13}NO_4P$	1.0	0.6	2.2↑	0.0025
PC(37:6)	$C_{45}H_{78}NO_8P$	10.0	$[M+H]^+$	792.5536	792.5538	-0.2	184.07: $C_5H_{13}NO_4P$	1.0	0.6	2.5↑	<0.0001
PC(38:4)	$C_{46}H_{84}NO_8P$	11.5	$[M+H]^+$	810.6002	810.6007	-0.6	184.07: $C_5H_{13}NO_4P$	1.0	0.7	-1.7↓	0.0068
PC(40:6)	$C_{48}H_{84}NO_8P$	11.2	$[M+H-H_2O]^+$	816.5884	816.5878	0.7	184.07: $C_5H_{13}NO_4P$	-	-	2.9↑	<0.0001
PC(46:2)	$C_{54}H_{104}NO_8P$	16.4	$[M+H]^+$	926.7522	926.7572	-5.4	184.07: $C_5H_{13}NO_4P$	1.0	0.5	3.7↑	0.0001
PC(O-30:0)	$C_{38}H_{78}NO_7P$	11.1	$[M+H]^+$	692.5581	692.5589	-1.2	184.07: $C_5H_{13}NO_4P$	1.0	0.0	2.2↑	<0.0001
PC(O-32:1)	$C_{40}H_{80}NO_7P$	11.3	$[M+H]^+$	718.5742	718.5745	-0.5	184.07: $C_5H_{13}NO_4P$	0.6	0.0	2.5↑	<0.0001
PC(O-34:1)	$C_{42}H_{84}NO_7P$	12.0	$[M+H-H_2O]^+$	728.6027	728.5952	10.3	184.07: $C_5H_{13}NO_4P$	-	-	2.9↑	0.0012
PC(O-34:2)	$C_{42}H_{82}NO_7P$	10.6	$[M+Cl]^-$	778.5582	778.5523	7.6	168.04: $C_4H_{10}NO_4P$; 255.23: $C_{16}H_{28}O_2$	0.7	0.0	1.5↑	0.0015
PC(O-34:2)	$C_{42}H_{82}NO_7P$	11.4	$[M+H]^+$	744.5895	744.5902	-1.0	184.07: $C_5H_{13}NO_4P$	1.0	0.0	2.7↑	<0.0001
PC(O-34:2)	$C_{42}H_{82}NO_7P$	12.2	$[M+H]^+$	744.5877	744.5902	-3.3	184.07: $C_5H_{13}NO_4P$	-	-	3.6↑	<0.0001
PC(O-36:4)	$C_{44}H_{82}NO_7P$	12.0	$[M+H-H_2O]^+$	750.5862	750.5796	8.7	184.07: $C_5H_{13}NO_4P$	-	-	2.0↑	0.0002
PC(O-38:2)	$C_{46}H_{90}NO_7P$	13.9	$[M+H-H_2O]^+$	782.6485	782.6422	8.0	184.07: $C_5H_{13}NO_4P$	-	-	-1.0↓	0.0357
PC(O-44:5)	$C_{52}H_{96}NO_7P$	15.1	$[M+H-H_2O]^+$	860.6940	860.6891	5.7	184.07: $C_5H_{13}NO_4P$	-	-	3.2↑	<0.0001

***Table S1.1** (continued)*

Tentative compound	*Proposed formula*	*Retention time [min]*	*Adduct*	*m/z measured*	*m/z calculated*	*Error [ppm]*	*Relevant fragments*	*MetFrag Score*	*LipidFrag Score*	*log2FC*	*FDR*
PE(34:0)	$C_{39}H_{78}NO_8P$	12.4	$[M-H]^-$	718.5372	718.5392	-2.7	255.23: $C_{16}H_{30}O_2$; 283.26: $C_{18}H_{34}O_2$	1.0	1.0	-1.5↓	0.0001
PE(36:4)	$C_{41}H_{74}NO_8P$	10.7	$[M-H]^-$	738.5073	738.5079	-0.8	255.23: $C_{16}H_{31}O_2$; 303.23: $C_{20}H_{31}O_2$	1.0	1.0	-1.7↓	<0.0001
PE(40:5)	$C_{45}H_{80}NO_8P$	11.8	$[M-H]^-$	792.5534	792.5549	-1.9	140.01: $C_2H_7NO_4P$; 283.26: $C_{18}H_{33}O_2$; 329.25: $C_{22}H_{34}O_2$	1.0	1.0	2.5↑	<0.0001
PE(O-34:3)	$C_{39}H_{74}NO_7P$	11.6	$[M-H]^-$	698.5107	698.5130	-3.3	253.22: $C_{16}H_{26}O_2$; 283.26: $C_{18}H_{34}O_2$	1.0	0.0	2.0↑	0.0024
PE(O-35:3)	$C_{40}H_{76}NO_7P$	11.8	$[M-H]^-$	712.5266	712.5285	-2.6	267.23: $C_{17}H_{29}O_2$; 281.25: $C_{18}H_{30}O_2$	1.0	0.0	4.0↑	<0.0001
PE(O-36:5)	$C_{41}H_{74}NO_7P$	11.2	$[M-H]^-$	722.5115	722.5130	-2.1	303.23: $C_{20}H_{31}O_2$; 436.28: $C_{21}H_{43}NO_6P$	1.0	0.0	-1.7↓	<0.0001
PE(O-36:6)	$C_{41}H_{72}NO_7P$	10.6	$[M-H]^-$	720.4954	720.4974	-2.8	301.22: $C_{20}H_{29}O_2$; 436.28: $C_{21}H_{43}NO_6P$	1.0	0.0	5.5↑	<0.0001
PE(O-40:7)	$C_{45}H_{78}NO_7P$	11.4	$[M-H]^-$	774.5427	774.5443	-2.0	140.01: $C_2H_7NO_4P$; 283.24: $C_{21}H_{31}$; 327.23: C22H31O2	1.0	0.0	4.2↑	<0.0001
PI(36:5)	$C_{45}H_{77}O_{13}P$	6.7	$[M-H]^-$	855.5014	855.5029	-1.8	241.01: $C_6H_{11}O_8P$; 301.22: $C_{20}H_{29}O_2$; 391.23: $C_{19}H_{37}O_6P$; 553.28: $C_{25}H_{47}O_{11}P$	1.0	1.0	4.0↑	<0.0001
PI(40:6)	$C_{49}H_{83}O_{13}P$	7.2	$[M-H]^-$	909.5493	909.5499	-0.7	283.26: $C_{18}H_{35}O_2$; 419.26: $C_{21}H_{41}O_6P$; 581.31: $C_{27}H_{51}O_{11}P$	1.0	1.0	2.0↑	0.0003
PS(34:1)	$C_{40}H_{76}NO_{10}P$	7.9	$[M-H]^-$	760.5118	760.5134	-2.1	255.23: $C_{16}H_{31}O_2$; 281.25: $C_{18}H_{33}O_2$; 391.22: $C_{19}H_{37}O_6P$; 409.24: $C_{19}H_{37}O_7P$; 417.24: $C_{21}H_{39}O_6P$; 673.48: $C_{37}H_{70}O_8P$	1.0	1.0	2.1↑	<0.0001
PS(40:3)	$C_{46}H_{84}NO_{10}P$	10.4	$[M-H]^-$	840.5756	840.5760	-0.5	283.26: $C_{18}H_{33}O_2$; 419.26: $C_{21}H_{39}O_6P$; 437.27: $C_{21}H_{39}O_7P$; 753.54: $C_{43}H_{78}O_8P$	1.0	1.0	-1.3↓	0.0002
PS(40:4)	$C_{46}H_{82}NO_{10}P$	9.8	$[M-H]^-$	838.5583	838.5604	-2.5	283.26: $C_{18}H_{35}O_2$; 331.26: $C_{22}H_{35}O_2$; 419.26: $C_{21}H_{41}O_6P$; 437.27: $C_{21}H_{41}O_7P$; 467.26: $C_{25}H_{41}O_6P$; 751.53: $C_{43}H_{76}O_8P$	1.0	1.0	2.1↑	0.0001
					Sphingolipids						
SM(d32:1)	$C_{37}H_{75}N_2O_6P$	9.3	$[M+H]^+$	675.5433	675.5435	-0.3	184.07: $C_5H_{13}NO_4P$	1.0	0.0	2.4↑	<0.0001
SM(d40:2)	$C_{45}H_{89}N_2O_6P$	12.6	$[M+H]^+$	785.6521	785.6535	-1.8	184.07: $C_5H_{13}NO_4P$	1.0	0.0	2.2↑	0.0056
SM(d42:1)	$C_{47}H_{95}N_2O_6P$	14.7	$[M+H]^+$	815.6995	815.7000	-0.6	184.07: $C_5H_{13}NO_4P$	1.0	0.0	2.3↑	0.0182
SM(d42:2)	$C_{47}H_{93}N_2O_6P$	13.7	$[M+Na]^+$	835.6653	835.6663	-1.2	184.07: $C_5H_{13}NO_4P$	1.0	0.0	2.3↑	0.0137
SM(d43:2)	$C_{48}H_{95}N_2O_6P$	14.2	$[M+H]^+$	827.6985	827.7000	-1.9	184.07: $C_5H_{13}NO_4P$	1.0	0.0	3.2↑	0.0065
SM(d44:1)	$C_{49}H_{99}N_2O_6P$	15.6	$[M+H]^+$	843.7301	843.7313	-1.5	184.07: $C_5H_{13}NO_4P$	-	-	2.6↑	0.0005
SM(d44:2)	$C_{49}H_{97}N_2O_6P$	14.6	$[M+H]^+$	841.7147	841.7157	-1.2	184.07: $C_5H_{13}NO_4P$	1.0	0.0	3.3↑	0.0001
HexCer(d44:2)	$C_{50}H_{95}NO_8$	14.0	$[M+Formate]^-$	882.7026	882.7040	-1.6	179.06: $C_6H_{12}O_6$	-	-	3.2↑	0.0146

Table S2.1: *Sequencing and mapping overview. Triplicates were sequenced per cell line and oxygen treatment. For sample mock-H_2O_2-2 sequencing failed and was discarded. Around 51 million reads per sample were generated of which around 75 % mapped to the GRCm39 mouse reference genome.*

Sample ID	Accession	# Reads	Mean Quality Score	Mapped reads %
HN33-mock-normoxia-1	SRR20646231	54,631,566	35.93	75.93%
HN33-mock-normoxia-2	SRR20646230	43,220,304	35.81	74.81%
HN33-mock-normoxia-3	SRR20646219	51,775,704	36.00	78.57%
HN33-mock-hypoxia-1	SRR20646208	52,052,511	35.83	73.91%
HN33-mock-hypoxia-2	SRR20646202	58,723,186	35.81	76.67%
HN33-mock-hypoxia-3	SRR20646201	46,880,076	35.89	75.66%
HN33-mock-oxidative_stress-1	SRR20646200	30,508,905	35.97	74.34%
HN33-mock-oxidative_stress-2	SRR20646199	40,445,197	35.97	76.49%
HN33-nCLU-normoxia-1	SRR20646198	65,965,761	35.89	77.78%
HN33-nCLU-normoxia-2	SRR20646197	48,021,315	35.96	79.58%
HN33-nCLU-normoxia-3	SRR20646229	47,677,448	35.90	74.37%
HN33-nCLU-hypoxia-1	SRR20646228	58,624,401	35.87	72.79%
HN33-nCLU-hypoxia-2	SRR20646227	51,146,599	35.87	77.06%
HN33-nCLU-hypoxia-3	SRR20646226	48,122,292	35.96	77.99%
HN33-nCLU-oxidative_stress-1	SRR20646225	55,650,122	35.81	74.18%
HN33-nCLU-oxidative_stress-2	SRR20646224	43,358,527	35.75	70.73%
HN33-nCLU-oxidative_stress-3	SRR20646223	63,395,372	35.79	74.16%
HN33-sCLU-normoxia-1	SRR20646222	49,471,413	35.79	76.94%
HN33-sCLU-normoxia-2	SRR20646221	52,628,491	35.75	69.68%
HN33-sCLU-normoxia-3	SRR20646220	63,415,123	35.84	75.52%
HN33-sCLU-hypoxia-1	SRR20646218	52,775,071	35.86	75.87%
HN33-sCLU-hypoxia-2	SRR20646217	43,037,551	35.84	77.59%
HN33-sCLU-hypoxia-3	SRR20646216	40,234,863	35.95	80.70%
HN33-sCLU-oxidative_stress-1	SRR20646215	27,019,498	35.51	59.72%
HN33-sCLU-oxidative_stress-2	SRR20646214	54,622,362	35.85	75.17%
HN33-sCLU-oxidative_stress-3	SRR20646213	53,908,929	35.73	74.65%
HN33-S100B-normoxia-1	SRR20646212	53,322,771	35.81	76.70%
HN33-S100B-normoxia-2	SRR20646211	62,184,734	35.84	76.67%
HN33-S100B-normoxia-3	SRR20646210	58,811,703	35.97	79.11%
HN33-S100B-hypoxia-1	SRR20646209	55,875,817	35.81	76.60%
HN33-S100B-hypoxia-2	SRR20646207	40,033,728	35.95	78.91%
HN33-S100B-hypoxia-3	SRR20646206	43,408,060	35.92	79.04%
HN33-S100B-oxidative_stress-1	SRR20646205	46,397,569	35.90	72.36%
HN33-S100B-oxidative_stress-2	SRR20646204	47,776,179	35.97	75.28%
HN33-S100B-oxidative_stress-3	SRR20646203	82,370,114	35.78	74.25%

***Table S3.1a**: Primer sequences used in qPCR expression analyses for mice (Mmu), hooded seals (Ccr) and harp seals (Pgr).*

Primer name	species	Primer sequence (5'-3')
SOD1_fw	Mmu, Ccr, Pgr	GACCTGGGCAATGTGACTGC
SOD1_rev	Mmu, Ccr, Pgr	CACCTTTGCCCAAGTCATCT
GPX3_fw	Mmu	CTCCTGAGACCAGCCAAGAC
GPX3_rev	Mmu	GAGCCTAAGCCTGAATGCAC
GPX3_fw	Ccr, Pgr	TTCTCGCACTCTCTACAGCA
GPX3_rev	Ccr, Pgr	AAACATGTGCGTGCGATTGT
GSTK1_fw	Mmu, Ccr, Pgr	CAAATATGGGGCYTTTGGGCT
GSTK1_rev	Mmu, Ccr, Pgr	AGGGCCCATCCACTTCTCT
GSTO1_fw	Mmu	TTGGAGCTCAAGGAGTGTCTA
GSTO1_rev	Mmu	TCAGAGCCCATAATCACAGG
GSTO1_fw	Ccr, Pgr	TGATTGTGTAGACCACACTCC
GSTO1_rev	Ccr, Pgr	AGCCCATAGTCACAGGCCT
GLRX2_fw	Mmu	GAAAGAACCGTTCCCAGGATA
GLRX2_rev	Mmu	TGATGAACCAGAGGCAGCAAT
GLRX2_fw	Ccr, Pgr	CTGGTGAAAAAACTGTACCAAG
GLRX2_rev	Ccr, Pgr	ACTGATGAACTAGTGGAAGCAA
TXNRD3_fw	Mmu	AATTCGACAACGAACGTGTGGT
TXNRD3_fw	Ccr, Pgr	TCGACAATTATCGGGTGATAGG
TXNRD3_rev	Mmu, Ccr, Pgr	CTAGCCTCAGCAGCCTTTCT

***Table S3.1b**: Primer efficiencies for every gene, presented by species and brain regions.*

Gene symbol	Brain region	Species	Efficiency
GLRX2	visual cortex	Ccr+Pgr	0.98
GLRX2	visual cortex	Mmu	0.89
GLRX2	cerebellum	Ccr+Pgr	0.82
GLRX2	cerebellum	Mmu	0.90
GLRX2	hippocampus	Ccr+Pgr	0.92
GLRX2	hippocampus	Mmu	0.85
GPX3	visual cortex	Ccr	1.04
GPX3	visual cortex	Pgr	1.32
GPX3	visual cortex	Mmu	0.82
GPX3	cerebellum	Ccr	1.20
GPX3	cerebellum	Pgr	1.49
GPX3	cerebellum	Mmu	1.22
GPX3	hippocampus	Ccr	1.09
GPX3	hippocampus	Pgr	1.13
GPX3	hippocampus	Mmu	1.92
GSTK1	visual cortex	Ccr+Pgr	1.10
GSTK1	visual cortex	Mmu	1.13
GSTK1	cerebellum	Ccr+Pgr	1.01
GSTK1	cerebellum	Mmu	1.20
GSTK1	hippocampus	Ccr+Pgr	1.25
GSTK1	hippocampus	Mmu	1.29
GSTO1	visual cortex	Ccr+Pgr	0.94
GSTO1	visual cortex	Mmu	1.27
GSTO1	cerebellum	Ccr+Pgr	0.84

GSTO1	cerebellum	Mmu	0.85
GSTO1	hippocampus	Ccr+Pgr	1.10
GSTO1	hippocampus	Mmu	0.90
RBFOX3	visual cortex	Ccr	0.97
RBFOX3	visual cortex	Pgr	0.95
RBFOX3	visual cortex	Mmu	1.11
RBFOX3	cerebellum	Ccr	1.01
RBFOX3	cerebellum	Pgr	1.06
RBFOX3	cerebellum	Mmu	1.19
RBFOX3	hippocampus	Ccr	1.07
RBFOX3	hippocampus	Pgr	0.96
RBFOX3	hippocampus	Mmu	1.03
SOD1	visual cortex	Ccr+Pgr	1.30
SOD1	visual cortex	Mmu	1.61
SOD1	cerebellum	Ccr+Pgr	1.23
SOD1	cerebellum	Mmu	1.47
SOD1	hippocampus	Ccr+Pgr	1.15
SOD1	hippocampus	Mmu	1.38
TXNRD3	visual cortex	Ccr+Pgr	1.47
TXNRD3	visual cortex	Mmu	2.23
TXNRD3	cerebellum	Ccr+Pgr	1.23
TXNRD3	cerebellum	Mmu	1.16
TXNRD3	hippocampus	Ccr+Pgr	1.36
TXNRD3	hippocampus	Mmu	1.13

Table S3.2: *Expression of 49 antioxidant genes in neurons of the visual cortex of the mouse (Mus musculus, n = 3) and the hooded seal (Cystophora cristata, n = 3). Gene expression is presented as TPM (transcripts per million) values and the RNA-seq data were extracted from Geßner et al. (2022). Expression values of genes in the GO term „antioxidant activity" (GO:0016209) were taken from Geßner et al. (2022), while expression values of genes of the GO term „glutathione metabolic process" (GO:0006749) and from a list of human antioxidants (Gelain et al. 2009) were extracted in this study. Since some genes occur in more than in one GO term, we have listed them only once to avoid repetition.*

Annotated Term	Gene symbol	Fold change	FDR	TPM mouse	TPM hooded seal
antioxidant activity (GO:0016209) taken from Geßner et al. (2022)					
glutathione peroxidase activity	*ALOX5AP*	21.5	2.21E-29	0.5	12.7
	GPX1	2.2	2.52E-05	65.4	140.2
	GPX3	8.6	1.47E-11	4.0	34.2
	GSTK1	26.9	6.76E-72	0.7	19.1
	GSTO1	15.1	2.30E-30	3.6	53.9
	GSTO2	9.9	2.12E-07	0.1	1.1
	LTC4S	-8.9	1.77E-07	1.8	0.2
	*MGST1**	13.6	4.86E-21	0.2	1.3
	PTGES	4.5	1.50E-03	0.3	1.1
	PTGS2	-2.4	7.40E-03	2.9	1.2
glutathione-disulfide	*GSR*	2.0	1.50E-02	6.5	12.8
bromide peroxidase	*PXDN*	-2.5	3.69E-07	2.3	0.9

antioxidant activity	*PRDX2*	3.4	3.24E-16	114.1	388.0
	PRXL2A	3.5	6.17E-15	7.9	27.8
	PRXL2B	-4.3	1.35E-19	35.3	8.2
	S100A9	99.7	5.00E-03	0.1	6.1
	SELENOW	2.0	4.00E-02	15.0	30.1
	SOD1	9.1	7.29E-59	52.8	481.0
superoxide	*NQO1*	10.1	6.35E-24	1.5	15.2
catalase activity	*CYGB*	-2.7	8.72E-08	12.3	4.6
thioredoxin-disulfide reductase activity	*SELENOT*	17.6	6.79E-75	2.3	41.5
	TXNRD1	2.6	1.34E-06	7.6	20.0
	TXNRD3	4.7	6.03E-07	1.3	5.9
glutathione metabolic process (GO:0006749)					
glutathione metabolic process	*CTH*	10.6	9.03E-11	0.8	8.4
	CTNS	-2.2	6.40E-04	2.2	1.0
	ETHE1	2.1	1.10E-02	16.0	33.7
	GLO1	8.3	5.26E-28	8.4	70.3
	GSTM1	-69.7	4.85E-53	9.5	0.1
	GSTM3	-35.4	1.42E-111	50.1	1.4
	GSTM4	-9.4	1.75E-06	1.5	0.1
	GSTZ1	-2.9	1.07E-05	1.9	0.7
	NAT8	-17.3	2.38E-09	2.4	0.1
	NFE2L1	-4.1	0	64.9	15.7
glutathione biosynthetic process	*GCLM*	-5.7	3.38E-26	10.6	1.8
	GSS	2.3	1.30E-03	3.9	9.1
	SLC1A2	3.5	9.08E-11	12.5	43.8
positive regulation of	*NFE2L2*	15.2	4.32E-13	0.7	10.3
glutathione	*GGT7*	-2.8	7.46E-14	133.5	47.5
glutathione catabolic	*CHAC2*	-2.9	8.62E-06	5.0	1.7
Human antioxidant genes (Gelain et al. 2009)					
Thiol redox	*GLRX*	-3.7	2.79E-07	1.2	0.3
	GLRX2	-3.3	1.09E-08	3.8	1.1
	GLRX3	-2.4	3.12E-12	39.8	16.7
	MT1A	10.0	1.10E-02	0.1	1.7
	MT1M	-105.9	6.25E-54	66.2	0.6
	MT2A	-49.3	4.76E-46	20.2	0.4
	TXNDC5	-2.0	4.60E-04	2.5	1.3
	TXNIP	8.5	8.46E-14	2.3	19.3
additional genes with known antioxidant activity					
antioxidant defence	*HMOX2*	2.5	3.94E-07	40.3	99.0
antioxidant defence	*PON2*	4.0	3.55E-14	12.0	48.6

Table S3.3: *GenBank accession numbers of genes tested for positive selection. Sequences of the hooded seal were extracted from Geßner et al (2022) who deposited sequence files at the NCBI Sequence Read Archive (PRJNA785765). Dash (-) indicates missing sequences.*

Species	SOD1	GPX3	GSTO1	GSTK1	GLRX2	TXNRD3	GSR
Gray seal	XM_036070661.1	XM_036090652.1	XM_036072388.1	XM_036095820.1	-	XM_036078530.1	XM_036107086.1
Hawaiian monk seal	XM_021678086.1	XM_021700997.1	XM_021700263.1	XM_021692779.1	XM_021686656.1	XM_021695011.1	XM_044911945.1
Southern elephant seal	XM_035017588.1	XM_034999581.1	XM_035028644.1	XM_035021296.1	-	XM_045904193.1	XM_045879790.1
Harbour seal	XM_032393272.1	XM_032395275.1	XM_032423193.1	XM_032401423.1	XM_032422059.1	XM_032412074.1	XM_032413462.1
Weddell seal	XM_031041374.1	XM_006752411.2	XM_031040229.1	XM_006749538.1	XM_031041961.1	XM_031018881.1	XM_031026276.1
Walrus	XM_004406294.1	XM_004402830.2	-	XM_004414576.1	-	-	XM_004408281.2
Dog	NM_001003035.1	NM_001164454.1	XM_038440499.1	XM_005629528.4	XM_038448378.1	NM_001122778.1	XM_038689973.1
Ferret	XM_013058840.1	XM_004737800.2	XM_013054574.1	XM_004782546.2	XM_045081144.1	XM_004738666.3	XM_045073784.1
Polar Bear	XM_040621040.1	XM_040630394.1	XM_040623945.1	XM_008697303.2	XM_040636025.1	XM_040628356.1	XM_040643282.1
Grizzly Bear	XM_026514338.1	XM_026510805.1	XM_026494065.1	XM_026512905.1	XM_044390677.1	XM_026501505.2	XM_026508378.2
Giant Panda	XM_002928799.4	XM_002920757.4	XM_034663250.1	XM_002924165.4	XM_011230064.3	XM_034657258.1	XM_034647544.1

Table S3.4: *Antioxidant genes in pinnipeds show no signatures of positive selection when compared to non-diving carnivores using two models (BUSTED, aBSREL). Only when both models inferred positive selection were genes considered to have been positively selected.*

	BUSTED		aBSREL	
gene symbol	**p-value**	**alignment (%)**	**p-value**	**branch**
GPX3	0.5	-	-	-
GSTO1	0.5	-	< 0.001	gray seal
GSTK1	0.5	-	-	-
SOD1	0.056	-	-	-
GSR	<0.001	3,75	-	-
TXNRD3	0.058	-	0.002	hooded seal
GLRX2	0.304	-	-	-

Table S3.5: *All glutathione-s-transferases (GSTs) present in the hooded seal neuronal transcriptome with a TPM-value ≥ 1 in either species, mouse or hooded seal.*

Gene symbol	Fold change	FDR	TPM mouse	TPM hooded seal
GSTK1	26.9	6.76E-72	0.7	19.1
GSTM1	-69.7	4.85E-53	9.5	0.1
GSTM3	-35.4	1.42E-111	50.1	1.4
GSTM4	-9.4	1.75E-06	1.5	0.1
GSTM5	-745.3	2.07E-71	6.0	0.0
GSTO1	15.1	2.30E-30	3.6	53.9
GSTO2	9.9	2.12E-07	0.1	1.1
GSTZ1	-2.9	1.07E-05	1.9	0.7
SUM			**73.5**	**76.5**

13 Acknowledgements (Danksagung)

In erster Linie möchte ich Dr. Cornelia Geßner meinen besonderen Dank aussprechen für die Möglichkeit diese Doktorarbeit durchzuführen und die wundervolle Betreuung mit der diese Arbeit erst gelingen konnte.

Prof. Dr. Thorsten Burmester möchte ich in diesem Zug dafür danken dieses interessante Forschungsthema in seiner Arbeitsgruppe und die finanziellen Mittel zur Verfügung gestellt zu haben und wünsche ihm alles Gute für die Zukunft!

Des Weiteren gilt mein Dank Dr. Andrej Fabrizius, der diese Arbeitsgruppe souverän in Vertretung geleitet hat und für seine Bereitschaft als Zweitgutachter dieser Arbeit zu fungieren.

Vielen Dank an dieser Stelle auch an Prof. Dr. Susanne Dobler, die spontan als Erstgutachterin dieser Arbeit eingesprungen ist.

Prof. Dr. Lars P. Folkow möchte ich dafür danken das Probenmaterial für diese Arbeit zur Verfügung gestellt zu haben (Kapitel I & III) und für sein konstruktives Feedback zu den Manuskripten.

Dr. Marina Creydt und Prof. Dr. Markus Fischer möchte ich für die Möglichkeit danken massenspektrometrische Experimente in ihrem Labor durchzuführen, für die methodische Expertise und den wissenschaftlichen Austausch.

Dr. Carina Osterhof und Prof. Dr. Thomas Hankeln danke ich für die freundliche Aufnahme in ihrer Arbeitsgruppe und die Unterstützung bei der Analyse der Sequenzierdaten an der Johannes-Gutenberg-Universität Mainz.

Ganz herzlich möchte ich auch Katja Reimann, Maria Machola, Michelle Wisniewsky und Marilou Kloock für die ausdauernde Hilfe rund ums Labor danken.

Leonie Lancelle möchte ich für ihren experimentellen Beitrag zu dieser Arbeit danken und die Möglichkeit ihre Bachelor-Arbeit zu betreuen.

Danke an alle meine Mitstreiter am Institut, besonders meinen Büro-Mitbewohnern Raphael Koll, Dr. Alena Krüger, Dr. Julia Lüdemann und Paressa Papadopoulou-Wörner sowie meinen Büro-Nachbarn Sarah Beyer, Eda Dönmez, Dr. Kathrin Helfenrath, Soraya Safavi und Annette Schlosser. Danke für interessante Gespräche innerhalb und außerhalb der Wissenschaft sowie für schöne und lustige Erinnerungen auf Konferenzen und Feiern.

Auch meinen wunderbaren Mitbewohnern und Freunden möchte ich für die Unterstützung danken und die willkommene Abwechslung zu tagelangen Schreib-Sessions.

Ohne die Unterstützung meiner Eltern wäre ich heute nicht, wer und wo ich bin. Danke, dass ihr mir immer mit Rat und Tat zur Seite steht und alles ermöglicht habt, was ich mir in den Kopf gesetzt habe. Dafür möchte ich euch von Herzen danken.

Nicht zuletzt, Elisabeth Riedel, die mir immer ein Lächeln aufs Gesicht zaubert und aus dem Alltagstrott holt. Danke, dass du in mein Leben gefunden hast und danke für deine Liebe. Bleib so wundervoll, wie du bist.

14 Declaration upon oath (Eidesstaatliche Versicherung)

I hereby declare upon oath that I have written the present dissertation independently and have not used further resources and aids than those stated in the dissertation.

Hiermit erkläre ich an Eides statt, dass ich die vorliegende Dissertationsschrift selbst verfasst und keine anderen als die angegebenen Quellen und Hilfsmittel benutzt habe.

Hamburg, July 2023

Place, date

Gerrit Alexander Martens